Continuous Flow Rheometry for Settling Slurries

by

Timothy James AKROYD

Thesis submitted for the degree of
Doctor of Philosophy

School of Chemical Engineering
Faculty of Engineering, Computer and Mathematical Science
The University of Adelaide

November 2004

It's kind of fun to do the impossible.

Walt Disney

Declaration

This work contains no material which has been accepted for the award of any other degree or diploma in any university or other tertiary institution and, to the best of my knowledge and belief, contains no material previously published or written by another person, except where due reference has been made in the text.

I give consent to this copy of my thesis, when deposited in the University Library, being available for loan and photocopying.

SIGNED : ……. **DATE : ……..**

Acknowledgements

I am extremely grateful to my supervisor A/Professor Dzuy Nguyen for his guidance, support and advice throughout the entirety of this project.

This work is supported by a grant from the Australian Research Council under the Strategic Partnership with Industry- Research and Training Scheme, in conjunction with Rio Tinto Technical Services. I also would like to acknowledge and thank the involvement of Mark Coghill and Nick Vagias in this project and their kind hospitality during my visits to Melbourne.

I would like to thank Dr Denier from the Department of Applied Mathematics for some invaluable discussions on instabilities in fluid flow.

I would also like to extend my sincere appreciation to the Chemical Engineering workshop staff; Brian, Peter and Jason, for their assistance in the construction and development of the numerous pieces of experimental apparatus which I required for this project. I cannot thank you enough. To Mary and Elaine thank you for your assistance in all non-technical matters and to Andrew thank you for your assistance in laboratory matters.

To Peng thank you for your assistance, advice and friendship over the years we worked together in room A309, though I'll never look at coal in the same way again!

To all my friends, thank you for your friendship, support and numerous creative diversions during the course of this project. It was much appreciated!

Finally I would especially like to thank my Parents, Philip and Sarah for their endless support and assistance throughout this entire project. I could not have done this without you.

To my much-loved family I dedicate this thesis.

Publications

Akroyd, T.J. and Nguyen, Q.D., (1999), 'Continuous On-Line Rheological Measurements for Mineral Slurries', *Chemeca '99*, Newcastle.

Akroyd, T.J., Nguyen, Q.D. and Vagias, N., (2001), 'Rheological Characterisation of Rapid Settling Slurries', *Aust. Korean Rheol. Conference*, Melbourne.

Akroyd, T.J. and Nguyen, Q.D., (2001), 'Rheological Characterisation of Heavy Mineral Slurries', *Chem. Eng. World Congress 2001*, Melbourne.

Akroyd, T.J. and Nguyen, Q.D., (2001), 'Continuous Rheometry for Industrial Slurries', *14 Aust Fluid Mech Conference*, Adelaide.

Akroyd, T.J., Nguyen, Q.D., and Denier, J.P., (2003), 'The Stability of Helical Flow of Pseudoplastic Fluids', *Chemeca '03*, Adelaide.

Akroyd, T.J. and Nguyen, Q.D., (2003), 'Effect of Density Difference between the Solids and Suspending Liquid on the Rheological Properties of Settling Slurry', *Chemeca '03*, Adelaide.

Papers

Akroyd, T.J. and Nguyen, Q.D., (2003), 'Continuous On-line Rheological Measurements for Rapid Settling Slurries', *Minerals Eng.*, **16**, pp. 731-738.

Akroyd, T.J. and Nguyen, Q.D., (2003), 'Continuous rheometry for industrial slurries', *Exp. Thermal and Fluid Science*, **27**, pp. 507-514.

Summary

The rapid settling nature of some industrial mineral slurries can cause problems in the measurement of their rheological properties. To address this problem a flow rheometer based on the principles of helical flow was developed. The rheometer designed, is a modified Couette flow system, whereby slurries are circulated through the concentric cylinders by the addition of an axial flow. The purpose of this axial flow is to prevent particles from settling and to maintain a homogeneous suspension. However, the addition of an axial flow component to Couette flow complicates the analysis procedure for non-Newtonian fluids particularly in wide gap geometries. Thus a specific emphasis in this study was placed on developing a correct analysis procedure for helical flow that eliminated the need for rudimentary calibration procedures.

Experimental measurements with different liquids, including those with Newtonian and non-Newtonian flow properties showed good agreement between data obtained from the flow rheometer and data obtained using other standard laboratory instruments. Typical differences between the results from the flow rheometer and results from other laboratory instrument varied between 1-2%, with standard deviations in the flow rheometer data of between 2-4%. The flow properties of several non-Newtonian slow settling slurries were examined using the flow rheometer and also with a specially modified tube rheometer. As with the pure liquid results good agreement was obtained between the results from the flow rheometer and those obtained with the modified tube rheometer. Several rapid settling slurries were examined using the flow rheometer, but due to the rapid settling nature of these slurries they could not be examined with any other laboratory instruments. However, internally consistent results were obtained from different tests with the flow rheometer using different values of axial flow rate. These results demonstrate that the correct data analysis method was developed for the helical flow of non-Newtonian fluids

Particle migration is a phenomenon known to affect the results of both rotational and axial flow rheological equipment. Whilst the motion of particles within the helical

flow geometry could not be directly observed, careful examination of the results from several experiments with slurries showed that the effects of particle migration were minimal or non-existent within the flow rheometer. It is presumed that the circulation of the fluid through the geometry minimises the residence time in the geometry, which reduces the likelihood of particle migration.

The development of Taylor vortices in a Couette type geometry can cause substantial errors in any rheological measurements. The flow rheometer is based on helical flow, which is a combination of both Couette and axial flow and as such may also suffer from measurement errors if instabilities develop in the flow. A stability criterion for the helical flow of non-Newtonian fluids is therefore required to ensure measurements from the flow rheometer were obtained in the laminar flow region. The stability criterion for laminar Couette flow of a Newtonian fluid was well known, as was the effect of imposing axial flow on Newtonian Couette flow. However, the effect of the rate of acceleration of the inner cylinder and the effect of non-Newtonian fluids on the onset of Taylor vortices was unknown. An increase in the rate of acceleration of the inner cylinder was found to have a destabilising effect on Couette flow. A modified Taylor number was developed for non-Newtonian fluids using the power-law model and was experimentally validated for a range of non-Newtonian fluids. These results were then used to develop a laminar flow stability criterion for rheological measurements of non-Newtonian fluids in the flow rheometer.

To test the suitability of the results from the flow rheometer for use in the design and optimisation of process units, the power requirements to turn an impeller in a small baffled mixing vessel were investigated. Good agreement was obtained in the laminar and turbulent flow regions for a variety of Newtonian and non-Newtonian fluids between measured values of impeller power and those predicted using rheological measurements from the flow rheometer.

Altering the density of the solid particles in a slurry is known to affect the overall rheological properties of the slurry. However, the effects of changing the liquid density were not so clearly defined and thus several artificial slurries of PMMA (poly-methylmethacrylate) spheres in water/NaCl and water/glycerol solutions were used to investigate this phenomenon. It was found that the slurry rheology was altered by

changes in the suspending liquid density, however, these changes could be entirely attributed to changes in the liquid viscosity associated with the changes in liquid density.

To summarise, the work presented in this Thesis provides a fundamental approach for the absolute measurement of the rheological properties of settling slurries, under conditions that more accurately represent those found in actual mineral processing operations.

Table of Contents

APPENDICIES

List of Figures

List of Tables

Nomenclature

English Letters

A	pre-exponential parameter, power-law model	Pas^n
a	shear stress calculation parameter, vane	
a_x	Shi and Napier-Munn (1996) model parameters	$mV(s/rad)^x$
b	constant of integration	
C	height of the impeller above the base of the tank	m
c	differential pressure parameter	$kg/(m^2s^2)$
D_T	turbine diameter	m
d_x	x% of particles have a smaller diameter	m
dv	particle diameter (volume average)	m
ELF	entrance length parameter	
e	displacement of inner cylinder axis from centre axis	m
g	gravitational acceleration	m/s^2
H	axial length of a Taylor vortex	m
He	Headstrom number	
h	gap width between parallel plates	m
I_P	impeller blade pitch	m
J	width of baffles	m
k	ratio of cylinder speeds (inner/outer)	
k_1	Krieger and Maron model parameter	
k_2	Krieger and Maron model parameter	
k_n	mixing parameter used by Sinevic et al. (1986)	
L	length	m
L_B	length of impeller blade	m
L_e	entrance development length	m
M	torque	Nm
N_B	number of baffles in a tank	
N_I	number of impeller blades	
n	exponential parameter, power-law model	
P	Taylor's turbulence parameter	
p	pressure	Pa

Q	flow rate	m^3/s
R	outer cylinder radius	m
Re	Reynolds number	
Re'	modified Reynolds number for mixing tank systems	
S	radius ratio (outer/inner) (=1/κ)	
SC	stability criterion	
Ta	Taylor number	
Ta'	Taylor number (= Ta^2)	
Ta_c	critical Taylor number	
v	velocity	m/s
v_m	minimum velocity to maintain homogeneous conditions	m/s
$\langle v_z \rangle$	average annular axial velocity	m/s
W	width of an impeller blade	m
z	axial length	m

Greek Symbols

α	angle between cone and plate	rad
Δ	difference	
ε	eccentric Ratio (= e / average gap width(R-κR))	
η	apparent viscosity	Pas
Φ	solids volume concentration	
Φ_P	power number	
ϕ	fluidity function (=1/η)	1/Pas
$\dot{\gamma}$	shear rate	1/s
φ	co-axial cylinder shape factor	
κ	radius ratio (inner/outer) (=1/S)	
λ	radius ratio (axial velocity peak/outer)	
Ω	angular velocity	rad/s
$\wp$	combined pressure (= p + ρgz)	Pa
μ	viscosity	Pas
ν	kinematic viscosity	m^2s
ρ	density	kg/m^3

τ	shear stress	Pa
τ_y	yield stress	Pa
θ	cone and plate angle (= $\pi/2-\alpha/2$)	rad
υ	acceleration of the inner cylinder	rad/s
Ψ	wave number	

Subscripts

b	property at bob (inner cylinder) wall
l	property of the liquid
p	property of the solid fraction (particle)
r	radial direction, cylindrical co-ordinates
w	property at the system wall
s	property of the slurry
z	axial direction, cylindrical co-ordinates
θ	annular direction, cylindrical co-ordinates

Superscripts

c	CMC solution
g	glucose-water solution
m	moderate gap geometry
n	narrow gap geometry
p	polyox (PEO) solution
w	wide gap geometry

SECTION A INTRODUCTORY CONCEPTS AND TECHNIQUES

CHAPTER 1 INTRODUCTION

1.1 Background

An economically viable ore body may contain only 1% valuable mineral or even less for exceptionally valuable products such as gold where only a few grams per tonne may be economically viable. Thus it is usual that a lot of gangue material will also be unearthed as part of the mining process. The transportation and processing of ore is often in the form of slurries. Water is therefore a key component of every mining and mineral-processing operation and in 1996-97 Australian mine sites used over 570 GL of water (Australian Bureau of Statistics 2001). However, Australia is one of the driest continents and is characterised as having a high spatial and temporal variability in climatic conditions (Australian Bureau of Statistics 2001), making water an extremely valuable and expensive commodity. The plant life cycle cost of a mining operation is typically influenced greatly by the throughput or processing rate, the solids concentration and rheological properties of the slurries (Wills 1976). In more

recent years a greater focus is being placed on improving the design and optimisation of mineral-processing operations to reduce costs. In order to achieve this goal it is crucial that the actual physical properties of the slurries being processed including the rheological properties be determined under conditions that realistically represent those found in actual site operations.

Solid / liquid solutions can be divided into two broad categories; settling slurries and suspensions. Suspensions (non-settling / slow-settling slurries) usually consist of fine particles (smaller than 40 μm) at high solids concentrations. The slow settling rate of particles in these suspensions means that their rheological properties can be measured using generic standard rheological instruments. However, while only standard rheological instruments are required; slip, the presence of a yield stress and possible thixotropic behaviour often means that advanced measurement techniques are required (Steffe 1992, Van Wazer et al. 1963).

Compared to suspensions, settling slurries consist of a diverse range of particle sizes, which include large particles (greater than 40 μm) and lower solids concentrations. A significant problem encountered when measuring the rheological properties of these slurries in standard instruments including: parallel plate, bob and cup and capillary tube, is that the particles settle during any measurements. The formation of a concentration gradient within the instrument can lead to substantial errors in the measurement of the slurry's rheological properties.

The challenge is therefore to develop a rheological instrument that is capable of determining the actual rheological properties of settling slurries whilst maintaining homogeneous conditions. This thesis outlines the development of an instrument capable of measuring the actual rheological properties of settling slurries. The design of this instrument was based on the addition of axial flow to Couette flow to generate helical flow (Nguyen et al. 2000). The purpose of the axial flow was to circulate fluid through the Couette geometry thereby maintaining the particles in a homogeneous suspension. Most mineral suspensions however, are characterised by non-Newtonian behaviour and the large sized particles in settling slurries often mean that narrow gap geometries cannot be used. Particular emphasis in this work was therefore placed on

developing the correct analysis procedures for the measurements of non-Newtonian fluids in wide gap geometries in helical flow.

1.2 Research Objectives

The primary objective of this project was to develop an instrument and a data analysis procedure that is capable of determining the rheological properties of non-Newtonian settling slurries. This primary objective can be divided into a number of smaller objectives and these are outlined as follows.

- Examine and evaluate existing modified concentric cylinder rheometers in the literature.
- Develop a design for a flow rheometer with a particular emphasis on an ability to maintain rapid settling slurries in a homogeneous suspension.
- Develop a data reduction procedure with a particular emphasis on non-Newtonian fluids in wide gap geometries.
- Evaluate the flow rheometer with a wide range of fluids including ideal Newtonian, pseudoplastic and yield-pseudoplastic fluids and settling and non-settling slurries.
- Determine the effect, if any, of particle migration on rheological measurements of slurries and suspensions from the flow rheometer, due to the helical nature of the flow profile.

The secondary objective of this project was to examine and develop a criterion for the onset of turbulent instabilities in the flow rheometer, which is based on helical flow. The onset of turbulent instabilities can cause errors during rheological measurements and it is therefore important to have a criterion, which can accurately predict the onset of these instabilities. A breakdown of the objectives of this project, relating to the onset of instabilities in helical flow are presented below.

- Develop an instrument to study (visualise) the onset of Taylor vortices in helical flow.
- Evaluate the effect of changes in the rate of acceleration of the inner cylinder on the onset of Taylor vortices in Couette flow.
- Modify and evaluate the Taylor number for non-Newtonian fluids.

- Determine the effect of axial flow on the stability of Couette flow for non-Newtonian fluids.
- Define a criterion of stability for the flow rheometer
- Evaluate the stability criterion with Newtonian and non-Newtonian fluids.

Another objective of this project was to show that the flow rheometer can be used to generate rheological results, which can be used in industrial and research applications. To simulate an industrial application rheological measurements from the flow rheometer were used to predict the power requirements of a mixing tank system. As a research application the flow rheometer was used to examine the effect that changes in the density of the suspending liquid can have on the rheological properties of a slurry.

1.3 Thesis Outline

This thesis is directed towards developing an instrument capable of measuring the actual rheological properties of settling slurries with a particular emphasis placed on developing the correct data analysis procedures for the helical flow of non-Newtonian fluids in wide gap geometries.

This thesis is divided into five distinct sections. In Section A the purpose for this work is introduced along with an overview of fundamental rheology knowledge. In Section B the design, development and experimental validation of the flow rheometer for settling slurries is presented. The onset of instabilities in the helical flow of non-Newtonian fluids is analysed in Section C. In Section D the flow rheometer is used in several different experimental studies. Finally Section E provides an overall summary of the finding from this study and presents possible directions for future work.

1.3.1 Section A: Introduction and Introductory Concepts and Techniques

In Chapter 1 the background and relevance of this project to the mineral processing industry is summarised. The research objectives and thesis outline are also presented.

Rheology is an important and fundamental component of this study and thus Chapter 2 presents a summary of basic rheological properties seen in liquids and slurries and some of the rheological models used to describe the different types of behaviour that can be observed.

1.3.2 Section B: The Flow Rheometer

Chapter 3 presents a comprehensive overview of different rheological instruments currently available. Particular emphasis is placed on examining the suitability of instruments based on modified Couette geometries to measure the properties of settling slurries. Other more specialised instruments developed for the measurement of settling slurries are also evaluated.

In Chapter 4 the theory and analysis of helical flow is examined. This chapter discusses methods for determining the rheological properties of non-Newtonian fluids from measurements with a helical flow geometry.

Chapter 5 presents a detailed description of the flow rheometer developed to measure the properties of settling slurries. The difficulties associated with the measurements of low viscous, rapid settling slurries are discussed with regards to instrument design. The auxiliary equipment including the pump and computer control program are also discussed.

Chapter 6 presents a description of the generic experimental apparatus, techniques and data analysis procedures used to support the unique experiments performed in this study. The techniques presented include; particle size analysis using a Malvern size analyser and generic rheological measurements in both controlled stress and

controlled rate instruments with a variety of different geometries. Finally a description of a modified tube rheometer, developed to measure the properties of slow settling slurries is presented.

The flow rheometer was extensively tested with a wide variety of liquids and slurries with different rheological properties including Newtonian, non-Newtonian and yield-stress behaviours. Some problems were encountered with the measurement of yield-stress fluids at low values of shear rate but a modified measurement method was devised to minimise this problem. A summary and discussion of the results obtained for the different types of fluids examined is presented in Chapter 7.

A significant complication of helical flow compared to Couette flow is the contributions of the additional axial flow component. In Chapter 8 the axial flow component of helical flow is examined with a focus on the errors that can arise when the contribution made by the axial flow component to the total shear rate in the system are ignored. An improvement to the analysis procedure, developed in Chapter 5, based on the findings is also presented.

The migration of particles in Couette flow, axial flow and helical flow is examined in Chapter 9. The migration of particles is known to affect the rheological measurements of slurries and suspensions in both axial and Couette flow and so it is possible that migration could also occur in helical flow. The extent of particle migration in the flow rheometer with respect to rheological measurements is examined.

Chapter 10 presents a summary of the results and findings of the work conducted with the flow rheometer presented in chapters 3 to 9.

1.3.3 Section C: Instabilities in Helical Flow

Chapter 11 presents a review of literature regarding the onset of instabilities in Couette flow, axial flow and helical flow. A particular focus of this chapter is a detailed examination of the various effects that alter the critical speed for the onset of Taylor vortices in Couette flow.

In Chapter 12 a detailed description is given of the specially developed equipment designed to visualise the onset of Taylor vortices in Couette and helical flow.

The onset of Taylor vortices in Couette flow is examined in chapter 13 with regards to rheological measurements. Particular emphasis is placed on the onset of Taylor vortices under conditions more regularly encountered in rheological measurements; fast acceleration rates of the inner cylinder and the presence of non-Newtonian fluids. The Newtonian Taylor number is suitably modified to better account for the different rheological properties observed in non-Newtonian fluids.

The onset of instabilities in a rotational type rheometer can cause errors in the torque measurements and thus it is necessary to ensure that laminar flow is present during any measurements. Chapter 14 presents a stability criterion for helical flow for both Newtonian and non-Newtonian fluids so that the presence of instabilities in the flow rheometer during any rheological measurements can be determined.

Chapter 15 presents a summary of the work regarding the onset of instabilities in helical flow.

1.3.4 Section D: Applications of the Flow Rheometer

Chapter 16 examines the suitability of measurements from the flow rheometer to be used in the design and optimisation of mineral processing units. The power requirements for a small mixing vessel are measured and these are compared to values predicted using rheological measurements from the flow rheometer.

In Chapter 17 the effect that altering the density of the suspending liquid has on the rheological properties of a slurry is examined. Artificial slurries of PMMA spheres and water, with sodium chloride salt or glycerol added to the water to adjust the suspending liquid density, were used to study this effect.

1.3.5 Section E: Conclusions and References

Chapter 18 provides an overview and summary of the major outcomes of this project and presents possible directions for future work as a result of this study.

CHAPTER 2 BASIC RHEOLOGY

2.1 Introduction

In order to improve the optimisation of mineral processing operations the rheological properties of settling slurries must be determined as accurately as possible under conditions that closely resemble actual site conditions. This chapter presents a review of rheology including the different types of fluids that exist and the different models available to characterise their rheological properties.

2.2 Rheology of Slurries and Suspensions

Settling slurries and suspensions of solids in liquid may exhibit a wide variety of rheological behaviours. The rheological properties are heavily dependent on the solids concentration of the slurry (Clarke 1967, Saraf and Khullar 1975). At low solids concentrations, constant viscosity, Newtonian behaviour is observed, but as the solids concentration increases the rheological behaviour becomes increasingly complex and non-Newtonian with the viscosity becoming dependent on the shear rate. The nature of the non-Newtonian behaviour depends on the solids concentration, the particle shape, the particle size, the particle size distribution and the suspending liquid rheological properties. The suspension/slurry may develop a yield stress and/or become time dependent in nature as structures develop within the fluid at higher solids concentrations (Barnes 1999). Two typical types of time-dependent behaviours are possible; Thixotropy, where the fluid thins with shear and time and the opposite rheopexy, where the fluid thickens with shear and time. This study however, is primarily focused on the measurement of the rheological properties of settling slurries where it is necessary to continuously circulate or shear the slurries to prevent settling. Under these conditions it is assumed that the fluid will be fully sheared and that the rheological properties will be unlikely to change further with time. Thus time-dependent effects will not be investigated further and the discussion will focus only on time independent behaviour.

2.2.1 Viscous Fluids

A settling slurry or suspension that flows under the influence of shear, no matter how small the shear, can be considered as a viscous fluid. Under these conditions it is assumed that for a given shearing condition (the shear stress, τ) there will only be one unique response in the fluid (the shear rate, $\dot{\gamma}$), represented in Equation (2.2-1).

$$\tau = f(\dot{\gamma}) \qquad (2.2\text{-}1)$$

The relationship between the shear stress and shear rate describes the fluids rheological behaviour. Figure 2.2-1 presents three of the more simple rheological behaviours observed in settling slurries and suspensions.

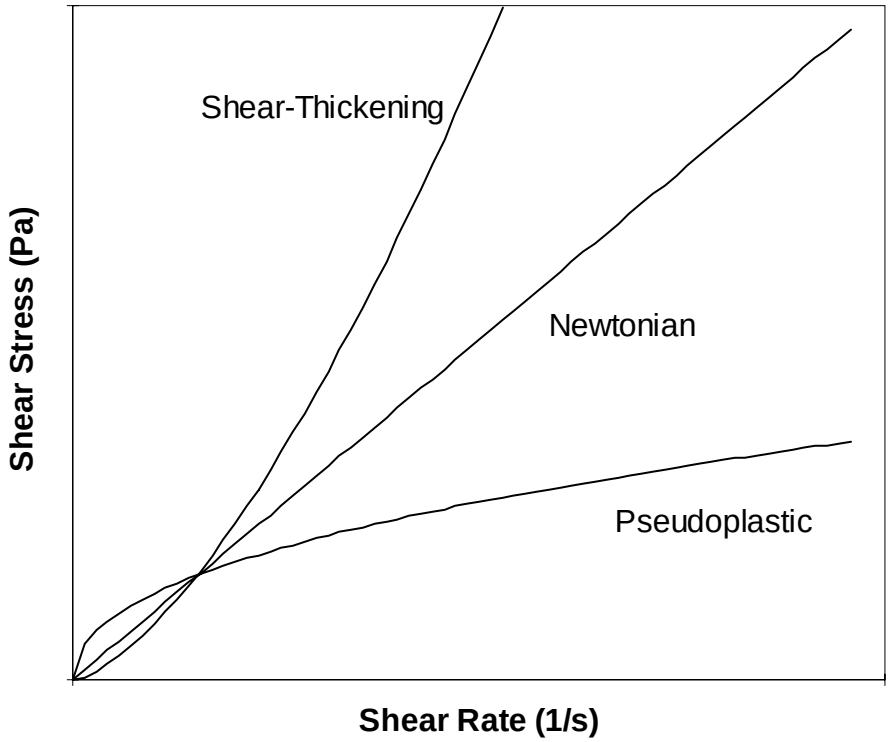

Figure 2.2-1 Flow curves for purely viscous fluids

2.2.1.1 Newtonian

The simplest relationship between shear stress and shear rate for a fluid, is one that is constant or directly proportional, Equation (2.2-2).

$$\tau = \mu \dot{\gamma} \qquad (2.2\text{-}2)$$

In this case the proportionality constant, μ, is referred to as the Newtonian viscosity. The flow curve (a plot of shear stress versus shear rate) is therefore a straight line passing through the origin, see Figure 2.2-1.

Newtonian behaviour is typically only observed in suspensions and slurries when the particles can be considered non-interacting or fully dispersed (Clarke 1967, Vand

1948a, 1948b). Under these conditions particle collisions are assumed to occur in a relatively insignificant number of cases. Thus the movement of particles in the flow field results in only an increase in the viscous energy dissipation.

2.2.1.2 Pseudoplastic

Pseudoplastic fluids are typically suspensions of solids or dissolved long chain polymer strands. As the shear rate increases the structure of the fluid becomes more ordered, which steadily reduces the apparent viscosity, see Figure 2.2-1. The power-law model also referred to as the Ostwald-de Waale model (Ostwald 1926), Equation (2.2-3), may be used to model the rheological behaviour of pseudoplastic fluids.

$$\tau = A\dot{\gamma}^{n} \tag{2.2-3}$$

The parameter A is defined as the pre-exponential factor or consistency index and n as the exponential factor or the flow-behaviour index. The relative value of A refers to the viscous behaviour of the fluid, while the value of n describes the deviation of the fluid behaviour from Newtonian behaviour. For pseudoplastic fluids n must be less than unity. If n is equal to one then Equation (2.2-3) reduces to the Newtonian model, Equation (2.2-2) and A becomes the Newtonian viscosity, μ. A value of n greater than one is used to describe the behaviour of a shear thickening fluid, see section 2.2.1.3. In reality however, most pseudoplastic fluids cannot be described by the power-law model over a wide range of shear rates, as there is typically a region of Newtonian behaviour at very low shear rates and a second Newtonian region at very high shear rates (Skelland 1967, Van Wazer et al. 1963).

More complex models based on the power-law model have been proposed to improve the description of pseudoplastic fluid behaviour over a wider range of shear rates. The Carreau model, Equation (2.2-4) incorporates two terms η_0 and η_∞, which correspond to the constant viscosity regions at very low and very high shear rates respectively.

$$\frac{\eta_0 - \eta}{\eta_0 - \eta_\infty} = \left[1 + \left(A\dot{\gamma}\right)^2\right]^{(n-1)/2} \tag{2.2-4}$$

2.2.1.3 Shear Thickening

Shear thickening behaviour should not be confused with dilatancy, which is a change in volume on deformation, though dilatancy is often used to describe shear thickening behaviour. Suspensions of solids in liquids are often capable of shear thickening behaviour over certain ranges of shear rate. The degree of shear thickening and its onset is a function of the solids concentration, the particle shape and size distribution. At rest the particles are assumed to be situated in such a way that the void space between particles is at a minimum, but as the shear rate increases the particles become more disordered and there may be insufficient liquid to fill the space between the particles leading to direct particle contact which causes an increase in the apparent viscosity of the fluid or shear thickening behaviour (daC.Andrade et al. 1949, Mondy et al. 1994).

A fluid that shows purely shear thickening behaviour is extremely rare, but in such cases the rheological models presented for shear-thinning fluids can be used to describe the behaviour of the fluid, except that pre-exponential parameter n must be greater than one. In more practical situations shear thickening behaviour may be observed over a particular range of shear rate values and in these cases several different rheological models may be needed to describe the fluids behaviour over a wide range of shear rates.

2.2.2 Yield Stress Behaviour

The yield stress of a fluid is commonly defined as the stress that is required to initiate flow of the material. Some of the more simple types of flow curves associated with yield stress behaviour in fluids are presented in Figure 2.2-2.

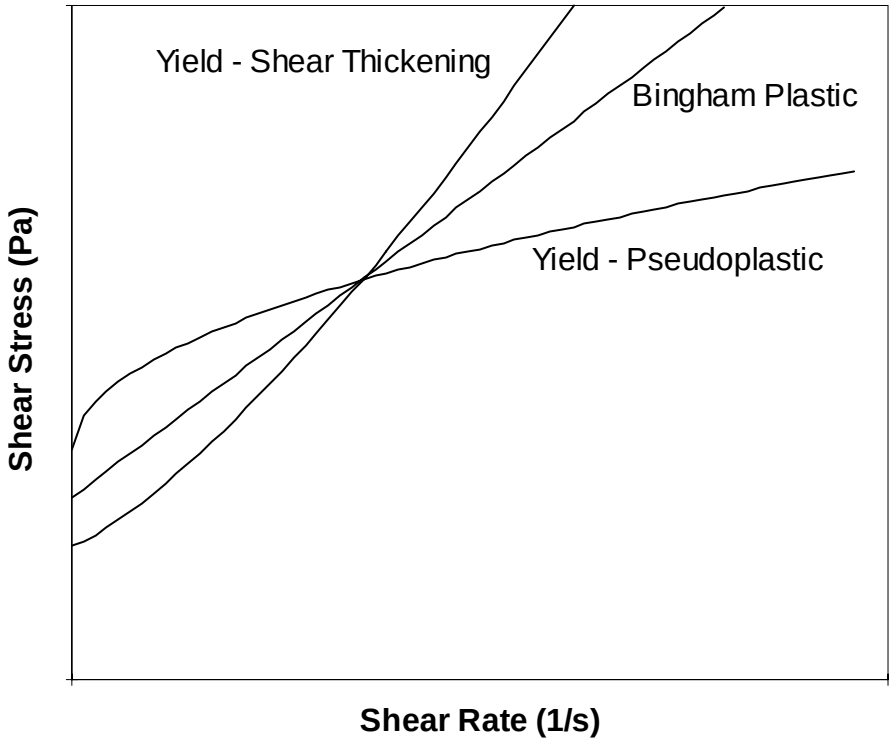

Figure 2.2-2 Flow curves for yield stress fluids

The yield stress, however, is not easily measured and values of the yield stress for a fluid will often vary depending on the measurement technique (Steffe 1992). It is believed that the material responds similar to an elastic solid until the yield stress is reached, at which point the fluid starts to flow. The yield stress is usual explained as the fluid contains an internal structure that is able to resist a certain amount of stress before flow commences. There is some discrepancy in the literature as to the true nature of the yield stress and whether or not it truly exists (Barnes and Walters 1985). If the yield stress does indeed exist then the variable nature in measured values of yield stress suggests that there may be multiple types of structures involved that have varying levels of significance during different types of tests (Cheng 1986). Cheng

(1986), proposed a two-structure theory; the first structure is a pseudo-time independent structure, where the structure is insensitive to changes in shear rate and serves to define the equilibrium flow curve of the fluid. While a true time independent structure is highly unlikely a time dependent structure that recovers extremely rapidly would give the impression of time independent behaviour (Steffe 1992). The other structure is a time dependent structure that builds up in the fluid during the absence of shear. If this structure is more significant than the time independent structure it explains why the yield stress of a fluid changes depending on the rest time, the shear rate and the type of test performed (Steffe 1992).

The two most common types of tests to determine the yield stress are direct measurement and extrapolation. Numerous methods have been proposed for the direct determination of the yield stress, but one of the more simple methods uses a generic rotational rheometer and a vane geometry (Nguyen and Boger 1985). If a direct measurement is not possible then rheological data must be obtained at shear rates as low as possible and then an extrapolation procedure (Murdoch and Kearsey 1960, Kearsey and Cheney 1961) must be used to obtain an estimated value for the yield stress.

2.2.2.1 Bingham Plastic Model

The simplest type of yield stress fluid model is the Bingham plastic model (Bingham 1922), shown in Equation (2.2-5). For this model once the yield stress is exceeded it is assumed that the fluid behaves like a Newtonian fluid, where the shear stress increases proportionally with increases in shear rate. However, there are few suspensions and slurries for which the Bingham model can be used to describe the rheological behaviour over a wide range of shear rates. But over a small range of low values of shear rate the Bingham model may be more applicable for a wider range of suspensions and slurries.

$$\tau = \tau_y + \mu \dot{\gamma} \qquad (2.2\text{-}5)$$

2.2.2.2 Yield Pseudoplastic Fluids

Generally most suspensions and slurries can be described as yield-pseudoplastic fluids; once the yield stress is exceeded the fluid can be expected to act similar to a non-yield stress shear thinning fluid, described previously, in section 2.2.1.2. Two of the more simple models that exist for yield pseudoplastic fluids are the Casson and Herschel-Bulkely model. Initially developed to describe the properties of printing inks but later shown to be suitable for some yield stress fluids, the Casson model is shown in Equation (2.2-6) (Casson 1959).

$$\sqrt{\tau} = \sqrt{\tau_y} + \sqrt{\mu\dot{\gamma}} \qquad (2.2\text{-}6)$$

The Herschel-Bulkley model (Herschel and Bulkley 1926a, 1926b) is a three parameter model that is quite similar to the power-law model previously described, section 2.2.1.2, with an additional yield stress term, τ_y, shown in Equation (2.2-7). The Herschel-Bulkley model is more widely used than the Casson model because the extra term increases the range of fluid behaviour that can be described by the model.

$$\tau = \tau_y + A\dot{\gamma}^{n} \qquad (2.2\text{-}7)$$

In the case of either the Casson or Herschel-Bulkley model the fluids yield stress must either be obtained from an experimental measurement, such as the vane method (Nguyen and Boger 1985), see section 3.2.2.5, or by extrapolation from measured rheological data; shear stress and shear rate (Kemblowski at al. 1988, Murdoch and Kearsey, 1960).

2.2.2.3 Yield Shear Thickening

Yield shear thickening behaviour is not common but as previously mentioned, over a certain range of shear rates, slurries and suspension depending on the properties of the solid particles and the suspending liquid can exhibit shear thickening behaviour. In the case of yield shear thickening behaviour, the Herschel-Bulkley model, Equation (2.2-7), previously outlined for yield-pseudoplastic fluids can be used to describe the

fluids rheological behaviour, except that pre-exponential parameter n must be greater than one.

SECTION B THE FLOW RHEOMETER

CHAPTER 3 RHEOLOGICAL INSTRUMENTATION

3.1 Introduction

The correct determination of the rheological properties of different fluids including suspensions and slurries is important to many research and industrial applications. To achieve this, the choice of the correct instrument for the application is essential, as many different methods and instruments exist for determining the rheological properties of fluids. Whatever the design of the instrument two essential components are required to correctly measure the rheological flow properties of a non-elastic fluid; these are an ability to apply a measured stress to the fluid and to measure the fluids response to the applied stress. Most common laboratory type instruments can be separated into two broad categories; rotational and tube type.

3.2 Standard Rotational Type Rheological Instruments

Of the two basic types of rheometers previously mentioned the rotational type is the most common and includes cones and plate, parallel plate, concentric cylinder and vane geometries. To achieve accurate rheological measurements steady laminar flow and no slip of the fluid at the surfaces of the geometry are required. A significant advantage of the rotational type rheometer is that only a small sample volume is usual required, which also means that control of temperature and pressure of the sample can be more readily achieved. Accuracy, reliability and easy of use make these instruments extremely common, though they are significantly more expensive than other types of rheometers (Steffe 1992, Van Wazer et al. 1963).

3.2.1 Plate Type

3.2.1.1 Parallel Plate

The parallel plate geometry consists of two parallel disks separated by a defined distance, with the space between two disks filled with the sample liquid, see Figure 3.2-1. One of the two discs rotates at a defined speed and the resistance of the fluid to the motion is recorded as a torque. It is also possible to apply a certain torque and measure the speed of rotation. The shear rate is not uniform across the radius of the geometry, with a significantly higher shear rate observed at the outer edge of the plate compared to the centre. Due to this difference an average shear rate must be determined and while this is a relatively simple task for a Newtonian fluids, errors in the calculations will increase with increasing non-Newtonian behaviour of the tested fluid. The shear stress and shear rate may be determined from the measured values of torque and rotational speed respectively as shown in Equation (3.2-1) and (3.2-2), where, M is the torque, Ω is the rotational speed, R is the radius of the plates and h is the gap width between the two plates.

$$\tau = \frac{3M}{2\pi R^3} \qquad (3.2\text{-}1)$$

$$\dot{\gamma} = \frac{\Omega R}{h} \qquad (3.2\text{-}2)$$

Measurements of slurries and suspensions with the parallel plate geometry can be affected by slip and settling particles.

Slip can occur when the gap width between the two shearing surfaces is small compared to the particle size (a gap to particle ratio of less than 10:1). Under these conditions the assumed boundary conditions that the velocity of the first layer of fluid equals that of the adjacent plate can become invalid. The effect of this phenomenon can to a certain extent be offset in the parallel plate geometry as the gap width can be varied.

The only direction of shear in the parallel plate geometry is rotational in the horizontal plane, there is no vertical shear and thus the settling rate of particles cannot be reduced. As particles settle a concentration gradient will develop lending to incorrect values of measured torque and incorrectly determined rheological properties (Steffe 1992, Van Wazer et al. 1963).

A further problem with the parallel plate geometry is that there is often quite a low upper limit on the shear rates that can be examined, particularly with low viscosity fluids that can be ejected from the geometry due to centripetal forces at higher values of shear rate.

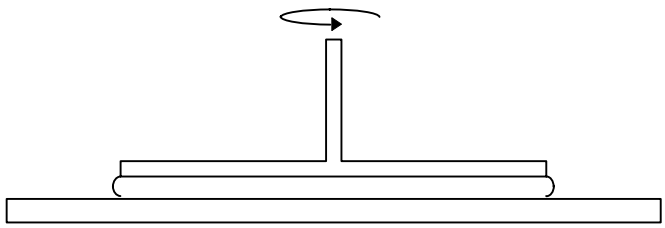

Figure 3.2-1 Parallel plate geometry

3.2.1.2 Cone and Plate

The cone and plate geometry is shown in Figure 3.2-2 and either the cone or the plate can rotate at a set speed and the resistance of the fluid to the motion, the torque, is measured. Due to the changing gap size with radius, the shear rate across the conical shaped gap can be considered constant, providing that the cone angle, α, is less than 3° (Van Wazer et al. 1963).

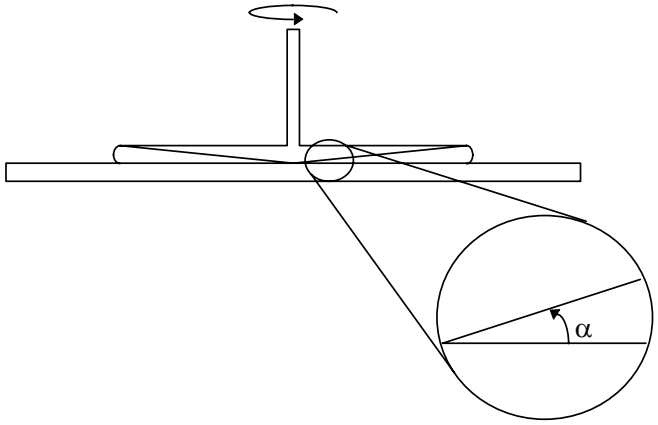

Figure 3.2-2 Cone and plate geometry

The calculations to determine the shear stress and shear rate require that the tip of the cone touch the plate, but because this is often impractical a truncated cone can be used instead. In a truncated cone a small portion of the tip of the cone is removed but the cone is positioned as if the cone was complete. The equations to determine the shear stress and shear rate are shown in Equation (3.2-3) and (3.2-4), where θ is related to the cone angle, α, ($\theta = \pi - \alpha/2$).

$$\tau = \left(\frac{3M}{2\pi R^3 \sin^2 \theta} \right) \tag{3.2-3}$$

$$\dot{\gamma} = \frac{\Omega}{\tan \alpha} \approx \frac{\Omega}{\alpha} \tag{3.2-4}$$

The small clearance between the cone (whether truncated or not) and the stationary plate means that particles can become easily trapped. Trapped particles significantly increase the measured resistance (the torque) and this can lead to significant errors in the calculated shear stress. Thus the size of particles in suspensions that can be measured with the cone and plate geometry is quite limited. Settling and slip may also affect the measurements from a cone and plate geometry, in the same way that the parallel plate geometry is affected and test samples can also be ejected from this geometry at higher rotational speeds (Steffe 1992, Van Wazer et al. 1963).

3.2.2 Concentric Cylinders

The concentric cylinder system, shown in Figure 3.2-3, consists of a bob or inner cylinder and a cup or outer cylinder, with the fluid placed in the annular region between the two cylinders. Usually the inner cylinder is rotated and the resistance of the fluid to the motion measured as a torque. It is however possible to rotate either cylinder, though in most practical applications it is significantly easier to rotate the inner cylinder.

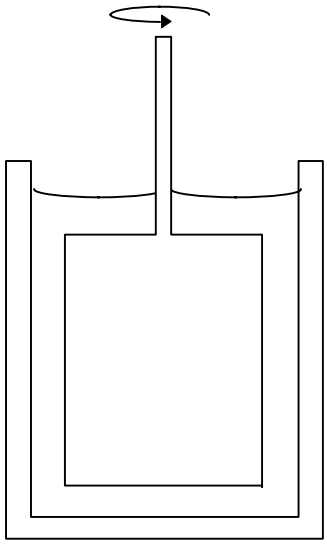

Figure 3.2-3 Concentric cylinder geometry

3.2.2.1 Shear Stress

For a concentric cylinder geometry, it is easier to calculate the shear stress compared to the shear rate, as the calculations are not dependent on the dimensions of the geometry or the rheological properties of the fluid being examined. Thus from the measured torque, the shear stress may be determined as shown in Equation (3.2-5), where κ represents the ratio between the radius of the two cylinders (inner/outer), L the length of the cylinders and R the radius of the outer cylinder.

$$\tau = \frac{M}{2\pi(\kappa R)^2 L} \tag{3.2-5}$$

3.2.2.2 Shear rate

The shear rate across the gap between the two cylinders in the concentric cylinder geometry is not constant for any type of fluid, but if a Newtonian fluid is examined then shear rate at the wall of the inner cylinder may be determined as follows.

$$\dot{\gamma} = \frac{2\Omega}{\left(1-\kappa^2\right)} \tag{3.2-6}$$

If a non-Newtonian fluid is examined in a small gap then the shear rate may be approximated using the Newtonian method, Equation (3.2-6).

When a wide gap is used to examine a non-Newtonian fluid other methods must be used to determine the correct shear rate. If a rheological model can accurately describe the rheological behaviour of the fluid over the shear rate range of interest then the shear rate may be determined directly. For the case of the power-law model the shear rate at the inner cylinder may be determined using Equation (3.2-7).

$$\dot{\gamma} = \frac{2\Omega}{\left(1-\kappa^{2/n}\right)n} \tag{3.2-7}$$

The parameter n may be obtained from the slope of a plot of the natural log of torque versus the natural log of rotational speed.

If the non-Newtonian behaviour of the fluid is unknown or cannot be described by a model then the Krieger and Maron method (Krieger and Maron 1953, 1954) may be used to determine the shear rate in a wide gap geometry where the radius ratio, κ is greater than 0.833.

$$\dot{\gamma} = \frac{2\Omega}{\left(1-\kappa^2\right)}\left[1 + k_1\left(\frac{1}{n'}+1\right) + k_2\left(\frac{1}{n'}+1\right)\right] \tag{3.2-8}$$

where:

$$k_1 = \left(1-\kappa^2\right)\frac{1+\left(\frac{2\ln\left(1/\kappa\right)}{3}\right)}{2} \tag{3.2-9}$$

$$k_2 = \left(1-\kappa^2\right)\frac{\ln\left(1/\kappa\right)}{6} \tag{3.2-10}$$

The parameter n' will depend on the rotational speed but it's value for a given rotational speed may be determined from the slope of a plot of the natural log of torque versus the natural log of rotational speed.

For larger gaps ($\kappa < 0.833$) Krieger (1968), proposed a more complex method of solution.

In the case of a yield stress fluid the presence of a plug or a region of zero shear must be determined so that the shear rate can be properly calculated. The presence of a plug may be determined using Equation (3.2-11), where τ_y is the yield stress and τ_b is the shear stress at the bob.

$$\kappa^2 \frac{\tau_b}{\tau_y} > 1 \qquad \text{(No Plug)} \tag{3.2-11}$$

If a plug is not present then the Krieger and Maron method described previously may be used to calculate the shear rate. However, if a plug is present then the shear rate may be determined in the same method as that of a bob rotating in an infinite medium as shown below.

$$\dot{\gamma} = \frac{2\Omega}{n'} \tag{3.2-12}$$

3.2.2.3 End Effects

The set of concentric cylinders shown in Figure 3.2-3 will be subject to end effects due to the design of the inner cylinder. In the calculations to determine the shear stress, Equation (3.2-5), it is assumed that the only shearing surface is the cylindrical wall of the bob and not the top or the base. As can be seen in Figure 3.2-3 additional liquid contact with the top and base will increase the value of the measured torque for a given rotational speed. This will lead to a higher determined value of shear stress for a given value of shear rate. One procedure to determine the extent of end effects in a concentric cylinder system involves measuring values of torque at different immersion depths of the bob for a given rotational speed. By extrapolating a graph of torque versus immersion depth an additional imaginary length may be determined. This additional length is assumed to account for the additional drag due to the ends of the bob and must be added to the length of the bob in the shear stress calculation, Equation (3.2-5) (Van Wazer et al. 1963). It is however, preferable to minimise end effects through modifications to the design of the bob and cup rather than continuously calibrating the equipment with different liquids. An example of a modified bob is shown in Figure 3.2-4, which is an automatic immersion depth type; the hollow at the base of the bob creates a pocket of air, which greatly reduces the drag on the base of the inner cylinder. The top of the bob also contains a hollowed region where any excess fluid in the cup can flow into, which leaves the liquid filled to exactly the correct depth. The only shearing surface is then the sidewall of the inner cylinder and the integrity of Equation (3.2-5) is preserved.

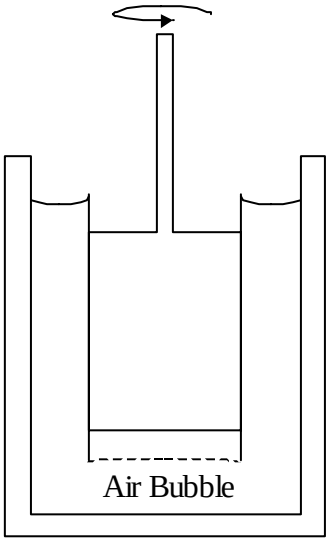

Figure 3.2-4 Automatic immersion depth concentric cylinder geometry

3.2.2.4 Particulate systems

The measurement of the rheological properties of suspensions or slurries in a concentric cylinder can be affected by slip and settling particles. Incorrect choice of the measurement geometry (a gap width that is too small) can lead to slip. However, this effect can be minimised through the correct choice of gap width and/or by employing ribbed walled cylinders. On the other hand settling cannot be slowed or prevented in a standard concentric cylinder geometry as there is no vertical shear under laminar flow conditions. Thus a concentration gradient will develop and lead to errors in any measurements performed under these conditions (Klein et al. 1995, Steffe 1992, Van Wazer et al. 1963).

A further problem that can occur when a small gap width concentric cylinder geometry is used to measure the properties of a slurry or suspension is particle bridging. As discussed in section 2.2.1.3 suspensions and slurries may, under certain shear conditions, exhibit shear thickening behaviour. It is suggested that the reason for this shear thickening behaviour is the formation of clusters of particles due to the shear in the geometry (Bender and Wagner 1996). It has been shown (Chow and

Zukoski 1995a and 1995b) that the onset of this shear thickening behaviour can be influenced by the gap width of the geometry in which the suspension is examined. Chow and Zukoski (1995a and 1995b) also showed that if the gap width of the geometry is particularly narrow then the clusters of particles that form can span the entire width of the gap and may become jammed. These jammed clusters of particles can cause abrupt shear thickening, which is referred to as particle bridging.

3.2.2.5 Vane Geometry

As outlined briefly above slip can cause measurement errors in a concentric cylinder system, especially when suspensions, slurries and yield stress fluids are examined. A vane geometry, shown in Figure 3.2-5, can be used to eliminate the problem of slip. The vane geometry however, cannot prevent particles settling and so it is generally restricted to those systems where particles either don't settle or settle very slowly. Like the bob in a concentric cylinder system the vane is rotated in a cup and the shear stress and shear rate determined from measurements of torque and rotational speed respectively. To analyses measurements from the vane geometry it is assumed that the fluid between the vane blades is not sheared and that the vane blades will describe a cylinder shape in the fluid with a radius equal to the width of a blade. In this case the system can be treated the same as a bob and cup geometry for the purpose of analysis (Barnes and Nguyen 2001). This assumption however, is only valid for very shear thinning fluids or yield stress fluids. It cannot be used with Newtonian fluids or low viscosity fluids where inertial effects become important. In the case of Newtonian fluid or low viscosity fluids the Couette flow lines can become distorted and at higher rotational speeds vortices can form behind the blade tips of the vane, which will lead to measurement errors (Barnes and Nguyen 2001).

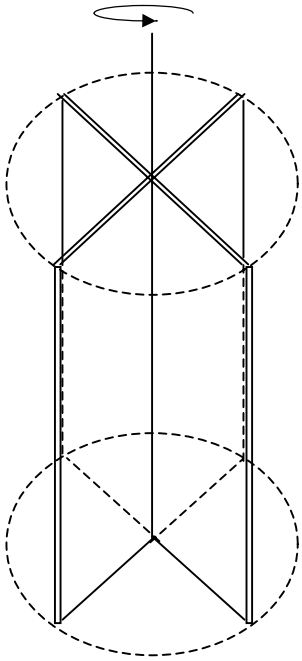

Figure 3.2-5 Schematic of a vane geometry

Another important use of the vane geometry is in the direct determination of the yield stress of a fluid. In the case of a direct yield stress measurement certain geometrical restrictions are placed on the dimensions of the vane and the cup so as to minimise end effects and wall effects. To perform a measurement the vane is typically rotated at speeds of 0.5 rpm or slower and the torque is recorded as a function of time. The torque curve will typically show a distinct peak or a plateau and this maximum value of the curve indicates the yield stress of the fluid (Nguyen and Boger 1985). The actual yield stress may then be determined from the maximum torque value, using Equation (3.2-13), where the parameter a is equal to 1/6 if the top of the vane is level with the top of the fluid or 1/3 if the vane is fully submerged to a depth of one vane diameter.

$$\tau = \frac{M}{\frac{\pi(2\kappa R)^3}{2}\left(\frac{L}{(\kappa R)} + a\right)} \qquad (3.2\text{-}13)$$

3.3 Generic Tube Type Rheometer

A tube rheometer is shown in Figure 3.3-1 and primarily consists of a pressurised reservoir and a capillary tube. Fluid is held in the reservoir and forced out through the tube under a certain pressure and the flow rate is recorded. Usually the tube is placed in a vertical position though measurements with horizontal tubes are possible.

Unlike the rotational type rheometers the tube rheometer is based on pipe flow, which means that it better represents the conditions found in actual industrial pipelines. Higher values of shear rate can also be achieved in a tube rheometer compared to a rotational type rheometer. These features make the tube rheometer much more suitable for pipeline design than rotational type geometries.

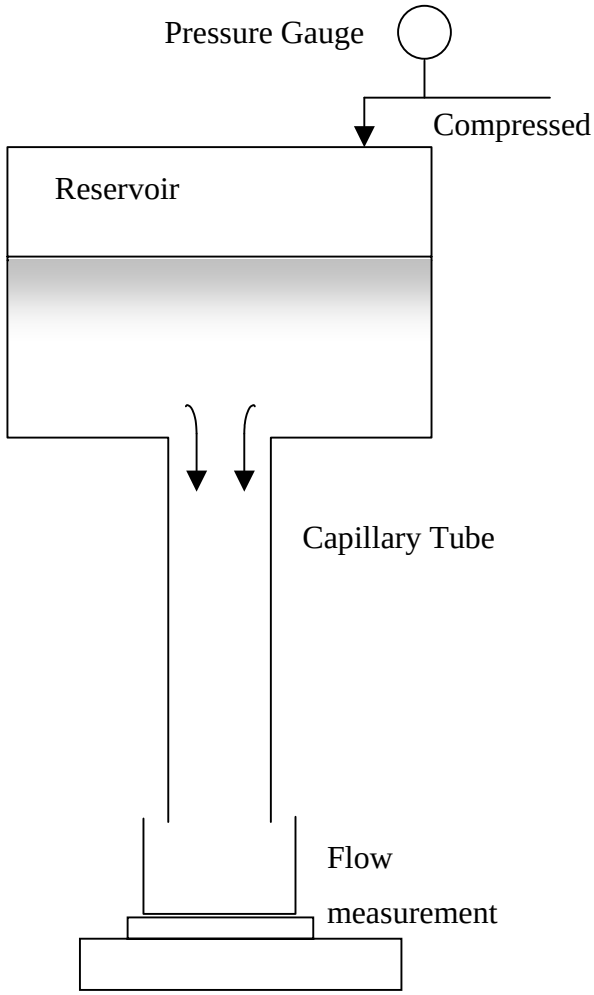

Figure 3.3-1 Schematic of a generic tube rheometer

The wall shear stress, τ_w, for any fluid may be determined from the pressure drop across the length of the tube, as in Equation (3.3-1), where D is the diameter of the tube, L is the tube length and Δp the pressure drop along the length of the tube. For the case of the tube rheometer used in this investigation, section 6.5 the pressure drop across the length of the tube was equal to the applied gauge pressure plus the head of liquid in the reservoir.

.

$$\tau_w = \frac{D(\Delta p)}{4L} \tag{3.3-1}$$

For a Newtonian fluid the wall shear rate may be determined using Equation (3.3-2), where Q is the volumetric flow rate of fluid out of the tube and the R is the tube radius.

$$\dot{\gamma}_w = \frac{4Q}{\pi R^3} \tag{3.3-2}$$

When non-Newtonian fluids are examined the shear rate is not constant across the tube width (Metzner 1956) and a correction to the Newtonian wall shear rate calculation is required. The true corrected wall shear rate may be determined using Equation (3.3-3) which is known as the Weissenberg-Rabinowitsch-Mooney equation (Rabinowitsch 1929) and is suitable for any type of fluid.

$$\dot{\gamma}_w = \left(\frac{3n'+1}{4n'}\right)\frac{4Q}{\pi\left(D/2\right)^3} \tag{3.3-3}$$

Where n’ may be determined from the slope of a plot of the natural logarithm of τ_w vs the natural logarithm of $4Q/\pi R^3$.

It is usual when determining the pressure drop across a tube rheometer to assume that the fluid has no (or a minimal) velocity when it exits the end of the tube. This assumption will not always be valid and under certain conditions can lead to

significant errors that are referred to as “kinetic effects” (Sarmiento et al. 1979). The observed pressure drop can be corrected as shown in Equation (3.3-4). Where Δp is the corrected differential pressure, Δp_{obs} is the observed value of differential pressure, ρ is density of the fluid under examination and α is the kinetic energy correction factor. The value of the correction factor α can vary with different types of fluids and the size of tube used, but it is generally assumed that α has a value of unity for Newtonian fluids (Van Wazer et al. 1963).

$$\Delta p = \Delta p_{obs} - \frac{\rho Q^2}{\alpha \pi^2 R^4} \tag{3.3-4}$$

End effects, which are the combination of entrance and exit effects, may influence the results from a tube rheometer. When the fluid enters the tube a certain length is required for a laminar flow profile to fully develop, but the shear stress and shear rate calculations described previously assume fully developed laminar flow along the entire length of the tube. However, if the tube is sufficiently long (length to diameter ratio greater than 200 (McKelvey et al. 1957)), then the additional pressure loss due to the fluid entering and exiting the pipe will be insignificant compared to the total pressure loss across the length of the tube and end effects may be ignored. If it is impractical to use long tubes then any end effects may be accounted for as follows. Values of pressure drop over the tube length at different L/R ratios and different flow rates are measured. Lines of constant flow rate are constructed on a graph of L/R versus pressure drop over the tube length. If the intercept of these lines on the x-axis (L/R) is zero, then end effects will have no impact on the results. However, if the intercept is negative then the absolute value of the intercept is equal to the additional length required to account for the entrance effects and must be added to the length term in the shear stress calculation, Equation (3.3-1) (Bagley 1957).

When suspensions, slurries or very viscous fluids are examined there is the possibility of wall effects influencing the measurements. Wall effects or slip occurs when the first fluid layer next to the tube wall no longer conforms to the zero velocity boundary condition. Particles in the fluids can often cause this phenomenon especially if their

diameter is large compared to the diameter of the tube. This effect can also sometimes be seen in viscous fluids at higher values of velocity.

Wall effects can also manifest in the form of particle migration, particularly shear induced particle migration, which is more common in highly concentrated suspensions and slurries (Allende and Kalyon 2000, Shauly et al. 1998, Sinton and Chow 1991). Particle migration is discussed in further detail in CHAPTER 9 but briefly, in concentrated suspensions the imperfect nature of particle collisions leads to the migration of the particles, generally towards the centre of the tube. This concentration gradient leads to an increase in the fluid velocity of the suspension near the wall, because of the reduced solids volume concentration. Particle migration can also occur in low solid concentration suspensions under a mechanism referred to as inertial effects (Segre and Silberberg 1962a, 1962b, Tehrani 1996). However, the effects of this migration on rheological measurements are less pronounced due to the lower initial solids concentration.

3.4 Rheological Instruments for Settling Slurries

The control of the rheology of settling suspensions is of great importance to the mineral processing industry, as it is a critical factor in optimising plant life cycle costs. However, many processes involve handling particles of diverse sizes, usually in the form of rapid settling (unstable) slurries and it is the slurry viscosity not the solids concentration that affects the energy consumption and many of the design factors of mineral processing units (Thomas et al. 1998). It is therefore essential that the rheological properties of these slurries be determined accurately under conditions that closely represent those conditions found in the actual industrial processes. A significant problem faced in the design of a suitable rheometer for settling slurries is that the slurries are typically heterogeneous and settling in nature. Many existing rheometers using standard geometries, such as cone and plate, parallel plate, bob and cup and capillary tube are not suitable for measuring the rheological properties of settling slurries, as they cannot prevent the particles from settling during experimental measurements. To illustrate the effect that settling solid particles in a slurry can have on rheological measurements from a concentric cylinder geometry, Figure 3.4-1 is

presented. The fly ash sample settles rapidly (0.017 cm/s, see Table 6.2-I) under the influence of gravity and under no circumstance can a stable torque reading be obtained. The final flattening of the curves represents the final settled position of the particles and does not represent the true rheological properties of the slurry. Examination of the sample at the end of the test confirmed that the sample had settled during the test and thus it is extremely unlikely that the results are due to a thixotropic behaviour of the slurry.

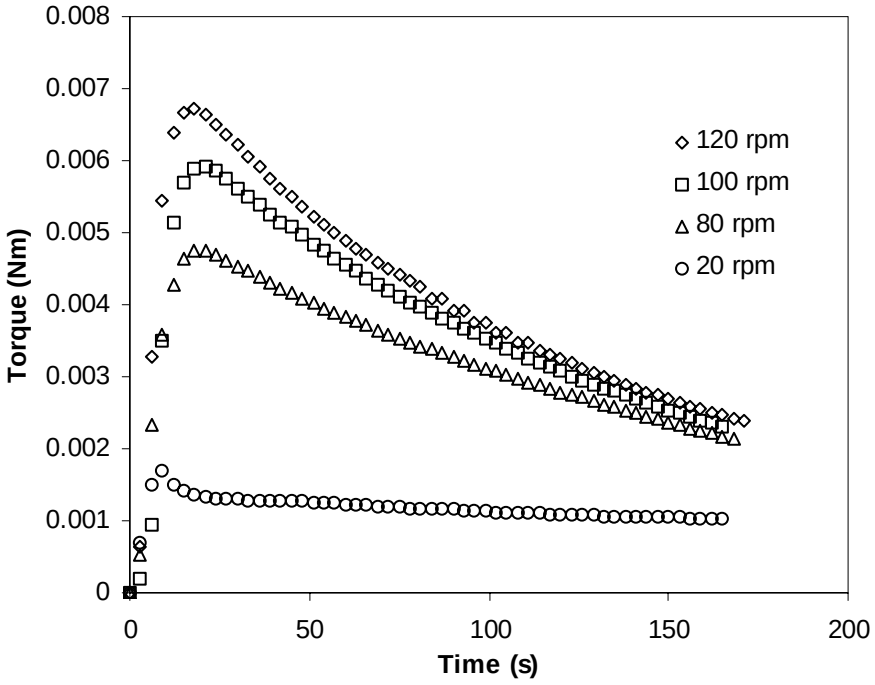

Figure 3.4-1 Rheological measurements of a fly ash slurry using a standard bob and cup geometry

3.4.1 The Impeller Geometry

One option, which can be extremely effective, providing the correct operating conditions are maintained, is to use an impeller to maintain homogenous conditions (Kassim and Killick 1996). However, the procedure to determine the rheological properties of a slurry or suspension from an impeller-based geometry is extremely complex. Typically the torque required to turn the impeller, usually a Rushton turbine or marine impeller, at a certain speed is measured. Once the rotational speed and

torque are measured it is necessary to solve the equations of motion for the impeller geometry. However, the mathematics needed to define such a system are very complex and make numerical solutions extremely difficult (to impossible) to develop, especially for non-Newtonian slurries. To avoid solving the equations of motion for the impeller geometry calibration procedures are required either by using standard Newtonian liquids of known viscosities or by employing an average mixing shear rate method for non-Newtonian liquids (Metzner and Otto 1957, Metzner and Taylor 1960). Thus, while numerous data sets and correlation procedures have been reported in the literature for mixing tank systems, in general they are highly empirical and system-specific (Calderbank and Moo-Young 1959, 1961) and thus errors in these correlations can be quite significant. As an example, experimental work by Calderbank and Moo-Young (1959), produced results for a variety of different fluids with errors as high as 20%.

A more complex method of solution was proposed for a helical screw impeller (Chavan and Ulbrecht 1972, Kemblowski et al. 1988, Valverde et al. 1997). Instead of calibrating the impeller system an effective radius (equivalent to a bob and cup geometry) was determined. With this effective radius, the measured torque and rotational speed were used to determine the shear stress and shear rate using bob and cup calculations. Kemblowski et al. (1988) tested various fluids in an instrument consisting of a helical screw impeller in a draft tube. The results while more accurate than those of Calderbank and Moo-Young, still showed significant errors of 10-15%.

To maintain a homogeneous mixture of solid particles in the liquid medium it is often necessary to maintain highly turbulent conditions within the mixing vessel (Shi and Napier-Munn 1996, Warren 1975). Results are therefore generated and analysed under turbulent flow conditions, which can lead to considerable errors.

Thus, in conclusion regardless of the calibration procedures performed the impeller viscometer is fundamentally imperfect, as the equations of motion for the geometry cannot be solved. Until this situation can be rectified other geometries and methods must be employed to measure the rheological properties of settling slurries under homogeneous conditions.

3.4.2 Modified Coaxial-Cylinders

To avoid the complications associated with using mixing impellers as rheometers, simpler geometries must be used. However, they must be suitably modified so that homogenous conditions in a slurry can be maintained during rheological measurements. The concentric cylinder viscometers used in its standard form is obviously not capable of maintaining homogenous conditions. However, in situations where the particle settling rate is known, it is possible to design a concentric cylinder viscometer where the shearing surface is only in the hindered settling zone, see Figure 3.4-2. By measuring only in the hindered settling zone the solids concentration is known and should remain relatively constant. Such a device was designed and tested by Klein et al. (1995), who demonstrated good reproducibility for results with coal-water slurries although there was no comparison of the results with measurements on other instruments. This design however, is unlikely to be suitable for characterising slurries in which the particles settle rapidly as a zone of known concentration may only exist for a few seconds if particularly rapid settling materials are examined.

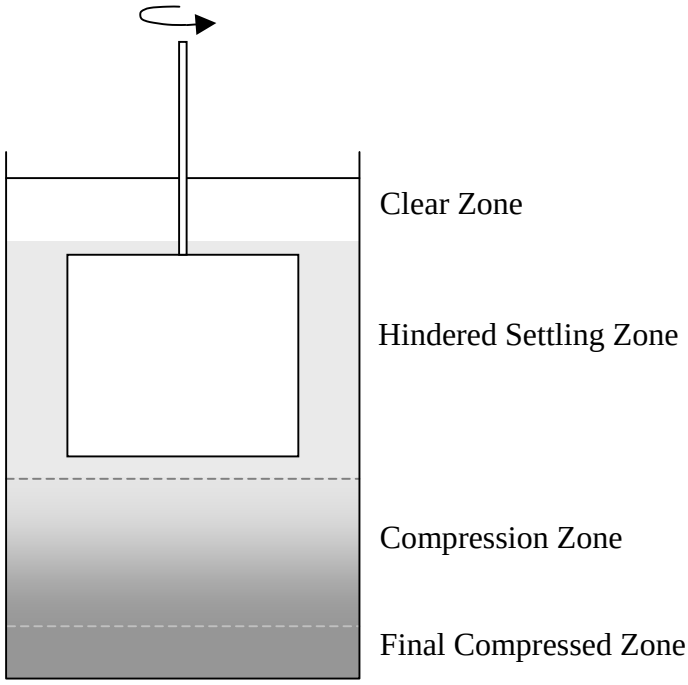

Figure 3.4-2 Modified concentric cylinder geometry, with the bob in the hindered settling zone

Another development based on the concentric cylinder geometry, proposed by Reneham et al. (1987), was to place a set of concentric cylinders in a concrete mixing bowl, which when rotated would keep the slurry particles suspended, see Figure 3.4-3. The flow patterns however, within the rotating mixing bowl, especially when the bowl is rotated at higher rotational speeds, which are often required to keep the particles suspended, are more complex than those present in standard Couette flow. These complex flow patterns will alter the Couette flow between the concentric cylinders and thus the total shear rate experienced by the fluid will be greater than that due to the rotation of the inner cylinder alone. The change in the total shear rate between the concentric cylinders is however, extremely difficult to quantify, but this difference will affect the results of non-Newtonian fluids, as the rheological properties of these fluids are dependent on the shear rate. The design of the instrument is such, that end effects may also reduce the accuracy of the torque measurements, due to measurement fluid coming into contact with the ends of the rotating cylinder.

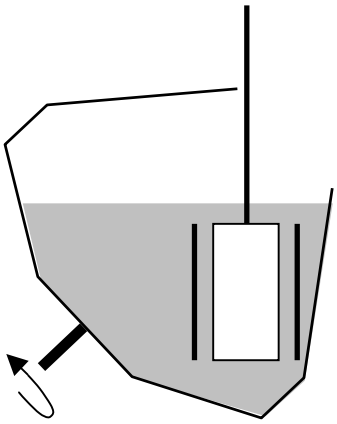

Figure 3.4-3 Concentric Cylinder – Bob in a mixing vessel

3.4.3 Addition of Axial Flow to Concentric Cylinder Geometries

The concentric cylinder system is inherently unable to accurately measure the properties of settling slurries because there is no shear in the vertical or axial direction and thus particle settling cannot be slowed. The addition of an axial flow to the concentric cylinder system would overcome this inherent deficiency and prevent the particles from settling. Various technique and instruments have been developed to impose axial flow in a concentric cylinder system and their design and effectiveness are discussed below.

3.4.3.1 Shielded Mixing Impeller

One option by which axial flow may be imposed on a Couette system is to use a mixing impeller and a series of baffles and plates to direct the flow of the circulating liquid so as to provide adequate mixing of a slurry. A series of experimental apparatus were designed and constructed by Clarke (1967), Purghit and Roy (1965) and Saraf and Khullar (1975). Figure 3.4-4 presents schematic of the instrument, which was used by all three research groups.

A six-baffle tank was used to prevent excess turbulence. A marine impeller was fixed a short distance off the base to maintain homogeneous conditions. To prevent a vortex forming a disc was attached to the baffles and used to shield the bob from the impeller. A second smaller tube, the cup, was placed inside the baffled tank above the impeller and shielding disk. Careful design of the tank and impeller meant that the test suspensions circulated up along the baffles and down through the smaller tube. Good mixing was obtained in the tank with a minimal (± 5%) variation in the solids concentration throughout the tank (Saraf and Khullar 1975). In one instance a Brookfield disc was placed inside the smaller inner tube (Saraf and Khullar 1975), in other cases a more standard concentric cylinder bob was used (Clarke 1967, Purghit and Roy 1965).

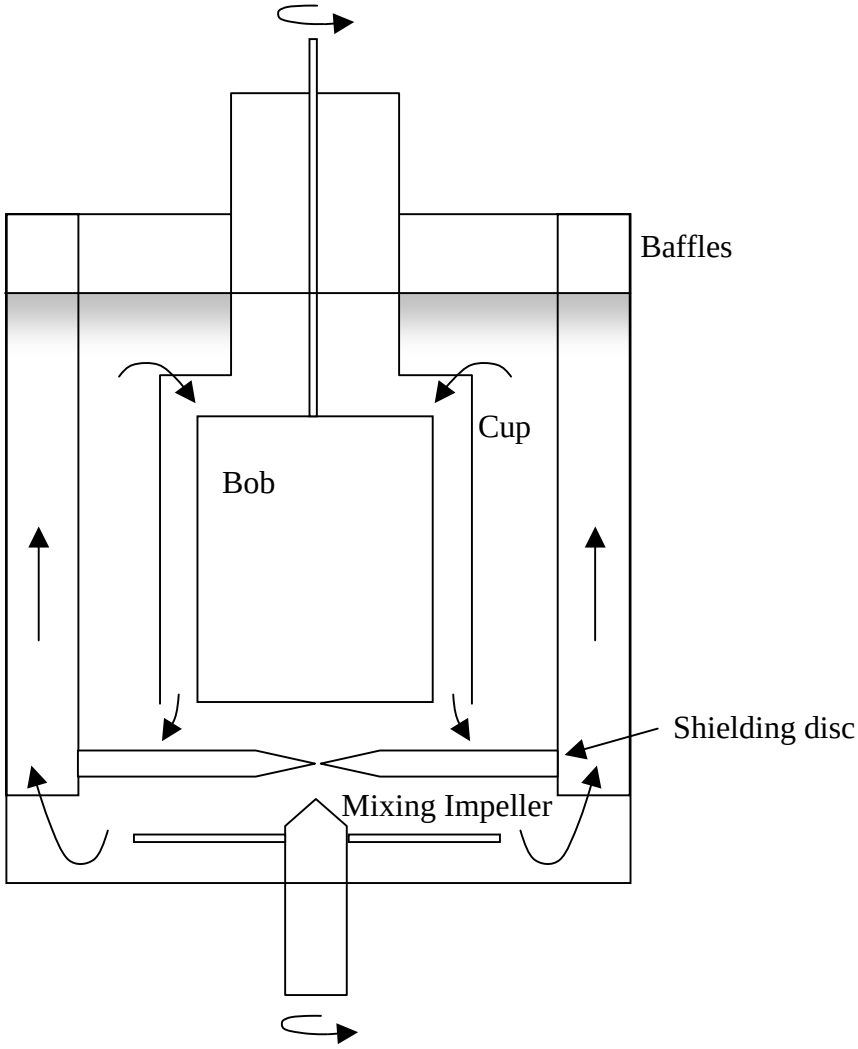

Figure 3.4-4 Concentric Cylinder – with shielded mixing impeller

For the Brookfield system (Saraf and Khullar 1975) the viscosity was only determined at one rotational speed. No tests were performed with standard materials or the experimental results compared with measurements on other instruments. The effect of the fluid circulation on the total shear rate was also not discussed or accounted for.

For the case of the concentric cylinder arrangement (Clarke 1967, Purghit and Roy 1965) the bob was attached to a Ferranti portable viscometer, which was used to rotate the bob and measure the torque. Purghit and Roy (1965) and Clarke (1967) obtained good agreement with Newtonian calibration liquids. However, this is to be

expected, as the viscosity of the fluid is independent of changes in the shear rate due to the circulation of the fluid. Unfortunately other results generated by Purghit and Roy (1965) for several slurries appear to have been obtained in the presence of Taylor vortices. The vortices were made visible by the presence of the solid particles in the liquid. Whether or not the Newtonian results were obtained under the same condition cannot be determined, but the presence of Taylor vortices in some of the results affects the accuracy of the measurements. It is also probable that results generated by Clarke (1967) were also obtained in the presence of Taylor vortices, as the results of Clarke (1967) show dilatant behaviour in all the suspensions examined with solid volume concentrations greater than 10%. While this result is possible, given that the results of Purghit and Roy (1965) were obtained under Taylor vortex flow and Taylor vortex flow is known to cause an increase in measured torque values, see section 11.3.1, it must be concluded that the results from Clarke's experimental work may have also been obtained under Taylor vortex flow conditions.

While this system has been shown to provide adequate mixing of the slurry and thus maintain the particles in a homogeneous suspension the axial flow rate cannot be readily determined. This makes the determination of the total shear rate very difficult and although this will not affect the measurements of Newtonian fluids because the rheological properties are independent of the shear rate, the rheological properties of complex non-Newtonian fluids cannot be reliably determined.

3.4.3.2 External Axial Flow Source

The inability to measure the flow rate in the mixing impeller system described previously may be overcome by the use of an external axial flow source instead of the mixing impeller. Various researches Bhattacharya et al. (1990), Blaszczyk and Petela (1986), Ferrini et al. (1979), Reeves (1985) and Shi and Napier-Munn (1996) all used similar helical flow rheometers to measure the properties of settling suspensions. Helical flow is the combination of axial and Couette flow. A schematic of the instrument used by Ferrini et al. (1979) is shown in Figure 3.4-5. The instruments used by Bhattacharya et al. (1990), Blaszczyk and Petela (1986), Reeves (1985) and Shi and Napier-Munn (1996) were all similar in design, with rotating inner cylinders and axial flow in a downwards direction, the only difference being the type of pumps

used to generate the axial flow. However, although pumps were used in the instruments to aid in the fluid circulation, the actual external force used to generate the downward axial flow was provided by gravity alone.

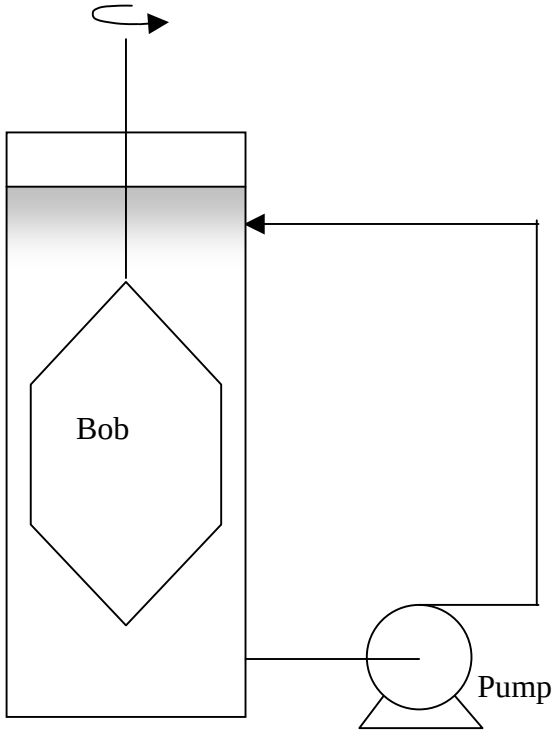

Figure 3.4-5 Schematic of a concentric cylinder geometry, with an external pumping source

Ferrini et al. (1979) recognised that the axial flow component would affect the total shear in the system, but chose to calibrate with standard fluids rather than calculate the actual total shear rate. Few results were compared between measurements with the helical flow rheometer and other standard instruments but errors of approximately 10% were observed. The instrument used by Blaszczyk and Petela (1986) used only a small axial flow rate and thus the effects on the total shear rate were ignored in the calculations, resulting in errors of about 7%. The instrument used by Reeves (1985) differed from the previous two in that baffles were placed around the inside wall of the outer cylinder. A calibration with standard Newtonian fluids was performed, instead of trying to correctly determine the shear rate in the system. The large gap width between the inner and outer cylinders promoted turbulence within the instrument and this is thought to have affected the results, especially those results

where suspensions showed shear thickening behaviour (Shi and Napier-Munn 1996). The rheometer used by Shi and Napier-Munn (1996), was similar to that used by Reeves (1985), including the baffles around the outer cylinder. Complex calculations and correction factors were employed to account for the turbulent conditions and the resulting additional torque that would be measured by the instrument under these conditions. The procedure appeared to be quite successful for the several ideal fluids tested, but the turbulence correction method used is not very suitable, as it appears to depend on the rheological properties of the fluid, which is usually unknown at the time of testing.

The device employed by Bhattacharya et al. (1990), used an external screw in a draft tube to lift the slurry above the concentric cylinders. It again relied on the force of gravity to generate the fluid flow between the cylinders. However, the instrument was designed with a narrow gap geometry, which limited its use to the measurement of slurries with small particle sizes. A narrow gap assumption was also used in the calculation procedure. Good results were obtained with a Newtonian fluid but for shear thinning fluids at higher values of axial flow rate a certain amount of error in the results was apparent.

3.4.3.3 Helical Flow Instruments

Albert et al. (1966) developed a helical flow instrument, with axial flow in an upward direction. The design of the instrument was such that the outer cylinder was rotated instead of the inner one. The analysis was quite unusual in that no attempt was made to measure the drag on either cylinder, instead the pressure drop across the length of the cylinders was measured. A comparison of results between computed and experimentally determined angular velocities showed excellent agreement. Despite the fact this instrument was not tested with slurry materials it does show that experimental results from helical flow could be matched to theoretical predictions.

Nguyen et al. (2000) reported on the development of a rheometer, for settling slurries based on the principles of helical flow, where, unlike most of the previously mentioned instruments and measurement procedures the contributions made by the axial flow component were included in the calculations to determine the fluid's

rheological properties. Thus for this instrument no calibration procedures were required and the rheological properties could be determined absolutely. Figure 3.4-6 shows the experimental system, with a detailed schematic of the instrument shown in Figure 3.4-7. The axial flow in the instrument is provided by an external pump, with the direction of flow upwards through the concentric cylinders.

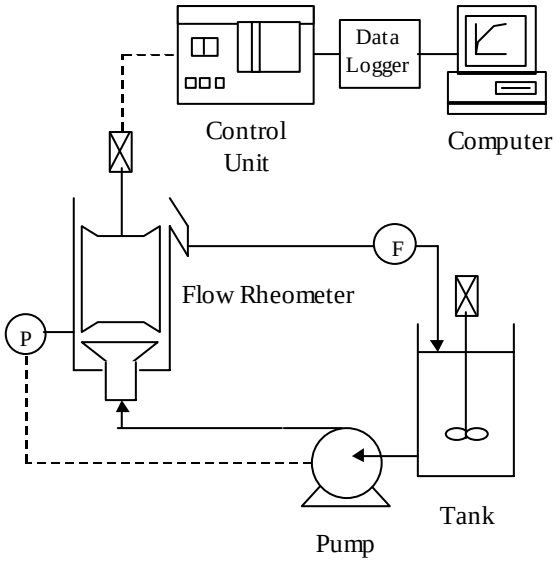

Figure 3.4-6 Complete experimental system for a helical flow rheometer

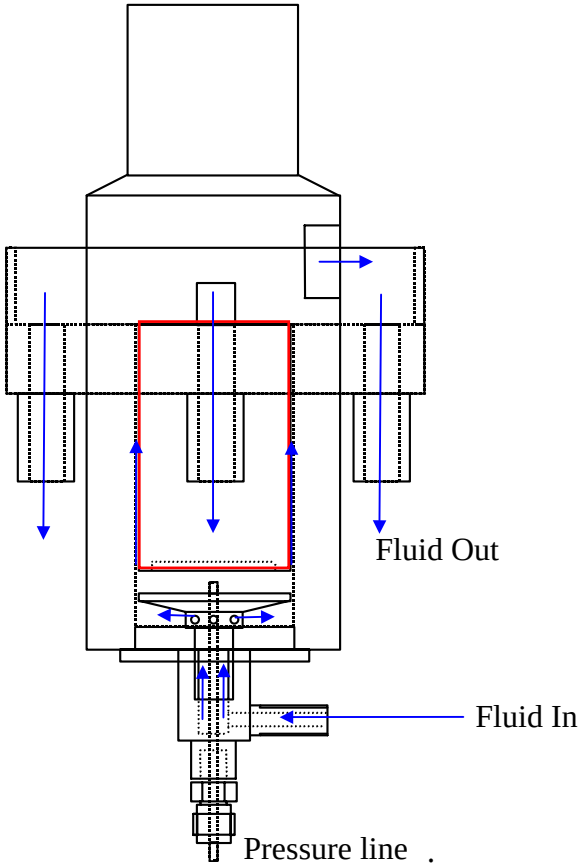

Figure 3.4-7 Schematic of a helical flow rheometer

The data analysis procedure proposed by Nguyen et al. (2000), assumed a narrow gap between the cylinders and while this assumption may be valid for an instrument that is used to test viscous ideal solutions, mineral slurries often contain many large diameter particles. It is often assumed, as a rule of thumb, that a gap width of ten times the largest particle diameter is required within an instrument to minimise wall effects (Barnes 1995). However, it was later shown by Barnes (2000) that the gap width required to minimise wall effects is dependent on the solid phase volume fraction and that gap widths much greater than ten can often be required for high volume fraction slurries and suspensions. Thus the presence of large particles in mineral slurries means that a narrow gap assumption cannot be reliably used.

3.4.4 Modified Tube Rheometers

A tube style rheometer offers another possibility for measuring the properties of settling slurries if suitably modified for the purpose. Thomas et al. (1998) presented a rheometer that consisted of an inverted U-tube connected to a process stream via a control valve. The pressure drop over the length of the tube was measured for a given flow rate, which was set using a control valve, and from this the shear stress and shear rate were determined. However, the u-bend section in the geometry caused some complications in the analysis of the data, especially for non-Newtonian fluids. Minimal comparison work with standard fluids and other instruments was performed, though promising results were presented for Newtonian fluids.

A more conventional straight tube rheometer was proposed by Kawatra et al. (1999). In this instrument a sample stream is removed from a main process stream, the sample stream then flows through a capillary tube across which the pressure drop and flow rate are measured. A complex arrangement of pressurised vessels is used to control the sample flow rate through the tube, though a conventional data analysis procedure can be used because of the straight tube. Reasonably good agreement was observed between this modified tube rheometer and other laboratory instruments, though a minimal amount of comparative results were reported. This instrument is also more susceptible to particle settling because the measurement tube is horizontal rather than vertical.

3.4.5 Other Instruments

3.4.5.1 A vibrating sphere and concentric cylinder geometry

A device for settling slurries was proposed by Kawatra and Bakshi (1996), which incorporated a rotational viscometer and a vibrating sphere viscometer. Using two different geometries in combination extended the operating shear rate range of the instrument; with the vibrating sphere operating in a higher shear rate range, while the rotating Brookfield portion of the instrument covered the lower region of the measurement range.

The rotational component of the device was extremely similar to the systems proposed by Blaszczyk and Petela (1986), Ferrini et al. (1979), Reeves (1985) and Shi and Napier-Munn (1996), in that an external pump was used to transport the experimental fluid above the geometry and the fluid allowed to flow through the system under the influence of gravity. But also like these previous instruments the results were compromised because the additional shear rate due to the axial flow was not properly accounted for in the analysis procedure.

In the vibrating sphere section of the instrument the fluid was pumped directly into the tank containing the vibrating sphere and allowed to return to the main storage tank via gravity. The main advantage of the vibrating sphere as a rheometer for slurries is that it can operate within an unspecified gap width and as such the gap width between the sphere and the wall of the surrounding vessel can be made sufficiently large so as to minimise particle related problems. One significant problem with the vibrating sphere is that it is sensitive to external vibrations and thus requires good damping. However, mineral-processing plants can be subject to significant amounts of vibrations, which could affect measurements from the vibrating sphere. Another significant problem with the vibrating sphere is that it is very difficult to determine the actual operating shear rate and thus the rheological properties of non-Newtonian slurries cannot be accurately determined (Kawatra and Bakshi 1995).

Good agreement was observed internally between both components of the system for measurements with Newtonian fluids and reasonable differences were observed when shear thinning fluids were examined. The difference in results for shear thinning fluids is expected because the operating shear rate range of the two components is different. However, the results were not compared with results from other rheological instruments and so while it is accepted that the instrument can detect non-Newtonian abehaviour, whether it can accurately characterise this behaviour is unknown.

3.4.5.2 Modified Parallel Plate

Vlachou and Piau (2000) designed a modified parallel plate geometry to measure the properties of cement slurries. The geometry consisted of three rotating plates with

four stationary plates, which were placed top and bottom and in between each rotating plate. Each plate whether stationary or rotating had a series of openings cut out of it, see Figure 3.4-8 below. The holes served two purposes, to allow particles to settle and to provide surface roughness to reduce slip. Results from experiments with Newtonian calibration fluids showed errors of 8-17% for a wide range of shear rates. For settling materials the rate of settling must be known so the device can be placed in the zone of constant solids concentration. Experiments with settling slurries showed that the geometry could measure the properties of the slurries without the results being adversely affected by settling particles. However, the results from the modified geometry were consistently higher than those recorded in a standard parallel plate geometry before the settling nature of the slurries affected the parallel plate results. Like the modified concentric cylinder device designed by Klien et al. (1995), discussed previous in section 3.4.2, this design is unlikely to be suitable for characterising rapid settling slurries.

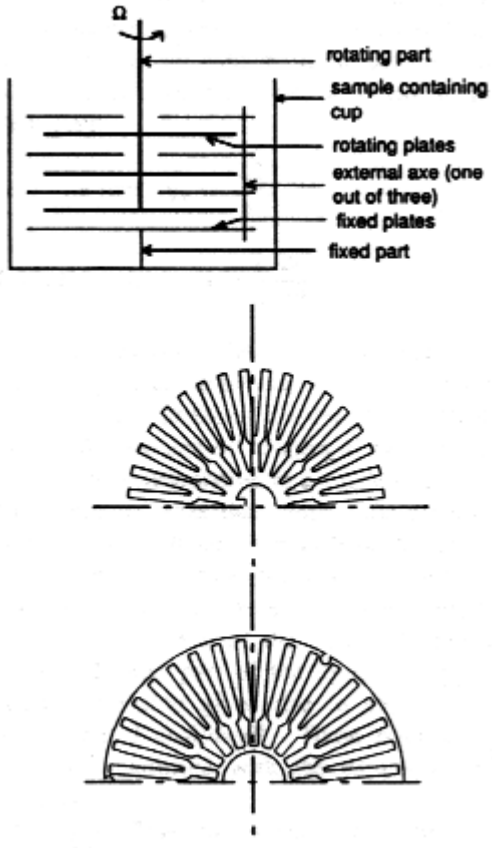

Figure 3.4-8 Schematic of the modified parallel plate geometry proposed by Vlachou and Piau (2000).

3.5 Statement of Purpose

To correctly examine the rheological properties of settling slurries it is critical that homogeneous conditions are maintained within the measuring instrument. However, this criterion cannot be satisfied by most standard rheological equipment and so while the concentric cylinder geometry has many positive features that make it highly desirable, in its standard form it cannot prevent particles settling. A lot of research has been focused on modifying Couette geometries to make them more suitable for the measurement of settling slurries. The majority of these modifications involve the addition of an axial flow to the system to create helical flow. However, most measurement and analysis procedures then ignore the contributions made to the total shear by the axial flow component or merely rely on calibration procedures to account for the additional shear. Thus the proposal for this research is to develop an instrument that is capable of measuring the absolute properties of settling mineral suspensions without the need for complex calibration procedures. Particular emphasis will be placed on developing the correct method of data analysis for helical flow especially for wide gap geometries and non-Newtonian fluids. The design of the instrument is also important and consideration must be given to its ultimate purpose, which is to measure the properties of settling slurries. The instrument must therefore be designed, such as to minimise areas of slow flow where particle settling may occur and cause erroneous measurement errors and/or unexpected equipment failure due to blockages.

CHAPTER 4 THEORY AND ANALYSIS OF LAMINAR HELICAL FLOW

4.1 Introduction

Many laboratory rheometers utilise a rotational type Couette geometry, the advantage of such an instrument is the need for smaller sample volumes than some other rheometers and also accurate measurements of torque and rotational speed, from which shear stress and shear rate are determined. However, when settling suspensions are measured the direction of fluid motion is perpendicular to the direction that the particles settle and so there is no applied force to reduce the settling rate of the particles. As discussed in CHAPTER 3 the most suitable design for a rheological instrument to measure the properties of settling slurries is based on helical flow (which is the addition of Couette and axial flow). However, in almost all previous studies (discussed in CHAPTER 3) a proper complete analysis procedure for helical flow was not developed. In this chapter a correct analysis procedure for helical flow is developed, particularly for non-Newtonian fluids in wide gap geometries.

4.2 Summary of Variables

A schematic representation of helical flow is presented in Figure 4.2-1 below using cylindrical coordinates (r,z,θ). The liquid flows between the two concentric cylinders, where the inner radius of the outer cylinder is defined as, R and the outer radius of the inner cylinder as a fraction of, R, κR. Either or both cylinders may rotate in either direction, though in the example presented below, only the inner cylinder rotates clockwise with an angular velocity Ω. The rotational motion of the cylinders imparts a rotational flow on the fluid, ω, which is a function of the radial position, r. A differential pressure (not shown), $\partial p/\partial z$ is applied across the length of the cylinders, L, which imparts an axial velocity on the fluid, u, which is also function of the radial position, r.

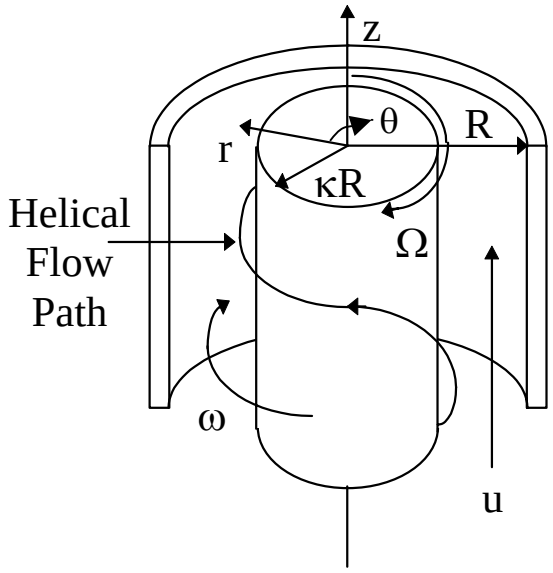

Figure 4.2-1 Schematic of Helical flow

4.3 Rheological Measurements from Helical Flow

Under helical flow conditions a non-uniform shear rate is known to exist across the gap between the two concentric cylinders. The system however can be solved for a Newtonian fluid, but further complexities are introduced when non-Newtonian fluids are examined. A number of theoretical investigations of this type of flow have been performed (Coleman and Noll 1959, Rivlin 1956), but the results from these investigations did not lead to a full solution to the problem for the case of non-Newtonian fluids. Thus the problem of solving the equations of motion for helical flow may only be solved exactly for simple fluid models (Dierckes and Schowalter 1966, Dostál et al. 1993, Rea and Schowalter 1967). However, some simplifications can be made to develop a solution for more complex fluids under certain conditions. If the gap width between the cylinders is very small then the curvature of the cylinders may be ignored and the system may be considered as channel flow with a moving wall (Chiera et al. 1992, Garcia-Ramirez and Isayev 1992, Tanner 1963a, 1963b).

One reason for the difficulty of solution for non-Newtonian fluids is the interaction between the axial flow and the Couette flow. It has been theoretically predicted and proven experimentally that for a shear thinning “power-law” fluid the speed of rotation of the inner cylinder can affect the flow rate through the annulus for a given value of differential pressure. That is for a given constant pressure drop over the cylinder the flow rate will increase with an increase in the speed of rotation of the inner cylinder (Dostál et al. 1993).

In the following sections of this chapter an analysis procedure will be developed to solve the helical flow system for non-Newtonian fluids, so that a fluids rheological properties can be determined from measurements of rotational speed, torque, pressure drop and flow rate from a helical flow system.

4.4 Theory of Analysis

Consider the helical flow between two concentric cylinders as shown in Figure 4.2-1. The inner cylinder of radius, κR, is rotating at a constant angular velocity, Ω, under an applied torque, M. The outer cylinder of radius, R, is stationary. The fluid flow in the axial direction is caused by a pressure gradient, ($\partial p/\partial z$). The velocity of a particle of fluid in cylindrical co-ordinates {r, z, θ} in the annulus may be described by Equation (4.4-1).

$$v = \{v_r, v_z, v_\theta\} = \{0, u(r), r\omega(r)\} \quad (4.4\text{-}1)$$

The axial and tangential components of the fluid velocity u and ω respectively are assumed to be a function only of the radial position, r. Thus the boundary conditions associated with the flow are as follows:

$$u(\kappa R) = 0; \qquad \omega(\kappa R) = \Omega \quad (4.4\text{-}2)$$

$$u(R) = 0; \qquad \omega(R) = 0 \quad (4.4\text{-}3)$$

It is assumed that the rheological behaviour of the fluid can be described by a unique relationship between the total shear stress and the total shear rate as shown in Equation (4.4-4).

$$\tau = f(\dot{\gamma}) \quad (4.4\text{-}4)$$

The aim is therefore to determine the shear stress and shear rate from the measured variables from which a function describing the rheological behaviour of the fluid can be determined.

4.4.1 Determining the Shear Stress

From the theory of helical flow by Coleman and Noll (1959) and from further developments by Huilgol (1990), it follows that the total shear stress experienced by the fluid consists of an axial component and a tangential component. The total stress tensor of the fluid consists of nine components in cylindrical co-ordinates. It can be shown (Huilgol 1990) that the only two non-zero tensors are τ_{rz}, the axial component and $\tau_{r\theta}$, the rotational component. Thus the total shear stress may be determined as follows.

$$\tau = \sqrt{\tau_{rz}^2 + \tau_{r\theta}^2} \tag{4.4-5}$$

where:

$$\tau_{rz} = \frac{b}{r} - \left(-\frac{\partial p}{\partial z} + \rho g \right) \frac{r}{2} \tag{4.4-6}$$

$$\tau_{r\theta} = \frac{M}{2\pi r^2 L} \tag{4.4-7}$$

Equation (4.4-6) may be simplified as follows

$$\tau_{rz} = \frac{b}{\kappa R} - \frac{c(\kappa R)}{2} \tag{4.4-8}$$

where:

$$c = -\frac{\partial p}{\partial z} + \rho g \tag{4.4-9}$$

The parameter b is a constant of integration that appears when Equation (4.4-10) is integrated to yield Equation (4.4-6) and physically represents the radial location of the peak in the axial velocity profile.

$$\frac{\partial p}{\partial z}+\frac{\partial \tau_{rz}}{\partial r}+\frac{\tau_{rz}}{r}-\rho g=0 \qquad (4.4\text{-}10)$$

The axial flow component of the shear stress must be solved, but to do so requires parameter b. Examination of the physical nature of the system indicates that b must lie somewhere between the outer boundaries of the system in this case the inner and outer walls of the concentric cylinders and so the following equation must be satisfied.

$$\left(-\frac{\partial p}{\partial z}+\rho g\right)\frac{R^2}{2}<b<\left(-\frac{\partial p}{\partial z}+\rho g\right)\frac{(\kappa R)^2}{2} \qquad (4.4\text{-}11)$$

The helical flow system, as previously mentioned can be solved for a Newtonian fluid and as such, b can be directly determined for a Newtonian fluid (Huilgol 1990) as shown in Equation (4.4-12).

$$b=\frac{1}{4}\left(-\frac{\partial p}{\partial z}+\rho g\right)\frac{R^2-(\kappa R)^2}{\ln\left(\frac{R}{\kappa R}\right)} \qquad (4.4\text{-}12)$$

If a non-Newtonian fluid is examined under narrow gap conditions then the variation in possible radial positions for the parameter b are limited and thus the following approximation, Equation (4.4-13), may be made to determine the value of b.

$$b\approx\frac{3}{10}\left(-\frac{\partial p}{\partial z}+\rho g\right)\frac{R^5-(\kappa R)^5}{R^3-(\kappa R)^3} \qquad (4.4\text{-}13)$$

The situation where a non-Newtonian fluid is flowing in a wide gap geometry will be discussed in further detail, section 4.4.5.

4.4.2 Determining the Shear Rate

Similar to the total shear stress the total shear rate is a function of only two tensor components, $\dot{\gamma}_{rz}$, the axial component and $\dot{\gamma}_{r\theta}$, the rotational component and thus the total shear rate may be determined as follows.

$$\dot{\gamma} = \sqrt{\dot{\gamma}_{rz}^2 + \dot{\gamma}_{r\theta}^2} \tag{4.4-14}$$

where:

$$\dot{\gamma}_{rz} = -\frac{du}{dr} = -u'(r) \tag{4.4-15}$$

$$\dot{\gamma}_{r\theta} = -r\frac{d\omega}{dr} = -r\omega'(r) \tag{4.4-16}$$

To determine the shear rate the velocity profile of both the axial and rotational components of the flow must be known. However, without a PIV (Particle Imaging Velocimetry) system or some other form of velocity measuring device this cannot be achieved.

4.4.3 Determining the Rheological Properties without determining the Shear Rate

By using the boundary conditions defined in Equation (4.4-2) and Equation (4.4-3) the equations of motion can be partially solved and the following relationships developed (Huilgol 1990).

$$\int_{\kappa R}^{R} \phi(\tau)\left[\frac{b}{r} - \frac{cr}{2}\right]dr = 0 \tag{4.4-17}$$

$$\int_{\kappa R}^{R} \phi(\tau)\frac{M}{2\pi r^3 L}\,dr = \Omega \qquad (4.4\text{-}18)$$

$$\pi\int_{\kappa R}^{R} \phi(\tau)\left[br - \frac{cr^3}{2}\right]dr = -Q \qquad (4.4\text{-}19)$$

Where the fluidity function, ϕ, is the inverse of the apparent viscosity.

Thus to determine the rheological properties of the fluid without determining the shear rate a rheological model must be used so that an expression for the fluidity function, ϕ, can be developed. It is assumed that this model will fit the rheological properties of the fluid over the range of shear rates examined experimentally. For this study the power-law model is chosen, as it provides a reasonably good fit to most fluid behaviour over a moderate range of shear rates, yet it is relatively simple as it is comprised of only two parameters. For the power-law model the fluidity function, ϕ, may be defined as follows.

$$\phi(\tau) = \left(\frac{1}{A}\right)^{\frac{1}{n}}\left[\left(\frac{M}{2\pi r^2 L}\right)^2 + \left(\frac{b}{r} - \frac{cr}{2}\right)^2\right]^{\frac{1-n}{2n}} \qquad (4.4\text{-}20)$$

By using the relationships described in Equation (4.4-18) or Equation (4.4-19) the experimentally measured variables Ω, Q, M and $(\partial p/\partial z)$ can be used to determine the values of the power-law model parameters A and n. The experimental values of Q or Ω are compared to calculated values and used to optimise the power-law model parameters, see section 4.4.4.

The shear stress may then be determined using Equation (4.4-21) (Huilgol 1990).

$$\tau = \sqrt{\left[\frac{M}{2\pi(\kappa R)^2 L}\right]^2 + \left[\frac{b}{\kappa R} - \frac{c(\kappa R)}{2}\right]^2} \qquad (4.4\text{-}21)$$

Because the shear rate cannot be determined from the measured variables directly it may be determined using the already calculated values of shear stress and the optimised power-law parameters, using the following equation.

$$\dot{\gamma} = \left(\frac{\tau}{A}\right)^{\frac{1}{n}} \qquad (4.4\text{-}22)$$

The calculation procedure outlined above to determine the rheological properties of a fluid from helical flow measurements is summarised in a flow chart, see Figure 4.4-1.

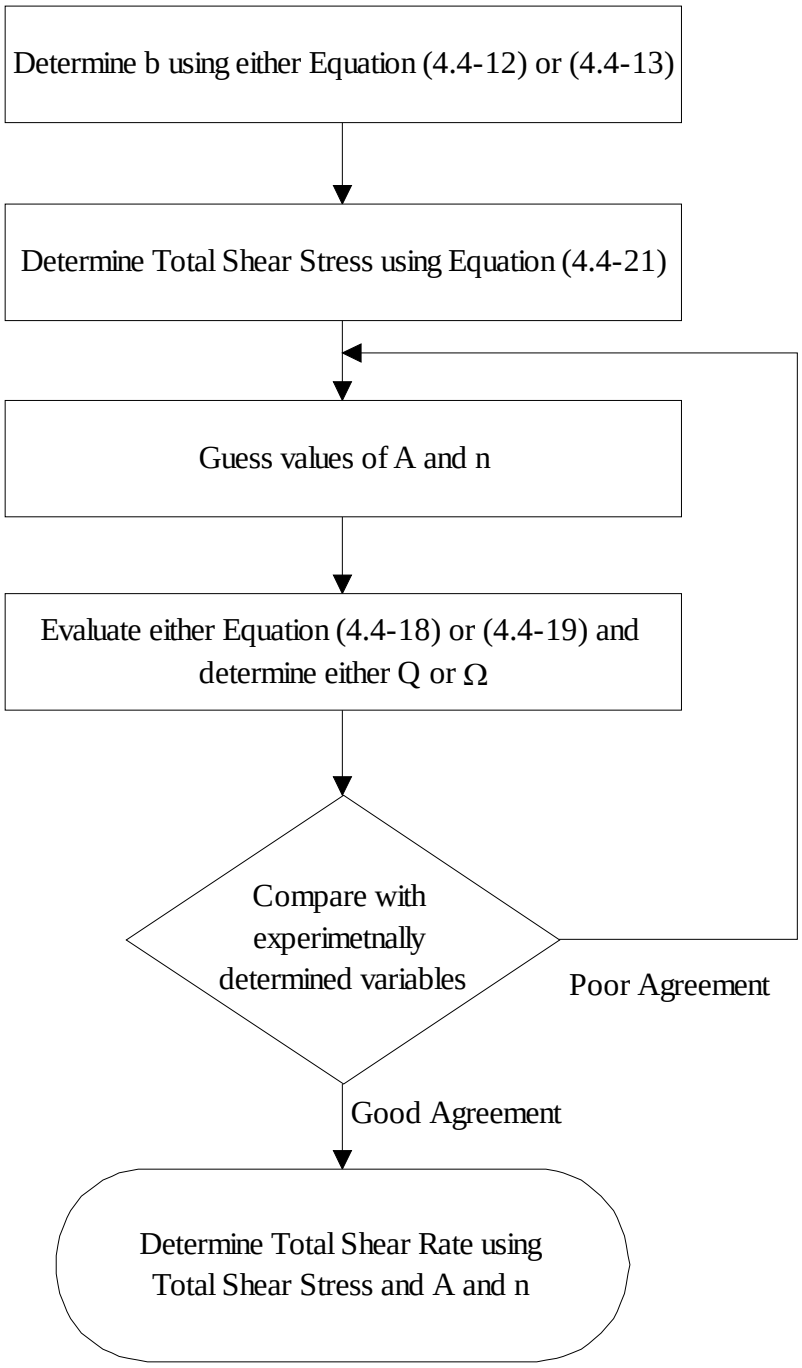

Figure 4.4-1 Basic data analysis procedure for helical flow

4.4.4 Optimisation Procedure

The optimisation procedure used was the Levenberg-Marquardt technique for non-linear regression (Marquardt 1963).

The Levenberg-Marquardt technique is the combination of two non-linear regression techniques, the method of linear descent and the Gauss-Newton technique. Non-linear regression involves fitting a particular equation to given a set of data. To start the process it is usual to guess a set of initial values for the variables in the fitting equation. The variables are then adjusted so that the fitting equation gives the best fit to the set of data.

The method of linear descent is a relative simple technique where by the initially guessed values are adjusted by a small amount and the affect on the accuracy of the fit of the equation to the data set is examined. If the fit of the data improves then the direction of change was correct and another small change is taken in that direction. If the fit however, is worse then the direction of change was incorrect and a change is made in the opposite direction. As the optimal solution is approached the step size is adjusted (usually reduced) to give a more accurate fit.

The Gauss-Newton technique involves examining the slope of the rate of change of the accuracy of the fit with changes in the fitting variables. If the fitting equation were linear then this would be enough to determine the most accurate fit, but because the equation is non-linear there is not enough information in one step to find the optimal solution. However, the correct direction of alteration is given and repeating the process will eventual give the most optimal solution.

Generally the method of linear descent works well for early iterations and slows down as the optimal solution is approached. The Gauss-Newton method is the opposite; initially the method can be quite slow but works well in later iterations. The Levenberg-Marquardt method utilises both techniques, in early iterations the method of linear descent is used and then this is gradually changed to the Gauss-Newton method in later iterations (Marquardt 1963, Press et al. 1990).

As mentioned the Levenberg-Marquardt procedure fits a function of a given number of variables to a given set of data. In this case the function used was a modification of Equation (4.4-18), though Equation (4.4-19) could have also been used. The angular velocity, Ω, measurements were used as the optimisation data set because the experimentally measured values were considered more accurate than the axial flow rate measurements, Q. The actual function optimised is shown in Equation (4.4-23).

$$\Omega = \frac{M}{2\pi L}\left(\frac{1}{A}\right)^{\frac{1}{n}} \int_{\kappa R}^{R} \left(\left[\frac{M}{2\pi r^2 L}\right]^2 + \left[\frac{b}{r} - \frac{cr}{2}\right]^2 \right)^{\frac{1-n}{2n}} \frac{1}{r^3} dr \qquad (4.4\text{-}23)$$

The Levenberg- Marquardt method also requires the derivatives of this function with respect to the fitting variables, which in this case were A and n. The derivatives are shown below.

$$\frac{\partial \Omega}{\partial A} = \frac{-M}{2n\pi L}\left(\frac{1}{A}\right)^{\left(\frac{1}{n}+1\right)} \int_{\kappa R}^{R} \left(\left[\frac{M}{2\pi r^2 L}\right]^2 + \left[\frac{b}{r} - \frac{cr}{2}\right]^2 \right)^{\frac{1-n}{2n}} \frac{1}{r^3} dr \qquad (4.4\text{-}24)$$

$$\frac{\partial \Omega}{\partial n} = \frac{M}{2n^2\pi L}\left(\frac{1}{A}\right)^{\frac{1}{n}} \int_{\kappa R}^{R} \left(\left[\frac{M}{2\pi r^2 L}\right]^2 + \left[\frac{b}{r} - \frac{cr}{2}\right]^2 \right)^{\frac{1-n}{2n}} \ln\left(\frac{A}{\sqrt{\left[\frac{M}{2\pi r^2 L}\right]^2 + \left[\frac{b}{r} - \frac{cr}{2}\right]^2}} \right) \frac{1}{r^3} dr \qquad (4.4\text{-}25)$$

A weakness of the Levenberg- Marquardt procedure is that an initial guess of the fitting variables is required and the poorer the guessed value of these variables the more likely the procedure will not reach the most optimal solution. To improve the chance of determining the correct values of A and n the initial guess values were determined by analysing the experimental data from the flow rheometer using Couette

flow theory, that is the axial flow component was ignored. This simplifies the analysis procedure, reduces the number of iterations that must be made and increases the chance of finding the most appropriate solution.

4.4.5 Determination of b for a Non-Newtonian Fluid in a Wide Gap

The data analysis procedure previously outlined relied on determining a value for the parameter b in one of two ways, either because the fluid under examination was a Newtonian fluid or because a narrow gap geometry was used. However, slurries are generally non-Newtonian in nature and in most cases cannot be examined in a narrow gap geometry because to avoid wall effects a gap width of ten time the largest particle diameter is required (Barnes 1995). Thus b cannot be determined in such a case and thus the rheological properties of the fluid cannot be calculated either.

It can be shown, APPENDIX A, that the parameter b is a function only of the system dimensions, the rheological properties of the fluid and the pressure drop across the bob. Therefore for a given set of experimental tests performed at a constant value of differential pressure the parameter b should be constant providing that the rheological properties of the fluid do not significantly change over the shear rate range of investigation.

An iteration procedure was developed to determine the value of the parameter b for non-Newtonian fluids in a wide gap geometry. In order to achieve this, a range of b values were selected, based on the limits imposed by Equation (4.4-11). Optimal values of A and n were then determined for each of the assumed values of b, using the Levenberg-Marquardt non-linear regression procedure. The correct set of A, n and b must satisfy Equation (4.4-26), which is a combination of Equation (4.4-17) and Equation (4.4-20).

$$\int_{\kappa R}^{R}\left[\frac{1}{A}\right]^{\frac{1}{n}}\left[\left(\frac{M}{2\pi r^2 L}\right)^2+\left(\frac{b}{r}-\left(\frac{\partial p}{\partial z}+\rho g\right)\frac{r}{2}\right)^2\right]^{\frac{1-n}{2n}}\left[\frac{b}{r}-\left(\frac{\partial p}{\partial z}+\rho g\right)\frac{r}{2}\right]dr=0 \qquad (4.4\text{-}26)$$

The left-hand side of Equation (4.4-26) was evaluated for each set of A, n and b and the set of variables that best satisfied the equation were used to describe the rheological properties of the fluid. The variations in the values of Equation (4.4-26) with b are illustrated in Figure 4.4-2. A single distinct value of b is noted when the value of the integral equals zero indicating the suitability of the method devised.

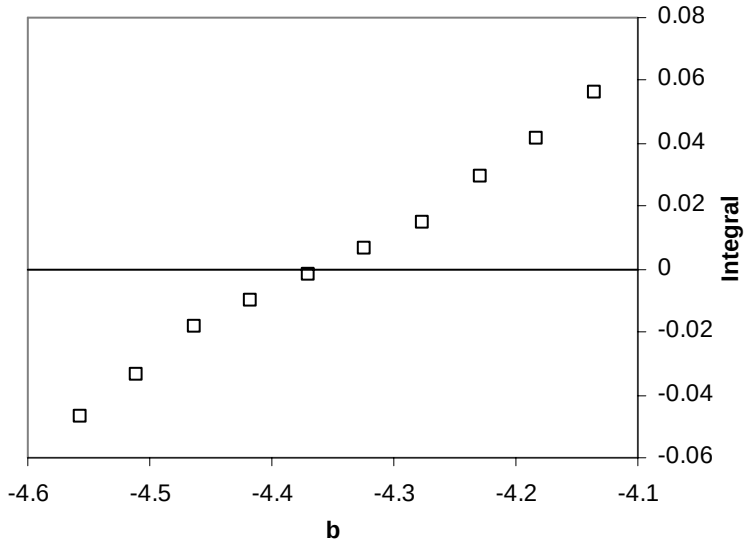

Figure 4.4-2 Plot of the values of Equation (4.4-26) versus b

4.5 Summary of the Data Reduction Procedure

The measured variables from a helical flow experiment are angular velocity, Ω, the torque, M, the pressure drop ($\partial p/\partial z$) and the flow rate, Q. A range of b values are selected based on the limits imposed by Equation (4.4-11). For each value of b an optimal value of the rheological parameters A and n are determined using the Levenberg-Marquardt procedure, where the starting guess values of A and n are determined using Couette analysis. Each set of A, n and b are examined using

Equation (4.4-26) and the set that best satisfies the equation (i.e. the value of the integral is zero) are used to describe the rheological properties of the fluid. The calculation procedure is outlined in Figure 4.5-1.

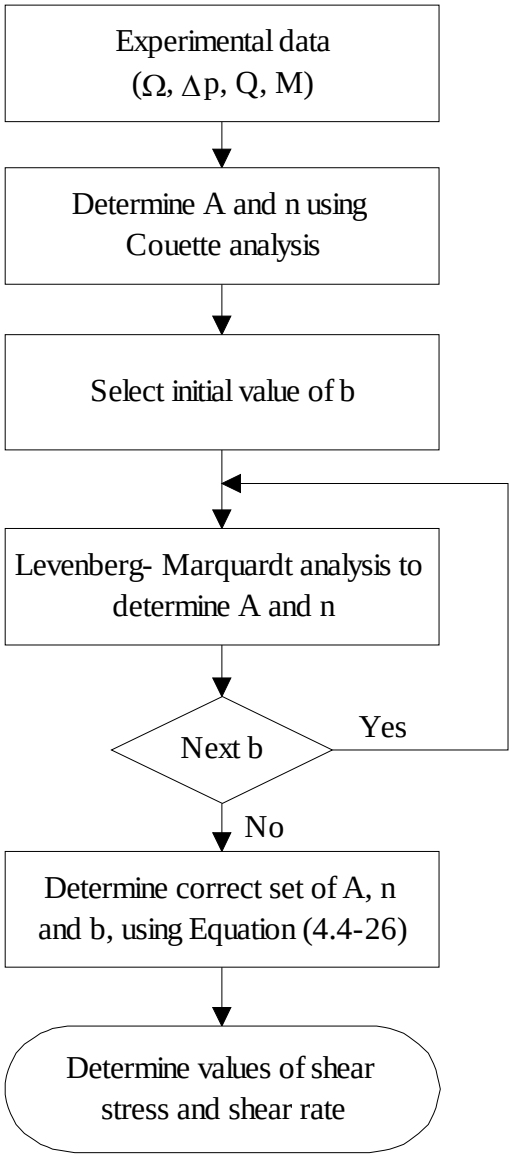

Figure 4.5-1 Data analysis procedure

4.6 Computer Analysis

To reduce analysis times the data reduction procedure described previously was adapted into a computer program. The raw experimental data was imported into a specially prepared Microsoft Excel spreadsheet using a custom written Macro. A second Macro was used to perform the data analysis, to determine the best combination of A, n and b and to present the rheological data in term of shear stress and shear rate. The most complex portion of the analysis was the Levenberg-Marquardt non-linear regression. To improve the speed and reliability of the analysis, the Levenberg-Marquardt procedure was written in a separate Pascal program, which was run when required by the Excel Macro. The actual Levenberg-Marquardt technique was programmed using a standard procedure (Press et al. 1990), which was used as a framework for the rest of the Pascal program. The numerous definite integrals in these equations were solved using a fourth order Runge-Kutta procedure (Kreyszig 1993).

CHAPTER 5 THE FLOW RHEOMETER - DESIGN AND DEVELOPMENT

5.1 Introduction

The design, development and commissioning of the flow rheometer is presented in this chapter. Several unique problems were encountered in the operation of the equipment used to measures the properties of low viscous, rapid settling slurries and these difficulties and the solutions are presented and discussed. Auxiliary equipment including pumps and pressure measurement devices are also discussed with a focus on operation in a settling slurry environment. The automation incorporated into the measurement procedure for the flow rheometer is also presented.

5.2 Description of the Flow Rheometer

The flow rheometer and the experimental system are shown in Figure 5.2-1 and Figure 5.2-2. The helical flow geometry consists of a stationary outer cylinder with an inner diameter of 38mm, with two interchangeable inner cylinders (bobs) with outer diameters of 36mm and 32mm and both 130mm in length. The helical flow geometry is attached to an existing Haake VT 550 viscometer, which is used to control the speed of rotation of the inner cylinder from 0.05 to 800rpm and also to measure the torque acting on the rotating bob. Measurements of torque from the VT 550 are sent to a computer for storage and data processing. A pressure transducer is used to measure the value of differential pressure across the concentric cylinders. The voltage output signal from the pressure transducer is sent to a Data Taker (DT 50, manufactured by Data Taker Australia) where it is analysed and then sent to a computer for storage and data processing.

A variable speed positive displacement pump was used to circulate the sample fluid from a feed tank up to and through the geometry. The design of the pump is detailed in section 5.4. The force of gravity is used to return the fluid from the helical flow geometry to the feed tank. The feed tank was specially built from Perspex with a conical base and ball valve at the outlet. The Perspex allows the test material to be visually examined and to ensure that homogeneous conditions are maintained when settling slurries are examined. A Rushton turbine connected to a variable speed drive was used to mix the slurries in the tank and maintain homogeneous conditions. For viscous liquids heating of the re-circulating fluid was found to alter the rheological properties and so to prevent this problem a copper cooling coil was placed in the feed tank, which was connected to an existing water bath. A cooling coil was not placed around the helical flow geometry because the residence time in the geometry was insufficient for adequate heat transfer to take place and to allow for accurate control of the fluid temperature.

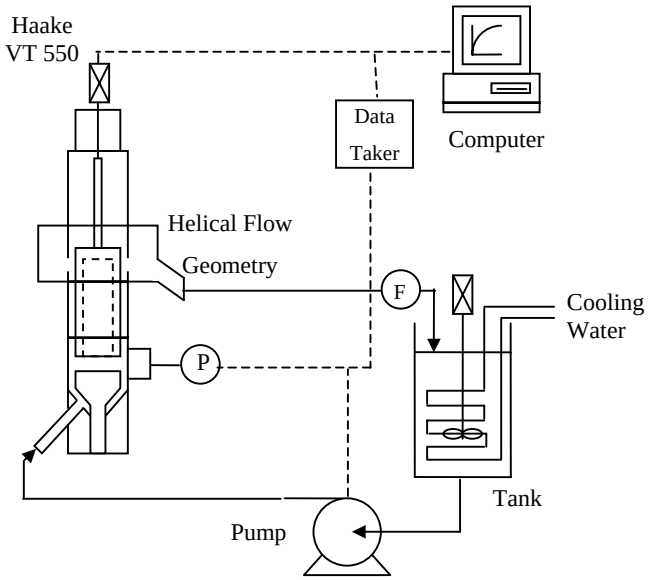

Figure 5.2-1 Schematic of the flow rheometer

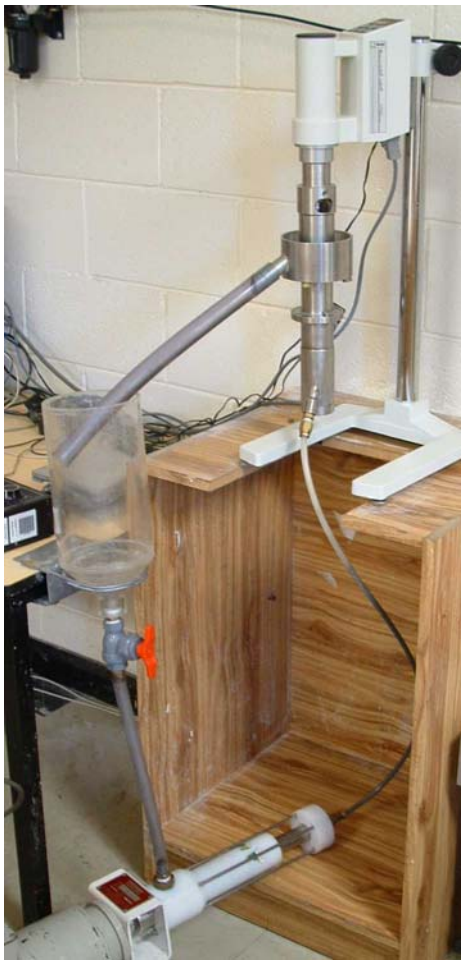

Figure 5.2-2 Photograph of the flow rheometer (cooling coil is not shown)

5.3 The Helical Flow Geometry

A detailed schematic of the design of the helical flow geometry is shown in Figure 5.3-1 and a photograph is shown in Figure 5.3-2.

Flowing fluid enters at the base of the geometry through the inlet pipe and is distributed by the lower insert into annular flow. Flow continues in a vertical direction past the pressure transducer and along the length of the bob. However, before the top of the bob is reached outlet holes allow the fluid to exit the geometry. This reduces the effective bob length to 116 mm. A single outlet pipe is used to transport the fluid from the geometry back to the feed tank.

The geometry is designed to attach directly to a Haake VT 550 viscometer using the existing holding screws. The bobs used in the helical flow geometry are also designed to screw directly into the Haake VT 550, similar to the generic Haake bobs. To assists in cleaning, the outer (stationary) portion of the geometry is made of three interconnecting parts; flanged joints connect the three parts together with Teflon gaskets used between the sections to prevent leaks. The entire geometry was manufactured from stainless steel to avoid corrosion problems, because in many industrial applications mineral slurries are not processed at neutral pH values.

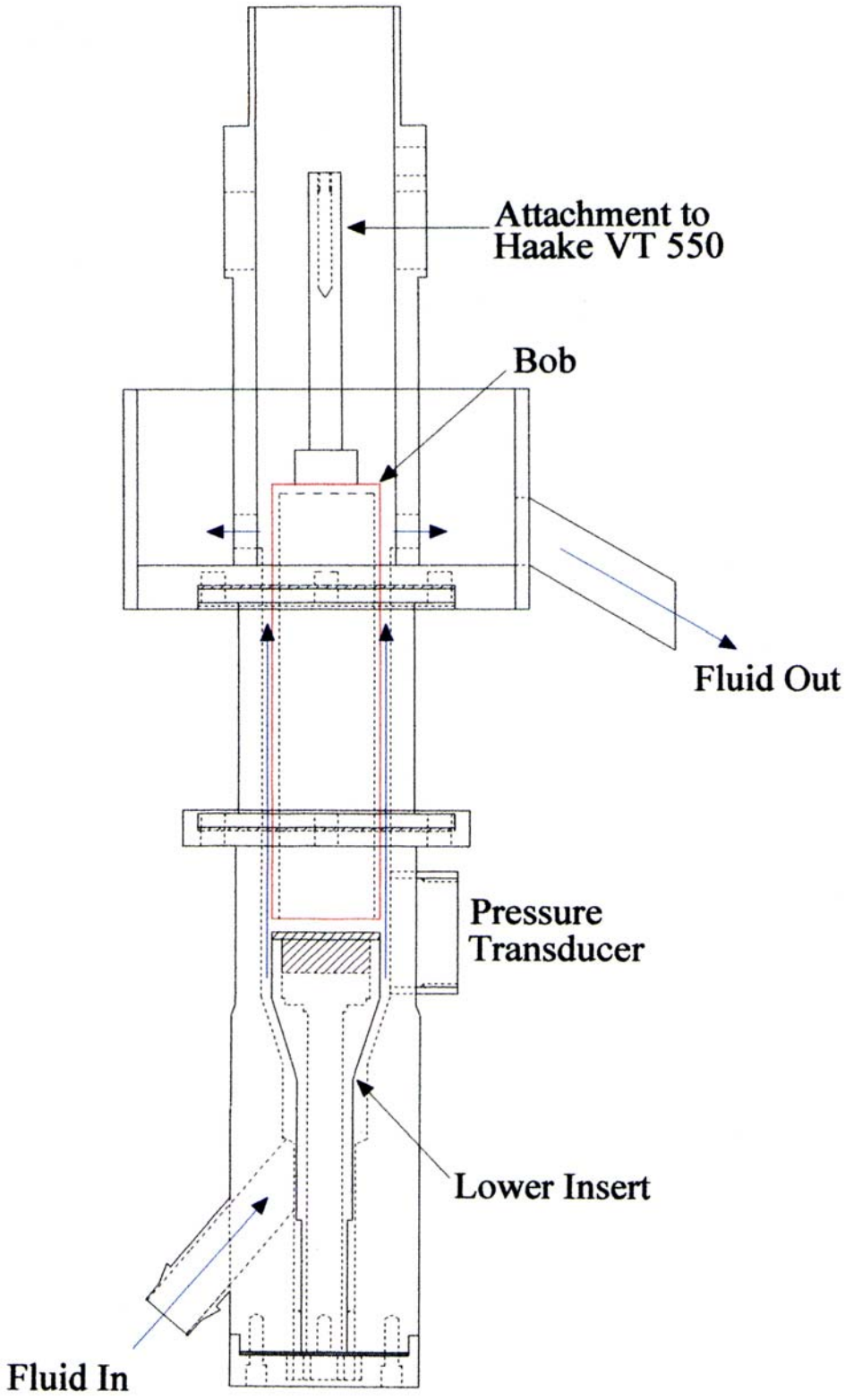

Figure 5.3-1 Schematic of the helical flow geometry

Figure 5.3-2 Photograph of the helical flow geometry

5.3.1 Pressure and Flow rate Measurement

The four essential variables that must be measured for the determination of rheological properties are the rotational speed of the inner cylinder, Ω, the torque required to turn the inner cylinder, M, the axial flow rate and Q and the pressure drop required to generate the axial flow, $\partial p/\partial z$. The torque and rotational speed are measured using the Haake VT 550 viscometer, but other methods are required to measure the differential pressure across the concentric cylinders and the axial flow rate through the geometry.

The differential pressure across the instrument can be determined by measuring the gauge pressure at the base of the inner cylinder, using the pressure transducer shown in Figure 5.3-3. Specific issues relating to pressure measurements and settling slurries are discussed in section 5.3.2.1. Before the top of the bob is reached the fluid flows out of the geometry, see Figure 5.3-1, which gives an exit pressure approximately equal to the surrounding atmosphere and thus the differential pressure across the bob must be equal to the gauge pressure at the base of the bob. For this assumption to be valid the fluid must exit the geometry with no kinetic energy and while this is practically impossible, the fluid will have a lower value of kinetic energy if a positive displacement pump is used. The characteristics of a positive displacement pump are such that for a given flow rate the pump outlet pressure generally matches the system head (McGuire 1993), leaving the fluid with little excess head pressure when it leaves the system.

Figure 5.3-3 Pressure transducer (IMT, Germany)

Initially the flow rate was determined by collecting a certain volume of the fluid (in a measuring cylinder) flowing out of the rheometer in a given time. It was later established that the flow rate measurement was not required to determine the rheological properties and so axial flow rate measurements were abandoned. The justification for not measuring the axial flow rate is discussed in detail in CHAPTER 8.

5.3.2 Critical Design Issues

During design and development several critical issues were identified as possible sources of measurement problems. These were unreliable pressure measurements, the blocking of the instrument by settling solid particles, end effects and entrance length effects.

5.3.2.1 Pressure Measurement and Settling Particles

The pressure measurement is a critical variable that can be affected by a build-up of settling particles. It is common for pressure to be measured by running a capillary line away from the main process stream to an external pressure measurement device. If this procedure were used in the flow rheometer the capillary line would rapidly block with settling solids. To eliminate this problem a pressure transducer with the sensing element at its very end, see Figure 5.3-3, was used. When this transducer was screwed into position in the helical flow geometry the sensing element was flush with the vertical pipe wall and thus there was no region with a reduced flow rate or an area in which particles could settle and interfere with the pressure measurement.

5.3.2.2 Settling Particles within the Helical Flow Geometry

In the transport of settling slurries it is important to maintain a sufficiently high velocity to keep the solid particles in a homogeneous suspension and to prevent them from settling. The critical velocity to avoid deposition of the particles varies with the orientation of the flow and a considerably higher velocity is required for horizontal

flows compared to vertically orientated flows (Spells 1955). The following correlation, Equation (5.3-1), was proposed by Spells 1955, to determine the minimum flow required in a horizontal pipe to prevent particles settling, where v_m is the minimum average flow velocity to maintain particles in a homogeneous suspension, 85% of particles have a diameter smaller that $d_{85,}$ R is the pipe radius, η is the apparent viscosity of the suspending liquid, ρ the density and the subscripts s, p and l refer to the slurry, the particles and the liquid respectively. This correlation may be used to determine the minimum flow rate necessary in the delivery pipe to prevent settling in the flow rheometer, if measurements at particularly low flow rates are required.

$$v_m^{1.225} = (0.0251) d_{85} g \left(\frac{2R\rho_s}{\eta} \right)^{0.775} \frac{\rho_p - \rho_l}{\rho_l} \qquad (5.3\text{-}1)$$

The design of the flow rheometer is such that particles will settle first in the delivery pipe rather than in the instrument as this pipe is not directly vertical but is positioned at an angle of approximately 60º from horizontal. Bends or changes in the direction of the flow can also lead to regions of low flow rate where settling can occur. To further minimise the chance of particles settling and blocking the flow rheometer a “straight through” design was used. In this design fluid enters at the base of the geometry and travels in a vertical direction until the exit holes are reached, where it flows out of the geometry. This design makes for a long geometry, which can lead to construction issues with the rotating bob. If the bob has a small offset at the top of the geometry, then this can be magnified over the total length of the bob resulting in considerable wobble at the base of the rotating bob. However, the advantage of this design is that the flow is predominately in a vertical direction, which means there are very few places where solid particles can settle and block the instrument.

5.3.2.3 End Effects

Rotational rheometers in particular suffer from reduced accuracy due to end effects, but careful design of the geometry can significantly minimise these errors. One way this can be achieved in a Couette geometry is to use an automatic immersion depth

bob with a hollow end (Steffe 1992), see Figure 6.4-3a. The air trapped in the hollow significantly reduces the drag on the end of the geometry. In order to minimise end effects in the helical flow geometry a hollow ended bob was also used. The use of a hollow ended bob in the presence of axial flow may lead to problems as illustrated in Figure 5.3-4a. If the axial flow impacts directly on the base of the bob it may displace the air from inside the hollow increasing the measurement errors due to end effects. The problem of air displacement is reduced in the helical flow geometry by the addition of the lower insert, Figure 5.3-4b. The lower insert directs the fluid flow around the bob and protects the pocket of air from direct exposure to the axial flow. Examination of the bob after experiments showed only a small ingress of fluid into the hollow region.

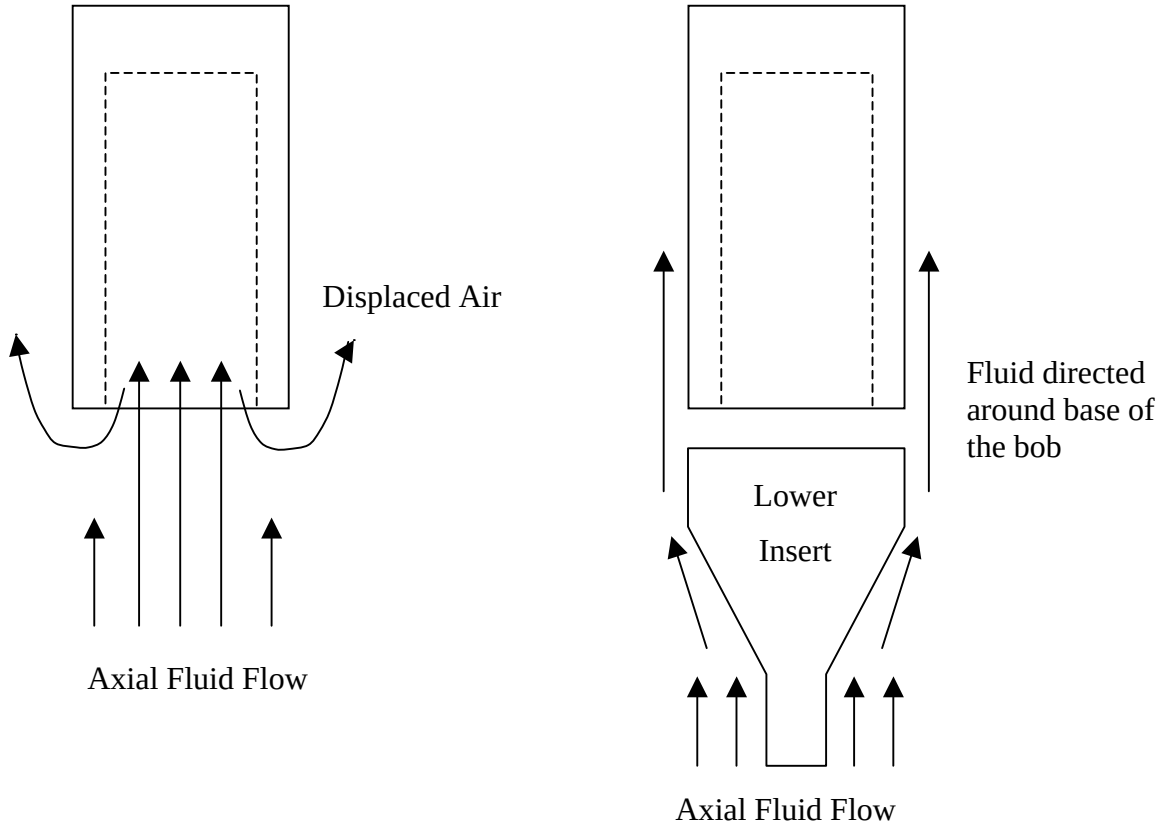

Figure 5.3-4 a: Axial Flow impacts on the base of the bob; b: Axial flow directed around the bob

End effects may also manifest at the top of the bob. In the case of the helical flow geometry the fluid flows out of the geometry before the top of the bob is reached, see Figure 5.3-1, which avoids fluid contact with the top of the bob. In this case the bob length used in any calculations must be determined as the length of the bob in contact with the fluid and not the manufactured length of the bob.

5.3.2.4 Laminar Flow Development

The circulation of the sample fluid in the helical flow geometry means that in terms of fluid flow the geometry has a lot more in common with a tube rheometer than a standard Couette geometry. Even under steady-state conditions fluid is continuously entering the geometry from a pipe and a certain length is required for a full laminar flow profile to develop. Calculations that can be used to determine the entrance development length for laminar flow entering an annulus are described in section 11.2.2. Assuming a viscosity of 0.01 Pas, a density of 1000 kg/m^3, a maximum axial flow rate of 4 L/min and using the wide gap geometry (32mm bob), an axial flow development length of 10mm can be calculated (axial flow development length calculations are discussed in section 11.2.2). The total effective measurement length of the inner bob in the flow rheometer is 116mm, which means that the axial flow development length is less than 10% of the total length. This value of 116mm does not include the length of the lower insert, which also provides an additional region for laminar flow to develop, before the bottom of the bob is even reached. It is therefore unlikely that development of laminar axial flow will affect experimental measurements in the flow rheometer.

5.3.3 Sizing the Geometry

The critical variables that must be measured (rather than those which are preset) are the torque and the differential pressure. The dimension of the rheometer needed to be carefully selected in order that lower viscosity materials such as mine tailings could be successfully measured. Ideal fluids such as CMC and glycerol tend to be highly viscous, with values of apparent viscosity typically 50 to 100 times that of mine tailings.

A computer-based simulation was developed to determine the optimal dimensions for the flow rheometer. The different factors and effects that were considered in determining the optimal dimensions are discussed in the following sections. The dimensions of the Haake MV II geometry (see section 6.4.2.1.) were used as preliminary starting values for the analysis.

5.3.3.1 Differential Pressure Measurement

If the magnitude of the pressure drop is very small then accurate measurement can be very difficult. To increase the value of the differential pressure across the instrument at a given volumetric flow rate, several dimensional changes can be made, based on Equation (5.3-2).

$$\Delta p = \frac{8Q\mu L}{\pi R^4}\left(\frac{\ln(1/\kappa)}{\left(1-\kappa^4\right)\ln(1/\kappa)-\left(1-\kappa^2\right)^2}\right) \qquad (5.3\text{-}2)$$

Equation (5.3-2), describes the pressure drop through an annulus when a Newtonian fluid is flowing at given flow rate. Examination of this equation shows that the pressure drop can be significantly increased if the outer radius of the instrument is reduced, whilst maintaining a constant gap ratio, as shown below.

$$\Delta p \propto \frac{1}{R^4}$$

Since the pressure drop is also directly proportional to the length of the bob, a further increase in pressure can be obtained by lengthening the bob.

$$\Delta p \propto L$$

The gap ratio, κ, between the outer cylinder and the rotating bob can also have a significant effect on the pressure drop, see Figure 5.3-5.

$$\Delta p \propto \left(\frac{\ln(1/\kappa)}{(1-\kappa^4)\ln(1/\kappa) - (1-\kappa^2)^2} \right)$$

As shown in Figure 5.3-5 the value of differential pressure decrease rapidly with increasing gap width and approaches a value 1000Pa which represents the static head pressure for the system defined at the beginning of this analysis. To maximise the value of differential pressure the smallest gap width possible is necessary. However, the final minimum gap width is controlled by the size of particles and the requirements necessary to minimise wall effects (Barnes 1995).

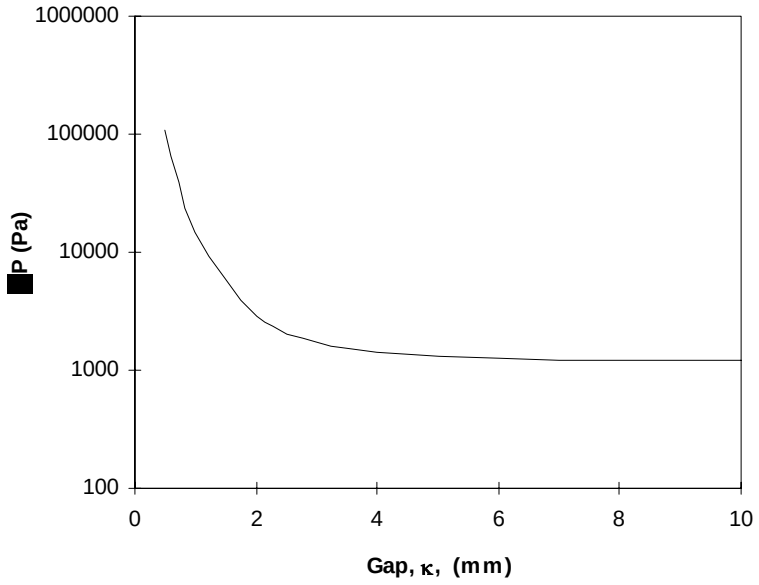

Figure 5.3-5 The effect of gap width on the pressure drop of a flow in an annulus

5.3.3.2 Torque Sensitivity

The torque acting on a bob rotating in a Newtonian fluid in an annulus can be determined using Equation (5.3-3).

$$M = 4\pi\mu L\Omega\left(\frac{R^2}{1-\kappa^2}\right) \qquad (5.3\text{-}3)$$

The measured torque is dependent on the square of the radius of the outer cylinder, providing that the gap ratio is constant and will increase with an increase in the outer cylinder radius, as shown.

$$M \propto R^2$$

However, the measured torque will decrease with an increase in the gap ratio for a constant outer cylinder radius.

$$M \propto \frac{1}{1-\kappa^2}$$

Lengthening the bob will proportionally increase the measured torque values.

$$M \propto L$$

5.3.3.3 Laminar Flow Criteria

Laminar flow in the helical flow geometry must be present for any rheological measurements to be performed. To ensure laminar flow, it is necessary to maintain the axial Reynolds number and the Taylor number below the respective critical transition values. Calculated Reynolds numbers for maximum axial flows of four litres a minute with a low viscosity liquid (10cp) were approximately 250 times less than the critical value. This indicates that it is extremely unlikely that the axial flow component will ever become turbulent. However, unlike the axial flow component, calculations (see

APPENDIX B) revealed that Couette turbulence or Taylor vortices could develop in the helical flow geometry and thus the criteria for laminar Couette flow was incorporated into the optimisation. The Taylor number shown in Equation (5.3-4) can be used to determine the onset of turbulent flow in a Newtonian fluid in a concentric cylinder system.

$$\mathrm{Ta} = \frac{v_0 R(1-\kappa)}{\nu}\sqrt{\frac{(1-\kappa)}{\kappa}} \qquad (5.3\text{-}4)$$

The critical speed for the onset of instabilities will increase proportionally with an increase in the outer cylinder radius at a constant gap ratio.

$$\mathrm{Ta} \propto R$$

An increase in the gap ratio can significantly lower the critical rotational speed at which instabilities in the flow appear.

$$\mathrm{Ta} \propto \frac{(1-\kappa)^{3/2}}{\kappa^{1/2}}$$

5.3.3.4 Summary

Several key findings were drawn from the analysis performed on the helical flow geometry and are listed as follows.

- Reducing the outer radius and lengthening the bob will increase the differential pressure across the geometry.
- A Reduction in the outer cylinder radius reduces the measured torque but increasing the length of the bob can offset this.
- The onset of Taylor vortices can be delayed by reducing the outer cylinder radius.

By combining these key results the following dimensional changes were made. Compared to a standard Haake MV II geometry (see section 6.4.2.1) the outer cylinder radius was reduced and the entire geometry lengthened, to better optimise the measurements of torque and differential pressure. The final dimensions of the helical

flow geometry are presented in Table 5.3-I. These design modifications also had an advantage of further minimising any end effect at the base of the bob by increasing the length to gap ratio and the onset of Taylor vortices was delayed by reducing the radius of the outer cylinder.

Table 5.3-I Summary of the dimensions of the helical flow geometry

Dimension	(mm)
Outer Cylinder Diameter	38
Bob Diameter – Narrow Gap	36
Bob Diameter – Wide Gap	32
Bob Length – Manufactured	130
Bob Length – Effective	116

Using the dimensions presented in Table 5.3-I, the operational limits of the Haake VT 550 viscometer and a maximum flow rate value of 4 L/min from the helical rotor (Mono) pump the operating range of the flow rheometer was calculated and is shown in Figure 5.3-6.

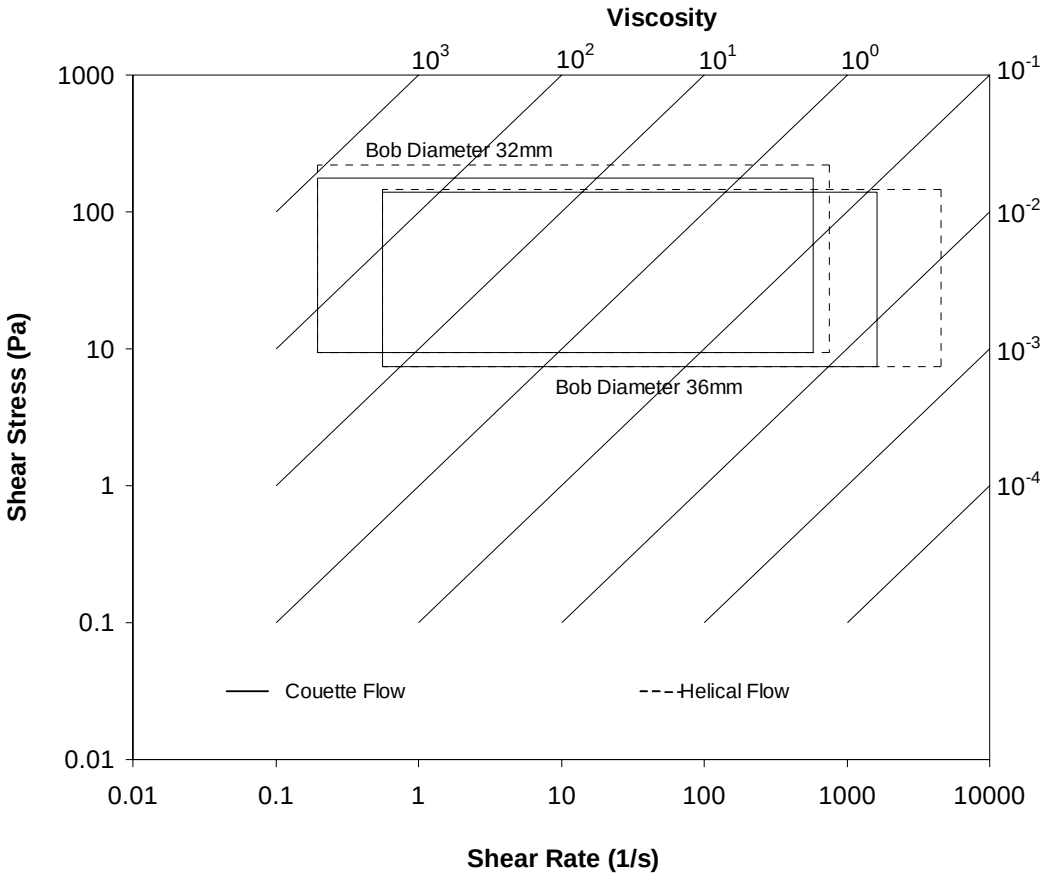

Figure 5.3-6 Operating range of the flow rheometer

5.4 Pump Selection

A significant problem associated with the operation of the flow rheometer with settling slurries was the selection of a suitable pump to circulate the settling slurries. The pump was required to meet several specifications; an ability to handle solid and abrasive particles and to provide non-pulsed flow. A slurry centrifugal pump would have been most suitable except that the smallest of these pumps that could be sourced was rated at 30L/min., well above the maximum requirements of 4L/min. A standard centrifugal pump would have been eroded rapidly by the abrasive particles and accurate variable flow control of these types of pumps is often difficult without an elaborate wear resistant control valve. Most positive displacements pumps including diaphragm and peristaltic pumps resist erosion better than centrifugal pumps but the flow delivered is pulsed in natured. Even the flow from an eight roller peristaltic pump was considered too pulsed for use in the flow rheometer. The pump that was eventually selected for this application was a helical rotor pump. The helical rotor pump is a positive displacement pump with a continuously variable pumping volume created by the voids between a single spiral helical rotor and a double “angle-rate” helical spiral stator, see Figure 5.4-1 below. To resist erosion the stator is made of a natural rubber and the rotor made of hard chrome plated steel. Many helical rotor pumps including the mono pump used in this study have a large cavity before the pumping head where solids can settle out, see Figure 5.4-1. However, the drive shaft also goes through this cavity and thus it was possible to attach a set of custom-made paddles to the drive shaft that kept the solid particles suspended during pumping operations.

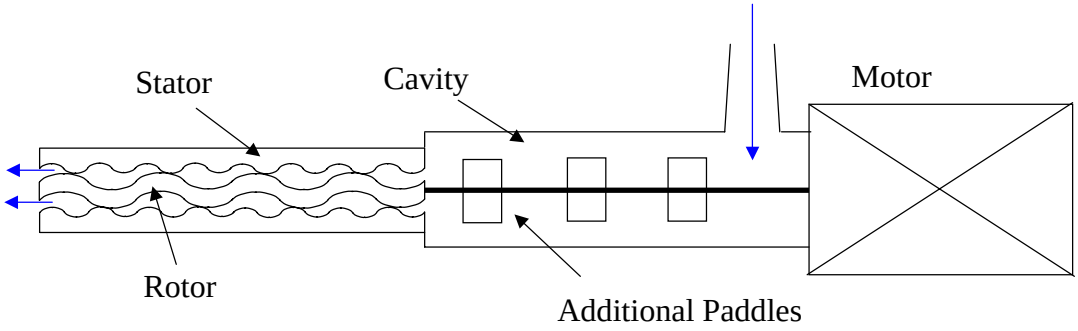

Figure 5.4-1 Schematic of the modified helical rotor pump

5.5 Computer Control and Interface / Data Acquisition Program

The unique design and operation of the flow rheometer required the development of specialised data acquisition and control software. The analysis procedure restricted the type of tests that could be performed to the measurement of torque as a function time at a constant rotational speed. Thus to generate a rheological profile of the experimental fluid a series of tests at different values of rotational speed were required and thus the control aspect of the program incorporated an ability to pre-program a sequential series of experiments at different values of rotational speed.

A requirement for the correct analysis of helical flow is that the differential pressure across the geometry be maintained at a constant value for different values of rotational speed, see CHAPTER 4. This is particularly important when non-Newtonian fluids are examined as the rotational speed of the bob can affect the differential pressure across the concentric cylinders. Thus the data acquisition program needed to not only interface with the Haake rheometer but also with the pressure transducer through the data logger, to provide real-time measurements of the differential pressure, so that changes in the flow rate could be made to keep the differential pressure constant. Visual Basic was used to write the code for the control/acquisition program as it allowed for the development of a user-friendly input interface. The data from each experiment was stored in a modified text file (a ".hfr" file) that could be later accessed by the excel macro for data analysis, see section 4.6.

CHAPTER 6 GENERAL EXPERIMENTAL APPARATUS AND TECHNIQUES

6.1 Introduction

To support the development of the flow rheometer and the other unique apparatus developed as part of this study, several generic pieces of experimental apparatus were required. These apparatus and the experimental techniques used are discussed in detail in this chapter. The rheological instruments used included standard commercial instruments and geometries (a Bohlin CVO–50 and a Haake VT 550) and also a specially developed modified tube rheometer. A Malvern particle size analyser was also used. A variety of different fluids were used in this investigation and included ideal Newtonian fluids (glycerol, glucose water solutions and standard rheological oils), both pseudoplastic and yield-pseudoplastic solutions (CMC, polyox, xanthan gum and carbopol) and both settling and non-settling slurries (fly ash, gold mine tailings, diamond mine tailings, a clay slurry and a PMMA in water slurry).

6.2 Preparation of Experimental Fluids

6.2.1 Liquid Solutions

6.2.1.1 Newtonian Fluids

The Newtonian solutions used were a standard rheological oil, glycerol-water solutions and glucose-water solutions. The standard rheological oil (s200 grade, supplied by Cannon Oils, Cannon Instrument Company, USA) is a mineral oil of certified viscosity and density at selected temperatures and is used with no additional preparation.

Glycerol (supplied by ACE Chemicals, South Australia) is a significantly polar molecule that readily hydrogen bonds and is thus quite viscous at room temperature with a viscosity of 1.1 Pas (at 20°C) (Dean 1985). However, water may be absorbed from the atmosphere and even a small amount of water can significantly reduce the viscosity. For this reason when comparative rheological experiments were performed on different instruments the tests were performed as close as possible, to minimise the chance of changes in the rheological properties of the glycerol.

Glucose (MCY grade, supplied by Fielders, Australia) is an isomer of a group of eight sugars known as the Altohexoses, but is only one of two that occur naturally (McMurry 1992). The glucose was diluted to a variety of concentrations with reverse osmosis (ro) water. This dilution however meant that the newly prepared solution was highly susceptible to microbial attack. So as to prevent a build-up of mould in the solution a small quantity of Dettol Antiseptic liquid (manufactured by Reckitt and Coleman, UK) was added. Evaporation of the water in the solution could cause the viscosity to increase with time, so to prevent evaporation the solutions were kept in sealed buckets. As with the glycerol when comparative test work was performed on different instruments minimal time was allowed to elapse between tests.

6.2.1.2 Non-Yield Stress Pseudoplastic Fluids

The pseudoplastic fluids used, were various concentration solutions of the polymers CMC and polyox. As with the previously discussed Newtonian solutions evaporation could cause the rheological properties to change so these solutions were stored in sealed buckets and a testing program, the same as previously discussed for the glycerol and glucose solutions was used.

CMC or carboxymethyl-cellulose (c600 grade, supplied by ACE Chemicals, South Australia) is a derivative of a natural cellulose polymer and finds many uses from a paper covering to a depressant in mineral flotation. The same standard procedure was used to make the various different concentration solutions. The correct quantity of CMC was first weighed and placed into a suitable container; the correct quantity of ro-water was then weighed and added. The solution was then left to rest for several days except when it was occasionally stirred by hand, to allow an aqueous dispersion to form (Wright 1999). It was found that this method for producing a CMC solution provided a more viscous and shear thinning solution than using an impeller to aggressively mix the CMC powder into the water.

Polyox is the trade name for polyethylene oxide resins (supplied by Union Carbide, USA), which are high molecular weight homopolymers produced by the heterogeneous catalytic polymerisation of ethylene oxide (Hubbe 2003). A quantity of ro-water was weighed and placed within a glass beaker of known weight, which in turn was placed on a magnetic stirring/heating element. A magnetic stirring piece was placed in the water and the heating element and magnetic stirrer switched on. The desired amount of polyox was measured and slowly added to the water at a temperature of approximately 80°C (Wei and Willmarth 1992). Once the solution had cooled, further water was added and mixed in to equalize that which was lost to evaporation. Often a larger quantity of solution was required than could be heated on the mixer/heater and in these cases a more concentrated solution was created and then later diluted to the desired value

6.2.1.3 Yield-Pseudoplastic Fluids

The yield-pseudoplastic fluids used, were various concentration solutions of the polymers xanthan gum and carbopol. As with the previous solutions evaporation could cause the rheological properties to change so the same storage and testing regimes as previously discussed were used.

Xanthan gum (Food grade, supplied by ACE Chemicals, South Australia) is a high molecular weight polysaccharide that is produced by fermentation (Chaplin 2003). The preparation of the xanthan gum was similar to that of the CMC solutions; correct quantities of water and polymer powder were weighed and placed in a suitable container and then left for several days (Vlaev et al. 2002), except when they were occasionally stirred by hand

Carbopol (940 grade, supplied by B.F. Goodrich Co.) is a manufactured polymer, which belongs to a class of resins, known as carbomers. Carbomers are a polyacrylic based polymer cross-linked with allypentaerithritol and modified with C10 to C30 acrylates (Curran et al. 2002)]. The preparation of the carbopol solution is again similar to that of the CMC solutions; correct quantities of water and polymer powder were weighed and placed in a suitable container and then left for several days, except when they were occasionally stirred by hand. The rheological properties of a carbopol solution are heavily influenced by the pH of the solution (Curran et al. 2002) and thus the pH of the solutions needed to be carefully monitored and adjusted were necessary.

6.2.2 Slurries

A variety of different artificial and real slurries were used in this investigation.

6.2.2.1 Artificial Slurries

PMMA or polymethylmethacylate (IF 850 grade, supplied by LG Chem, Korea) is an injection moulding grade polymer in spherical form. Before these spheres could be used they were first washed to remove any remaining monomer on the surface (Abbott et al. 1991, Graham et al. 1991, Tetlow et al. 1998). Once washed the spheres were dried in a drying oven at approximately 90°C, to prevent the particles melting and fusing together. The PMMA particles were then combined with ro-water to form a slurry. Varying amounts of sodium chloride salt was added to the water to adjust the density of the liquid and the settling rate of the solid particles.

6.2.2.2 Real Slurries

The diamond mine tailings (supplied by Rio Tinto Technical Services) and the fly ash (supplied by the CSIRO Minerals) were provided in a slurry form and could be used as supplied, though ro-water was added to adjust the solids volume concentration.

The clay slurry (supplied by Rio Tinto Technical Services) was provided in a dry powder form. The solids were added to ro-water, well mixed and allowed to rest for several days before rheological experiments were performed.

The gold mine tailings (supplied by Rio Tinto Technical Services) were provided in a dry solid form. Care was taken when handling the gold mine tailing due to the possibility of residual cyanide within the sample. As with the clay slurry the dry solids were added to ro-water, well mixed and allowed to rest for several days.

6.2.3 Determining the Solution Density

For solutions containing no solid particles a 50mL density bottle was used to accurately determine the density. A water bath was used to control the temperature of the bottle and any liquid contained within. To determine the correct volume of the density bottle a fluid of know density was used (s200 grade standard oil, supplied by Cannon Oils)

The presence of solid particles in a slurry prevented the density bottle from being used as solid particles interfered with the operation of the stopper. Standard oil (s200 grade, supplied by Cannon Oils) was used to calibrate the volume of two small 25mL measuring cylinders. To reduce measurement errors two cylinder were used and the average result recorded.

6.2.4 Determining the Settling Rate

The settling rates of particles in the slurries used in this study were determined using a 500mL glass measuring cylinder. A quantity (approx 350mL) of the slurry was placed in the measuring cylinder (where the solid volume fraction was the same as that used in the rheological tests) and thoroughly mixed by up-turning the cylinder multiple times. The settling velocity of the clear zone interface was then observed. Where the settling rate varied dramatically between different particles present, usually due to the difference in the size of the particles, the fastest settling rate is presented.

Table 6.2-I Settling Rate of Slurry Particles

Slurry	wt% Solids	Particle Settling Rate (cm/s)
Clay slurry	71	Negligible
Fly ash	68	0.017
Gold mine tailings	36	0.48
Diamond mine tailings	49	1.33

6.3 Particle Size Analysis

The size and size distribution of particles in a slurry can have a significant influence on the rheological properties of the slurry (Clarke 1967, Moreland 1963, Ward and Kammermeyer 1940, Ward and Whitmore 1950). The size of the particles can also limit the size of the geometry and the type of instrument used to perform the rheological characterisation (Barnes 1995). For this reason accurate measurements of the particle size is important.

For this study a Malvern Particle Size Analyser, 2600 series was used. The Malvern instrument uses a light scattering technique to determine the particle size. Numerous attachments for the instrument are available to enable a wide range of particle sizes to be measured.

6.3.1 Experimental Apparatus

The Malvern Particle Size Analyser consists of a He-Ne Laser, a beam expander, a ultrasonic and mechanical mixing tank, a liquid measurement cell, a receiver lens and detector plane. The set-up of the apparatus is shown in Figure 6.3-1. Several different receiver lenses are available depending on the size range of particles to be measured as shown in Table 6.3-I.

Table 6.3-I Malvern Size Analyser -Lenses

Lens Size (mm)	Size Range (μm)
63	1.2 – 118
100	1.9 – 188
300	5.8 – 564
600	11.6 – 1128

In operation the sample of slurry is pumped from the mixing tank through the liquid measurement cell and returned to the mixing tank, see Figure 6.3-1. The laser beam passes through the sample and the scattered light collects on the detector plane.

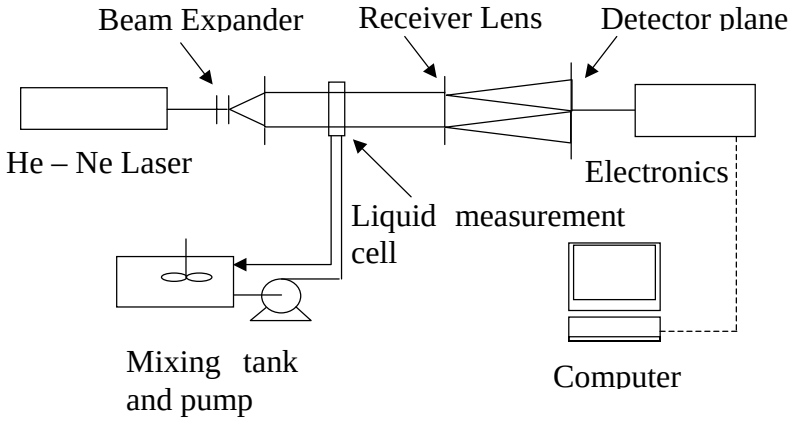

Figure 6.3-1 Malvern particle size analyser

6.3.2 Experimental Results

6.3.2.1 Standard Material

To test the accuracy of the Malvern particle size analyser a sample of glass beads of known particle diameter were measured. The particle size distribution of the glass beads (supplied by ATA Scientific, Australia) is shown in Table 6.3-II. Results from the Malvern particle size analyser are shown in both Table 6.3-II and Figure 6.3-2. Good agreement, within the limits of the instrument and variation in the bead sample, is observed between the manufacturer's data and the experimental data. This agreement verifies the accuracy of the experimental procedure used for the Malvern particle size analyser.

Table 6.3-II Particle size – Glass Beads

Particle Size	Manufacturer Mean Diameter (μm)	Measured Mean Diameter (μm)
d_{10}	53.2 ± 8%	55.7
d_{50}	67.8 ± 5%	68.7
d_{90}	87.7 ± 8%	94.7

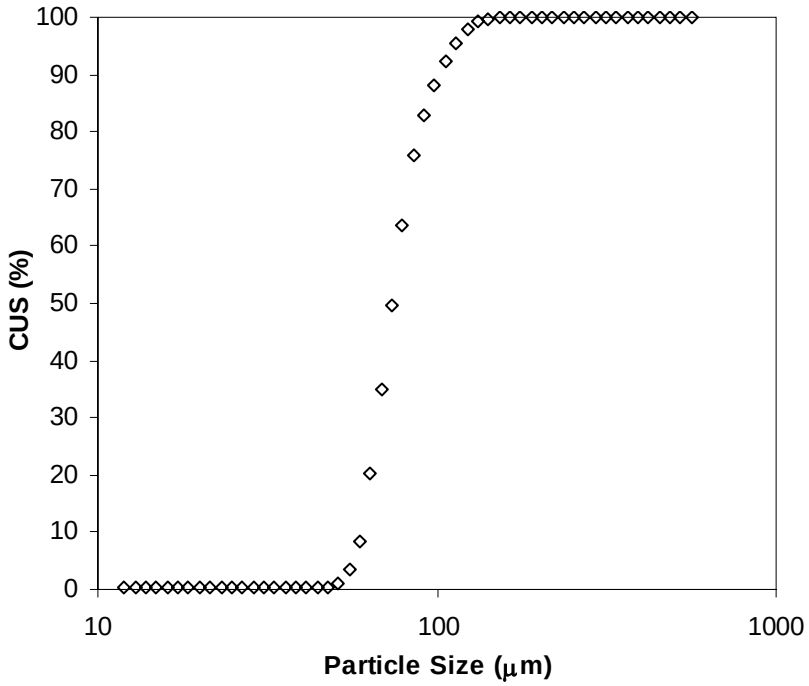

Figure 6.3-2 Results - Malvern particle size analyser, cumulative under size – Glass Beads

6.3.2.2 Slurry Results

Once the accuracy of the Malvern particle size analyser was confirmed using the glass beads the instrument was used to determine the particle size distributions of the various slurries used in this investigation. The results are present in Figure 6.3-3 below.

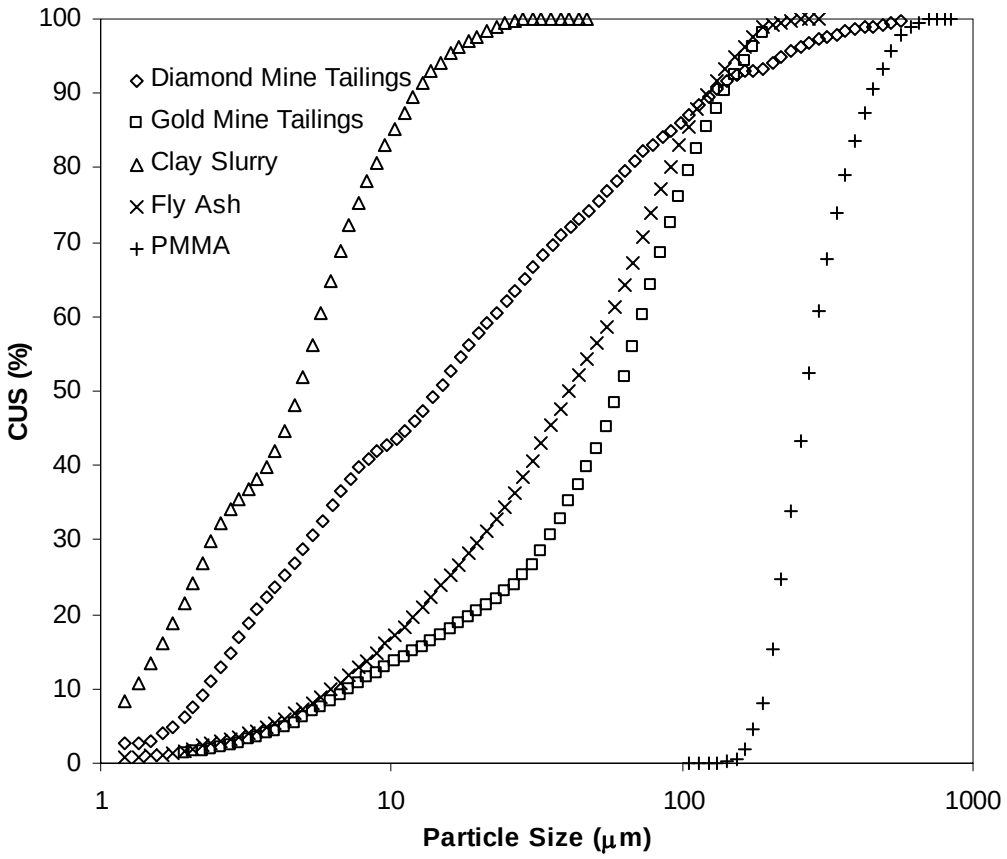

Figure 6.3-3 Cumulative under size plot – various different solid particles

6.4 Generic Rheological Instruments

The correct determination of the rheological properties of experimental fluids in the standard laboratory rheological instruments was an extremely important component of this study, as these results were needed for comparison with results generated on the unique instruments, which were developed during this project. The values of the viscosity for many common fluids may be found in books and literature, but when these results are compared to laboratory results there is often too much variation for the literature results to be accurately used. This variation between the literature results and laboratory results can be caused by many factors that are extremely difficult to control, including the length of time the fluid has been prepared for, the amount of exposure to the air and the ambient storage temperature. For this reason the rheological properties of a fluid must be determined immediately before or after its use in experiments rather than using literature values.

Two generic rheometers were used in this investigation, a Bohlin CVO-50 (manufactured by Bohlin Instruments, UK) and a Haake VT 550 (manufactured by ThermoHaake, Germany).

6.4.1 Bohlin CVO-50

The Bohlin CVO-50 is a controlled stress rheometer that can also be used in a simulated constant rate mode. A supply of dry compressed air was required for the air bearing in the instrument, so a three stage drying unit, which consists of a drain catcher, mist separator and a membrane dryer, was installed on the air supply line from the main compressor. The CVO unit consists of a torque motor and a deflection sensor. Measurements involve applying a torque to a sample and measuring the resulting deflection. A separate water bath is attached the CVO to control the temperature of the fluids under examination.

6.4.1.1 Geometries Available for use on the Bohlin CVO-50

A wide variety of geometries are available for use on the CVO including, parallel plates (40mm and 20mm diameter), cone and plates (4°/40mm diameter, 2°/40mm diameter, 4°/20mm diameter), a Money bob and cup (bob: 14mm diameter, 22.3mm long and a cup 15.4mm diameter) and a vane (vane: 10mm diameter, 20mm long and a cup 15.4mm diameter). All the cone and plate geometries are truncated cones, where the degree of truncation is 0.07mm for the 2° cone and 0.15mm for the 4° cones. For the rheological analysis of liquids that contained no solid particles, the 4°/40mm cone and plate geometry was used as the larger diameter increases the sensitivity of the measurement and the use of a cone and plate geometry, as opposed to the other geometries available, ensured a constant shear rate across the measurement gap.

6.4.1.2 Rheological Measurements

The sample was then loaded as shown in Figure 6.4-1, with the liquid filled to the edge of the cone but not overflowing. When aqueous samples were tested the small sample volume meant that any amount of evaporation could potentially affect the results, so to prevent evaporation a layer of light olive oil was placed around the sample as shown in Figure 6.4-1. The viscosity of the oil was significantly less than that of the sample so that there was only a minimal additional increase in the measured torque due to the presence of the oil.

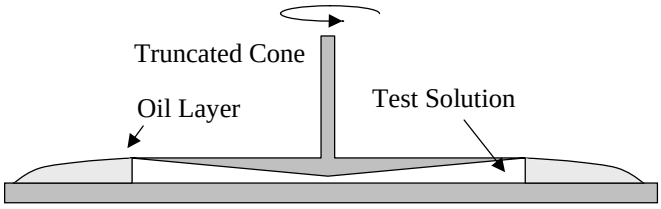

Figure 6.4-1 Correctly loaded - cone and plate geometry

For basic rheological measurements to determine the relationship between shear stress and shear rate the CVO had several modes of operations that could be used. Other

more complex tests to examine elasticity are also possible on the instrument but these types of tests are beyond the scope of this investigation.

Controlled Stress Experiments

When operating in the controlled stress mode several different experimental tests were possible. As the CVO is a controlled stress instrument, these tests in general were more accurate and reliable than the simulated controlled rate tests, which are also described below.

Stress Sweep

The stress sweep was the most basic test that could be performed on the CVO. However, Krieger (1990) described the problems that instrument inertia in sweep tests can have on the results. In a sweep test the response time of the fluid and the machine can lead to the development of a hysteresis loop in the results, even when the fluid does not exhibit thixotropic behaviour and for this reason the stress sweep test was not usually performed

Constant Stress as a Function of Time

The constant stress test involved measuring the shear rate response in a fluid to a particular applied stress as a function of time. This type of test was typically used because it was more accurate and reliable than the controlled rate mode, described below and did not suffer from the hysteresis effects associated with the stress sweep, described above.

Controlled Rate Experiments

As with the controlled stress mode both sweep and constant speed as a function of time tests were possible in controlled rate mode. However, this mode of operation was found to be unreliable and was not regularly used. For the machine to operate in a controlled rate mode a feed back loop control circuit was used to adjust the applied torque to keep the rotational speed constant. However, the software used to control this feedback loop appeared to be unsuitable for higher values of shear rate, as the control loop would become unstable and the speed of the machine would continue to increase until the fluid was expelled from the geometry.

6.4.1.3 Analysis of the Results

The control software that was used for the CVO automatically determined the shear stress and shear rate data from the measurements of torque and rotational speed respectively. However, the calculation were only based on Newtonian fluid mechanics, where the rotational speed and toque are multiplied by a constant which is a function of the geometry to determine the shear rate and shear stress respectively. This method of solution is not generally applicable when non-Newtonian fluids are examined and the shear stress and shear rate values should not be used. However, it was possible when more complex types of fluids were examined to determine the actually values of torque and rotational speed by using the geometry constants in reverse. An advantage of using the cone and plate geometry was that even for non-Newtonian fluids the shear rate was essentially uniform across the measurement gap and thus no corrections to the shear rate were needed and the simple calculations performed by the software were acceptable. The calculations associated with the cone and plate geometry are discussed in section 3.2.1.2.

6.4.1.4 Experiments with Standard Fluids

A standard rheological oil (s200 grade) was used to test the accuracy of the measurements from the CVO. These experiments involved measuring the shear rate (rotational speed) for a series of approximately eight constant stress tests, see section 6.4.1.2, conducted in a random order to reduce the chance of systematic errors. A summary of the tests performed and the results are presented in Table 6.4-I and Figure 6.4-2.

Table 6.4-I Standard oil properties at various temperatures

Fluid	Temp (ºC)	Density (kg/m^3)	A ($Pa.s^n$)	n	Error* (%)	Std Dev# (%)
Standard Oil s200	25.0	876.1	0.407	1	0.7	0.9
Standard Oil s200	50.0	860.9	0.092	1	1.5	1.1
Standard Oil s200	80.0	842.8	0.025	1	2.2	1.9

* The error is the difference between the CVO data and the value of the viscosity specified by the manufacturer

The standard deviation (Std Dev) is the measured variation in the CVO results

From the data collected the CVO has an average error of 1.3% with an average standard deviation in results of 1.4%. The error and spread of the data increases as the fluid viscosity decreases, but even for the relatively low viscosity, seen in the standard oil at 80°C, the error is still acceptably small. However, this viscosity value probably represents the lower limit of the CVO's measurement range.

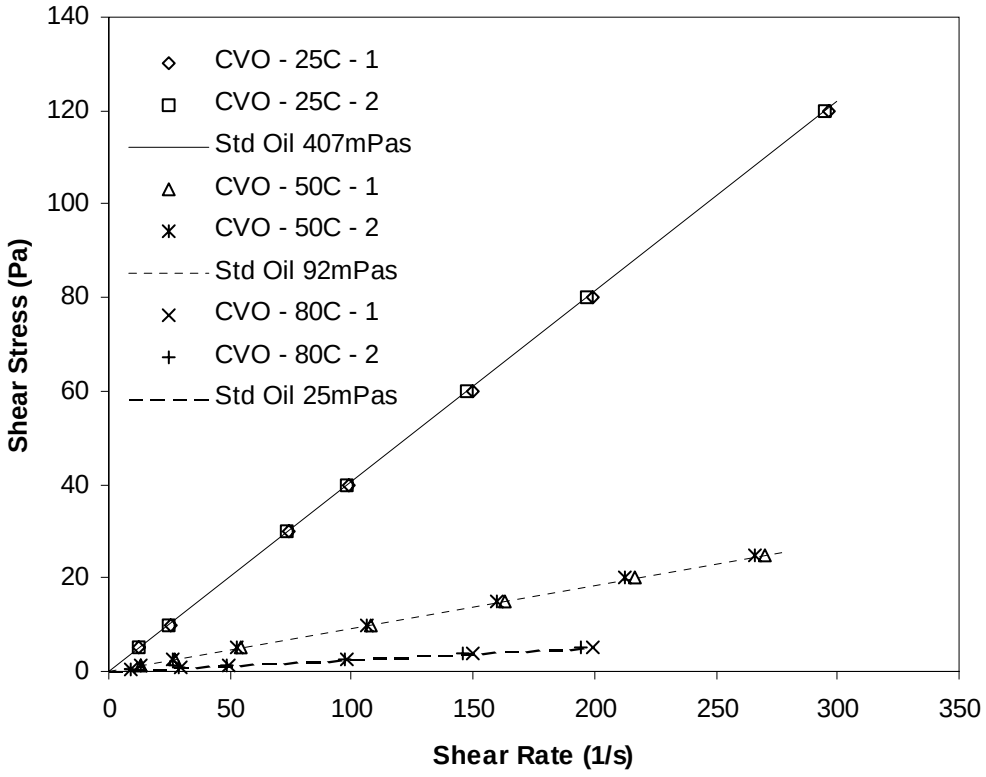

Figure 6.4-2 Rheological results for the Std Oil s200

6.4.2 Haake VT 550 – Controlled Rate Viscometers

The VT 550 is a controlled rate viscometer, manufactured by ThermoHaake and consists of a constant speed motor, torsion bar and position detector. The resistance to rotation of a solution being examined causes a deflection in the torsion bar when an attached bob or vane is rotated at a given speed. The degree of deflection is measured and this in conjunction with the stiffness of the torsion bar enables the resistive torque generated by the fluid and hence the shear stress to be determined. The VT 550 has an operating speed range of 0.5 to 800 rpm.

6.4.2.1 Measurement Geometries

The Haake VT 550 essentially uses bob and cup type geometries though other types of plate geometries can be used, with suitable attachments. For most experiments a single cup of 42mm diameter was used complete with a water jacket for temperature control. The water jacket is connected by silicon tubing to a Thermoline water bath (manufactured by Thermoline, Australia) which can be used to control the temperature from -10°C to 105°C. Three different, smooth surface, automatic immersion depth bobs, see Figure 6.4-3a, were available, MV I: 40.08mm diameter, MV II: 36.8mm diameter and MV III: 30.4mm diameter. Several different vanes, Figure 6.4-3b, were also available, a 20/40, a 10/20 and a 40/50, where the first number denotes the vane width in mm and the second number the vanes length in mm.

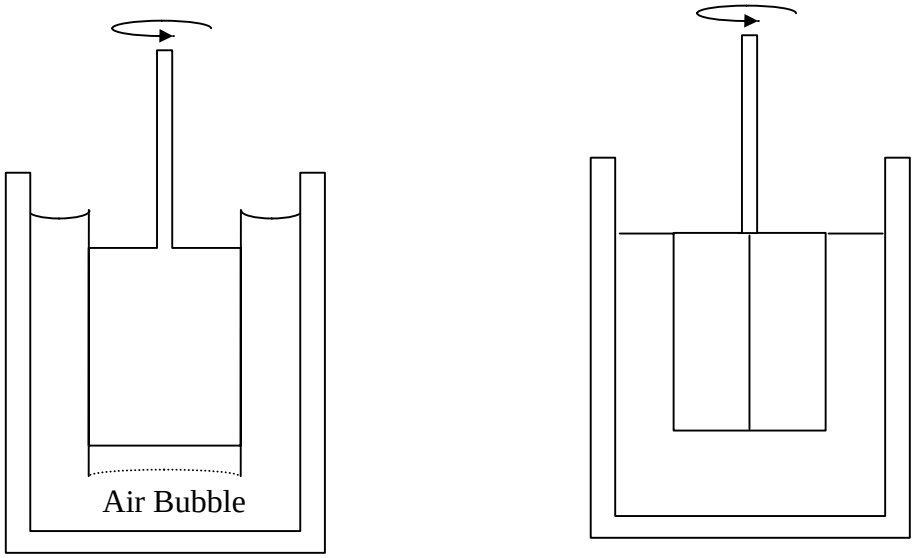

Figure 6.4-3 a: Automatic immersion depth bob; b: Vane in cup

6.4.2.2 Zeroing the Rheometer

To ensure that the Haake VT550 provided accurate measurements at low values of measured torque, where the sensitivity was likely to be reduced, an appropriate zeroing procedure was required. The selected geometry whether it was a bob or a vane was first screwed into place and then set rotating in air at an appropriate speed given the forth-coming test conditions and the torque measured. The measured value was adjusted until a value of zero was attained. The instrument was then stopped. At this point the instrument sometimes showed a torque value which was no longer zero. However, as it was the dynamic torque and not the stationary torque that was required to be zero, no further adjustments were made to the zero position.

6.4.2.3 Loading a Sample

Bob and Cup

The bob and cup geometry was loaded as shown in Figure 6.4-3a. Approximately the correct amount of sample was placed in the cup and the cup was then pushed up through the water jacket into position. The more viscous the liquid the slower the procedure was performed so as to ensure the integrity of the air bubble at the base of

the cup. Once secured in position the top of the bob was examined. A small amount of excess liquid could flow into the top recess of the cup. However, a large amount of excess liquid would fill this recess entirely leading to inaccurate results. This excess liquid if present was removed from the top of the bob with either a spatula or a syringe.

Vane

A suitable amount of test solution was loaded into the cup, such that when it was placed into position it matched that shown in Figure 6.4-3b. The cup was placed in position so as to minimise any lateral movement (also know as the stress of loading) so that the yield stress could be accurately determined. A bench top scissor-lift was often used to aid the loading process.

.

6.4.2.4 Modes of Operation/ Data Acquisition

Essentially two different types of tests can be performed with the Haake VT 550 rheometer, a sweep or ramp test and a constant rate test.

Sweep Test

The sweep test involved a continuous acceleration of the instrument from a set rotational speed to another set speed in a given period of time, followed usually by a return to the original speed in usually the same period of time. This test procedure can produce a hysteresis loop if the acceleration rate is set too high, especially if the fluid and instrument response times are slow. A hysteresis loop should normally only be observed when time dependent fluids are examined, so to avoid incorrectly identifying the fluids rheological properties this test procedure was not regularly used.

Constant rate

To determine the rheological properties from a constant rate experiment a series of tests were performed and the average steady state values of torque and rotational speed from each test were used. This procedure was less susceptible to errors from slow machine and fluid response times, though generally more experimental time was needed to develop the rheological profile of the fluid, so problems such as evaporation

and particle settling were also considered. This test procedure because of its greater accuracy and reliability was used almost exclusively.

Data Acquisition

A desktop computer with a specially developed Visual Basic program was used to control the VT 550 and perform the data acquisition. This data acquisition software was specifically developed for the flow rheometer, see section 5.5. This software proved to be quicker and more reliable than the Rheowin software that was supplied with the VT 550 and so was used in preference.

6.4.2.5 Analysis of results

The analysis procedures for measurements from the VT 550 with different geometries are outlined below, but in general the aim is to determine the shear stress and shear rate from the measurements of torque and rotational speed respectively.

Bob and Cup

The shear rate in a concentric cylinder, particularly a wide gap geometry, is not constant across the measurement gap width, which is particularly relevant if non-Newtonian fluids are examined. The Krieger and Maron method described in section 3.2.2.2 may be used to determine the shear rate in a wide gap concentric cylinder geometry for an unknown non-Newtonian fluid. On the other hand, if the behaviour of the fluid is known and can be well described by a simple rheological model, eg. Newtonian or power-law, then the shear rate may be directly determined, see the discussion in section 3.2.2.2. The shear stress calculation is independent of the rheological properties of the fluid examined and is described in section 3.2.2.1.

Vane

When the vane geometry is used to determine the yield stress property of a fluid, then only the torque is measured as the shear rate is assumed to be approximately zero. The peak in a graph of torque versus time is used to determine the yield stress. The calculations to determine the yield stress or shear stress from a vane geometry are described in section 3.2.2.5.

6.4.2.6 Experiments Involving Standard Liquids

To determine the accuracy of measurements from the Haake VT 550 and also the data analysis procedure a variety of basic fluids were tested with the instrument. The particular emphasis in this series of experiments was to examine the accuracy of measurements of non-Newtonian fluids in wide gap Couette geometries, where corrections to the calculations are required to determine the correct shear rate in the geometry. The fluids examined are presented in Table 6.4-II, as are results from the Haake VT550, which are compared to measurements from the Bohlin rheometer (CVO). Measurements from the Bohlin rheometer were performed using the cone and plate geometry as it provided the most accurate results for Newtonian and non-Newtonian liquids that contained no solid particles. The reason for this is that the shear rate calculations for a cone and plate geometry require no corrections when non-Newtonian fluids are examined. The experiments performed on the VT550 were a series of constant rate tests performed in a random order to reduce the chance of systematic errors.

Table 6.4-II Experimental Fluids

Fluid	Temp (^oC)	τ_y (Pa)	A ($Pa.s^n$)	n	Error (%)	Std Dev (%)
Std Oil s200	20	-	0.587	1	0.2	2.4
CMC 0.5 wt% (c600)	20	-	0.449	0.65	1.0	3.2
Polyox 1.2 wt%	20	-	0.047	0.92	0.4	7.3
Xanthan gum 0.25 wt%	20	1.8	0.065	0.73	0.8	2.0

The results of the experimental measurements of the various fluids are presented in Figure 6.4-4 to Figure 6.4-7 with the comparative errors between the VT550 and CVO presented in Table 6.4-II. In general good agreement is noted between the measurements from the VT550 and the CVO with no more than a 1% error in the results from the VT550 and a standard deviation in results of generally between 2-3%. The results of the measurements with the polyox solution show a larger degree of

deviation of 7.3%, which is not unexpected given the very low viscosity of the polyox solution, which makes measurements in a wide gap geometry like the MV III more difficult. Therefore this probably represents the lower limit of the VT550's measurement range with the MV III geometry.

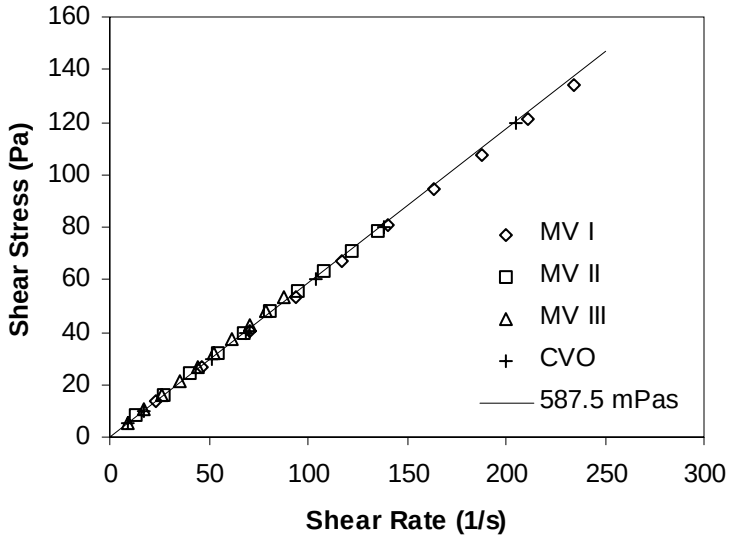

Figure 6.4-4 Rheological results for the Std. Oil s200

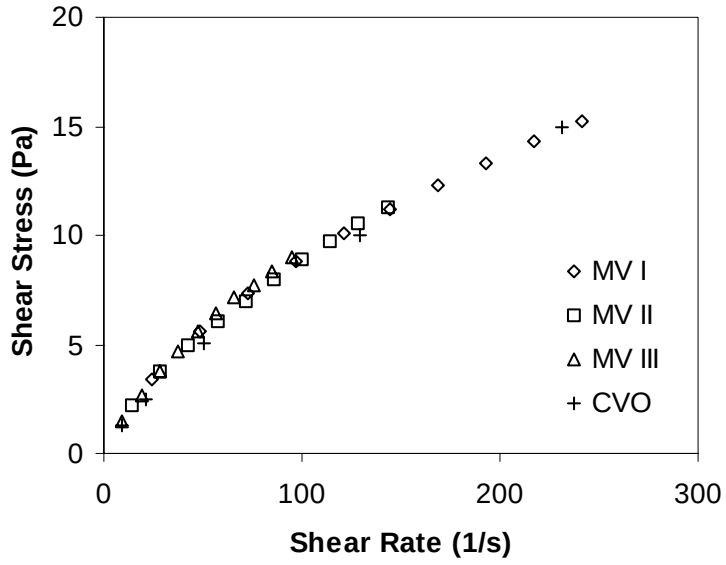

Figure 6.4-5 Rheological results for the CMC 0.5wt% (c600)

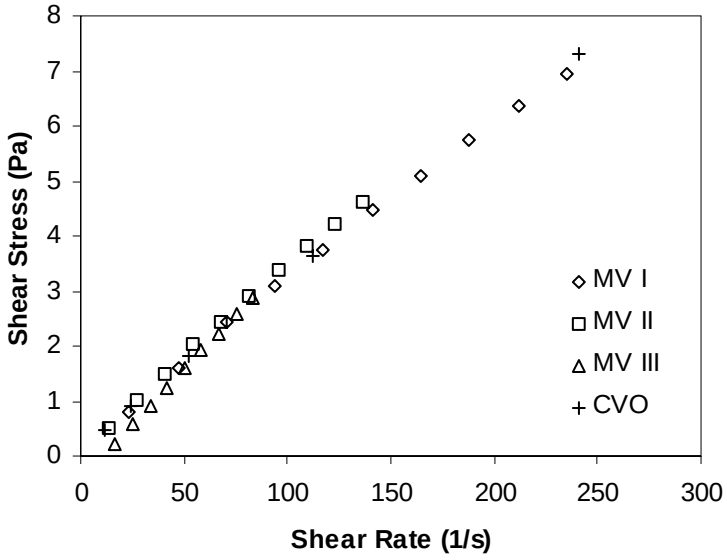

Figure 6.4-6 Rheological results for the polyox 1.2 wt%

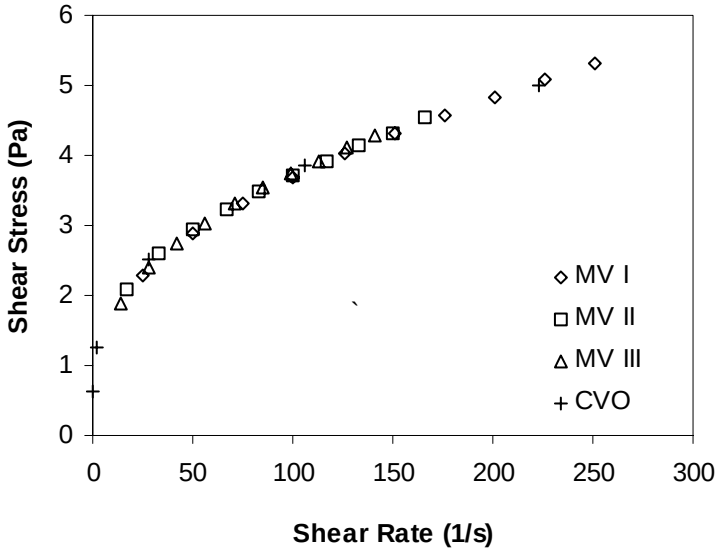

Figure 6.4-7 Rheological results for the xanthan gum 0.25wt%

6.5 Tube Rheometer

The two instruments previously discussed, the Bohlin CVO and the Haake VT 550 are generally not suitable for the measurement of particulate systems where the particles settle under the influence of gravity. To enable a comparison of measurements of settling slurries performed with the flow rheometer, described in Section B, another instrument that could reliably measure particulate suspensions was required. A modified tube rheometer was designed and constructed as part of this study and is described below.

6.5.1 Experimental Apparatus

Typically a tube rheometer consists of three major components: a pressurised holding tank or reservoir, tubes of varying length and diameter and a flow rate measurement device. To enable the tube rheometer to measure slow settling slurries an impeller was placed within the reservoir. A schematic of the tube rheometer is presented in Figure 6.5-1 and photograph is presented in Figure 6.5-2. The pressurised reservoir was made of 3mm 316 stainless steel and had an internal diameter of 161mm and a length of 343mm giving a total volume of approximately 7L. The top and bottom end plates were attached via 30mm flanges and eight bolts. With 2mm thick rubber gaskets used to seal the top and bottom flanges of the vessel. A boss was attached to the centre of the top plate to hold two sealed roller bearings, which were used to locate and seal the drive shaft for the impeller. The top plate also contained a 1” BSP threaded hole with plug, so that a sample of test fluid could be placed within the vessel without removing the top plate. Finally two ¼” fittings were placed in the top plate for the supply of compressed air and for a safety relief valve. The base plate contains a single ¾” olive type fitting through which the various tubes could be attached.

Several different tubes were available, all were 1000mm in length, but had varying internal diameters of 4.6mm, 4.98mm, 6.78mm and 7.95mm. By careful selection of the tube length to diameter ratio end effects could be avoided or significantly minimised (Bagley 1957, Van Wazer et al. 1963).

Several different impellers were tried; a combined helical screw and anchor impeller and a combined Rushton turbine and anchor impeller. When operated at even relatively slow rotational speeds, the helical screw and anchor impeller provided so much lift that liquid flow down the tube was significantly reduced when this impeller was in operation and thus the combined Rushton turbine and anchor impeller was used instead.

The impeller was driven by a 0.18kW single-phase DC electric motor (manufactured by Balder Electric Co. USA) with an analogue variable speed controller (manufactured by KB Electronics Inc. USA).

Compressed air was supplied to the laboratory by the main building compressor. A high flow rate, high precision pressure regulator (manufactured by Norgren UK) in conjunction with a Norgren 1” pressure gauge was used to control the pressure within the reservoir.

The flow rate of the test liquid exiting the apparatus was measured using a mass balance (manufactured by Ohaus Corporation USA) and a suitable collection bowl, both of which were placed approximately 10cm directly below the tube outlet. The balance was connected to a computer using an RS232 interface. A computer program written in Visual Basic was used to record the mass measured on the balance every three to five seconds. This mass flow when combined with the known density of the fluid was used to determine the flow rate of fluid exiting the tube.

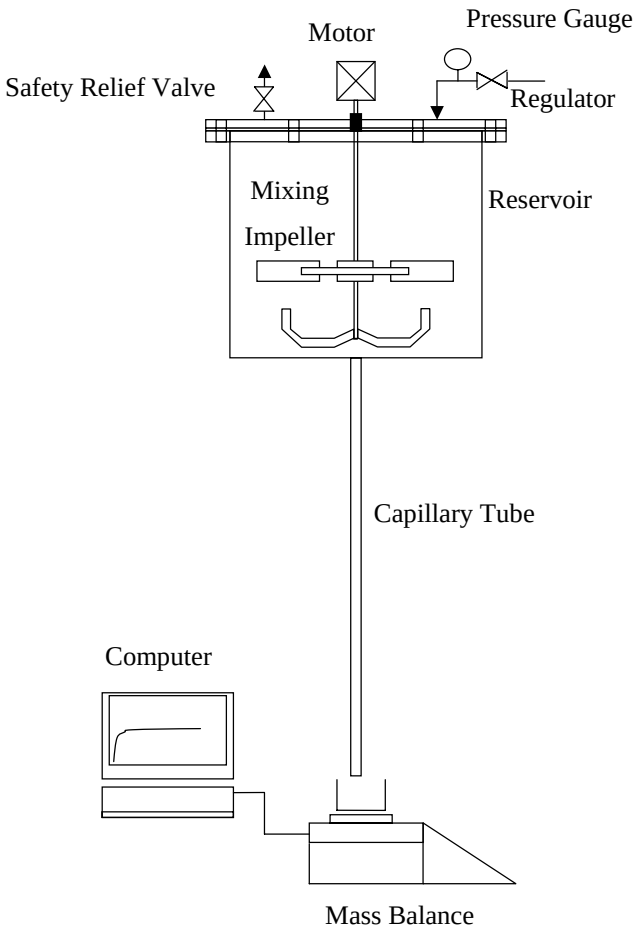

Figure 6.5-1 Schematic of the tube rheometer

Figure 6.5-2 Photograph of the tube rheometer

6.5.2 Experimental Techniques

Experiments with the tube rheometer generally required the preparation of approx 7-8L of test solution. A variety of liquids were used to test the accuracy of the instrument, see section 6.5.4. The density of the experimental fluid was needed to complete the calculations and thus before a fluid was tested in the tube rheometer the density of the fluid was measured using a 50mL-density bottle, see section 6.2.3.

For an experiment with the tube rheometer, the test fluid was transferred to the reservoir and the impeller switched on if required. A small Teflon plug was used to prevent fluid escaping from the end of the tube. The temperature of the sample was measured, as was the depth of fluid within the reservoir. The Visual Basic computer program was started and once connection with the balance was established the Teflon plug was removed and the desired pressure set using the regulator. The fluid flow rate out of the tube was then measured until a constant flow rate was established. To ensure the flow rate had reached a constant value the measurement period was typically two minutes though this value sometimes varied depending on the fluid flow rate. At the completion of the test, the pressure was returned to zero gauge, the Teflon plug was replaced and the total mass of fluid that had flowed from the reservoir was recorded. A series of six to ten tests were then performed at various different values of gauge pressure.

6.5.3 Analysis of Results

Raw data from the tube rheometer tests were saved in specially formatted text files by the Visual Basic program and these files were then imported into Excel using a macro-based program. A series of calculations were performed to determine the rheological properties of the fluid, these calculations are discussed in section 3.3

6.5.4 Experiments Involving Standard Fluids

To determine the accuracy of the data acquisition and analysis procedure for the tube rheometer a variety of simple fluids were examined within the instrument, Table 6.5-I and the results compared to those obtained on the Bohlin rheometer (CVO) using the 4°/40mm cone and plate geometry.

Table 6.5-I Experimental Fluids

Fluid	Temp (°C)	Density (kg/m^3)	τ_y (Pa)	A (Pa.s^n)	n	Error (%)	Std Dev (%)
Glycerol	16	1258	-	1.05	1	1.9	2.7
CMC 1.5wt % (c600)	16.5	1012	-	15.9	0.36	1.5	3.4
Carbopol 1.5wt% pH 2.7	16.5	1005	14	0.59	0.67	1.2	4.0

The results are presented in Figure 6.5-3 to Figure 6.5-5, and results from the tube rheometer are distinguished by the tube diameter used. When compared to the CVO results, the tube rheometer results show an average error of 1-2% with a standard deviation of 3-4%. While these values are somewhat less accurate than the Haake VT 550, section 6.4.2.6, the results show that the tube rheometer was still acceptably accurate for rheological measurements. There is some variation (~10%) visible at high values of shear rate (+1000 1/s) in the CMC data, Figure 6.5-4. The actual flow rates necessary to obtain these shear rates in the 7.95mm tube were approximately 50 mL/s and these high values of flow rate probably represent the measurement limit of the apparatus. Wall and end effects appear to be minimal as tests with different tubes with different length to diameter ratios give the same results for the different types of fluids examined.

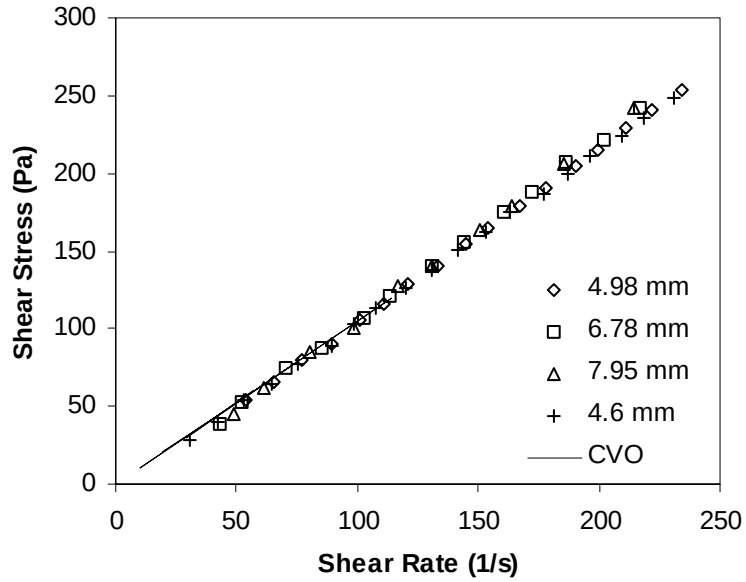

Figure 6.5-3 Rheological results for the glycerol solution

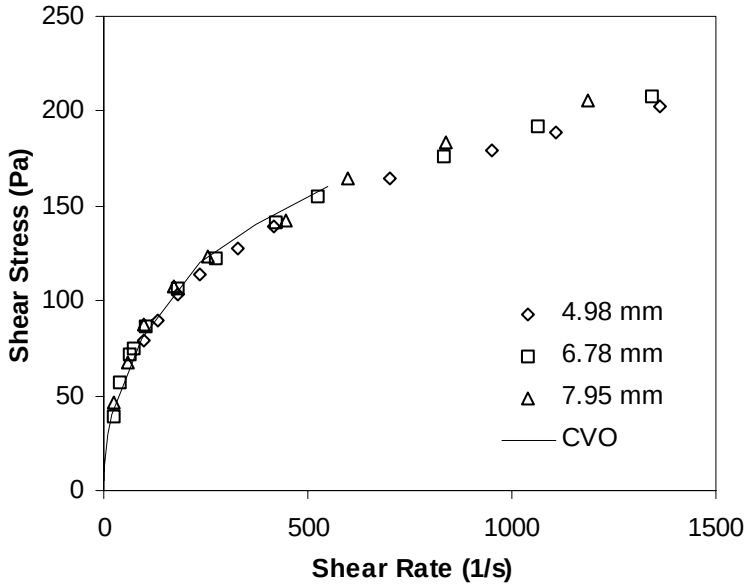

Figure 6.5-4 Rheological results for the CMC 1.5 wt% solution

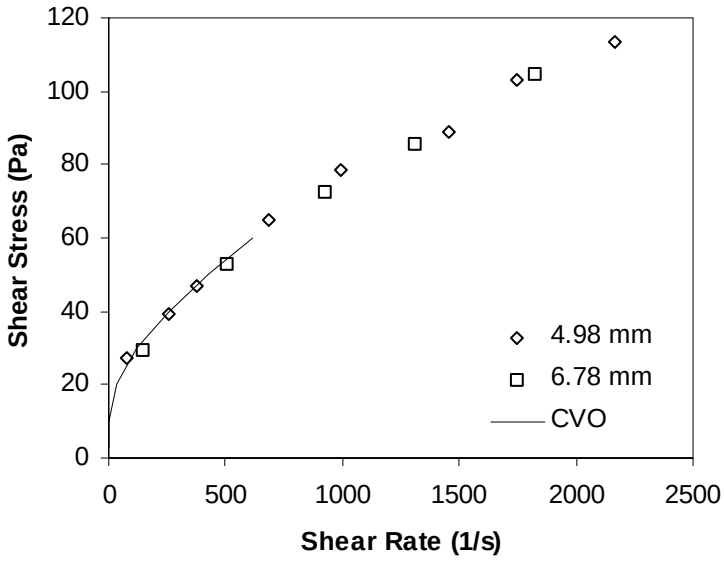

Figure 6.5-5 Rheological results for the 1.5wt% carbopol solution, pH 2.7

6.6 Summary

A wide variety of experimental fluids (including Newtonian, pseudoplastic and yield stress) were used to study the accuracy of rheological measurements from a variety of different laboratory instruments, including a controlled stress rheometer (CVO), a controlled rate rheometer (Haake VT 550) and a purpose built modified tube rheometer. Experimental results indicate the accuracy of the measurement techniques for a variety of different fluids with varying rheological properties. Other measurement techniques and apparatus used to determine density and particle size distributions were also successfully validated.

CHAPTER 7 EXPERIMENTAL VALIDATION OF THE FLOW RHEOMETER

7.1 Introduction

To demonstrate the accuracy and reproducibility of the experimental techniques and the data analysis procedure for the flow rheometer a wide variety of liquids and slurries with different rheological properties including Newtonian, pseudoplastic and yield pseudoplastic behaviours were tested. The results of these measurements were compared with results generated on other laboratory instruments and are presented and discussed in this chapter. A difficulty in the measurement of yield stress materials at low values of shear rate was encountered; this problem and its solution is also presented and discussed.

7.2 Experimental Procedures

For an experiment with the flow rheometer the differential pressure across the bob was first selected by adjusting the rotational speed of the pump. If settling particles were present it was necessary to ensure that the axial flow rate was sufficient to maintain the particles in a homogeneous suspension, particularly if very slow flow rates were required. The following Equation (5.3-1), can be used to determine the minimum velocity to prevent particles settling in a horizontal section of pipe (Spells 1955).

$$v_m^{1.225} = (0.0251) d_{85} g \left(\frac{2R\rho_s}{\eta} \right)^{0.775} \frac{\rho_p - \rho_l}{\rho_l} \qquad (5.3\text{-}1)$$

The bob was then set rotating at a constant speed and the torque measured as a function of time. Once a stable torque reading was established another rotational speed was selected and the torque again measured. The change in rotational speed could alter the value of differential pressure across the bob and so the speed of the pump and thus the fluid flow rate was adjusted to maintain a constant value of differential pressure. For a single value of differential pressure a series of eight to ten different values of rotational speed were selected and the torque and flow rate measured. The differential pressure was then adjusted to a new value and the procedure repeated. A graphically summary of the experimental procedure is presented in Figure 7.2-1.

Given that sufficient time must elapse for the flow rate, differential pressure and rotational speed to stabilise, a ramp test (where the rotational speed is continuously increasing and/or decreasing with time) cannot be reliably performed, as the axial flow significantly dampens the measurement response time. Also if the speed of rotation of the bob affects the differential pressure the feedback time required to adjust the flow rate through the pump to compensate for this change would be too slow and the accuracy and reliability of the readings would be affected.

The density of the experimental liquid was also required and this measurement was performed using either a density bottle or a pair of small measuring cylinders, see section 6.2.3.

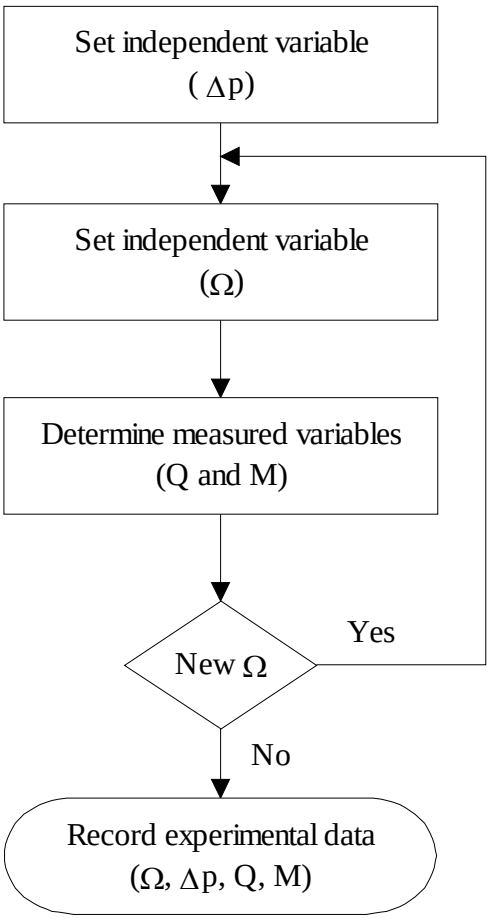

Figure 7.2-1: Experimental procedure for the flow rheometer

7.3 Results from the Flow Rheometer

During the validation of the flow rheometer a complication was encountered when measuring the properties of yield stress fluids at low values of shear rate. The analysis procedure, CHAPTER 4, assumes that the power-law model can predict the rheological properties of the experimental fluid, but at very low values of shear rate the power-law model cannot accurately predict the properties of a yield stress fluid. This chapter has therefore been separated in to two sections; firstly those fluids, which are not characterised by a yield stress are examined and then those fluids that are characterised by a yield stress are separately discussed in detail.

7.3.1 Non – Yield Stress Materials

The non - yield stress fluids examined are shown in Table 7.3-I and include a Newtonian liquid; a glycerol solution, a non-Newtonian polymeric solution; a 1.5% wt. CMC solution (C600 Grade), a settling mineral slurry; a 68wt% fly ash slurry (provided by CSIRO Minerals) and a rapid settling mineral slurry; a 36wt% gold mine tailings (provided by Rio Tinto Technical Services). The particle size distribution of the fly ash slurry and the gold mine tailings may be found in section 6.3. The rheological properties of the two pure liquids were measured using the Bohlin CVO rheometer, see section 6.4.1, using the 4°/40mm cone and plate geometry. The rheological properties of the fly ash slurry were measured using the tube rheometer, see section 6.5.

Table 7.3-I Experimental Fluids

Fluid	Temp (ºC)	Density (kg/m^3)	A ($Pa.s^n$)	n	Error (%)	Std Dev (%)
Glycerol solution	20	1248	0.773	1.0	0.7	2.2
CMC 1.5wt % (c600)	24	1003	8.68	0.45	0.3	1.6
Fly ash slurry 68wt%	15.5	1544	0.39	1.0	1.2	3.5
Gold mine tailings 36wt%	17.8	1854	0.73	0.81		0.9

The results of the experimental work are presented below in Figure 7.3-1 to Figure 7.3-4. Results from the flow rheometer are presented as shear stress versus shear rate for a variety of different values of differential pressure, where this value refers to the value of differential pressure across the geometry during the measurement period. To distinguish between results from the two different bobs of the flow rheometer; results obtained using the 32mm bob (a wide gap width) are represented by a ^{w}. The results from the tube rheometer are distinguished on the graphs below by reference to the diameter of the tube in which the measurements were performed.

A set of sample calculations relating to the measurements and analysis of the CMC solution is presented in APPENDIX C.

The results from the pure liquids and the fly ash slurry demonstrate good agreement between the flow rheometer and either the CVO (using the 4º/40mm cone and plate geometry) or the tube rheometer. As seen in Table 7.3-I there is a maximum error of only 1.2% with a maximum standard deviation of 3.5%. These results cover a wide range of values of differential pressure and different gap widths, thus validating the experimental and calculation procedures for non-Newtonian fluids in wide gap geometries.

The gold mine tailings, because of the settling rate, could not be measured in any other laboratory rheometer including the modified tube rheometer, so the standard deviation in the results presented is only a comparison between the results obtained on

the flow rheometer at different values of differential pressure. The gold mine tailings did not appear to have yield stress, which is probable due to the relatively low solids concentration, compared to the other mineral slurries examined in section 7.3.2.

The results for the non-Newtonian fluids are particularly important as they demonstrate that the data analysis procedure used to analyse the helical flow is correct. The addition of axial flow in a Couette flow system will increase the total shear rate in the system, which will change the rheological properties of a non-Newtonian fluid. Thus if the data analysis procedure did not properly account for the changes in the shear rate due to the additional axial flow, then different value of differential pressure (different axial flow rates) would be expected to produce different relationships between shear stress and shear rate for the one type of fluid. However, for the results presented in this study, for any given fluid, data obtained at different values of differential pressure (which is directly related to the axial flow rate) collapse on to a single curve, which validates the data analysis procedure for non-Newtonian fluids.

An important criteria in the design of the bob for the flow rheometer is that it should significantly reduce the errors associated with end effects. Examination of the bob at the end of experiments with slurries and other materials revealed only minimal penetration (2-3mm) of the fluid into the hollow base of the bob. There was also a distinctly clean section at the top of the bob confirming that the fluid was flowing out of the geometry at the correct point and not overflowing around the top of the bob.

Particle settling was an issue that could have affected the results from the flow rheometer. Examination of the interior of the flow rheometer at the conclusion of experiments with settling slurries showed some build up of solids on top of the lower insert. This build up however, did not appear to interfere with the rotation of the bob. For further conformation that there was minimal particle settling occurring within the flow rheometer, on several occasions the instrument was run for a period of several hours during which time no blockages occurred, thus validating the design of the instrument.

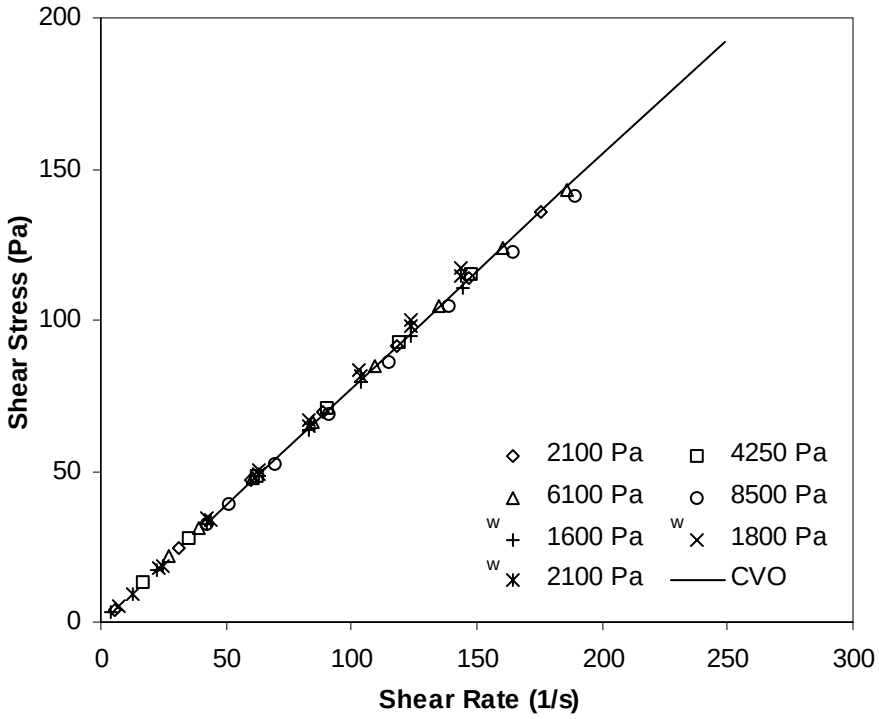

Figure 7.3-1 Rheological results for the glycerol solution

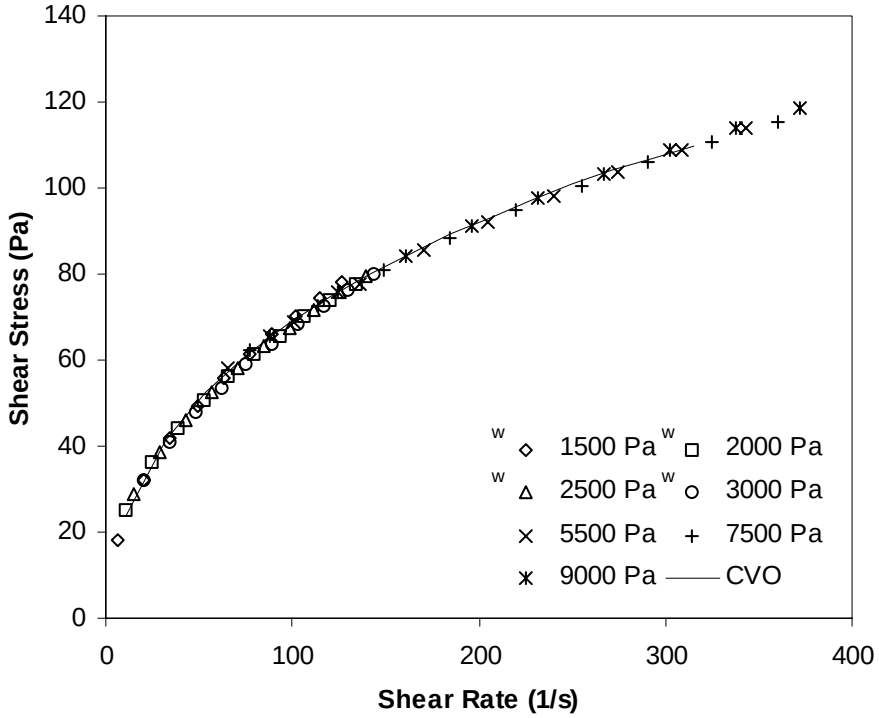

Figure 7.3-2 Rheological results for the 1.5wt% CMC solution

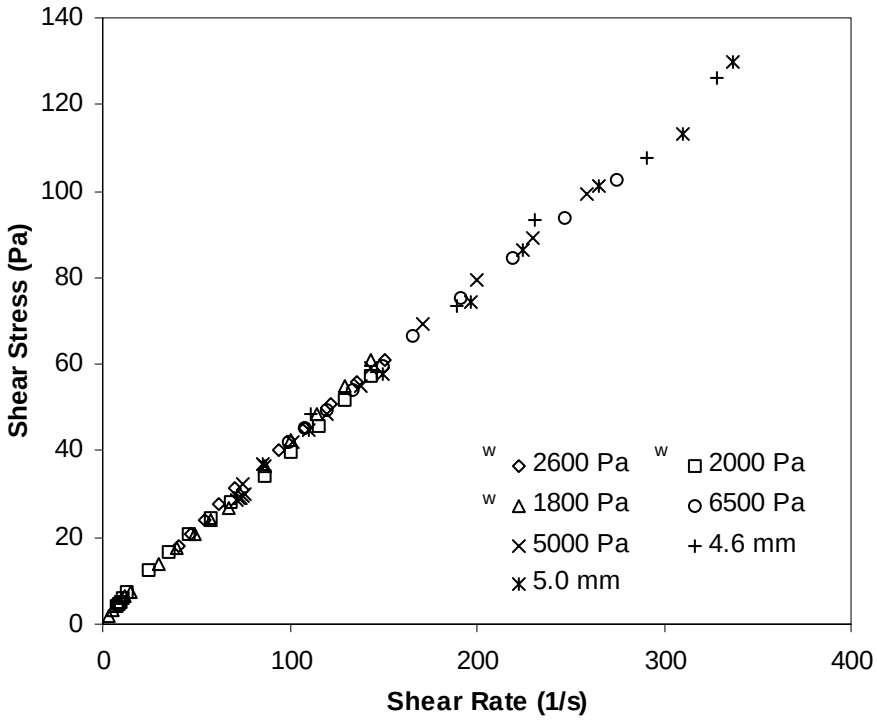

Figure 7.3-3: Rheological results for the 68wt% fly ash - water slurry

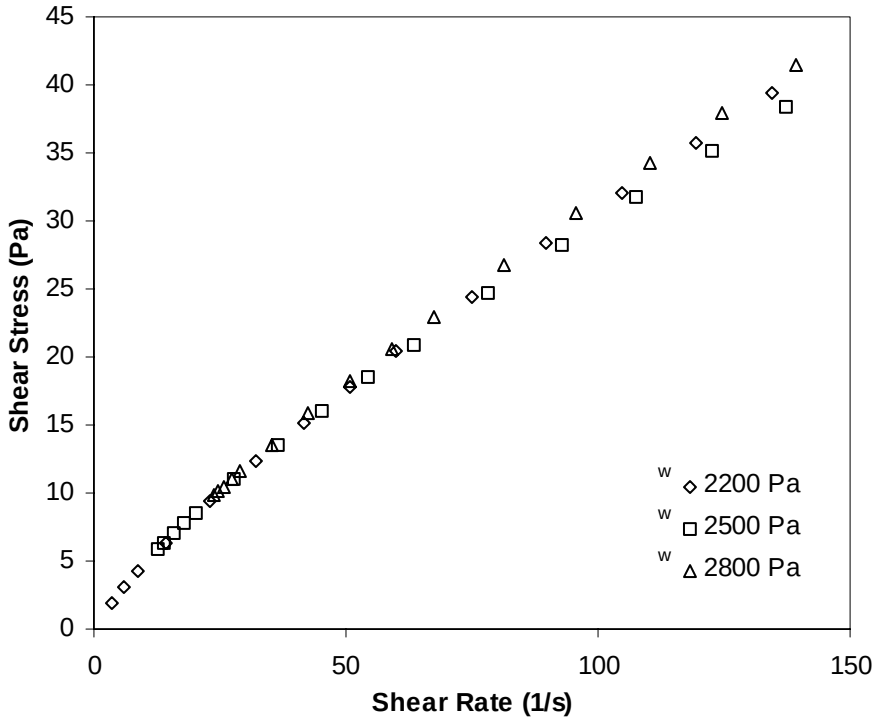

Figure 7.3-4 Rheological results for the 36wt% gold mine tailings

7.3.2 Yield Stress Fluids

In the analysis procedure it was assumed that the power-law model will fit the rheological properties of the experimental fluid over the range of shear rates examined. Under low shear rate conditions when a yield stress fluid is examined a significant difference could develop between the predicted rheological properties and the actual properties, see Figure 7.3-5.

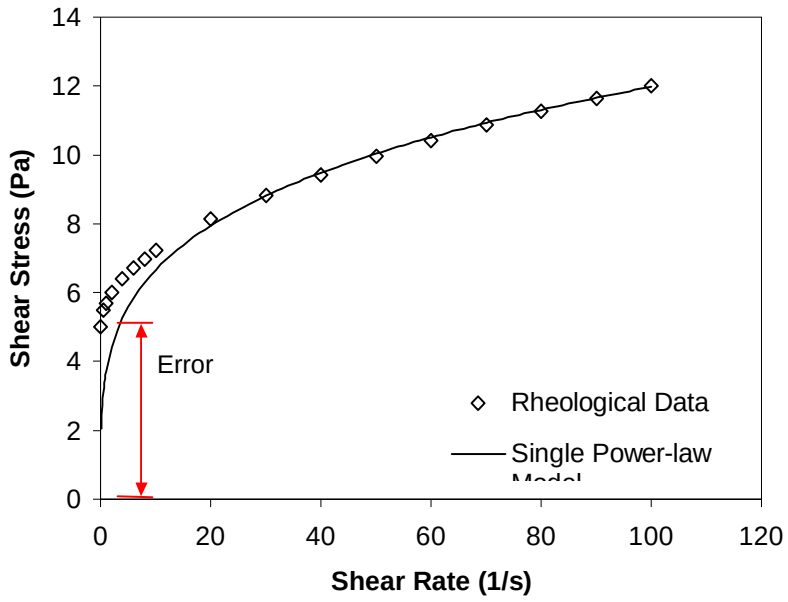

Figure 7.3-5 Representation of the error in predicting properties of a yield-stress fluid using the power-law model

7.3.2.1 Modifications to the Calculations

To improve the accuracy of the fit of the rheological data of a yield stress fluid by the power-law model, a multi-power-law model is used. For the multi-power-law model several different power-law models, each covering a smaller range of shear rates, are used to improve the description of the rheological properties of the yield stress fluid over a given range of shear rates. The improved fit can be seen in Figure 7.3-6 and also in Table 7.3-II, where there is a significant improvement in the R^2 fitting parameter of both segments of a two-part power-law model compared to the single power-law model.

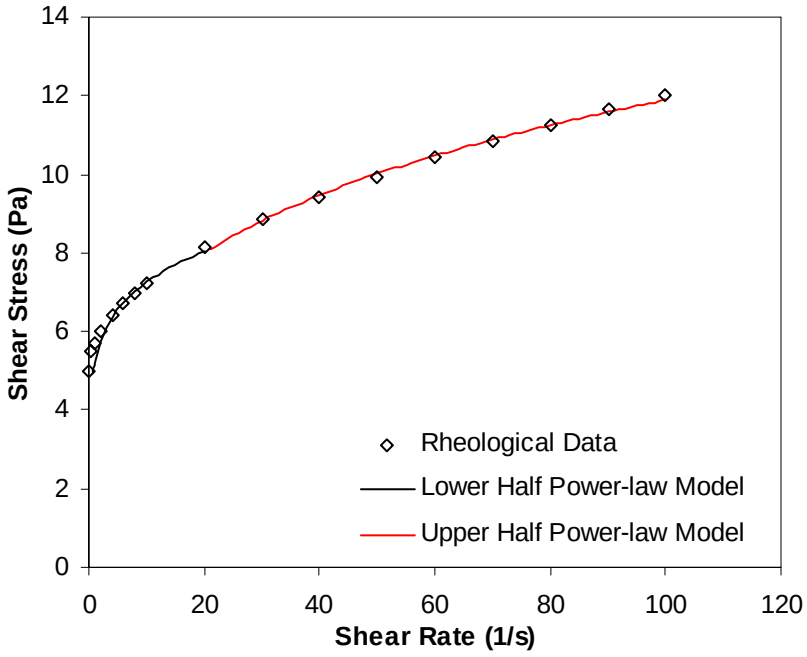

Figure 7.3-6 Error in predicting yield-stress fluid properties using two power-law models

Table 7.3-II Comparison between a single power-law model and a two-part power-law model

Model	τ_y	A	n	R^2
Herschel-Bulkley (rheological data)	5	0.7	0.5	-
Predictive models				
Single power-law	-	3.7	0.26	0.895
Two-part power-law (lower-half)	-	5.2	0.15	0.978
Two-part power-law (upper-half)	-	3.8	0.25	0.997

For experimental measurements of a non-yield stress fluid with the flow rheometer, between eight and ten different values of rotational speed are selected for a particular value of differential pressure. For yield stress materials the test procedure was modified to minimise the errors at low shear rate values due to the poor fitting of the

single two-parameter power-law model, see Figure 7.3-5. The standard test of eight to ten measurements was broken down into a series of smaller sub-tests so that a smaller range of rotational speeds (or shear rate values) were covered by each test, but overall the same range of shear rates would be covered as the single larger test. For example three groups of five measurements at a particular value of differential pressure were performed instead of the standard single group of eight to ten measurements. The procedure was then repeated for several different values of differential pressure. This procedure is summarised in Figure 7.3-7.

Typically the raw data from the measurements of a non-yield stress fluid are analysed in an Excel spreadsheet, as one group of measurements for each value of differential pressure. For each value of differential pressure a single value for each of the two model parameters A and n is then determined. For yield stress fluids the procedure is a little different, each of the smaller sub-tests is individually analysed and thus for one value of differential pressure a series of A and n values are determined for each of the sub-test that comprise the total test. Once the shear stress and shear rate values from each sub-test are determined they are recombined and presented as one complete data set for each value of differential pressure. In this way by allowing multiple sets of A and n to describe the fluid's rheological behaviour the two-parameter power-law model, Equation (2.2-3) can be used to describe the rheological properties of a yield pseudoplastic fluid, which would normally require a three-parameter model such as the Hershel-Bulkley model. This modification to the analysis procedure is also outlined in Figure 7.3-7.

A possible future development of the data analysis procedure for the flow rheometer would be to incorporate the Herschel-Bulkley three parameter model instead of the two parameter power-law model, to eliminate the need for a modified measurement procedure. This further development of the analysis procedure and other possible directions for future work are discussed in section 18.3.

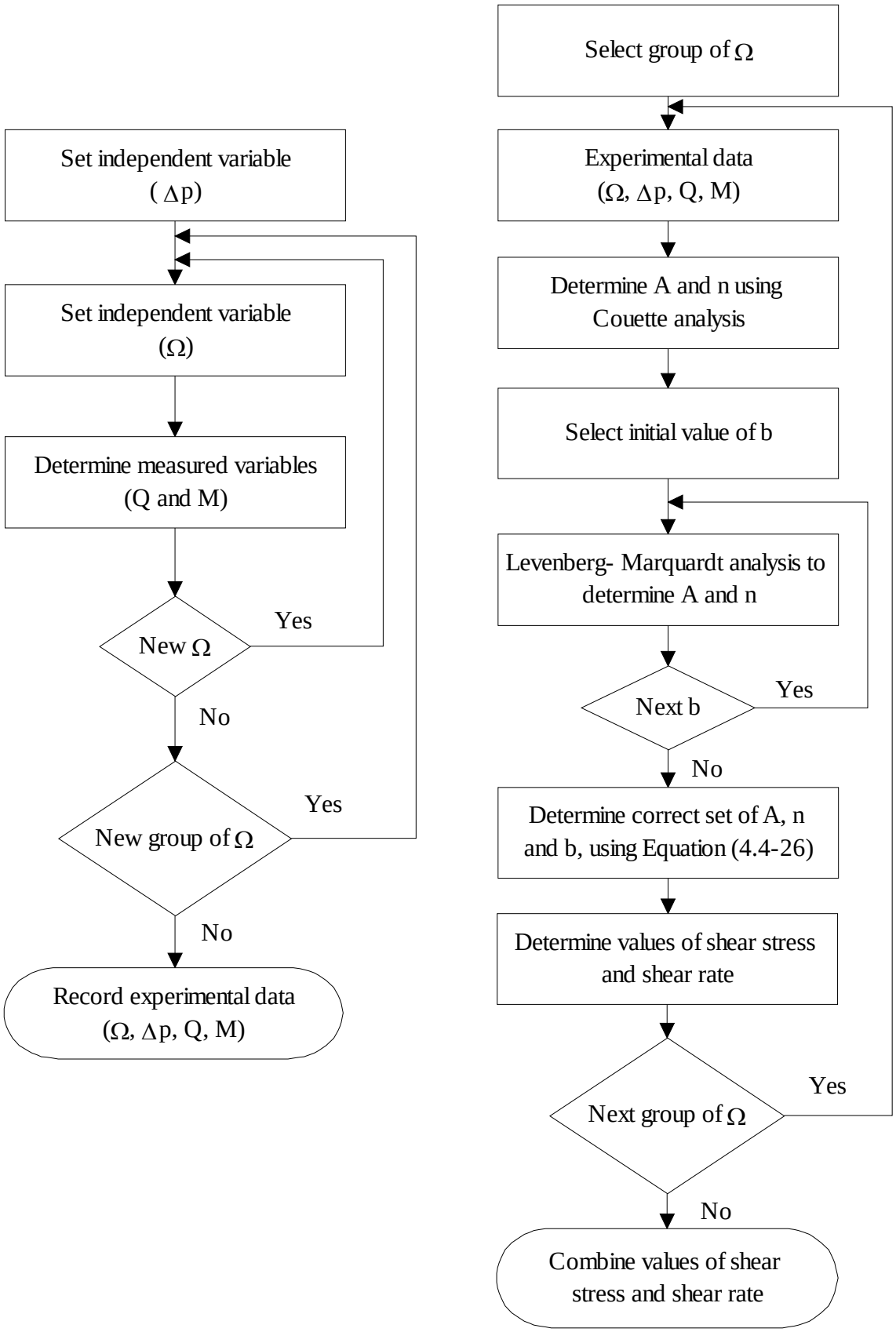

Figure 7.3-7: Experimental and data analysis procedures for yield stress fluids

7.3.2.2 Results

The yield stress fluids used in this investigation are shown in Table 7.3-III and include a yield pseudoplastic polymeric solution; 1.5wt% carbopol (940 Grade), pH 2.7, a slow settling mineral slurry; 71wt% clay slurry, provided by Rio Tinto Technical Services and a rapid settling slurry, 49wt% diamond mine tailings, also provided by Rio Tinto Technical Services. The particle size distribution of the slurries may be found in section 6.3.

The carbopol solution was examined on the CVO rheometer using the 4°/40mm cone and plate geometry, however because of the solid particles in the slurries it was impossible to test them in the small gap cone and plate and parallel plate geometries of the CVO rheometer. The clay slurry was examined using the tube rheometer, section 6.5, however the settling rate of the diamond mine tailings was too rapid for the tube rheometer and so it was only examined using the flow rheometer. The results from the tube rheometer are distinguished on the shear stress, shear rate graphs below by reference to the diameter of the tube in which the measurements were performed. As with the previous section, results obtained using the 32mm bob in the flow rheometer are distinguished by a ^{w}. The results for the various fluids are presented in Figure 7.3-8 to Figure 7.3-10.

Table 7.3-III Experimental Fluids

Fluid	Temp (°C)	Density (kg/m^3)	τ_y (Pa)	A (Pa.s^n)	n	Error (%)	Std Dev (%)
Carbopol 1.5wt% pH 2.7	16.5	997	5.5	0.865	0.6	0.8	2.5
Fly ash slurry 68wt%	15.5	1544	3.1	0.39	1.0	1.2	3.5
Clay slurry 71wt%	16	1788	6.8	3.02	0.49	2.2	4.3
Diamond MT 49wt%	16.5	1442	6.3	0.44	0.48	-	1.5

The results from the yield stress fluids demonstrate a good agreement between the flow rheometer and the Bohlin CVO rheometer (for the carbopol solution) or the tube

rheometer (for the clay slurry). The large diameter of some of the particles in the diamond mine tailings also meant that only the wide gap geometry (32mm bob) could be used. The yield stress of the clay slurry was also determined using the vane method (Nguyen and Boger 1985), due to the slow settling rate, while extrapolation procedures were used to determine the yield stress of the diamond mine tailings (Kearsey and Bakshi 1996, Murdoch and Kearsey 1960). As can be seen in Table 7.3-III there is a maximum error of only 2.2% in the results between the flow rheometer and other laboratory instruments with a maximum standard deviation of 4.3% in the flow rheometer results. These results cover a wide range of values of differential pressure and different gap widths validating the modifications made to the data analysis procedure for yield stress fluids.

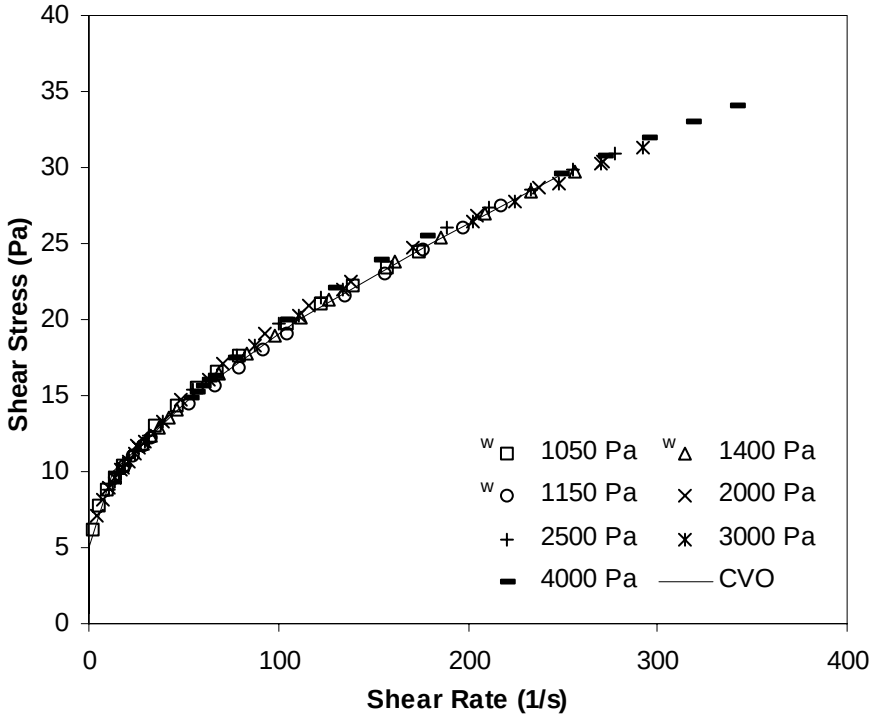

Figure 7.3-8: Rheological results for the 1.5wt% carbopol solution, pH 2.7

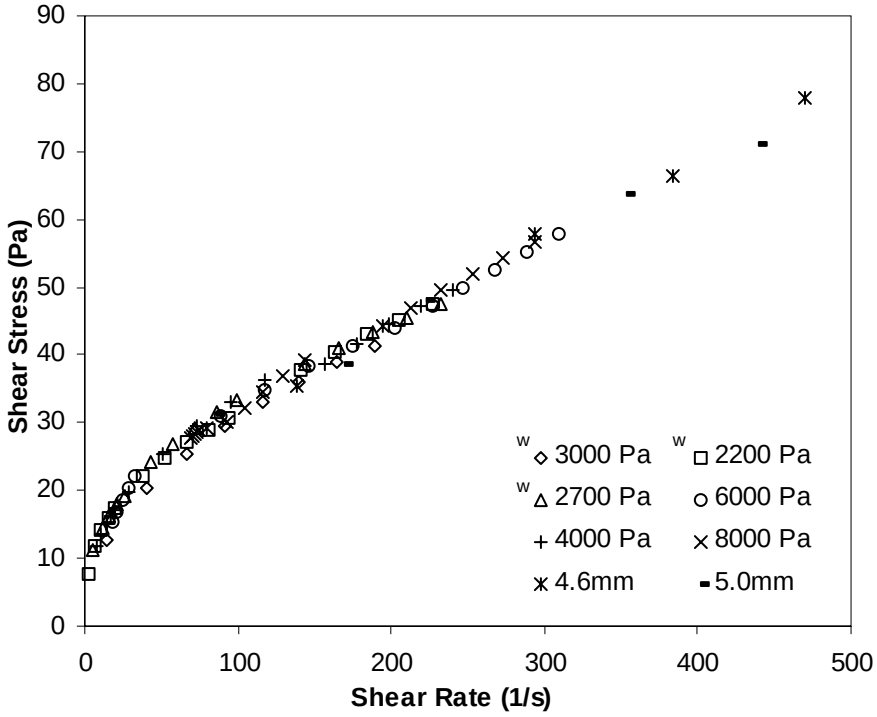

Figure 7.3-9: Rheological results for the 71wt% clay - water slurry

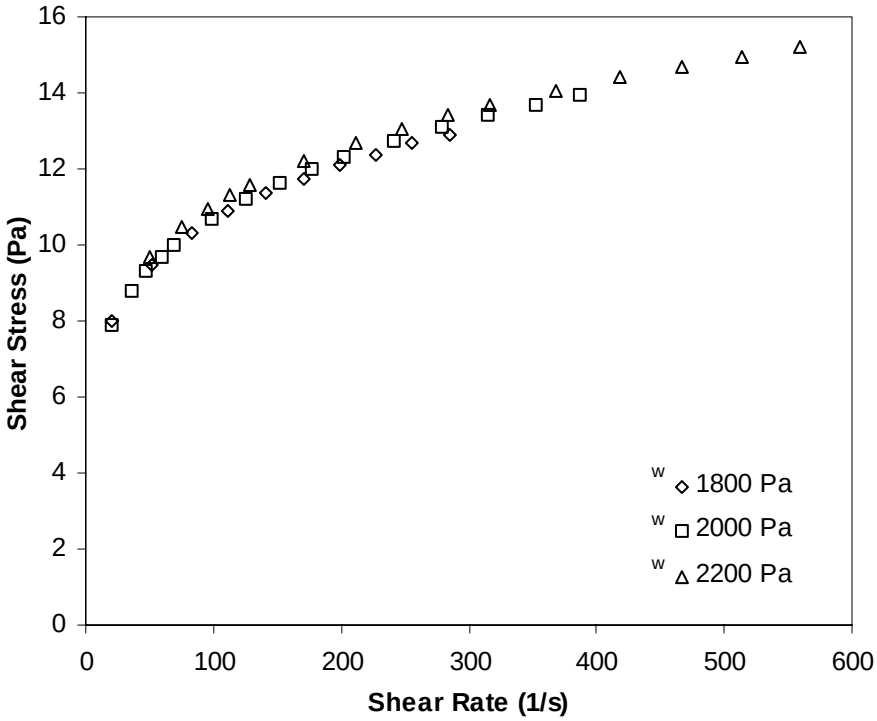

Figure 7.3-10: Rheological results for the 49wt% diamond mine tailings

7.4 Conclusions

To test and validate the accuracy of results from the flow rheometer a number of different fluids with different rheological properties were examined. These fluids included several Newtonian fluids a glycerol solution and a 68wt% fly ash slurry, several pseudoplastic fluids including a 1.5wt% CMC solution and a 36wt% gold mine tailing slurry and several yield stress fluids including a 1.5wt% carbopol solution, at pH 2.7, a 71wt% clay slurry and a 49wt% diamond mine tailing slurry. Each of these fluids were examined in the flow rheometer at different values of differential pressure and where possible (depending on the particle size distribution) the two different sized bobs were used.

For a comparison of the results from the flow rheometer, pure liquids were measured with the CVO using the 4º/40mm cone and plate geometry. For the slow settling slurries, comparison results were generated with a modified tube rheometer, also developed as part of this project. Good agreement was obtained between the results from the flow rheometer and results from both the CVO and tube rheometer.

The data analysis procedure for the helical flow of non-Newtonian fluids was validated by results from the flow rheometer generated at different values of differential pressure (or axial flow rate). The data obtained for different values of differential pressure for a given fluid all collapsed on to a single curve indicating that the changes in the total shear rate in the system due to changes in the axial flow rate were correctly predicted.

Complications and errors were introduced when yield stress fluids were examined and the power-law model was used to predict their rheological properties. However, a multi-power-law model was successfully used to improve the prediction of the rheological properties of yield stress fluids and reduce the errors associated with the measurement of these types of fluids.

CHAPTER 8 EXAMINATION OF THE AXIAL FLOW COMPONENT OF HELICAL FLOW

8.1 Introduction

A variety of researches Bhattacharya et al. (1990), Blaszczyk and Petela (1986), Ferrini et al. (1979), Reeves (1985) and Shi and Napier-Munn (1996) mentioned previously in section 3.4.3.2, used rheometers based on helical flow but ignored the contributions to the total shear rate made by the axial flow component in the data analysis. In most cases it was recognised that the rheological measurements would be affected by the addition of axial flow but in all cases the effect of the axial flow was not quantified and a calibration procedure was used to determine the rheological properties from the experimental measurements. In this chapter the errors in ignoring the axial flow component are discussed. Also discussed is an interesting consequence of the iterative analysis procedure used in this study, in which it has been shown that the calculations to determine the rheological properties of a fluid can be performed without measuring the axial flow rate.

8.2 Errors in Ignoring the Axial Flow Component

8.2.1 Newtonian Fluids

The errors associated with ignoring the axial flow component when a Newtonian fluid is measured are substantially less than those observed when non-Newtonian fluids are examined. A Newtonian fluid is unique compared to other types of fluids, as its rheological properties do not vary with shear rate and therefore any errors in the shear rate will not be apparent in any viscosity measurements, which should remain correct. However, there will be an error in the overall calculated value of shear rate that can be determined by comparing the axial flow portion of the shear rate, the 'rz' component, with the total shear rate, as shown in Equation (8.2-1).

$$\text{Error} = 1 - \frac{\dot{\gamma} - \dot{\gamma}_{rz}}{\dot{\gamma}} = -\frac{\dfrac{b}{\kappa R} - \dfrac{\kappa R}{2}\left(\dfrac{\partial p}{\partial z} + \rho g\right)}{\sqrt{\left[\dfrac{M}{2\pi(\kappa R)^2}\right]^2 + \left[\dfrac{b}{\kappa R} - \dfrac{c(\kappa R)}{2}\right]^2}} \qquad (8.2\text{-}1)$$

The actual error however, is highly dependent on the system dimensions and the operating conditions and a general error value cannot realistically be presented. An example of the wide variation in errors possible is shown in section 8.2.2 where non-Newtonian fluids are examined.

8.2.2 Non-Newtonian Fluids

For the case of a non-Newtonian fluid the apparent viscosity of the fluid is dependent on the shear rate and thus by ignoring the axial flow component in helical flow the calculated shear rate will be different to the actual shear rate within the geometry. As the rheological properties depend on the shear rate an incorrectly determined shear rate will lead to errors in the calculated rheological properties of the fluid.

The ratio of the two shear rate components (axial and rotational) to each other determines the size of the error, which will increase as the size of the axial flow rate component increases compared to the rotational component. To illustrate the effect that ignoring the axial flow rate can have on the results of non-Newtonian fluids, measurement data from the flow rheometer for a 1wt% CMC solution have been analysed with the axial flow component ignored. Thus experimental data collected from a helical flow test (torque and rotational speed) have been used to calculate shear stress and shear rate values using only Couette flow theory. For comparison, results are also provided which were calculated using full helical flow theory and are presented in Figure 8.2-1. The results from the Couette flow analysis are presented in Figure 8.2-2 and it can be seen that there is a significant disagreement between the Bohlin CVO rheometer and the flow rheometer data when pure Couette theory is used to analyse the helical flow data.

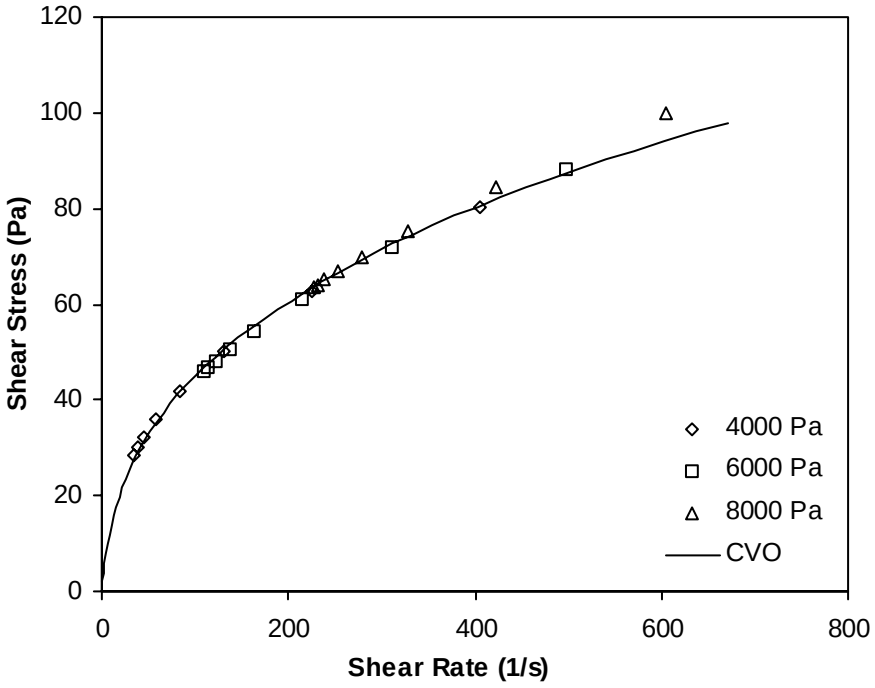

Figure 8.2-1 Helical Flow Analysis of 1 wt% CMC solution

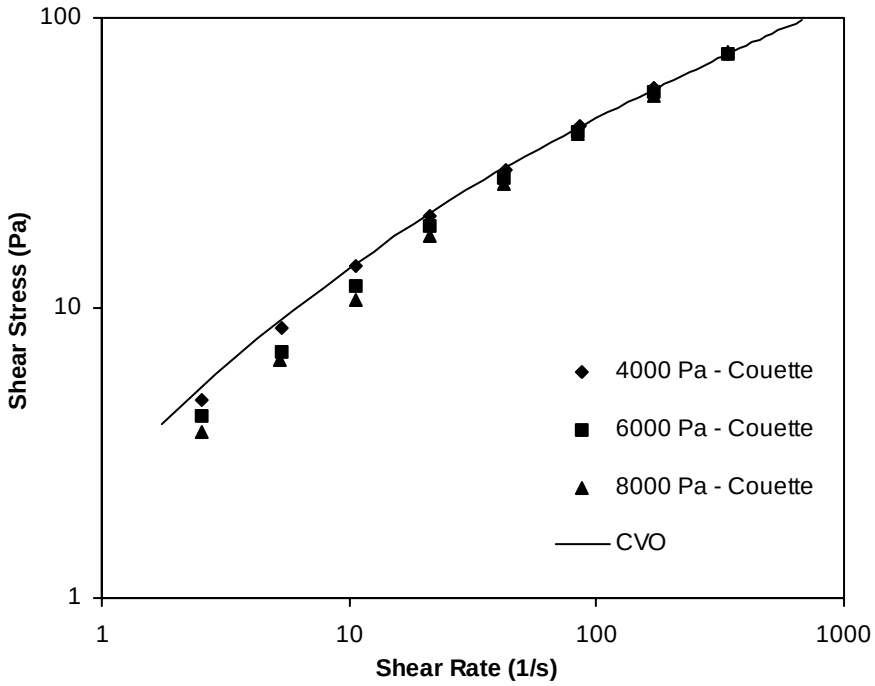

Figure 8.2-2 Couette Analysis of 1 wt% CMC solution

To further illustrate the error in ignoring the axial flow component, Figure 8.2-3 presents the difference in the shear rates calculated using helical flow theory and Couette theory, for the 1 wt% CMC solution. The error in the shear rate is determined using the Equation (8.2-2).

$$\text{Error} = \frac{\dot{\gamma} - \dot{\gamma}_{r\theta}}{\dot{\gamma}} \qquad (8.2\text{-}2)$$

The error in the shear rate can be seen to increase significantly with increasing values of differential pressure or axial flow rate but decreases with increasing values of rotational speed of the inner cylinder. At higher rotational speeds, but at constant values of differential pressure, the contribution to the total shear rate from the rotational speed becomes more significant, thus reducing the error in the shear rate calculations. However, even at the highest rotational speeds tested the error in the shear rate calculated using Couette flow theory is still as high as 45%, which is significant if the fluids are non-Newtonian in nature. It should be noted that these errors presented are extremely system specific but do however, illustrate the errors that can occur when the axial flow rate is ignored in any analysis of helical flow.

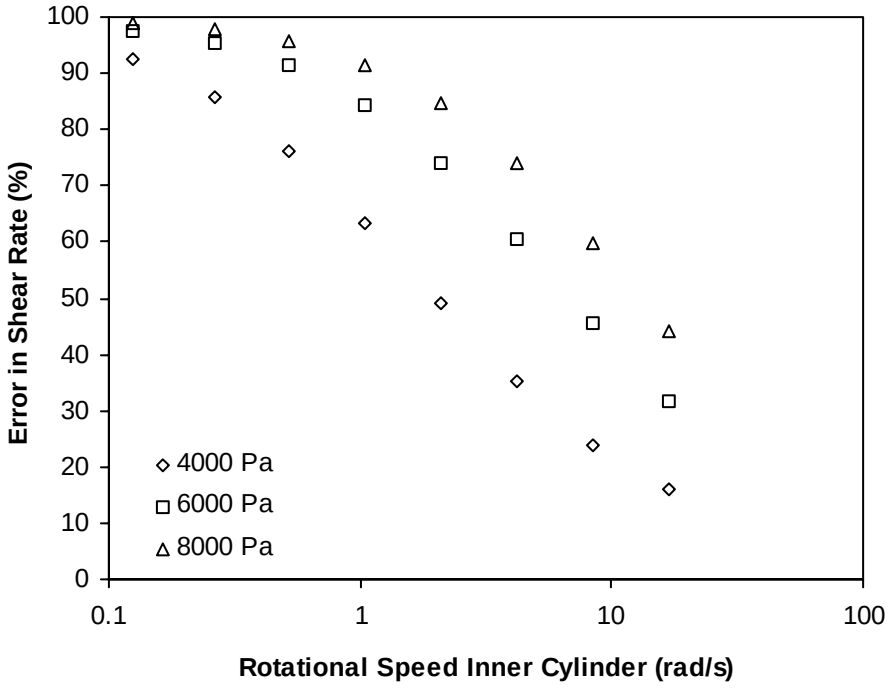

Figure 8.2-3 Error in shear rate between flow rheometer data analysed using helical flow and Couette flow theory for the 1 wt% CMC solution.

8.3 The Apparent Independence of Rheological Results on the Measured Value of Axial Flow Rate

A novel feature associated with the development of the flow rheometer is the data reduction procedure based on the principles of helical flow. Whilst the axial flow component was not ignored it was found that the rheological properties of a fluid could be determined without measuring the axial flow rate. To illustrate this affect a 0.7 wt% CMC solution is used. The rheological properties of the fluid were determined on the flow rheometer and also on the CVO (with a cone and plate geometry). The CMC solution is accurately predicted by the power-law model, with values of 0.16 and 0.88 for the parameters A and n respectively. The properties of the fluid are also presented in Figure 8.3-1, with the various values of differential pressure used to distinguish between the different tests performed with the flow rheometer.

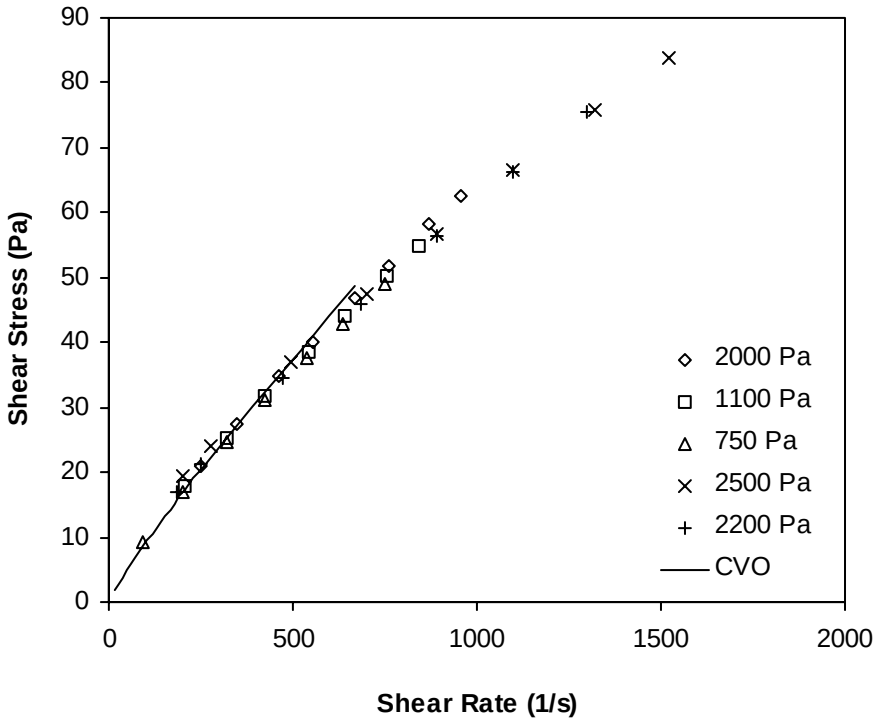

Figure 8.3-1 Rheological properties of the 0.7 wt% CMC Solution

To demonstrate the effective independence of the results on the axial flow rate a comparison of computed axial flow rate versus measured axial flow rate is presented in Figure 8.3-2. As can be seen there is a significant difference between the computed and the actual volumetric flow rates with an average error of 80.9% and a standard deviation of 9.2%. For comparison the computed angular velocity versus the measured angular velocity is presented in Figure 8.3-3. As can be seen there is a minimal difference between the computed and the actual rotational speeds with an average error of only 0.3% and a standard deviation of 1.2%. The significant error in the axial flow data is probably due to the measurement technique employed, which consisted of measuring a certain volume of fluid flowing out of the geometry in a given period of time. The fact that there is still good agreement in the rheological measurements between the CVO and the flow rheometer, despite the poor agreement between the calculated and measured values of axial flow rate, is discussed in the following section 8.4.

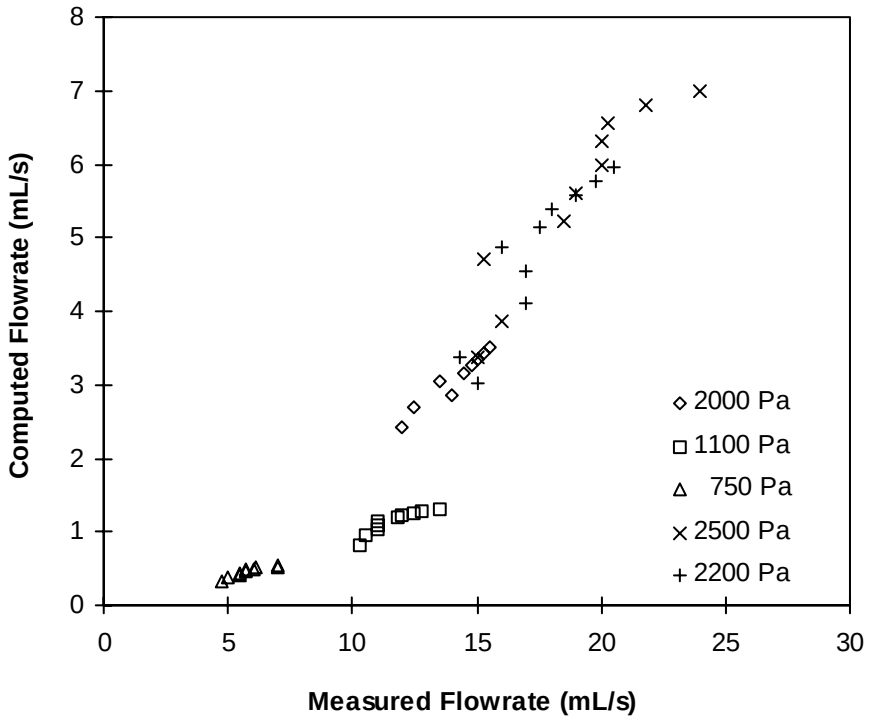

Figure 8.3-2 Computed versus experimental values of axial flow rate

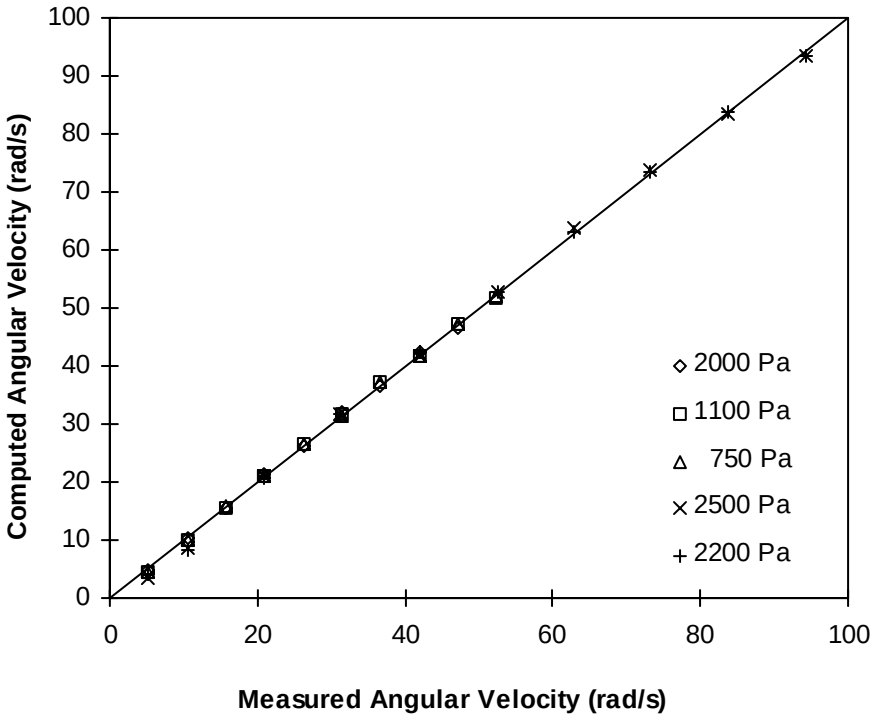

Figure 8.3-3 Computed versus experimental values of angular velocity

8.4 Calculating the Rheological Properties of a Fluid Without Measuring the Axial Flow Rate

It can be shown that the rheological properties of a fluid can be determined from helical flow measurements without measuring the axial flow rate. Examination of Equation (4.4-23) shows that the rotational speed is a function of (M, b, c(∂p/∂z), A, n, R and κR).

$$\Omega = \frac{M}{2\pi L}\left(\frac{1}{A}\right)^{\frac{1}{n}}\int_{\kappa R}^{R}\left(\left[\frac{M}{2\pi r^2 L}\right]^2+\left[\frac{b}{r}-\frac{cr}{2}\right]^2\right)^{\frac{1-n}{2n}}\frac{1}{r^3}dr \qquad (4.4\text{-}23)$$

Examination of the variables the aren't experimentally measured (b, A, n, R and κR) shows that only the parameter b is dependent on the axial flow rate, providing that the fluids rheological properties i.e. A and n do not vary significantly over the range of shear rates examined. Given that the parameter b could not be directly determined because the axial velocity could not be measured as a function of radial position, an iterative procedure was employed to determine the correct value of b, see section 4.4.5. Once the correct value of b was known the rotational speed could be determined using Equation (4.4-23) without knowing the value of the axial flow rate. Thus in this way the rheological properties of a fluid can be determined without measuring the axial flow rate. It should be emphasised that this technique does not mean that axial components of the flow can be ignored, merely that the axial flow does not need to be measured or optimised in the calculations.

CHAPTER 9 PARTICLE MIGRATION

9.1 Introduction

Under the action of shear in laminar flow, particles in a suspension or slurry can move across streamlines under a process known as particle migration. The migration of particles causes a concentration gradient to form perpendicular to the flow. The occurrence of particle migration can cause problems in the rheological measurements of suspensions and slurries. The migration of particles causes zones of reduced concentration to form in the measuring device. This non-uniformity can cause the suspension or slurry to exhibit a non-linear relationship between flow rate and driving force leading to irregularities and errors in rheological measurements (Ho and Leal 1974, Leal 1979). The rheological measurement errors usually manifest in the form of a reduction in the apparent viscosity of the slurry or suspension with time, which should not be confused with thixotropic behaviour, though the observed effect would be similar (Leighton and Acrivos 1987).

9.2 Literature Review

9.2.1 Modes of Migration

Under laminar flow conditions there are two main theories to explain the migration of particles; inertial effects and shear-induced particle migration. For smaller particles and low solid concentrations inertial effects will be more predominant whereas shear-induced particle migration is more predominant when larger particles are present in higher solid concentration suspensions (Leighton and Acrivos 1987).

Inertial Effects

Inertial effects will predominately cause particle migration when the chance of collisions between particles is minimal due to smaller particle sizes and low particle concentrations. Under these conditions the motion of the suspending fluid is the dominant force that causes the migration of the particles (Leal 1979). Segre and Silberberg (1962a, 1962b) first demonstrated that small neutrally buoyant rigid spheres in a suspension, under Poiseuille flow conditions in a circular pipe, would migrate away from the pipe wall. These results were confirmed in several subsequent studies by Brenner (1966), Halow and Wills (1970) and Tachibana (1973).

For a small perfectly spherical particle moving in an infinite medium the streamline around the particle will be perfectly balanced and the particle should not move perpendicular to the flow. If however, the streamlines are not uniform because the particle is near a wall or in a capillary tube then there will be an imbalance in the forces around the particle causing it to move perpendicular to the flow. This phenomenon will also be observed if the particle surface is rough or the particle is not uniform in shape relative to the streamlines. Inertial effects are therefore the motion of particles across streamlines due to an imbalance of the forces around the individual particles (Ho and Leal 1974, Leal 1979).

In general the rate of migration due to inertial effects is dependent on the suspending fluids rheological properties, the velocity of the flow, the particle size and shape, the dimensions and shape of the pipe or duct, the particles position in the flow and the

particle Reynolds number. The final position of the particle is independent of the initial starting position of the particle, thought the time taken to reach the equilibrium position may substantially vary depending on the particle's starting location (Clift 1978, Segre and Silberberg 1962b).

Shear-Induced Particle Migration

Several problems were encountered when the inertial effect theory was used to explain the observations from a series of experiments by Gadala-Maria and Acrivos (1980). In these experiments it was observed that the apparent viscosity of a high solids concentration suspension decreased despite a constant shear rate until an equilibrium value was reached, approximately a factor of two lower than the initial starting value. Leighton and Acrivos (1987) showed that this reduction in viscosity was due to particle migration, but the migration was not due to inertial effects. They proposed a new theory of particle migration based on collision theory, which is referred to it as shear-induced particle migration.

The theory of shear-induced particle migration may be broken down into two parts "shear-induced particle drift" (two-body interactions) and "shear-induced self-diffusion" (three-body interactions). The collision between two smooth, spherical particles in a Newtonian liquid will produce a perfectly reversible collision, with no irreversible displacement of the two particles and therefore on average there will be no overall migration of the particles (Bartok and Mason 1959, Darabaner and Mason 1967). However, if the particles are not perfectly smooth and spherical, then an irreversible displacement in the location of the particles will occur; this migration is referred to as "shear-induced particle drift".

Shear-induced self-diffusion occurs when three particles collide simultaneously. The collision between three bodies simultaneously will generate an irreversible component to the collision (Leighton and Acrivos 1987) and thus there will be an overall migration of the particles. A three (or more) body interaction is the only method by which perfectly smooth spheres in a concentrated suspension can migrate under the influence of shear. The rate of migration due to shear-induced self-diffusion is approximately an order of magnitude slower than that due to shear-induced particle

drift (Phillips et al. 1991) because of the reduced chance of three particles simultaneously colliding.

The model proposed by Leighton and Acrivos (1987) for particle migration was tested by Philips et al. (1991) for both Couette and Poiseuille flow. Phillips et al. (1991) chose to ignore the motion of particles due to shear-induced self-diffusion because of its substantially lower effect on the rates of migration. Despite ignoring the effects of shear-induced self-diffusion good agreement was obtained between experimental measurements obtained under a variety of different conditions and theoretical calculations, thus validating the theory of shear-induced particle drift.

9.2.2 The Influence of the Physical Properties of the Suspension on Particle Migration

9.2.2.1 Effect of Solids Concentration

The concentration of particles in a suspension will determine the type of migration that is most predominant; for low solid concentration suspensions with small particles, when the chances of inter-particle collisions is low then the predominant migration effect will be inertial effects. In contrast when larger particles and higher solid concentrations are involved, then shear-induced particle migration will be more significant (Tehrani 1996).

9.2.2.2 Effect of Particle Size and Shape

Inertial Effects

When inertial effects are predominant, Segre and Silberberg (1962b) showed that when the suspending fluid is Newtonian then the rate of migration is independent of the particle size but is dependent on the non-uniformity of the particle shape. A similar effect was also observed by Gauthier et al. (1971a, 1971b) and Karnis and Mason (1966) in viscoelastic fluids.

Shear –Induced Particle Migration

When shear-induced particle migration is the predominant effect, the shape of the particles can have an effect on the type and rate of migration that takes place. The rate of migration has been observed to increase with increases in the particle size (Abbott et al. 1991) and with decreases in the particle sphericity (Allende and Kalyon 2000). However, the final equilibrium position of the particles appears to be independent of particle shape. Mondy et al. (1994) showed that for the shear-induced particle migration of rods of various aspect ratios the final equilibrium concentration gradient was the same as that for spheres, though the time taken to reach equilibrium varied.

9.2.3 Migration in Rheological Instruments

The migration of particles can occur in rheological instruments where the shear rate is not constant across the measurement gap (Cameron 1989, Leal 1979). This migration will generate regions of low solids concentration, which can result in errors in rheological measurements. Two instruments which are widely used in rheological measurements and which are likely to be affected by particle migration are the concentric cylinder geometry and the capillary tube rheometer. Cone and plate and parallel plate geometries are less frequently used with suspensions because the small gap associated with these systems is usually not suited to the measurement of suspensions and slurries (Steffe 1992). Of particular interest, with regards to rheological measurements, is the rate at which the migration of the particles occurs, for if the rate of migration is slow compared to the measurement time, then it is possible that the measurements can be performed and results obtained before significant amounts of migration occur and affect the results.

9.2.3.1 Couette Migration

In Couette flow the shear rate within the gap is a function of the rotational speed of either one or both of the concentric cylinders. The rate of migration for both inertial effects (Halow and Wills 1970b) and shear-induced particle migration (Abbott et al. 1991, Mondy et al. 1994, Phillips et al. 1991, Tetlow et al. 1998) has been shown in both cases to be dependent on the time and the rate of shear, but independent of the

direction of rotation. Generally for both types of migration the rate of particle migration is logarithmic in behaviour but is significantly faster in shear-induced particle migration compared to inertial effects. The final position of the particles is dependent on the type of migration and the rheological properties of the suspending fluid.

Inertial Effects

When the predominant migratory effects are inertial then the following migration will occur:

- For Newtonian fluids at low Reynolds numbers minimal migration was observed by Gauthier et al. (1971). However, Halow and Wills (1970a, 1970b) showed the significant migration of particles in a Couette geometry, towards the midpoint between the concentric cylinders. Migration rates for Newtonian fluids are typically very slow and it is possible that at the very slow rotational speeds used in the Gauthier et al. (1971) studies, that insufficient time was allowed for migration to occur.
- For pseudoplastic fluids at low Reynolds numbers the migration is towards the region of higher shear or the towards the inner cylinder (Gauthier et al. 1971)
- For viscoelastic fluids at low Reynolds numbers the migration is towards the region of lower shear or the towards the outer cylinder (Gauthier et al. 1971, Karnis and Mason 1966).

Shear-Induced Particle Migration

When shear-induced particle migration is most significant, then for Newtonian fluids migrations will be towards the region of lower shear or towards the outer cylinder (Abbott et al. 1991, Chow et al. 1994, Graham et al. 1991, Mondy et al. 1994, Phillips et al. 1991m Tetlow et al. 1998). When the cylinders are placed eccentrically then the particles will also migrate to the region of lowest shear which is the area located in the widest portion of the gap (Phan-Thien et al. 1995). When non-spherical particles are introduced the direction of the migration is the same but the rate of migration increases as the sphericity decreases (Mondy et al. 1994).

9.2.3.2 Poiseuille Migration

In Poiseuille flow the shear rate within the gap is a function of the flow rate within the pipe. The rate of migration for either inertial effects (Gauthier 1971b) or shear-induced particle migration (Allende 2000) is dependent on the flow rate, time and the particle size. As with Couette migration the rate of migration is initially quite rapid followed by a slowing with time, as the particles tend towards their equilibrium position (Segre and Silberberg 1962b). The final position of the particles is dependent on the type of migration and the rheological properties of the fluid.

Inertial Effects

When the predominant migratory effects are inertial, then the following migration will occur:

- For Newtonain fluids Segre and Silberberg (1962a, 1962b) showed the direction of migration of spheres was towards an annular shaped region, which is about 60% of the distance from the pipe wall to the central axis. This result was confirmed by Purdom and Richardson (1991) and Tachibana (1973).
- For pseudoplastic fluids the migration is towards the region of highest shear or towards the pipe wall (Gauthier 1971b).
- For viscoelastic fluids the migration is towards the region of lowest shear or towards the centre of the pipe (Gauthier 1971b, Karnis and Mason 1966, Tehrani 1996).

Shear-Induced Particle Migration

For shear-induced particle migration in Newtonian fluids the migration is towards the region of lowest shear rate or towards the centre of the pipe (Butler and Bonnecaze 1999, Hampton et al. 1997, Han et al. 1999, Shauly et al. 1998, Sinton and Chow 1991). If the pipe is square then migration is similar with the particles migrating towards the centre of the conduit (Koh at al. 1994).

9.2.4 Statement of Purpose

The migration of particles in Couette and Poiseuille flow can lead to the development of segregated flow or a solids concentration gradient, which in-turn, can influence rheological measurements from these systems. The helical flow in the flow rheometer is a combination of these two types of flow, which suggests that migration could occur within the instrument when slurries and suspensions are examined. However, there are no studies in the literature of particle migration under helical flow conditions.

The literature results previously discussed show that there are a wide range of effects that can alter the type, direction and speed of migration and it is therefore almost impossible to predict what migration, if any, would occur in the flow rheometer, particularly given the combination of Couette and axial flow. Thus the objective of this investigation is firstly to determine if particle migration occurs to a significant extent in the flow rheometer and secondly to determine what effect this migration has on rheological measurements.

9.3 Migration in the Flow Rheometer

It is expected that two directions of particle migration might be present in the flow rheometer due to the Couette and Poiseuille flow present in the helical flow geometry. Generally most slurries contain a high concentration of solid particles in a suspending fluid which is typically water, though low concentration polymer solution are also possible. Under these conditions shear-induced particle migration will be the predominant migratory effect (Leighton and Acrivos 1987). The direction of migration due to the Couette component of the flow will be towards the outer wall (Abbott 1991, Chow et al. 1994, Leighton and Acrivos 1987, Tetlow et al. 1998), whilst the migration due to the Poiseuille flow will be towards the inner wall (Allende and Kaylon 2000, Hampton et al. 1997, Han et al. 1999). Whilst these two directions of migration are opposite, it is highly unlikely that the flow conditions will be such that migration due to one of the flow directions (i.e. Couette) will completely cancel out the migration due to the other flow (i.e. axial flow).

It is possible to obtain rheological measurements in an axial Poiseuille flow system without the effects of particle migration, provided that the ratio of the particle diameter to the tube diameter or annulus is correctly selected (Nott and Brady 1994). Allende and Kaylon (2000) showed that for length to diameter ratios of between 10 and 60 there will be a minimal effect due to particle migration providing that the tube diameter to particle diameter is correctly selected. It is also possible to generate rheological results from a Couette flow system where particle migration occurs, providing that the measurements are performed relatively quickly compared to the rate of migration. Experimental observations show (Abbott et al.1991) that approximately 100 revolutions are required before significant migration is observed, though this value is affected by the initial solids concentration of the slurry or suspension.

The circulating nature of the flow profile through the flow rheometer means that fluid is only in the measurement portion of the geometry for a few seconds, depending on the axial flow rate, before it returns to the storage tank. As a consequence the fluid and suspended particles will only experience a small number of revolutions (<100)

before they flow out of the geometry, which may lead to minimal particle migration due to the short residence time.

To substantiate the hypothesis that the circulation of the fluid through the geometry minimises the chance of migration the results from the clay and the fly ash slurries were examined based on the following theory.

The nature of the helical flow is such that the total shear stress and shear rate in the system is the Pythagorean addition of the rotational and axial components, as shown below.

$$\dot{\gamma} = \sqrt{\dot{\gamma}_{rz}^2 + \dot{\gamma}_{r\theta}^2} \qquad (4.4\text{-}14)$$

axial rotational

Thus for a given total shear rate or shear stress there is more than one combination of axial and rotational components that can generate the same shear rate. However, different rates of shear in the individual components will likely lead to different amounts of particle migration, which should lead to differences in the measured values of torque which is used to determine part of the total shear stress. Thus by determining the shear stress from a number of different tests where the total shear rate is the same but the contributions from the axial and rotational components vary then differences in the calculated shear stress should indicate the presence of particle migration in the flow.

The results from the clay and the fly ash slurries are plotted in Figure 9.3-1 and Figure 9.3-2. These graphs present total shear stress values at different axial flow rates (differential pressure), for approximately constant values of total shear rate. Thus because the axial shear rate is varied (different values of differential pressure) the rotational component is also varying, because the overall total shear rate is the same. It can be seen in the results presented that there is some variation in the shear stress values at constant values of shear rate but it should be noted that the shear rate values from the different tests were not exactly the same and this probably accounts for the

deviation observed. However, in general it is observed that the shear stress is effectively constant for the various values of total shear rate. This result suggests that minimal particle migration is occurring within the flow rheometer.

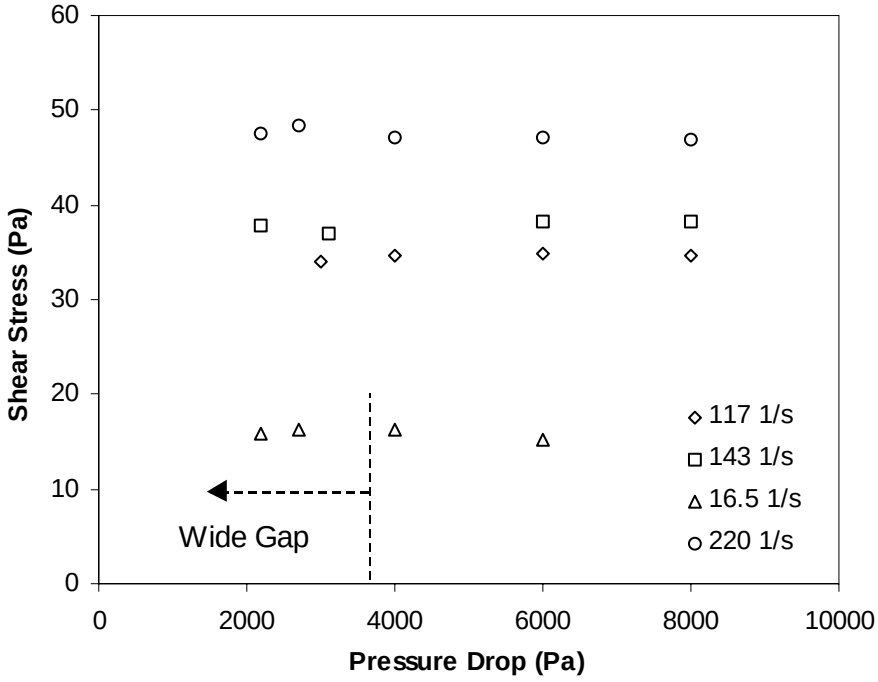

Figure 9.3-1 Effect of particle migration – clay slurry

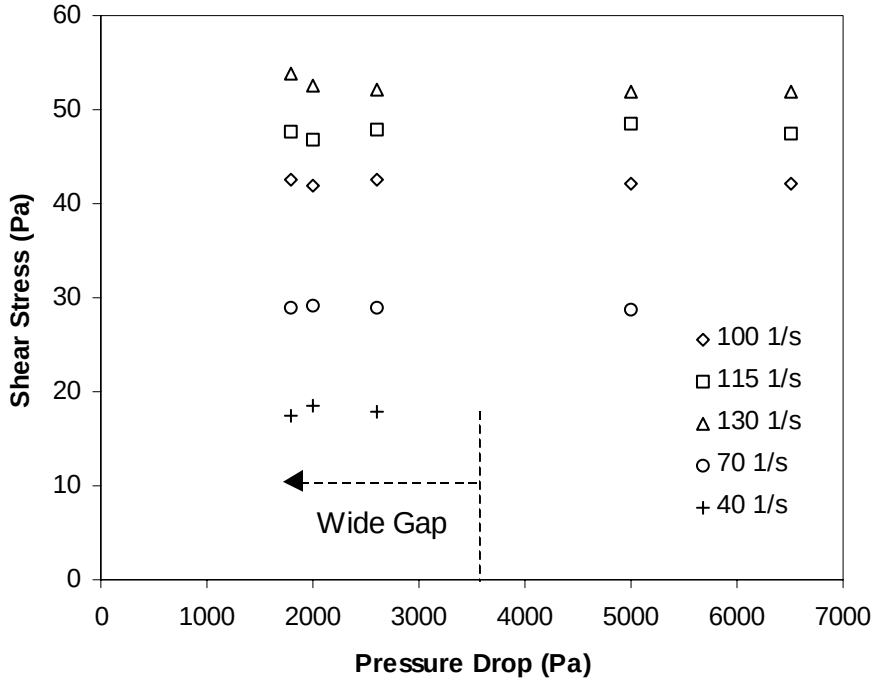

Figure 9.3-2 Effect of particle migration – fly ash slurry

To further substantiate the assumption that there is minimal migration occurring within the helical flow geometry the number of rotations experienced by the fluid and particles as they circulate through the flow rheometer is presented as a function operating differential pressure and total shear rate in Table 9.3-I. It can be seen from the data presented that under the most adverse conditions (low axial flow rate (or differential pressure) and high rotational speed) the greatest number of rotations experienced by the fluid and particles is approximately 50 and most values are significantly less. All of these values are less than the value of 100 revolutions suggested by Abbot et al. (1991) as being required before effects due to migration become noticeable. Thus based on these results it would seem probable that significant migration does not occur within the helical flow geometry under the operating conditions examined.

Table 9.3-I Number of rotations experienced by the fluid or a particle in the flow rheometer – fly ash slurry

	Operating Differential Pressure				
Total Shear Rate	6500 Pa	5000 Pa	2600 Pa	2000 Pa	1800 Pa
130 1/s	0.42	3.1	3.0	12.0	48.7
115 1/s	0.28	2.5	2.7	10.8	44.3
100 1/s	0.14	1.8	2.4	9.7	39.8
70 1/s	-	0.06	1.3	6.4	27.3
40 1/s	-	-	0.7	3.3	16.9

CHAPTER 10 THE FLOW RHEOMETER - CONCLUSIONS

10.1 Introduction

To improve the optimisation of mineral-processing operations the rheological properties of settling slurries need to be accurately determined under conditions that realistically represent those found in actual site operations. This is not an easy task when dealing with high rate settling slurries, as most rheological instruments cannot maintain the particles in a homogeneous slurry. The major purpose of this study was to address the need for an instrument capable of measuring the properties of settling slurries by developing the flow rheometer.

10.2 Development of the Flow Rheometer

The flow rheometer was specifically developed to measure the properties of settling slurries. Unique difficulties are associated with the operation of equipment used to measures the properties of low viscosity, rapid settling slurries. One of the principal design and operational issues was that of particles settling in the pipes and flow channels in the instrument leading to unexpected equipment shutdown due to blockage. In this respect the flow rheometer was specially designed to minimise the number of possible areas where particles are likely to build up due to settling in regions of slow flow.

The pumping requirements for this application that needed to be satisfied are unique and included; continuous non-pulsed flow, an ability to handle coarse settling particles and delivery a relatively slow flow compared to most other mineral processing applications. A helical rotor pump specially modified to prevent particles settling was used.

10.3 Data Analysis Procedure for the Flow Rheometer

The major problem with most rheological instruments, particularly the commonly used generic rotational type geometries, is that when settling slurries are examined heterogeneous conditions rapidly develop in the sample. Many unique instruments have been developed to better maintain homogeneous conditions of a slurry during the measurement period; this is often achieved by circulating the slurry with an axial flow through a set concentric rotating cylinders. However, the calculations associated with these instruments often ignored the contributions to the total shear rate made by the axial flow component. The increase in the total shear rate in the system, due to the axial flow, can have serious measurement implications if non-Newtonian fluids are examined and the correct shear rate is not determined. Calculations performed as a part of this study showed that errors as high 100% were observed in the shear rate when the axial flow component was ignored. However, it should also be noted that the actually value of this error is highly dependent on the physical size and operating conditions of the specific system and will vary widely in different system, but it does

give an indication of the dangers posed in ignoring the axial flow component of the flow. The significant advantage of the analysis procedure developed in this study is that the calculations are based on the fundamental principles of helical flow, which include the contributions to the total shear rate of the axial flow component and thus the true rheological properties of the fluid measured can be determined.

The particle size distribution of many slurries dictates that a wide gap geometry should be used for their measurement, but when the rheological properties of these slurries are non-Newtonian in nature significant complications in the analysis procedure are introduced. To determine the rheological properties of a non-Newtonian fluid from measurements from a helical flow system assuming a generalised rheological model would be extremely complex, so to simplify the calculations it was assumed that over the shear rate range examined, the power-law model could be used to describe the rheological properties of the fluid. An iterative numerical analysis procedure using Levenberg-Marquardt non-linear regression was used to determine the best set of power-law model parameters, A and n, that described the rheological properties of the fluid over the measured shear rate range.

While the assumption that the rheological properties of a fluid can be described by the power-law model over a particular range of shear rates works well for most fluids at higher values of shear rate, significant errors can be introduced when yield stress fluids are examined at low values of shear rate. At low values of shear rate there will an error between the power-law model which tends to a shear stress value of zero as the shear rate tends to zero whilst the fluids rheological properties tend towards τ_y, the yield stress. To reduce this error a modification was introduced to the experimental and analysis procedures, instead of using a single power-law model to describe the fluids behaviour over a wide range of shear rates, several power-law models were used, each covering a smaller range of shear rates and each with different values for the power-law model parameters. In this way the two-parameter power-law model can be used to describe more complex rheological behaviour that would usually require a model with at least three fitting parameters.

10.4 Summary of Results

To test and validate the accuracy of results from the flow rheometer a number of different fluids representing a range of rheological properties were examined. The fluids examined included several Newtonian fluids a glycerol solution and a 68wt% fly ash slurry, several pseudoplastic fluids including a 1.5wt% CMC solution and a 36wt% gold mine tailing slurry and several yield stress fluids including a 1.5wt% carbopol solution, at pH 2.7, a 71wt% clay slurry and a 49wt% diamond mine tailing slurry. Each of these fluids were examined in the flow rheometer at a variety of different axial flow rates and where possible (depending on the particle size distribution) using different geometries of varying gap width.

To compare the results from the flow rheometer the pure liquids were examined in a standard laboratory cone and plate instrument, the CVO. Good agreement was observed between the results of both the CVO and the flow rheometer, with an average error of approximately 1% and standard deviation in the results from the flow rheometer of approximately 2%.

To compare and validate the results from the flow rheometer for settling slurries a second rheological instrument capable of measuring the properties of slow settling slurries, a specially modified tube rheometer, was developed. This instrument incorporated a mixing impeller in the main reservoir, which was used to maintain homogenous conditions throughout the measurement period. However, while this instrument was able to measure the properties of some settling slurries, rapid settling slurries could not be reliably measured. The tube rheometer was used to examine the fly ash and clay slurries. Good agreement was observed between the results of the tube and flow rheometer, with an average error of approximately 2% and standard deviation in the results from the flow rheometer of approximately 4%.

The settling rate of the particles in the gold mine tailing and the diamond mine tailing slurries were such that they could not be measured in any other of the laboratory instruments except the flow rheometer. There is good agreement between the results

obtained at different values of axial flow rate for each of the slurries, with an average standard deviation in the results of approximately 2%

10.5 Examination of the Axial Flow Component of Helical Flow

The axial flow component of helical flow as previously discussed, section 10.3, is an extremely important component of the data analysis and ignoring it can lead to significant errors in the shear rate calculation. For non-Newtonian fluids this error in the shear rate calculation will lead to an error in the calculations of the fluid's rheological properties.

It was found that due to the nature of the equations that define the helical flow system and the iterative method of solution used in this study, that the system can be fully specified with the measurement of only three variables, M, dp/dz and Ω and thus the axial flow rate does not need to be measured.

10.6 Particle Migration

Migration of small particles is known to occur in both laminar axial pipe flow and laminar rotational Couette flow. Although this process occurs over a period of time, once migration occurs it can cause errors during the rheological measurements of suspensions and slurries as a concentration gradient develops in the sample. The flow rheometer has both axial and Couette flow components and it is possible that particle migration may occur during rheological measurements. The examination of results generated for the fly ash and clay slurries showed that particle migration had a minimal effect on rheological measurements from the flow rheometer. It is likely that the circulation of the slurry through the instrument minimised the residence time of the slurry in the actual measurement section of the geometry and thus significantly reduced the opportunity for particle migration to occur.

SECTION C INSTABILITIES IN HELICAL FLOW

CHAPTER 11 LITERATURE REVIEW - INSTABILITIES IN COUETTE, AXIAL AND HELICAL FLOW

11.1 Introduction

Under laminar flow condition a fluid flows with smooth constant streamlines and the velocity gradient has a smooth profile. However, all laminar flow may become turbulent if certain conditions are met. The reason for this breakdown in the fluid streamlines can be varied but it is often caused by a minor disturbance to the flow (Reynolds 1883). Reynolds (1883) showed that the relationship between inertial and viscous forces could be used to predict the onset of turbulent flow in pipeline flows. There is a transition point in the flow when the viscous forces of the fluid can no longer damp the transfer of energy from one fluid layer to another and turbulent motion of the flow begins (Davies 1972).

Instabilities and turbulence are of interest to many different engineering fields of research. However this examination of instabilities in fluid flow is based on the relevance to rheological measurements. The increased random nature of the flow increases the energy dissipated by the flowing fluid and affects the measured shear stress at a specific shear rate. This change in the relationship between shear stress and shear rate invalidates the theoretical assumptions made in most rheological measurements and calculations. It is therefore important in rheological measurements that the flow remains laminar and does not become turbulent. Thus a good knowledge of the conditions for the onset of instabilities is essential so that accurate and reliable rheological measurements can be performed.

11.2 Annular Pipe Flow

The flow rheometer developed as part of this study and discussed in Section B, has a flow regime that consists of two components; axial annular flow and rotational Couette flow. Focusing firstly on the axial component of the flow; as the axial flow rate increases the laminar flow will degrade and may become unstable and the conditions under which this is likely to occur must be defined.

11.2.1 Stability Criteria

The Reynolds number may be used to determine the onset of instabilities in a standard pipe flow, but must be suitably modified for annular flow. The modified Reynolds number for a Newtonian fluid flowing in an annulus is shown in Equation (11.2-1) (Bird et al. 1960), where $\langle v_z \rangle$ is the average annular axial velocity, R is the radius of the outer cylinder, κ is the ratio of the radii of the inner and the outer cylinders, ρ is the density and μ is the viscosity.

$$Re = \frac{2R(1-\kappa)\langle v_z \rangle \rho}{\mu} \qquad (11.2\text{-}1)$$

For non-Newtonian fluids that can be described by the power-law model, Equation (2.2-3), a modification to the Reynolds number, was devised and experimentally

validated by Tuoc and McGiven (1994). The modification is based on the Mooney and Rabinoswitsch derivation for the flow of non-Newtonian fluids in cylindrical pipes (Skelland 1967). The modified Reynolds number for the flow of a power-law model fluid in an annulus is presented below; the conditions for the onset of instabilities are the same as those used for the Newtonian Reynolds number.

$$\mathrm{Re} = \frac{\left[2R(1-\kappa)\right]^{n}\left\langle v_z\right\rangle^{2-n}\rho}{(8\varphi)^{n-1}A'} \tag{11.2-2}$$

Where the co-axial cylinder shape factor, φ, is defined as follows.

$$\varphi(\kappa) = \frac{(1-\kappa)^2}{\frac{\left(1-\kappa^2\right)}{\ln(\kappa)} + \left(1+\kappa^2\right)} \tag{11.2-3}$$

and

$$A' = A\left[\frac{3n+\varphi}{(3+\varphi)n}\right]^{n} \tag{11.2-4}$$

11.2.2 Entrance Effects

The development of a stable laminar flow profile is a critical criterion in any experimental investigation into helical flow stability. Any device must be long enough so that the axial component of flow is fully stabilised and developed. The development of axial flow profiles has been the subject of several investigations (Martin and Payne 1972, Simmers and Coney 1979, Sparrow and Lin 1964). It was found that the entrance length required to develop stable laminar flow increases with increasing axial flow rate and also with increasing radial gap width. However, unless the flow rate is particular high or the gap width particularly wide then the entrance length required for the development of laminar flow will be quite small. The following criteria developed by Sparrow and Lin (1964) may be used to determine the entrance length for a particular set of system dimensions and values of axial flow rate.

$$\text{Entrance Length} = \frac{(\text{ELF})\langle v_z \rangle (R - \kappa R)^2 \rho}{\mu} \qquad (11.2\text{-}5)$$

The parameter, ELF, is represented on the graph below, in Figure 11.2-1 as the total value of the x-axis and is dimensionless. As shown in Figure 11.2-1, the parameters u and ū refer to the axial velocity at a given radial location and the mean velocity, respectively. The inner and outer radii are defined by r_1 and r_2 respectively and the kinematic viscosity is represented by ν. Fully developed annular flow is represented by a flattening of the curves and this occurs at an x-axis value (or ELF value) of approximately 0.1. Thus given a set of system conditions r_1, r_2, ū and ν the entrance development length can be determined. Other graphs for different radius ratios are presented in the paper by Sparrow and Lin (1964).

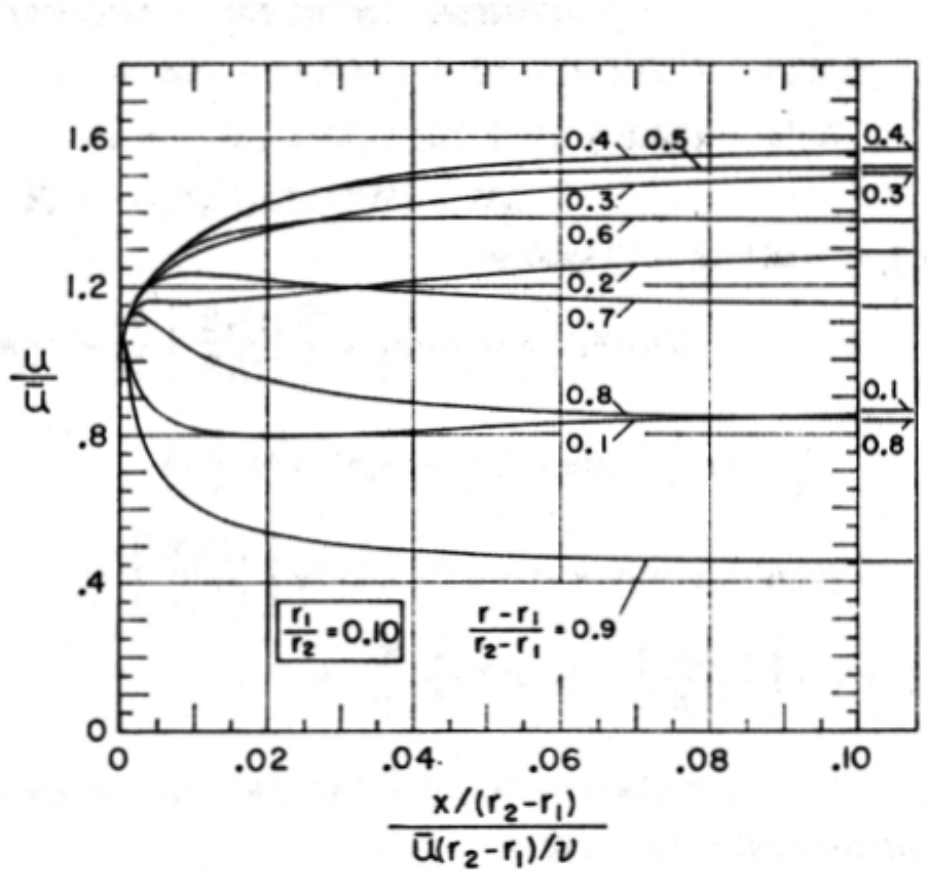

Figure 11.2-1 The velocity development in an annular duct with a radius ratio of 0.1 (Sparrow and Lin 1964)

11.3 Rotational Couette Flow

Similar to pipe flow, laminar rotational flow can become unstable and turbulent if certain conditions are met, but the transition to unstable flow in rotational systems is more complex than that observed in pipe flow. The first investigation into the stability of Couette flow was performed by Lord Rayleigh (1916) using a theoretical inviscid (or non-viscous) fluid. Rayleigh (1916) showed that laminar Couette flow could become unstable if the rotational speed of the inner cylinder was increased above a critical value. Taylor (1923) extended Rayleigh's stability theory to include viscous fluids. These instabilities were shown to take the form of toroidal vortices (Taylor vortices) regularly spaced along the axis of the cylinders, see Figure 11.3-1. These vortices develop when the fluid near the inner cylinder is radially displaced and there is insufficient pressure gradient to return the fluid to its original radial position (Von Kármán 1934). The motion of the fluid creates a rotating pattern, which leads to the development of Taylor vortices, which are shown in Figure 11.3-1.

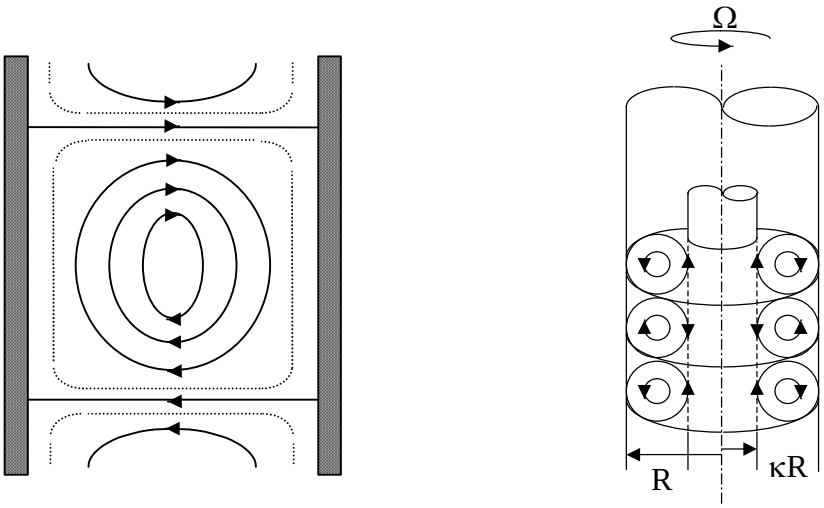

Figure 11.3-1 Taylor vortices

Taylor (1923) further showed that the transition to vortex flow was not only a function of the rotational speed of the inner cylinder, but that by rotating the outer cylinder (in either direction) the transition could be delayed. However, if only the outer cylinder was rotated then the flow would be stabilised by the centripetal forces (Schlichting 1968, Schulz-Grunow 1959).

11.3.1 The Effect of the Onset of Taylor Vortex Flow on Rheological Measurements

Couette (1890) was the first to notice a significant irregular increase in measured values of torque during a rheological measurement (in a concentric cylinder apparatus) when the speed of rotation of the inner cylinder increased above a certain value and attributed it to the onset of turbulence in the flow. The effects of the transition to Taylor vortex flow on the torque measurements within a concentric cylinder system were demonstrated by Taylor (1936) and later by Donnelly (1958). Donnelly (1958) used a modified Couette viscometer to determine the onset of Taylor vortex flow within a narrow gap system. Values of torque were recorded as a function of continuously increasing rotational speed and the onset of vortices caused a discontinuity in the torque readings, which was characterised by an increase in the slope of the torque (Di Prima and Eagles 1977, Donnelly 1958, Taylor 1936). This increase in torque will introduce a significant error in any rheological measurements, as the calculated value of viscosity will appear to increase when it ordinarily should not. Given that most concentric cylinder rheometers rotate only one cylinder and that if only the outer cylinder rotates then the flow will be stabilised, the discussion will be restricted to the case where only the inner cylinder is rotating.

11.3.2 Experimental Methods to Determine the Onset of Taylor Vortex Flow

A variety of different methods have been used to determine the onset speed at which Taylor vortices will develop in a concentric cylinder system, but the two most commonly used techniques are flow visualisation and measurements of torque as a function of rotational speed.

Flow visualisation techniques for liquids involve the addition of a small amount of solid flat (disc-like) flakes or liquid dyes (Van Dyke 1982). When the small flat flakes are placed in a moving liquid their direction of orientation is almost always in the same direction as the principle axis of the local rate of strain tensor (Coles 1965). As the fluid changes direction so also do the flakes leading to regions where the amount

of reflected light is reduced or increased. The use of small reflective metallic flakes enables the flow to be easily visualised by the naked eye. This method of flow visualisation is widely used in the study of the transition from laminar to turbulent instabilities in Couette flow (Coles 1965, Savaş 1985, Van Dyke 1982).

A different coloured dye may be injected into a fluid stream to track the fluid motion. This technique however is more appropriate for laminar flow, where there is little mass transfer between the streamlines and thus there will be minimal inter-mixing of the dye with the primary fluid. Under turbulent conditions the chaotic motion of the fluid cause rapid intermixing of the dye, reducing the effectiveness of further dye injections and limiting the time over which observations and measurements can be made with a given sample of fluid.

The measurement of torque as a function of rotational speed is another method that may be used to determine the onset of Taylor vortices (Donnelly 1958). For Newtonian fluids, the relationship between the torque acting on a rotating cylinder within a Couette laminar flow system is linearly proportional to the speed of rotation. When Taylor vortices form the torque will increase significantly above that which would normally be expected. The predicted results from such a measurement are presented in Figure 11.3-2, with the sharp inflection point indicating the onset of Taylor vortex flow.

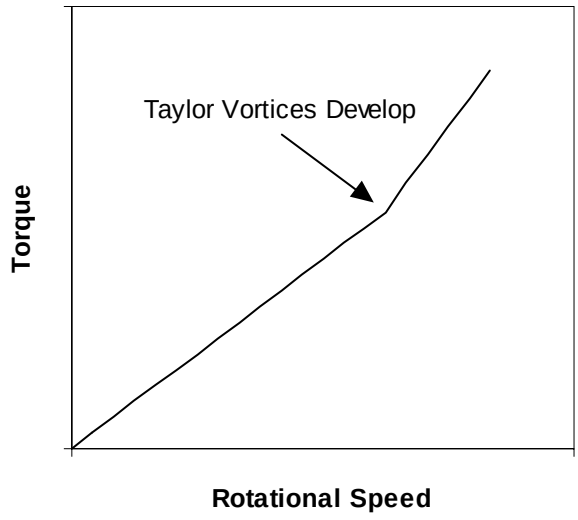

Figure 11.3-2 The onset of Taylor vortices in a Newtonian fluid

Another method to measure the onset of Taylor vortices, which has been reported, is referred to as the “ion technique” and is outlined in a series of papers by Donnelly (1965), Donnelly and Tanner (1965) and Donnelly et al. (1965). The method detects changes in a transmitted voltage between two concentric cylinders across a low electrically conductive fluid such as carbon tetrachloride. The presence of a vortex cause the voltage signal to change and by scanning up and down the cylinder walls the size of the vortices can be determined. Complex calculations and assumptions (Donnelly and Tanner 1965) are required to account for the three different ion (current) transportation mechanisms through a fluid (diffusion, conduction and convection) and how these mechanisms change in the presence of Taylor vortices. The complex nature of both the apparatus and the analysis procedure prevented further work with this technique.

11.3.3 Stability Criterion for Couette Flow – The Narrow Gap

To simplify the analysis of a concentric cylinder system the gap width may be assumed to be very small compared to the average radius, Equation (11.3-1). The critical speed of the inner cylinder at which vortices will appear can then be predicted by considering a linearised problem for the stability of Couette flow with respect to an asymmetrical disturbance (Chandrasekhar 1958).

$$\left(R-\kappa R\right) << \tfrac{1}{2}\left(R+\kappa R\right) \qquad (11.3\text{-}1)$$

In, 1923, Taylor presented an initial theoretical study on the instabilities of Couette flow for the case of a narrow gap. The resulting stability criterion developed is shown in Equation (11.3-2) and includes the option for either one or both of the concentric cylinders to rotate and in either direction.

$$P = \frac{\pi^4 \nu^2 \left(R+\kappa R\right)}{2\Omega_2^2 \left(R-\kappa R\right)^3 \left(\kappa R\right)^2 \left[1-\left(k\,R^2/\left(\kappa R\right)^2\right)\right]\left(1-k\right)} = 0.0571 \qquad (11.3\text{-}2)$$

The variable P is a dimensional parameter similar to 'Re' in the Reynold's number and k is the ratio of the cylinder rotational speeds (inner/outer), which should not be confused with κ, which is the radius ratio of the inner and outer cylinders. When the outer cylinder is stationary Taylor's stability criterion may be simplified, see APPENDIX D, to give Equation (11.3-3). The parameter P was inverted and renamed Ta (Taylor Number) in honour of Taylor's early work.

$$Ta' = \frac{2v_\theta^2(R-\kappa R)^3}{\nu^2(R+\kappa R)} = 1706 \qquad (11.3\text{-}3)$$

Further simplifications, APPENDIX D, will give Equation (11.3-4) the most simplified version of the Taylor number.

$$Ta = \frac{v_\theta R(1-\kappa)}{\nu}\sqrt{\frac{(1-\kappa)}{\kappa}} = 41.3 \qquad (11.3\text{-}4)$$

It is not clear from a review of the literature, which Taylor number is more commonly used and for this study Equation (11.3-4) will be used as the standard Taylor number with a critical onset value of 41.3, for the case of a narrow gap geometry.

11.3.4 The Effect of Radius Ratio or Gap Width

Whilst the narrow gap approximation allows for a significant simplification of the calculations it cannot be applied to many practical applications of the concentric cylinder system. Thus the effect that changes in the radius ratio have on the onset of Taylor vortices must be determined. The Taylor number, similar to the Reynolds number contains various terms to account for the dimensions of the system and as such the Taylor number could be expected to be independent of the system dimensions. Results from numerous theoretical examinations of the problem (Chandrasekhar 1958, 1962, Sparrow et al. 1964, Taylor 1923, Yu and Sun 1964) and equally numerous experimental studies (Andereck et al. 1986, Di Prima et al. 1984, Donnelly 1960, Gorman and Swinney 1982, Lewis 1928, Taylor 1923) show that the width of the gap between the concentric cylinders affects the critical speed of rotation

for the onset of Taylor vortices. The results from the literature are summarised below in Figure 11.3-3. Reasonable agreement is observed between the different data sets at smaller values of gap width, with more significant discrepancies at wider values of gap width.

By carefully selecting a large group of variables, Coles (1967) attempted to eliminate the effect of the gap width by modifying the expression for the Taylor number. The results were reasonably successful but the increased complexity in the Taylor number made the modifications impractical.

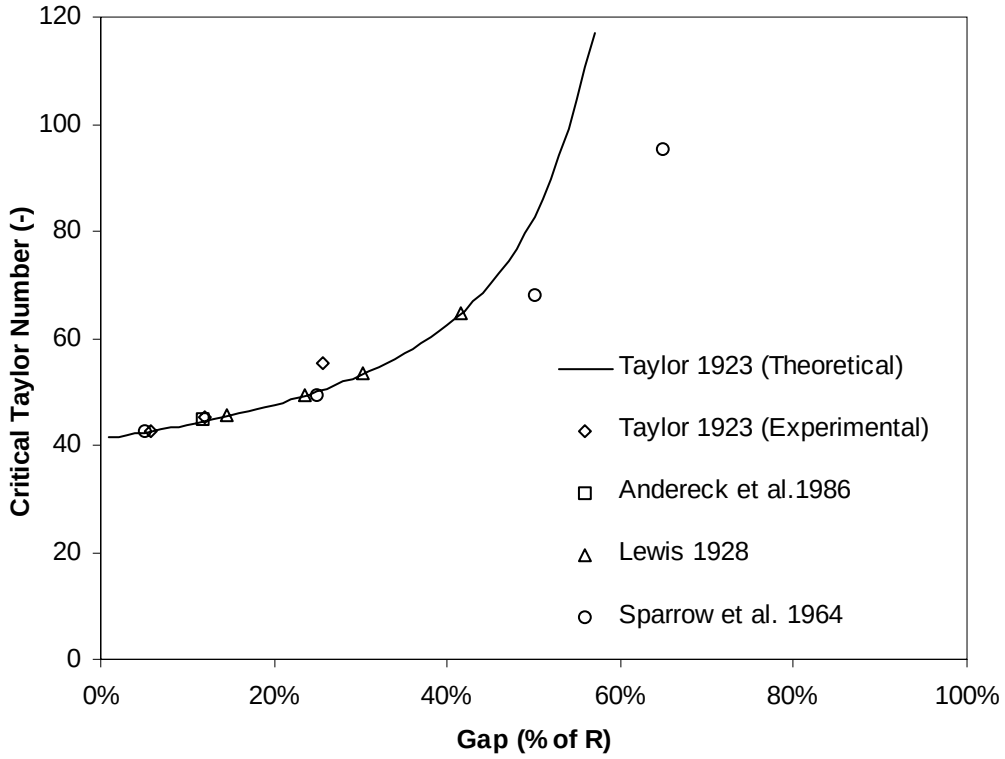

Figure 11.3-3 Literature data for the onset of Taylor vortices at varying gap widths

11.3.5 The Effect of Acceleration

The rate of acceleration of the inner cylinder can have a significant affect on the development of Taylor vortices. Theoretical studies and most of the experimental studies referred to previously assume quasi-steady state acceleration of the rotating cylinder. Quasi-steady state acceleration involves the very slow acceleration of the moving cylinder; the acceleration is so slow as to assume the acceleration rate is negligible (Andereck et al. 1986, Coles 1965). For many practical situations the assumption of quasi-steady state acceleration is not valid; this is particularly true for steady shear rheological experiments where the instrument is rapidly accelerated from rest to the operating shear rate.

There is some evidence from previous literature results that the rate of acceleration can have an effect on the onset and form of Taylor vortices. The rate of acceleration of the rotating cylinder has been shown to affect the vortex height or wavelength of Taylor vortices at Taylor numbers well above the critical value (Andereck et al. 1983, Burkhalter and Koschmieder 1974, Donnelly et al. 1965, Gorman and Swinney 1982) and also at extremely high Taylor Numbers (~40000Ta_c) (Koschmieder 1979). An example of this phenomenon is presented in Figure 11.3-4 below, where T/T_c, which represents the actual Taylor number divided by the predicted critical Taylor number for the onset of Taylor vortex flow under quasi-steady state acceleration conditions is plotted against the wave length of the Taylor vortices for a series of experiments performed under sudden start conditions (or high values of acceleration). It can be seen that the wavelength decreases from the critical onset point (T/T_c = 1.0), passes through a minimum at approximately $15T_c$ and increases back to the original critical onset wavelength at approximately $60T_c$. It is widely suggested that the reason for this change in wavelengths from sudden starts (or high values of acceleration) is because the fluid is availed of a choice in possible wavelengths, compared to quasi-steady state conditions or very slow acceleration conditions, when only one wavelength is possible (Burkhalter and Koschmieder 1974).

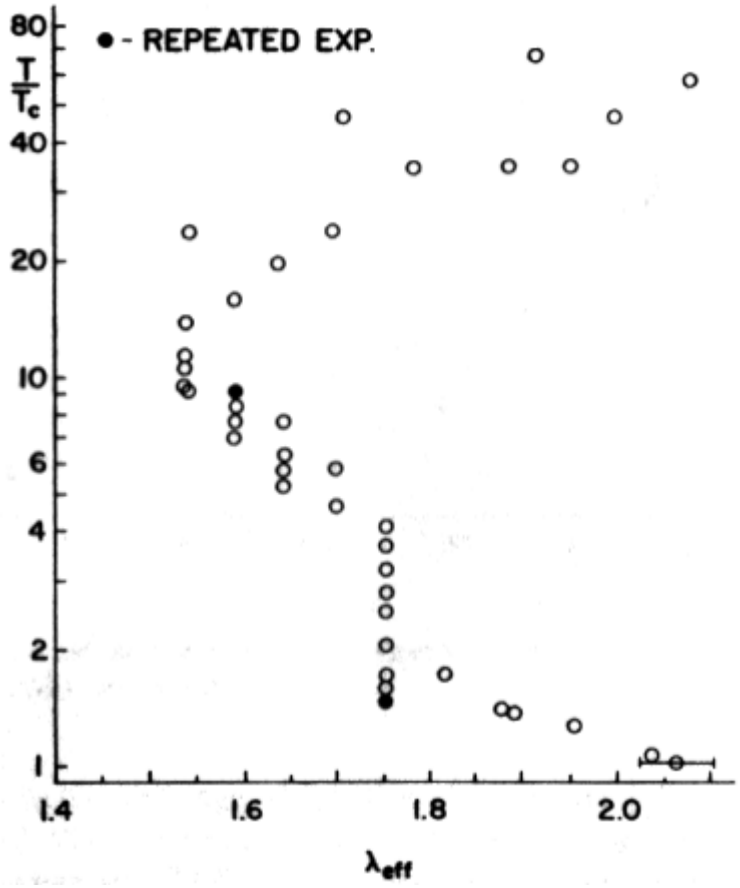

Figure 11.3-4 Wavelength as a function of super-critical Taylor vortices after sudden starts (Burkhalter and Koschmieder 1974)

The development of sub-critical vortices was reported by Mobbs and Ozogan (1984) and some of their results are represented in Figure 11.3-5. The term 'sub-critical Taylor vortices' refers to the formation of vortices at rotational speeds below the accepted critical value (i.e. $T/T_c < 1$). Mobbs and Ozogan (1984) suggest that the reason for these results is a failure of previous researchers to employ the correct measurement techniques. However, it would seem unrealistic to assume that much of the previous research in the field to be incorrect. No detailed description of the experimental technique is provided by Mobbs and Ozogan (1984) and thus it is not possible to determine the reasons for the sub-critical Taylor vortices, which could include effects due to acceleration.

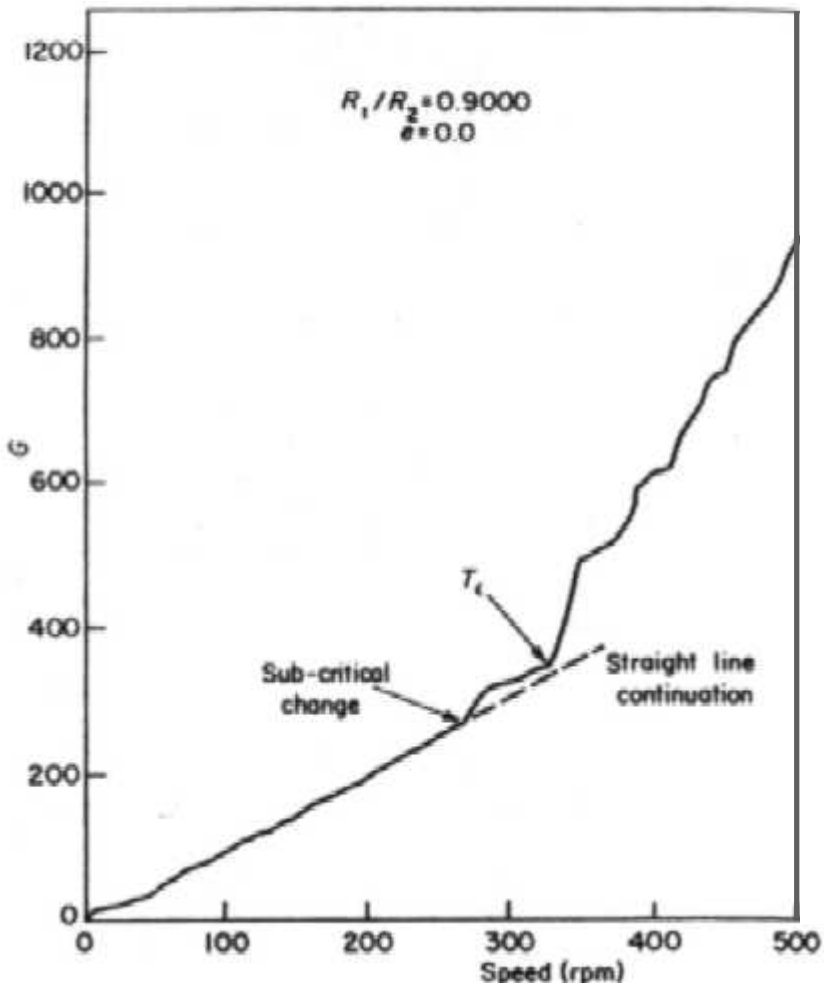

Figure 11.3-5 Measurement of sub-critical Taylor vortices in Couette flow (Mobbs and Ozogan 1984), where G is a function of the measured torque

A significant degree of hysteresis (up to 40%) in the onset of Taylor vortices was reported in acceleration and deceleration experiments, by Park et al. (1981). Initially no hysteresis was observed at quasi-steady state or very slow values of acceleration, but as the rate of acceleration was increased the hysteresis became more pronounced. However, these experiments were transitional type experiments, similar to a rheological stress or rate sweep, where the rotational speed of the inner cylinder is continuously varied with time. The problem with this type of experiment is that there will be a lag time in the system and thus it is not possible to determine whether the hysteresis is due to a purely acceleratory effect or whether it is due to a lag in the system.

To summarise, an examination of previous studies shows that the rate of acceleration can affect the development of Taylor vortices. This is evident from results that show changes in wavelength with changes in acceleration, the development of sub-critical Taylor vortices at unknown acceleration rates and hysterisis effects in the onset of Taylor vortices. While these acceleratory effects are evident, the actual effect of changes in the rate of acceleration of the inner cylinder on the critical rotational speed for the onset speed of Taylor vortices is unknown.

11.3.6 The Effect of Eccentricity

Experimental and theoretical investigations have shown that misalignment between the two concentric cylinder can have an effect on the onset of Taylor vortices (Castle and Mobbs 1967, Castle et al. 1967, Di Prima 1963, Di Prima and Stuart 1972, Frene and Godet 1974, Kamal 1966, Ritchie 1968, Vohr 1968, Zarti et al. 1979). Despite the fact that most rheological equipment consists of accurately machined concentric cylinders, possible defects in manufacture can lead to an eccentric positioning of the cylinders. The relationship therefore between eccentricity and the onset of Taylor vortices must be known as it will define the level of tolerance acceptable in the manufacture and operation of rheological equipment. As is clearly shown in Figure 11.3-6 a significant disagreement exists between the available literature data as to the effect of any misalignment in a concentric cylinder system. The data however, can be separated into two groups; those where the critical Taylor Number continually increases as the eccentric ratio increases and those where the critical Taylor number decreases before increasing. A theoretical explanation for the continuous increase in the Taylor number with an increase in the eccentric ratio is presented by Di Prima and Stuart (1975), using non-local stability theory. While a theoretical explanation for the decrease followed by the increase is also provided by Di Prima (1963), using local stability theory. A detailed examination of which of these two effects is more predominate in rheological measurements is beyond the scope of this investigation and although there are no real conclusions that can be drawn from the literature data, in most cases a significant degree of eccentricity ($\varepsilon > 0.1$) is required before a significant difference (greater ± 5%) in the critical Taylor Number is observed. The eccentricity parameter, ε, is described as the displacement of the inner cylinder's

central axis from the outer cylinder's central axis divided by the average gap width (outer cylinder radius – inner cylinder radius). In general most rheological equipment is built to a high level of precision and only a minimal degree of eccentricity is likely to be present, which should not affect the critical rotational speed at which Taylor vortices appear.

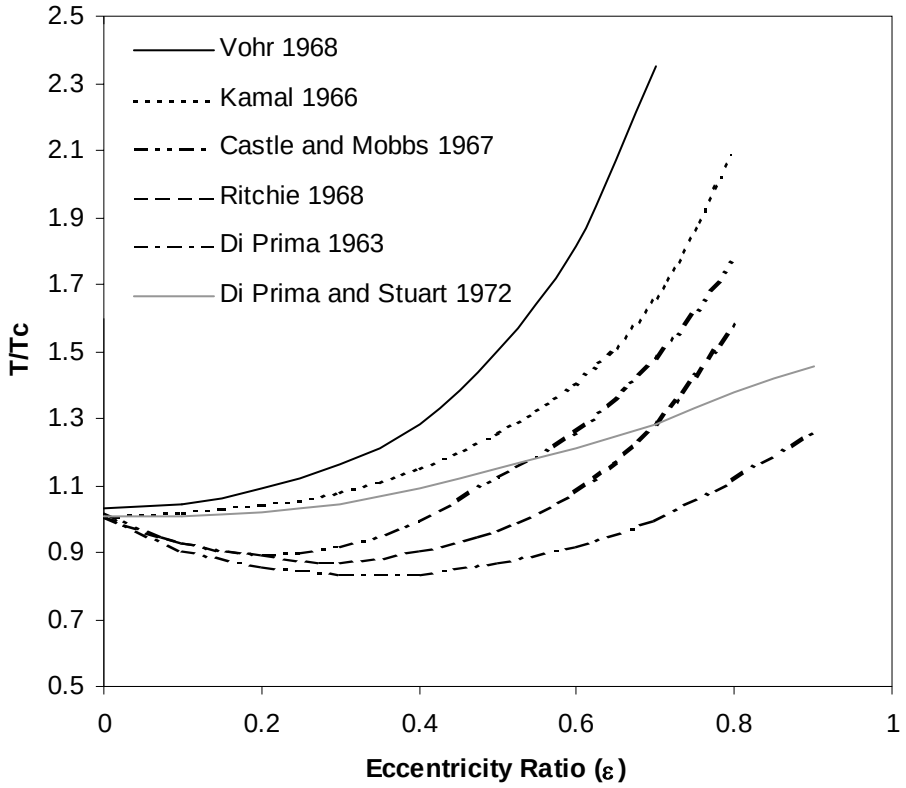

Figure 11.3-6 Normalised critical Taylor number versus eccentricity ratio.

11.3.7 The Effect of Aspect Ratio or End Effects

An assumption of infinitely long cylinders is typical in most theoretical and experimental investigations into the onset of Taylor vortices in Couette flow. However, in most practical situations including rheological applications the actual length of the concentric cylinders is often much less than that which could be assumed to be quasi-infinite. Therefore the effect of the aspect ratio of the cylinders (cylinder length divided by gap width) on the onset of Taylor vortices must be known. It is observed that for an aspect ratio of less than 40 the onset of wavy vortex flow is affected by the cylinder aspect ratio (Cole 1974). For Taylor vortex flow, which

occurs at slower rotational speeds the aspect ratio can be considerably less, as low as 10 before any effects are observed (Cole 1974, Snyder 1969a, 1969b).

11.3.8 The Effect of non-Newtonian Fluids

Whilst the transition from Couette flow to Taylor vortex flow has been extensively studied with Newtonian fluids only minimal investigations have been made into the transition to Taylor vortex flow with non-Newtonian fluids (Beavers and Joseph 1974, Sinevic et al. 1986).

Beavers and Joseph (1974) reported on the appearance of unusually high Taylor vortices in a polyacrylamide solution. However, minimal information was provided in regards to the acceleration rates and no Newtonian results were provided for comparison. It is therefore possible that these unusual vortex heights are due to acceleration effects rather than the nature of the pseudoplastic fluid examined, though no definite conclusion can be drawn due to the lack of information provided.

The degree of non-linearity in a non-Newtonian fluid or the value of the exponential parameter ‘n’ in the power-law model, Equation (2.2-3), was observed to effect the critical rotational speed at which Taylor vortices appeared (Sinevic et al. 1986). For shear-thinning fluids, the more non-Newtonian the fluid or the smaller the value of ‘n’ the greater the critical rotational speed observed. Sinevic et al. (1968) modified the Taylor number, Equation (11.3-5), using a procedure based on an impeller correction procedure for non-Newtonian fluids proposed by Metzner and Otto (1957) to account for the non-Newtonian nature of the fluids. However, significant differences were observed in the calculated critical Taylor numbers for the Newtonian and non-Newtonian fluids.

$$Ta = \frac{2\pi\rho R(\kappa R)(1-\kappa)}{Ak_n^{\,n-1}}\sqrt{\frac{1-\kappa}{\kappa}}N^{2-n} \qquad (11.3\text{-}5)$$

where

$$k_n = 4\pi[n(1-\kappa^{2/n})]^{-1} \qquad (11.3\text{-}6)$$

11.4 Helical Flow

Helical flow is the combination of both annular Poiseuille flow and rotational Couette flow. Either or both of these components of the flow can become turbulent if the correct conditions are met. Combining the two different types of flow can have a synergistic affect on the critical onset of turbulence in each individual flow. Figure 11.4-1 outlines the four different types of flow regimes that may be present in helical flow. By examining the typical operating conditions of the flow rheometer, see CHAPTER 5, it may be concluded that the most likely transition from laminar flow to turbulent instabilities will occur when Taylor vortices develop in the Couette component of the flow, while the axial flow component remains laminar. This conclusion is supported by a set of calculations presented in APPENDIX B. The focus of this investigation will therefore be to develop a detailed understanding of the effect of changes in the axial flow rate on the onset of Taylor vortices in Couette flow in Newtonian and non-Newtonian fluids.

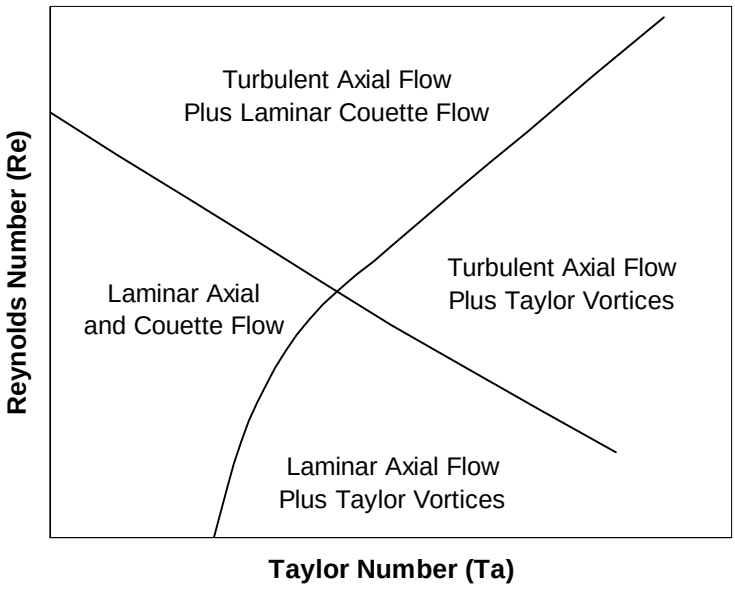

Figure 11.4-1 Flow regimes in helical flow (Di Prima 1960)

11.4.1 The Effect of Axial Flow on the Development of Taylor Vortices

The effect that axial flow can have on the onset of Taylor vortices in helical flow has been the subject of much research both experimentally (Kataoka et al. 1975, Lueptow et al. 1992, Schwarz et al. 1964, Snyder 1962, Takeuchi and Jankowski 1981, Tan et al. 2001) and theoretical (Di Prima 1960, Di Prima and Pridor 1979, Hasoon and Martin 1977, Hughes and Reid 1986, Krueger and Di Prima 1964, Takeuchi and Jankowski 1981). However, in all case the studies have been performed on Newtonian fluids. A summary of the results from these investigations is shown below in Figure 11.4-2. The most obvious conclusions that can be drawn from the results is that the axial flow can have a considerable stabilising effect on the development of instabilities in the Couette component of the flow. Initially at low Reynolds numbers ($Re < 10$) there is little or no effect due to the axial flow and the critical Taylor number remains relatively constant. One set of experimental results by Snyder (1962) shows a small initial increase in the critical Taylor number at a very low Reynolds number of approximately 2 followed by a region of relatively constant values. However, there is no other literature evidence to support this behaviour and the minimal difference is probably due to experimental error. Once a Reynolds number of approximately 10 is exceeded all previous studies show the critical Taylor number increases with further increases in the Reynolds number.

When pure Couette flow (no axial flow) becomes unstable and Taylor vortices develop the toroidal vortices appear one on top of one another along the length of the cylinder. When axial flow is applied, instead of observing a helical structure the vortices remain separated and the vortices proceed along the length of the cylinders, with minimal intermixing (Kataoka et al. 1975).

Most of the experimental work in this area has been performed through visual observation of the fluid flow in clear walled concentric cylinder apparatus (Kataoka et al. 1975, Lueptow et al. 1992, Schwarz et al. 1964, Snyder 1962, Takeuchi and Jankowski 1981). However, it has been shown that the torque method, see section

11.3.2, may also be used to determine the onset of Taylor vortices in a helical flow system (Tan et al. 2001).

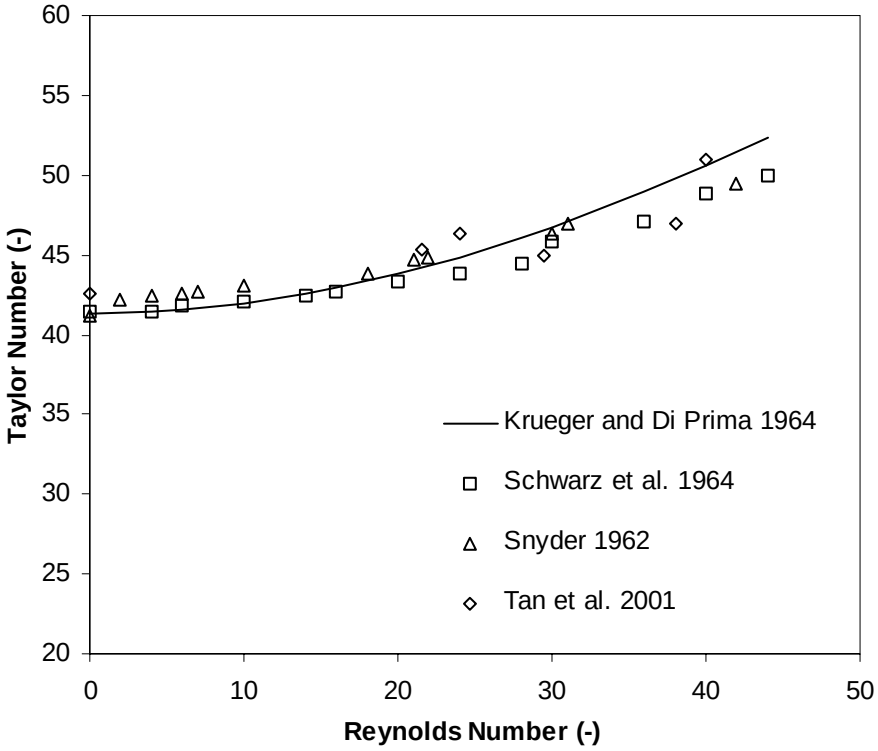

Figure 11.4-2 Effect of axial flow on the onset of Taylor vortices

11.5 Statement of Purpose

The onset of instabilities during rheological measurements in a Couette type geometry will generate errors in the final shear stress calculations. The most likely type of instability to occur in the flow rheometer is the onset of Taylor vortices in the Couette component of the flow. It is therefore important that a stability criterion for laminar helical flow can be defined and thus the purpose of this investigation to develop a stability criterion for the helical flow of non-Newtonian fluids. There are many factors that affect the speed of rotation at which Taylor vortices will first appear and many of these have been previously examined.

- Radius ratio between inner and outer cylinders (gap width)
- Eccentric alignment of the inner cylinder
- Aspect ratio (length to gap width) or end effects
- Additional axial flow rate

There are however, some other phenomena where the effect on the onset of Taylor vortices is unknown and these are discussed below.

Most previous investigations into the onset of Taylor vortices in rotational flow have been under quasi-steady state conditions where the actual acceleration rates are often not quantified. However, many practical applications including rheological measurements have acceleration rates that are faster than quasi-steady state and there are several findings in the literature, which suggest there may be an effect of changes in the rate of acceleration of the inner cylinder on the critical speed at which Taylor vortices appear. Thus one objective of this investigation is to quantify the effect of acceleration on the onset of Taylor vortices.

In calculations of the Taylor number the viscosity is used to describe the rheological properties of the fluid. However, many fluids are non-Newtonian in nature and it is therefore very difficult to correctly determine the Taylor number for these types of fluids. A suitable modification to the Taylor number will therefore be devised and quantified so that the critical rotational speed at which Taylor vortices appear can be determined for the helical flow of non-Newtonian fluids.

CHAPTER 12 EXPERIMENTAL EQUIPMENT

12.1 Introduction

A good knowledge of the transition to Taylor vortex flow is important in rheological measurements as it defines the stable operating limits of a Couette geometry. The onset of instabilities in a Couette geometry will cause measurements of the torque acting on the rotating inner cylinder to increase. By visually inspecting the fluid flow, using visual additives (metallic flakes) or by measuring the torque, the critical conditions at which these instabilities occur may be determined. Both of these methods form the basis of two different measurement techniques used in this investigation to determine the onset of instabilities in both Couette and helical flow.

12.2 Flow Visualisation

12.2.1 Experimental Apparatus

A schematic of the flow visualisation apparatus is shown in Figure 12.2-1 and a picture is shown in Figure 12.2-2. A detailed list of the significant components of the apparatus is presented in Table 12.2-I.

The flow visualisation apparatus consists of a stationary outer Perspex cylinder with an internal diameter of 277mm, a wall thickness of 3mm and a length of 1200mm and three interchangeable anodised aluminium inner cylinders with outer wall diameters of 160mm, 200mm and 250mm. The dimensions of the apparatus were selected using the criteria list below.

- The flow visualization was to be performed with the naked eye and thus the vortices had to be large enough to be clearly seen
- To minimise entrance effects a ratio between gap width and length of 10:1 was required (Cole 1976, Snyder 1969a, 1969b).
- Restrictions due the limited range of sizes available of Aluminium and Perspex tubes.

To seal the apparatus and to prevent vibrations in the central shaft, to which inner cylinders were attached, four roller bearings were used, two at the top and two at the bottom, including appropriate bearing seals.

To minimise end effects open chambers were placed at the top and the base of the concentric cylinders. These chambers were constructed of machined aluminium, which was anodized to prevent corrosion. To ensure an even distribution of the flow to these chambers, six ¾” Nylex tubes were used. The rest of the piping throughout the apparatus was 1” annealed copper tube, except for the inlet and outlet to the smaller rotameter where the diameter was ½” and the inlet and outlet pipes to the pump where 1” Ortac, reinforced flexible rubber tube (manufactured by Goodyear USA) was used to prevent the transfer of vibrations to the rest of the piping network. Two different sized (0-2 L/min and 0-20 L/min) KDG Mobrey 2000 series rotameters

(manufactured by Measurement Resources Pty Ltd, Australia) were used to increase the range of accurate flow rate control. An all stainless steel centrifugal pump (manufactured by Grudfos, Germany) rated at 0-30L/min of water was used to circulate the fluid through the apparatus. To prevent excess wear on the pump a bypass line was used when low flow rates were required.

A 0.55kW 3-phase synchronous AC motor (manufactured by Brook-Hanson (Australasia) Pty Ltd) was used in conjunction with a 690+ frequency inverter speed controller (manufactured by Eurotherm Drives, UK). The 690+ frequency inverter gave accurate speed control to within 0.01% of the maximum motor speed or 0.15 rpm. The frequency inverter also allowed the acceleration rate of the motor to be adjusted between 15.7 rad/s/s and 0.053 rad/s/s. To measure the temperature throughout the length of the annulus three K-type thermocouples were placed an equidistant along the length of the outer cylinder. The thermocouples were connected to a DataTaker DT50 (manufactured by DataTaker Australia Pty Ltd), which includes cold junction compensation and this was connected to a computer for data logging. Three 2mm injection ports were equally spaced along the opposite sides of the outer cylinder and these ports were used to either inject dyes to aid in the flow visualization or to withdraw samples of the fluid for analysis.

When operated fluid flows out of the storage tank (T - 01) via gravity and into the pump (P - 01). From the pump the fluid travels towards valve (V - 04), where depending on the position of the valve (V - 04) the fluid either returns to the storage tank or is forced towards the rotameters (R - 01 and R - 02). Valves (V - 05) and (V - 06) control the direction of the flow to either rotameter (R - 01) or (R - 02). The globe valves (V - 07) and (V - 08) respectively, control the rate of flow through the two rotameters. Once the fluid exits the rotameters the direction of flow is through the pipe to the distributor, which is located below the motor. The fluid then flows into the six delivery tubes to evenly distribute the flow into the concentric cylinders. The fluid in the six tubes enters the open chamber and then the concentric cylinders. The fluid leaves the concentric cylinders through another open chamber and another six-pipe distributor before returning to the storage tank. The return line of the storage tank includes an s-bend to prevent air entering the system.

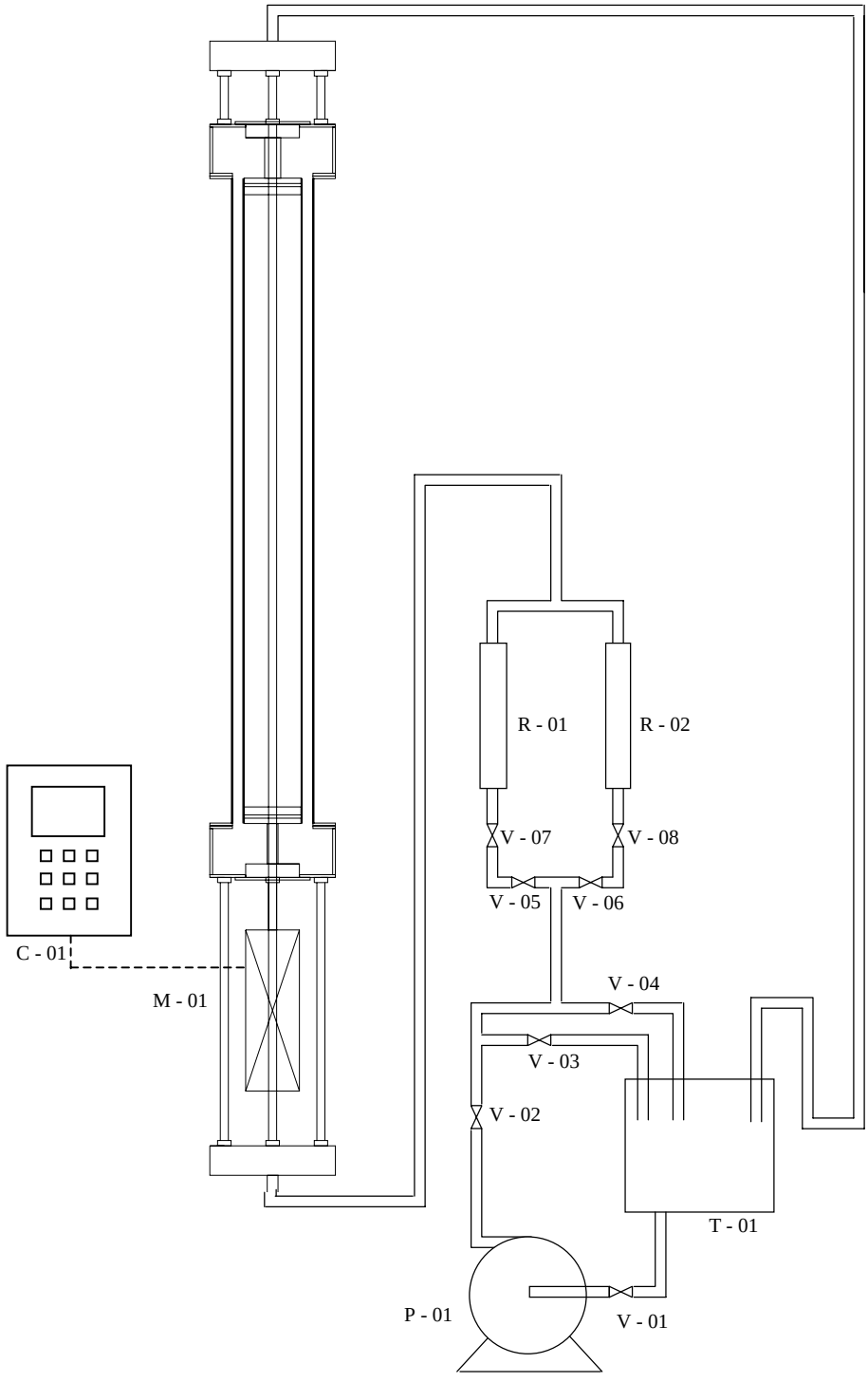

Figure 12.2-1 Schematic of the flow visualisation apparatus

Figure 12.2-2 Photograph of the flow visualisation apparatus

Table 12.2-I List of components of the flow visualisation apparatus

Equipment No.	Description	Manufacturer
V – 01	1” Ball Valve	John’s Valves, Australia
V – 02	1” Ball Valve	John’s Valves, Australia
V – 03	1” Ball Valve	John’s Valves, Australia
V – 04	1” Ball Valve	John’s Valves, Australia
V – 05	1” Ball Valve	John’s Valves, Australia
V – 06	0.5” Ball Valve	John’s Valves, Australia
V – 07	1” Globe Valve	John’s Valves, Australia
V – 08	0.5” Globe Valve	John’s Valves, Australia
R – 01	1” Rotameter	Measurement Resources, Australia
R – 02	0.5” Rotameter	Measurement Resources, Australia
C – 01	Motor Controller	Eurotherm Drives, UK
M – 01	Electric Motor	Brook-Hanson, Australasia
P – 01	Centrifugal pump	Grundfos, Germany
T – 01	Storage Tank	-

12.2.2 End Effects

When a flowing fluid enters a pipe, a certain distance is required for smooth laminar flow to develop (Gerhart et al. 1992). For accurate flow visualisation of fully developed helical flow the entrance development length had to be determined for the experimental flow visualisation system. The criterion proposed by Sparrow and Lin (1964), Equation (11.2-5), was used to determine the required entrance length for stable flow to develop in a Newtonian glucose – water solution. As can be observed from Figure 12.2-3 the entrance development length has a maximum value when the widest gap width is used and the pump is providing the maximum flow rate (approx. 30L.min.). Under these conditions the entrance development length is only 110mm, which is less than 10% of the total cylinder length of 1200mm, thus the results from the flow visualisation apparatus should not be affected by any entrance flow development effects.

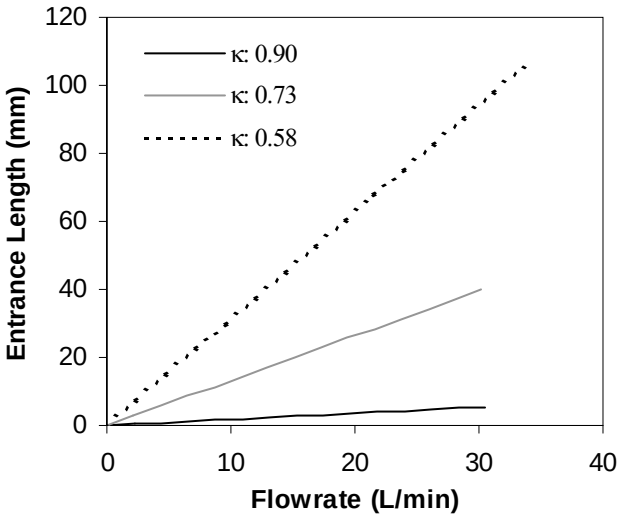

Figure 12.2-3 Entrance development length for a glucose water solution

12.2.3 Experimental Techniques

Experiments with the flow visualization apparatus required the preparation of approximately 45L of test solution. To enable flow visualisation a small quantity of Aluminium flakes were added to the solution (1-2g depending on the viscosity of the fluid). The Aluminium flakes, produced by Silberline Manufacturing Co USA, have a particle size less than 325 mesh and are inhibited against reaction with water. Once prepared a solution was transferred to the feed tank of the apparatus. The solution was then circulated through the apparatus for about 30 minutes before the flow was switched off to give the fluid time to stabilize and to give trapped air bubbles time to escape.

A small sample (120mL) of the fluid, including the Aluminium flakes, was withdrawn from the apparatus so that the density and viscosity could be determined. The size and low concentration of Aluminium flakes meant that their effect on either the rheological properties or the density would be minimal. However, to ensure there was no error, the measurements of the rheological properties and the density were performed with the flakes in the fluid at the same concentration as the actual test fluid. The Bohlin CVO-50 constant stress rheometer, with the 4°/40mm cone and plate geometry was used to determine the rheological properties of the fluid. This was achieved by performing a series of five to seven constant stress (as a function of time) tests, see section 6.4.1. A 100mL density bottle was used to determine the fluid density.

So that the effects of frictional heat build-up within the circulating fluid could be corrected for, the rheological properties and density of the test fluid were determined at three different temperatures typically 20ºC, 25ºC and 30ºC. A linear interpolation procedure was then used to approximate the rheological properties and density at any temperature within this range.

To determine the critical onset point of Taylor vortices a simple acceleration test was first performed with no axial flow rate. The speed of the inner cylinder was quickly increased and the rotational speed at the onset of Taylor vortices was noted, the

cylinder was then returned to rest. Axial flow through the instrument was then established and brought to a constant desired value. A rate of acceleration for the inner cylinder was pre-programmed, as was the desired final rotational speed, typically close to the observed critical onset point. The cylinder was then set in motion and the flow patterns observed. Once the flow patterns had stabilized the presence of any Taylor vortices was recorded as was the temperature and the height of the vortices (if present). The cylinder was then returned to rest. A new speed was then selected and the procedure repeated; this was done typically for a further 10-15 different values of rotational speed all of which were either slightly above or below the critical rotational speed. A new axial flow rate was then selected and the procedure repeated for a further 5-7 different values of axial flow rate.

12.2.4 Analysis of Results

The raw data obtained from the flow visualisation apparatus was rotational speed, vortex height and temperature. To determine the Taylor number a relationship was first developed between temperature and viscosity and temperature and density. For non-Newtonian fluids (described using the power-law model) it was determined that the value of the exponential parameter, n was relatively constant over a ten-degree temperature change as is shown in Table 12.2-II. An average value of n was therefore selected and the values of the pre-exponential parameter, A were recalculated using the new average value of n, Table 12.2-III. Thus only one relationship between the parameter A and temperature was then required instead of a complex relationship between the two power-law model parameters (A and n) and temperature.

Table 12.2-II Power-law model parameters for a CMC solution

Temperature (^oC)	A ($Pa.s^n$)	n
20	0.079	0.934
25	0.068	0.936
30	0.058	0.939

Table 12.2-III Updated power-law model parameters for a CMC solution

Temperature (°C)	A (Pa.s^n)	n
20	0.078	0.936
25	0.068	0.936
30	0.060	0.936

The Taylor number for each rotational speed was then determined using Equation (12.2-1). However as this equation is only valid for Newtonian fluids; a more detailed description of the calculations for non-Newtonian fluids is presented in section 13.4.

$$Ta = \frac{\Omega\rho(\kappa R)(R-\kappa R)}{\mu}\sqrt{\frac{(R-\kappa R)}{(\kappa R)}} \qquad (12.2\text{-}1)$$

The wave number was determined using Equation (12.2-2), where H equals the height of a Taylor vortex.

$$\psi = \frac{2\pi(R-\kappa R)}{H} \qquad (12.2\text{-}2)$$

For a set of results for a given value of acceleration, axial flow rate and fluid type the critical speed at which Taylor vortices appear was then determined, by plotting Taylor number versus wave number. The onset point was determined by a sharp increase in the curve, from a Wave number of zero to nearly 2π as illustrated in Figure 12.2-4.

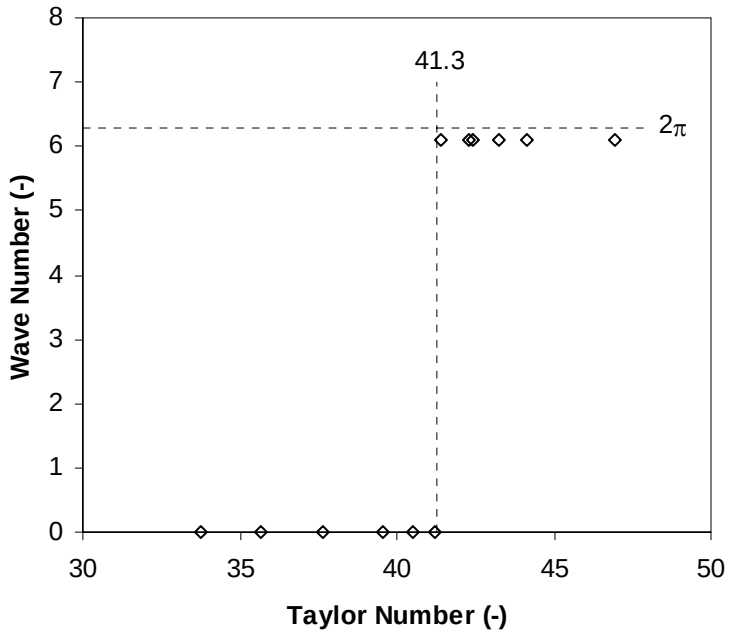

Figure 12.2-4 Graph of Taylor number versus wave number for a Newtonian glucose-water solution

12.3 Torque Method

12.3.1 Experimental Apparatus

Two different apparatus were used to investigate the turbulent transition to Taylor vortex flow in both Couette and helical flow using a torque measurement method. The standard geometries of the Haake rheometer outlined in section 6.4.2, were used in this investigation and in particular the MV III geometry was used. This geometry was selected because it had the largest gap width of 5.8mm, which meant that for most fluids instabilities could be generated in the flow at a rotational speed within the Haake VT550's operating range. For examination of helical flow turbulence the flow rheometer, described in Section B, was used. The smaller of the two bobs (32mm diameter) was used as again the larger gap width between the cylinders gave a lower rotational speed for the onset of Taylor vortices.

12.3.2 Experimental Techniques

The experimental techniques for both the Couette and the helical flow systems were quite similar. For Couette flow the rheometer was run at a series of different constant speeds from low to high values and the torque was measured as a function of time. The results were analysed, see section 12.3.3 and then further tests were performed, this time focusing on rotational speeds closer to the critical onset point. For helical flow experiments the two-test procedure was the same as for the Couette experiments but this time the fluid was pumped through the apparatus at a constant flow rate. The two-test procedure was then repeated at a variety of different flow rates to investigate the effects of flow rate on the onset of Taylor vortices.

12.3.3 Analysis of Results

The measured variable in these experiments was torque as a function of rotational speed. A plot of these two values allows the critical speed at which Taylor vortices appear to be directly determined, see Figure 12.3-1. As explained in section 12.3.2, Test 1 corresponds to a broad ranging test to roughly determine the critical speed for the onset of Taylor vortices, while Test 2 is used to more accurately determine the critical onset speed by examining a much smaller range of rotational speeds. The critical Taylor number for the system may then be determined using Equation (12.2-1), for Newtonian fluids and for non-Newtonian fluids see section 13.4.

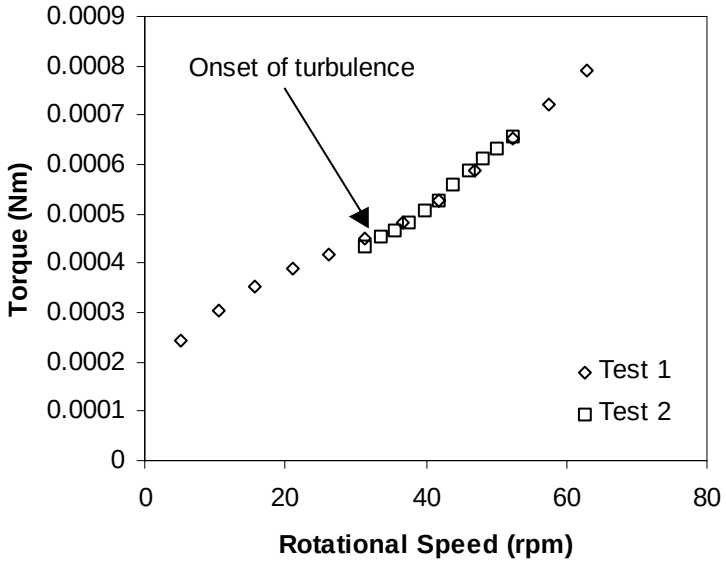

Figure 12.3-1 The onset of Taylor vortices in a non-Newtonian fluid

CHAPTER 13 INSTABILITIES IN COUETTE FLOW

13.1 Introduction

The onset of turbulence in a Couette flow system has been shown by Taylor (1936) and by Donnelly (1958) to increase the measured torque value, which will create errors in the rheological characterisation of a fluid. The flow rheometer discussed in Section B, is a Couette type system with the addition of axial flow and thus there is the possibilities that instabilities may develop in the flow rheometer. Furthermore the large gap width between the inner and outer cylinder and the fact that most mineral slurries have relatively low viscosity values means that turbulence may readily occur

under typical operating conditions. The aim of this investigation is therefore to define the transition from Couette flow to Taylor vortex flow for non-Newtonian fluids in a helical flow system.

Many rheological measurements and in particular those performed with the flow rheometer are torque versus time experiments and for these experiments the inner cylinder is rapidly accelerated from rest to the operating speed. Most of the previous studies regarding the onset of Taylor vortices have been performed under conditions where the acceleration rates are very slow, quasi-steady state, thus the effect of the rapid acceleration of the inner cylinder will also be investigated.

13.2 Experimental Study With Newtonian Fluids

To determine the suitability of the experimental apparatus and that the measurement techniques used in this study were correct, a series of experiments were performed with Newtonian liquids. Two different experimental techniques and apparatus, the flow visualisation apparatus and the MV III Couette geometry, as outlined in CHAPTER 12, were used to determine the critical rotational speed and the Taylor number at the onset of turbulence in a Newtonian liquid. The Newtonian liquid used in this investigation was a glucose-water solution. It is known that the water in the solution evaporates with time and so it is not possible to determine an exact value of the glucose concentration of the solution during the test period of several weeks. Due to the extended nature of the testing program and the evaporation of a portion of the test solution the viscosity and density of the glucose solution was determined daily before any tests were commenced. The viscosity and density of the glucose solution was also determined at three different temperatures, as described in 12.2.2, so that any changes due to viscous heating during experiments could be predicted.

Hysteresis in the onset of Taylor vortices has been observed in some experiments (Coles 1965) depending on whether the speed of the rotating cylinder has been increased or decreased. In the experiments performed in this investigation no hysteresis was observed in the results obtained. The speed of rotation was increased and decreased across the critical onset point with no change in the critical onset speed.

The difference between the tests performed in this study and those previously performed which showed hysteresis (Coles 1965) is that these tests are not dynamically changing with time. In the previous tests the rotational speed of the inner cylinder was constantly varied with time and this type of test can produce unexpected results because of lag times in the system. The experimental procedures used in this study should eliminate these effects, which is why hysteresis is not observed in the current experimental results. The results from the experiments with the Newtonian glucose-water solution are presented in Figure 13.2-1.

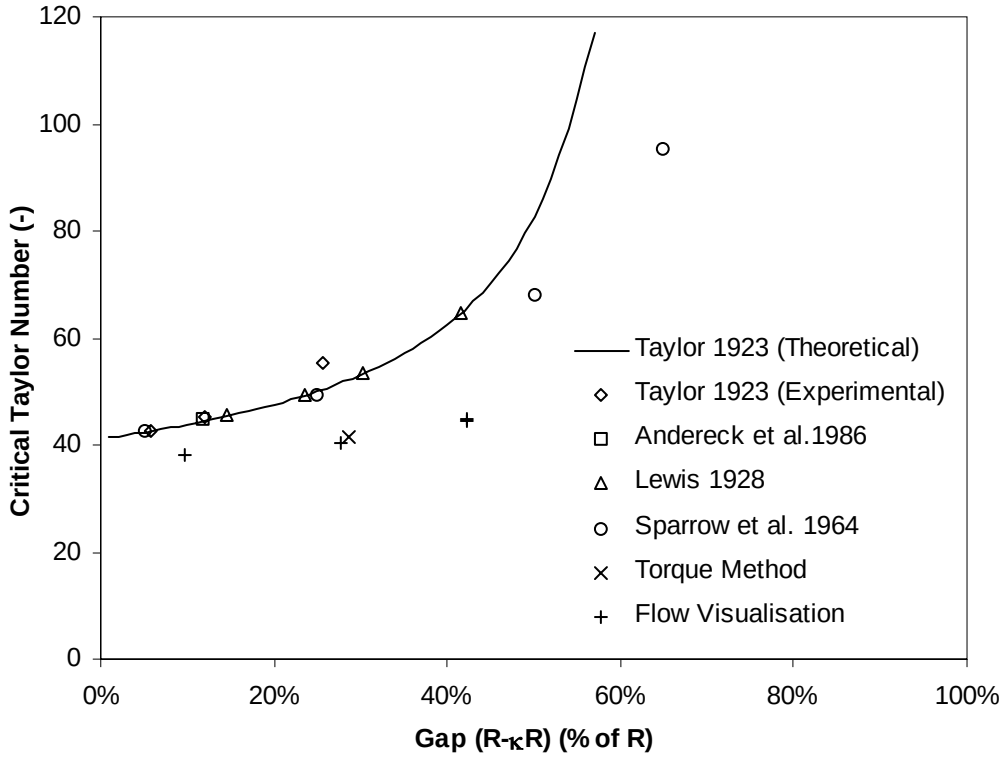

Figure 13.2-1 Comparison between experimental and literature Taylor numbers

A similar trend is observed between the literature data and the experimental results, with both sets of data showing an increase in the critical Taylor number with increasing gap width though the increase in the experimental results is less than the literature results.

This unusual result was further investigated by examining the vortex heights (or the wave numbers of the vortices that formed). A change in the wave number could

indicate the presence of an effect responsible for the lower than expected critical onset of speed shown in Figure 13.2-1. Wave numbers from measurements with the flow visualisation apparatus are presented in Table 13.2-I; wave numbers from experiments with the Haake concentric cylinder geometry could obviously not be determined. As is observed, the experimental results from the flow visualisation apparatus are extremely close to 2π (6.28); a wave number of 2π indicates the presence of square vortices. The presence of square vortices is to be expected (Taylor 1923) and thus does not indicate the presence of any unusual effects in the experimental results.

Table 13.2-I Table of experimental wave numbers at different gap sizes

Gap (% of R)	Length to gap ratio	Wave Number
9.8	177.8	5.9
27.7	62.5	6.2
42.2	41.0	6.1

Other effects which may be responsible for the formation of vortices at slower than expected rotational speeds include eccentricity and a small length to gap ratio. Visual inspection and measurement of the rotating cylinders shows that there is minimal eccentricity in the alignment of the cylinders. Examination of previously reported literature results, Figure 11.3-6, shows that significant levels of eccentricity are necessary before a significant change in the critical onset speed is observed. Thus it is not expected that an eccentric effect is responsible for the formation of vortices at slower than expected rotational speeds.

The dimensions of the flow visualisation apparatus are specified in section 12.2.1 and give length to gap ratios of between 89:1 for the smallest gap to 21:1 for the largest gap. All of these values are larger than the value of 10:1, which is reported by Cole (1976) and Snyder (1969a, 1969b) as the minimum length to gap ratio needed to avoid affecting the critical speed at which Taylor vortices form.

The literature data used for comparison in Figure 13.2-1 were obtained under very slow acceleration conditions, or quasi-steady state. The rate of acceleration of the inner cylinder in the experiments performed as part of this study could not be considered quasi-steady state, with an acceleration rate of approximately 5 rad/s/s. The possible effect that changing the rate of acceleration of the inner cylinder has on the critical speed at which instabilities occur is discussed in section 13.3.

13.3 The Effect of Acceleration

The rate of acceleration has been reported to effect the size of Taylor vortices (Andereck et al. 1983, Burkhalter and Koschmieder 1974, Donnelly et al. 1965, Gorman and Swinney 1982, Koschmieder 1979) and possibly to induce Taylor vortices at sub-critical rotational speed (Mobbs and Ozogan 1984). From examination of previous results there appears to be an effect due to the acceleration rate of the inner cylinder on the critical speed at which Taylor vortices develop. However, the actual values of the acceleration are seldom published in the literature except to state that the acceleration is quasi-steady state or very slow so any possible effect due to acceleration cannot be quantified with existing data.

Any possible effect on the critical rotational speed for the onset of Taylor vortices, due to a change in the acceleration rate is very important as most rheological measurements and many other practical applications involve acceleration rates above that which could be considered quasi-steady state. The aim of this investigation is to determine the effect that changing the rate of acceleration has on the critical rotational at which Taylor vortices appear.

Data for the onset of Taylor vortices was collected using both the flow visualization apparatus and the torque measurement technique at a variety of different acceleration rates and the combined results are presented below in Figure 13.3-1. A steady decrease in the critical onset speed or the Taylor number is observed as the acceleration rate is increased to a rate of 0.01 rad/s/s. However, beyond this value of acceleration the critical speed for the onset of Taylor vortices remains constant over a three-decade rise in the rate of acceleration of the inner cylinder. This result is

significant for most practical applications, as the speed at which Taylor vortices occur is likely to be independent of changes in the rate acceleration. This is because the range of acceleration rates used in most rheological measurements is well inside the region where the onset of Taylor vortices is independent of the rate of acceleration. It is important to note however, that the critical speed for the onset of these vortices is nearly 10% lower than that reported in the literature for quasi-steady state acceleration.

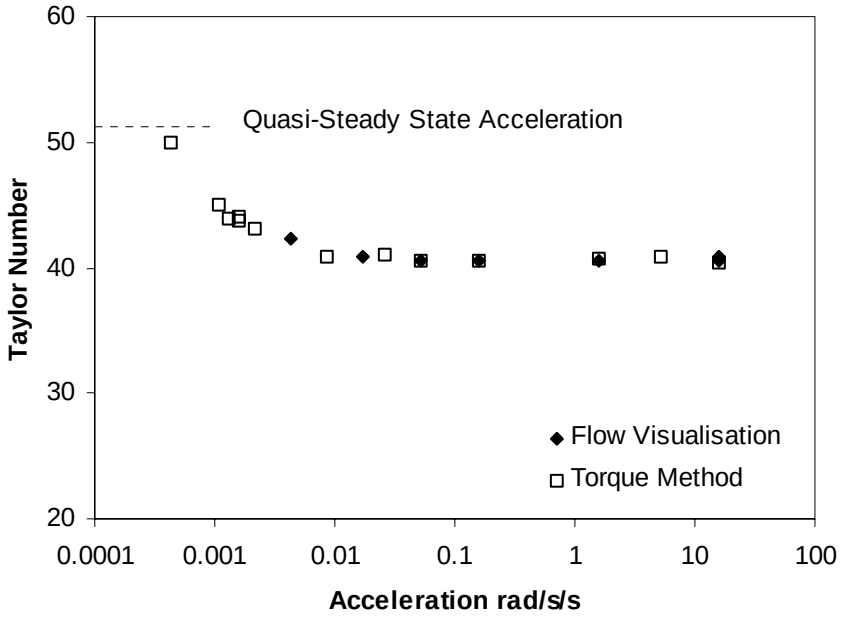

Figure 13.3-1 Effect of the rate of acceleration on the onset of Taylor vortices (Gap: 27.7 % of R)

The experimental data presented in Figure 13.2-1 is for results obtained under acceleration rates of approximately 5 rad/s/s. As can be seen from Figure 13.3-1, this is well inside the region where the critical speed for the onset of Taylor vortices is independent of the rate of acceleration, but also and importantly the critical value at which the vortices form is less than that previously reported in the literature. Thus it is expected that the results presented in Figure 13.2-1 should be less than those previously reported in literature because they are obtained at a higher rate of acceleration than quasi-steady state.

13.4 Non-Newtonian Fluids

The equation of the Taylor Number shown below is only applicable for Newtonian fluids. For many practical applications the fluid is non-Newtonian in nature so the effect that non-Newtonian fluids have on the Taylor number must be defined. There have been a minimal number of previous studies on the onset of Taylor vortices in non-Newtonian fluids and thus the aim of this study is to examine the effect of non-Newtonian fluids on the onset of Taylor vortices in Couette flow

$$Ta = \frac{v_\theta R(1-\kappa)}{\nu}\sqrt{\frac{(1-\kappa)}{\kappa}} \qquad (11.3\text{-}4)$$

Non-Newtonian fluids in general cover a wide range of fluid types, which makes their overall analysis complex. Calculations for non-Newtonian fluids from measurements with the flow rheometer assume that the rheological properties of the fluid can be described by the power-law model, Equation (2.2-3), over the range of shear rates under investigation. To simplify this investigation with non-Newtonian fluids it will also be assumed that the power-law model can be used to describe the rheological behaviour of the fluids at rotational speeds close to the critical speed for the onset of Taylor vortices. From rheological measurements described in section 7.3, the usual effect that invalidates the power-law assumption is associated with yield stress fluids at low values of shear rate, however, because the onset of turbulence generally occurs at higher values of shear rate this problem should be less prevalent

The Newtonian Taylor number contains a viscosity term, which is obviously not valid for non-Newtonian fluids. As previously discussed in section 11.3.8, the method used by Sinevic et al. (1986) to modify the Taylor number for non-Newtonian fluids is analogous to a mixing impeller design, where the speed of rotation of the inner cylinder is directly related to the shear rate via a parameter k_n.

In this study to modify the Taylor number for non-Newtonian fluids using the power-law model the apparent viscosity at the operating shear rate is determined. A similar procedure is detailed in Skelland (1967) for modifying the Reynolds number for non-

Newtonian fluids. The Krieger and Maron method (Krieger and Maron 1953, 1954) for estimating the shear rate in a Couette system for shear thinning fluids in a wide gap can be used to determine an approximate value if the rheological properties are unknown. However, if the power-law model, Equation (2.2-3), is used to describe the rheological behaviour of the fluid then the shear rate may be directly determined, using Equation (13.4-1) (Steffe 1992).

$$\dot{\gamma} = \left(\frac{2\Omega}{n}\right)\left(\frac{1}{1-\kappa^{2/n}}\right) \tag{13.4-1}$$

The apparent viscosity of a power-law model fluid may be determined using Equation (13.4-2).

$$\eta = A\dot{\gamma}^{n-1} \tag{13.4-2}$$

Substituting the expression for the apparent viscosity and the shear rate in to the Newtonian Taylor number the modified Taylor number for power-law model fluids can be written as follows.

$$Ta_{\text{power-law}} = \frac{\Omega\rho(\kappa R)(R-\kappa R)}{A\left(\left(\frac{2\Omega}{n}\right)\left(\frac{1}{1-\kappa^{2/n}}\right)\right)^{n-1}}\sqrt{\frac{(R-\kappa R)}{(\kappa R)}} \tag{13.4-3}$$

This modified Taylor number for power-law model fluids collapses to the Newtonian Taylor number when the exponential parameter n is set to a value of one and thus this modified Taylor number can be used for both Newtonian and non-Newtonian fluids.

A number of experiments were performed with different non-Newtonian fluids to examine the validity of the proposed modified Taylor number, Equation (13.4-3). Included also in this examination was data from the only literature experimental work involving the development of Taylor vortices in non-Newtonian fluids performed by Sinevic et al. (1986). The results from the investigation are presented in Figure 13.4-1. To eliminate the effect on the onset of Taylor vortices by other factors

including gap width and rate of acceleration, the Taylor number for power-law model fluids is divided by the Newtonian Taylor number predicted for the particular system and operating conditions, referred to as Ta_{crit}.

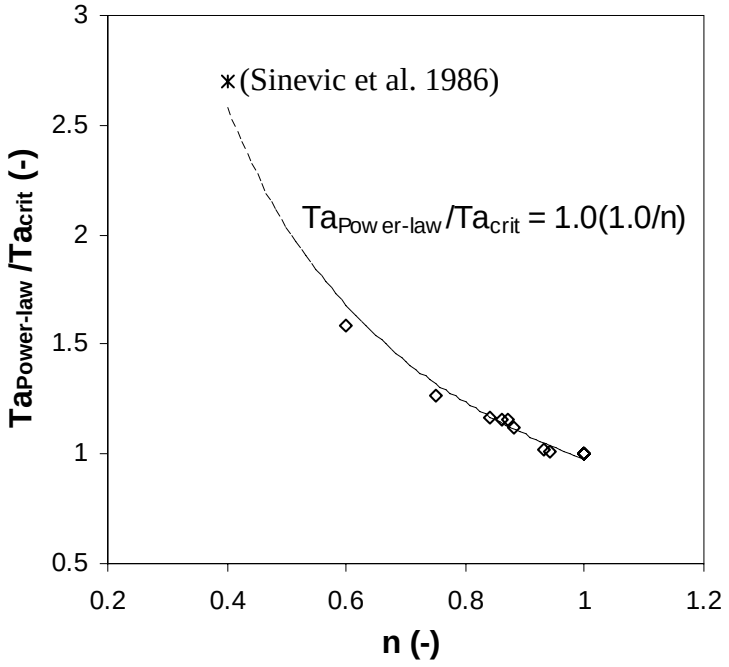

Figure 13.4-1 Effect of the power-law parameter n on the onset of Taylor vortices

From the results presented in Figure 13.4-1 a relationship between the critical value for the onset of Taylor vortices and the exponential parameter, n is observed. The relationship between n and the critical Taylor number is an inverse proportionality relationship for a range of n values from 1 to 0.4. This relationship was incorporated into the power-law Taylor number, Equation (13.4-3) and the modification is presented in Equation (13.4-4), which represents the final modified Taylor number for non-Newtonian fluids using the power-law model.

$$Ta_{power\text{-}law} = n\frac{\Omega\rho(\kappa R)(R-\kappa R)}{A\left(\left(\frac{2\Omega}{n}\right)\left(\frac{1}{1-\kappa^{2/n}}\right)\right)^{n-1}}\sqrt{\frac{(R-\kappa R)}{(\kappa R)}} \qquad (13.4\text{-}4)$$

13.5 Summary

Laminar Couette flow, which is found in concentric cylinder geometries, may become unstable when the speed of rotation of the inner cylinder is increased above a critical value. Several key factors, which had not been previously completely investigated, were identified as affecting the critical speed at which instabilities appear, particularly in rheological measurements and these included the rate of acceleration of the inner cylinder and the non-Newtonian nature of the fluid.

An increased rate of acceleration was found to have a destabilising effect on Couette flow. For as the rate of acceleration was increased above quasi-steady state (or very slow values) the critical speed for the onset of instabilities was observed to quickly decrease to a value approximately 10% lower than that previously reported in literature for quasi–steady state acceleration. Once this lower value was reached the critical rotational speed for the onset of Taylor vortices was independent of further changes in the rate of acceleration.

The Taylor number like the Reynolds number requires a description of the rheological properties of the fluid, which is usually represented by the viscosity. Most fluid and in particular mineral slurries do not conform to the Newtonian model but are instead non-Newtonian in nature. The concept of a single independent viscosity value to describe the rheological behaviour of the fluid cannot be used and thus the Taylor number was suitably modified such that the stability of Couette flow in non-Newtonian fluids could be predicted. The modification used the power-law model to describe the rheological behaviour of non-Newtonian fluids and whilst the power-law model may not be particularly accurate over a wide range of shear rate values, acceptable agreement can usually be obtained over a small range of shear rate values, particularly at higher values of shear rate, which is usual around the critical speed at which Taylor vortices form.

CHAPTER 14 INSTABILITIES IN NON-NEWTONIAN HELICAL FLOW

14.1 Introduction

Helical flow is the combination of axial flow and Couette flow and for the flow to become turbulent one or both components of the flow needs to become unstable. The addition of axial flow to Newtonian Couette flow can have a considerable stabilising effect on the Couette flow (Di Prima 1960, Kataoka et al. 1975, Krueger and Di Prima 1964, Lueptow et al. 1992, Schwarz et al. 1964, Snyder 1962, Takeuchi and Jankowski 1981, Tan et al. 2001). Couette flow can also affect the onset of turbulence in axial flow as shown below in Figure 14.1-1. However, calculation performed in APPENDIX B show in the flow rheometer the instabilities that are most likely to develop are Taylor vortices with laminar axial flow and thus the discussion will be restricted to this phenomenon.

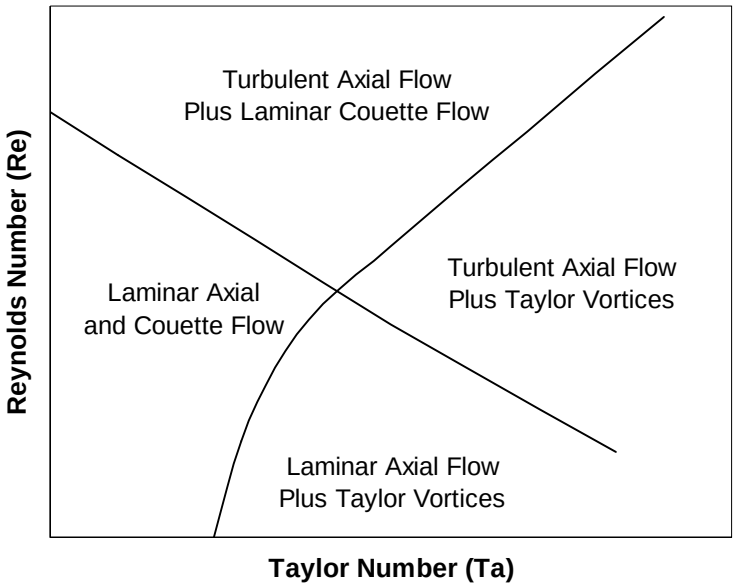

Figure 14.1-1 Flow regimes in helical flow (Di Prima 1960)

At axial flow Reynolds numbers below a value of approximately 10 the onset of Taylor vortices in the Couette rotational component of the flow is unaffected by the axial flow but beyond this Reynolds number, the onset of instabilities in the Couette flow is delayed.

When axial flow is applied to unstable Couette flow (Taylor vortex flow), contrary to expectation, the flow does not become helical in nature, but the vortices remain as they do in Couette flow with minimal intermixing between vortices (Kataoka et al. 1975). The only difference is that the vortices now move with a speed dependent on the axial flow rate.

14.2 The Effect of Axial Flow on the Onset of Taylor Vortices in Newtonian and non-Newtonian Fluids

It is known that when an axial flow is applied to a Newtonian fluid the onset of Taylor vortices in Couette flow is delayed. It is assumed that a similar response will be observed with non-Newtonian fluids, however there are no significant studies in the literature to substantiate this hypothesis. It is also know from the calculations to determine the shear stress and shear rate under helical flow conditions, as found in the flow rheometer, see CHAPTER 4 and CHAPTER 8, that the addition of axial flow can affect the total shear rate in the system. Thus to perform the calculations to determine the Reynolds number and Taylor number, the apparent viscosity of the fluid at the overall shear rate must be known. However, to do this would significantly complicate any calculations to determine the Reynolds number and the Taylor number. So to simplify the calculations, the Reynolds number and Taylor number are each determined independently and it is assumed that any synergistic effects between the two will be incorporated into the overall relationship between the critical Taylor number and the Reynolds number for non-Newtonian fluids.

As previously described in section 13.4 the power-law model is assumed to describe the rheological properties of the fluid over a small range of shear rate values close to the critical rotational speed for the onset of Taylor vortices.

The Reynolds number for fluids described by the power-law model in annular pipe flow is shown in Equation (11.2-2).

$$\mathrm{Re} = \frac{\left[2R(1-\kappa)\right]^{n}\left\langle v_z\right\rangle^{2-n}\rho}{(8\varphi)^{n-1}A'} \qquad (11.2\text{-}2)$$

The Taylor number for power-law fluids was derived previously, see section 13.4, and is shown in Equation (13.4-4).

$$Ta_{power\text{-}law} = n\frac{\Omega\rho(\kappa R)(R-\kappa R)}{A\left(\left(\frac{2\Omega}{n}\right)\left(\frac{1}{1-\kappa^{2/n}}\right)\right)^{n-1}}\sqrt{\frac{(R-\kappa R)}{(\kappa R)}} \qquad (13.4\text{-}4)$$

The effect of axial flow rate on the onset of Taylor vortices in both Newtonian and non-Newtonian fluids was examined using the flow visualisation technique. A variety of different fluids with varying rheological properties were examined under a variety of different gap widths. However, because the fluid properties changed on a daily basis (mostly through evaporation of water) and varied with temperature it is impossible to present all the rheological and physical property measurements, but to minimise errors due to this constant variation the rheological properties and density were measured on a daily and at three different temperatures as outlined in section 12.2.3.

To distinguish the different fluids and gap widths in the results the following superscripts are used (G: glucose-water solution; C: CMC solution; P: polyox solution; W: Wide-Gap (42.2% of R); M: Moderate-Gap (27.7% of R); N: Narrow-Gap (9.75% of R)). To eliminate the effect of gap width (as described in section 13.2) the experimentally determined critical power-law Taylor number for the different gap widths is normalised by dividing the experimentally determined result by the predicted critical Newtonian Taylor number (rotational flow only) for the particular gap width and rate of acceleration. In this way any effects due to the axial flow on the critical Taylor number in either Newtonian or non-Newtonian fluids can be isolated and observed without the effect of gap.

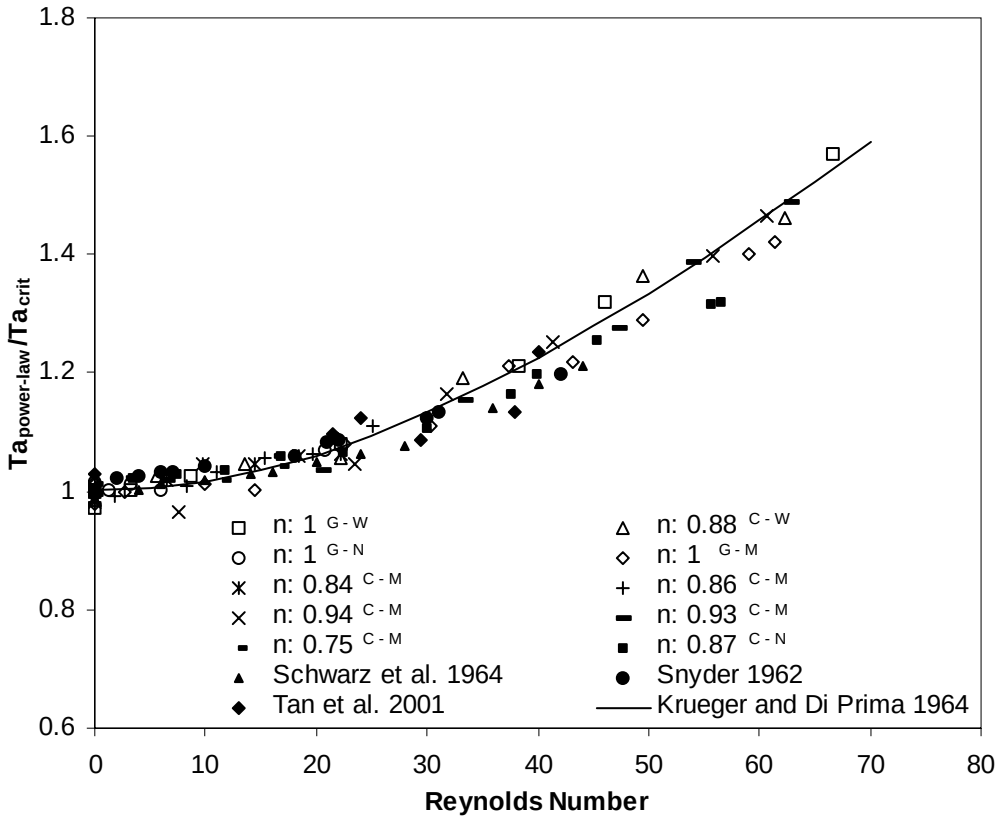

Figure 14.2-1 Combined results for the effect of axial flow on the onset of Taylor vortices in both Newtonian and non-Newtonian fluids

Combined results for both Newtonian and non-Newtonian fluids are presented in Figure 14.2-1. Good agreement is observed between the experimental results for Newtonian fluids and the literature data, with an average error of 0.6% and a standard deviation of 2.2%. Similarly good agreement is observed between the literature results and the experimental results for the non-Newtonian fluids with an average error of 0.9% and a standard deviation of 2.0%. These results indicate that there is no significant difference in the effect of axial flow on the formation of Taylor vortices in either Newtonian or non-Newtonian fluids.

14.3 Stability Criterion for Helical Flow

The flow rheometer outlined in Section B is based on the principles of helical flow, which is a combination of Couette and axial flow. Analysis of the two components of the flow and possible operating conditions, APPENDIX B, indicates that the rotational component of the flow can become unstable, but it is unlikely that instabilities will ever develop in the axial component of the flow. The axial flow component however, can delay the onset of instabilities in the Couette component and this can extend that operating range of the flow rheometer.

The purpose of this investigation is to describe a stability criterion for the onset of Taylor vortices in helical flow. The flow rheometer was specifically designed to analyse settling slurries, which are often non-Newtonian nature and it is therefore essential that the stability criterion incorporates the non-Newtonian nature of different fluids.

14.3.1 Axial Flow Stability

The Reynolds number may be used to determine the flow conditions in annular pipe flow and for a Newtonian fluid Equation (11.2-1) may be used (Bird et al. 1960).

$$\mathrm{Re} = \frac{2R(1-\kappa)\langle v_z \rangle \rho}{\mu} \qquad (11.2\text{-}1)$$

For non-Newtonian fluids that can be described by the power-law model, Equation (2.2-3), a modified Reynolds number is required. Equation (11.2-2) presented below, is a modified Reynolds for non-Newtonian fluids number that was devised and experimentally validated by Tuoc and McGiven (1994) and was previously discussed in section 11.2.1. This Reynolds number is also suitable for Newtonian fluids, for when the parameter n = 1 and A' = μ Equation (11.2-2) simplifies to give Equation (11.2-1). Thus this form of the Reynolds number will be used in the stability criterion for helical flow.

$$\mathrm{Re} = \frac{\left[2R(1-\kappa)\right]^{n}\left\langle v_z\right\rangle^{2-n}\rho}{(8\varphi)^{n-1}A'} \tag{11.2-2}$$

where

$$\varphi(\kappa) = \frac{(1-\kappa)^2}{\frac{\left(1-\kappa^2\right)}{\ln(\kappa)} + \left(1+\kappa^2\right)} \tag{11.2-3}$$

and

$$A' = A\left[\frac{3n+\varphi}{(3+\varphi)n}\right]^{n} \tag{11.2-4}$$

14.3.2 Rotational Flow Instability

For a Newtonian fluid under Couette flow conditions with only the inner cylinder rotating the Taylor number shown in Equation (11.3-4) may be used to determine the onset of instabilities in the fluid flow.

$$\mathrm{Ta} = \frac{v_\theta R(1-\kappa)}{\nu}\sqrt{\frac{(1-\kappa)}{\kappa}} = 41.3 \tag{11.3-4}$$

However, for a non-Newtonian fluid where the rheological properties are dependent on the shear rate the previously presented Taylor number cannot be used. Thus a suitably modified Taylor number was determined for non-Newtonian fluids, Equation (13.4-4) and is discussed in section 13.4. This modified Taylor number is also suitable for Newtonian fluids, for when the parameters n = 1 and A = μ, Equation (13.4-4) simplifies to give Equation (11.3-4). Thus this form of the Taylor number will be used in the stability criterion for helical flow.

$$Ta_{power\text{-}law} = n\frac{\Omega\rho(\kappa R)(R-\kappa R)}{A\left(\left(\frac{2\Omega}{n}\right)\left(\frac{1}{1-\kappa^{2/n}}\right)\right)^{n-1}}\sqrt{\frac{(R-\kappa R)}{(\kappa R)}} \qquad (13.4\text{-}4)$$

A substantial review of available literature and experimental work as part of this study has indicated that the following list of phenomena affect the critical rotational speed at which Taylor vortices form in both Couette and helical flow.

- Gap width
- Acceleration rate of the inner cylinder
- Axial flow rate

The effect that each of these phenomena have on the helical flow system will be described using a mathematical expression so that for a given set of operating conditions the onset of instabilities in helical flow in a non-Newtonian fluid can be determined, using the following expression.

$$\text{Stability Criterion} = E_A E_G E_{Re}\, Ta_{crit} \qquad (14.3\text{-}1)$$

Where E_A represents the effect of the rate of acceleration of the inner cylinder, E_G represents the effect of gap width and E_{Re} represents the effect of axial flow. The critical value for the onset of Taylor vortices in both Newtonian and non-Newtonian fluids is 41.3.

Several other factors including aspect ratio and eccentric alignment of the cylinders can lead to changes in the critical rotational speed at which Taylor vortices form. However, this stability criterion assumes that any effects due to the changes in the aspect ratio of the cylinders will be minimal as effects due to a small aspect ratio are only observed at values of 10 or lower (Cole 1976, Snyder 1969a, 1969b). Therefore this criterion will be valid for all concentric cylinder geometries with an aspect ratio of 10 or greater. The effect of eccentricity is only observed when the degree of eccentricity, ε, is greater than 0.1, below this value the variation in the Taylor number is less than ± 5%, see section 11.3.6 and Figure 11.3-6. It is therefore unlikely that

any effects due to eccentricity will be observed in rheological equipment, which is generally manufactured with high degree of precision and accuracy.

14.3.2.1 Effect of Acceleration Rate of the Inner Cylinder

The effect that changes in the rate of acceleration of the inner cylinder have on the onset of Taylor vortices is outlined in Figure 14.3-1. The critical Taylor number for the onset of instabilities in Couette flow is observed to decrease with increases in the rate of acceleration of the inner cylinder. However, beyond a value of 0.01 rad/s/s (5.7 rev/min/min) there is no change in the critical Taylor number with further increases in the rate of acceleration of the inner cylinder. Thus the effect of changes in the rate of acceleration of the inner cylinder on the onset of Taylor vortices can be described using the following set of equations outlined below. However, this criterion presented is only valid for a gap width of 27.7% of R. The expressions for E_A, presented below were obtained by first fitting the experimental results with a series of curves, see Figure 14.3-1 and then dividing by the quasi-steady state Taylor number (51.2 for a gap width of 27.7% of R, see Figure 13.2-1).

$$\upsilon < 0.0004 \qquad E_A = \frac{51.2}{51.2} = 1$$

$$0.0004 < \upsilon < 0.01 \qquad E_A = \frac{0.852\ln^2(\upsilon) + 7.73\ln(\upsilon) + 58.39}{51.2}$$

$$E_A = 1.66\times10^{-2}\ln^2(\upsilon) + 1.51\times10^{-1}\ln(\upsilon) + 1.14$$

$$0.01 < \upsilon < 20 \qquad E_A = \frac{40.7}{51.2} = 0.79 \qquad (14.3\text{-}2)$$

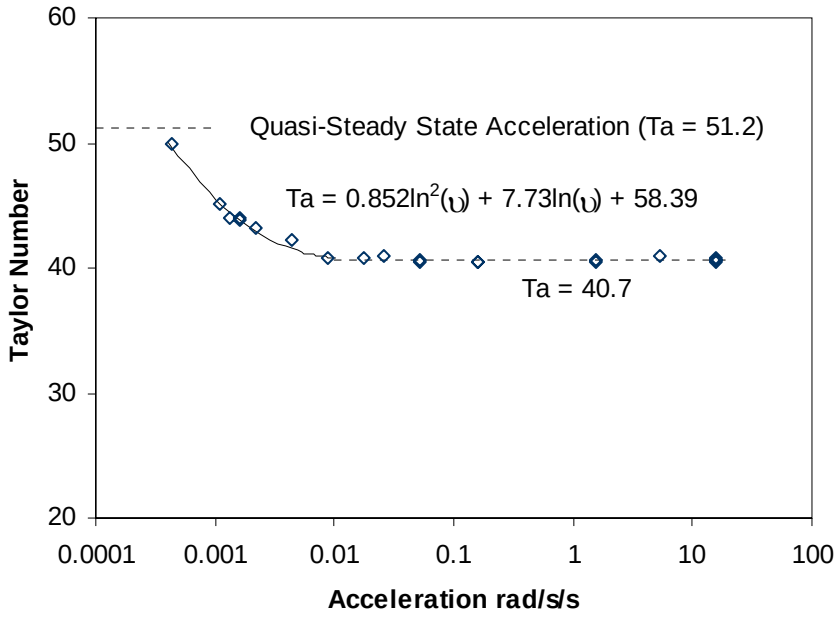

Figure 14.3-1 Effect of the rate of acceleration on the onset of Taylor vortices (Gap: 27.7 %)

It is clear from the results presented in Figure 14.3-1, that there are three distinct regions of acceleration; quasi-steady state, an intermediate region and fast acceleration region and each of these regions have a different effect of the onset of Taylor vortices.

There are no effects due to acceleration in the quasi-steady state region and thus E_A can be set to a value of one.

The effect of fast acceleration on the onset of Taylor vortices is constant across a wide range of acceleration values (0.01rad/s/s < υ < 20 rad/s/s), but as can be seen in Figure 14.3-2 the effect of gap width is also dependent on the rate of acceleration, thus the effect of fast acceleration will be defined when then gap width is infinitely small (0% of R). Under this gap width condition the onset of instabilities under quasi-steady acceleration occurs at a Taylor number of 41.3 compared to a Taylor number of 35.8 for fast acceleration, see Figure 14.3-2. Thus the value of E_A will be set at 0.87 as shown in Equation (14.3-3).

$$E_A = \frac{35.8}{41.3} = 0.87 \qquad (14.3\text{-}3)$$

Of these three regions the intermediate region is the most complex and difficult to describe, but it covers a range of low acceleration values (0.0004 rad/s/s to 0.01 rad/s/s), which are generally slower than the acceleration rates used in many practical applications including rheological measurements. A significant amount of additional measurements (and extra equipment) would be needed to fully describe the effect of acceleration in this intermediate region at different gap widths and this is beyond the scope of this investigation, which is to determine a stability criterion for rheological measurements in the flow rheometer, where the rate of acceleration is always in the fast region.

14.3.2.2 Effect of Gap Width, E_G

A review of the available literature reveals that the effect of gap width under very slow rates of acceleration may be described by Equation (14.3-4) below (Taylor 1923).

$$Ta = \frac{1}{2}\left[T'\left(\frac{2\kappa R + (R - \kappa R)}{\kappa R}\right)\right] \qquad (14.3\text{-}4)$$

where

$$T' = \frac{3414}{\left[\left(1 - 0.652\left(\frac{1-\kappa}{\kappa}\right)\right) + 0.0098\left(1 - 0.652\left(\frac{1-\kappa}{\kappa}\right)\right)^{-1}\right]} \qquad (14.3\text{-}5)$$

From this an expression the gap width parameter, E_G, under quasi-steady state acceleration conditions may be developed as shown in Equation (14.3-6).

$$E_G = \frac{1}{2}\left[T''\left(\frac{2\kappa R + (R - \kappa R)}{\kappa R}\right)\right] \qquad (14.3\text{-}6)$$

where

$$T'' = \frac{T'}{41.3}$$

$$T'' = \frac{82.3}{\left[\left(1-0.652\left(\frac{1-\kappa}{\kappa}\right)\right)+0.0098\left(1-0.652\left(\frac{1-\kappa}{\kappa}\right)\right)^{-1}\right]} \qquad (14.3\text{-}7)$$

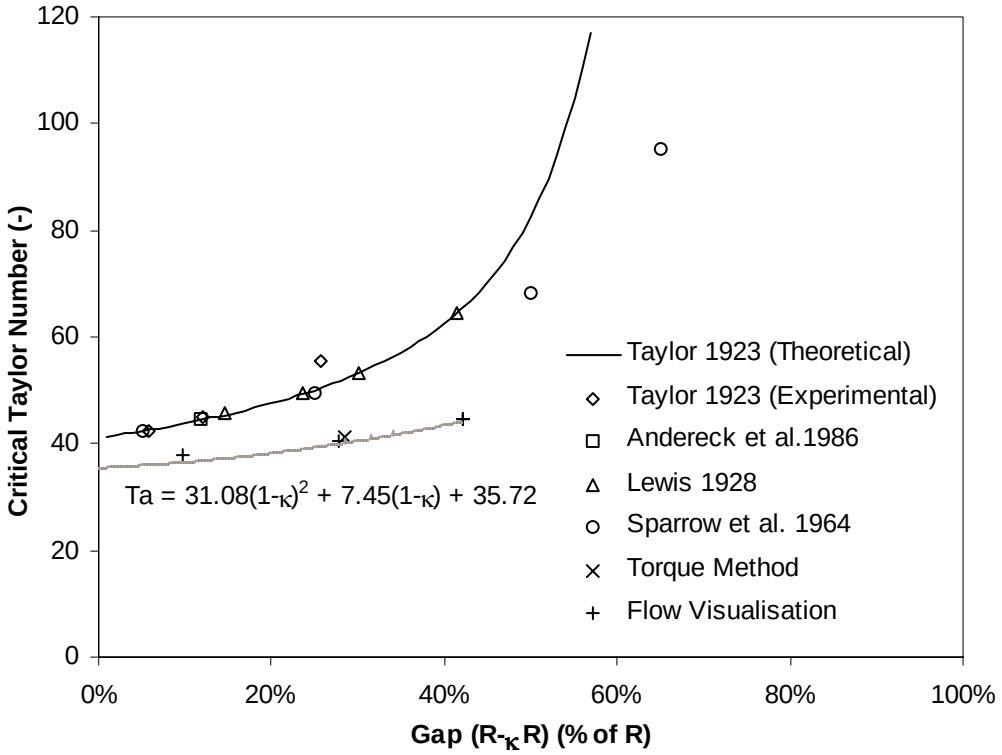

Figure 14.3-2 Effect of the rate of acceleration on the onset of Taylor vortices (Gap: 27.7 %)

For fast values of acceleration the effect due to the gap width is different than that for quasi-steady state acceleration, as shown in Figure 14.3-2. Examination of the experimental results (torque method and flow visualisation) presented in Figure 14.3-2 shows the effect of gap width at high values of acceleration and thus an expression for the gap width parameter, for fast acceleration can be developed as outlined below. This gap width parameter for fast values of acceleration is valid for

gap widths of 45% of the outer radius or smaller and for values of acceleration from 0.01 rad/s/s to 20 rad/s/s.

$$E_G = \frac{31.08(1-\kappa)^2 + 7.45(1-\kappa) + 35.72}{35.72}$$

$$E_G = 0.87(1-\kappa)^2 + 0.21(1-\kappa) + 1 \qquad (14.3\text{-}8)$$

14.3.2.3 Effect of Axial Flow Rate, E_{Re}

The effect of axial flow rate on instabilities in Couette flow with Newtonian fluids has been extensively studied in previous literature (Di Prima and Pridor 1979, Hasoon and Martin 1977, Krueger and Di Prima 1964, Schwarz et al. 1964, Snyder 1962, Tan et al. 2001). Experimental results from this study, see section 14.2, indicated that a similar effect was observed in non-Newtonian fluids providing that the Reynolds number and Taylor number were suitably modified and that the correct power-law model parameters were selected to describe the fluids properties under the appropriate shear rate conditions. Thus the following Equation (14.3-9), which is a modification of an expression discussed by Krueger and DiPrima (1964), can be used to develop the parameter, E_{Re}, for Newtonian and non-Newtonian fluids. This expression for the effect of axial flow on the onset of Taylor vortices is valid for axial flow Reynolds numbers of 70 or less.

$$Ta = \sqrt{1708 + 05325\,Re^2} \qquad (14.3\text{-}9)$$

$$E_{Re} = \frac{\sqrt{1708 + 05325\,Re^2}}{41.3}$$

$$E_{Re} = \sqrt{1 + 3.12 \times 10^{-4}\,Re^2} \qquad (14.3\text{-}10)$$

Where Re may be calculated using Equation (11.2-2), for Newtonian and non-Newtonian fluids.

14.3.3 Prediction of Instabilities in Helical Flow

Several different fluids were used to verify the stability criterion developed. The fluids were a Newtonian (glycerol-water solution) and two polymeric pseudoplastic solutions (0.5wt% CMC and 1.2wt% polyox). The properties of the fluids were determined using the MV II bob and cup and the Haake VT 550 and the results of these measurements are presented in Table 14.3-I. The fluids were examined in the flow rheometer, using the 32mm bob and a high acceleration rate (approximately 15.3 rad/s/s). The torque was measured as a function of rotational and time and at a variety of different flow rates. The experimental results obtained were compared with the predicted results determined using the stability criterion as shown below. A sample calculation of the prediction of the onset of turbulence in the polyox solution is found in APPENDIX E.

$$\text{Prediction} = E_A E_G E_{Re}\, 41.3 \qquad (14.3\text{-}11)$$

Table 14.3-I Summary of the physical properties of the experimental fluids

Experimental Fluid	Temperature (ºC)	Density (kg/m^3)	A ($Pa.s^n$)	n
Glucose – water solution	21	1231	0.032	1.0
CMC 0.5wt% (c600)	19	1001	0.012	0.88
Polyox 1.2wt%	25	998	0.0095	0.82

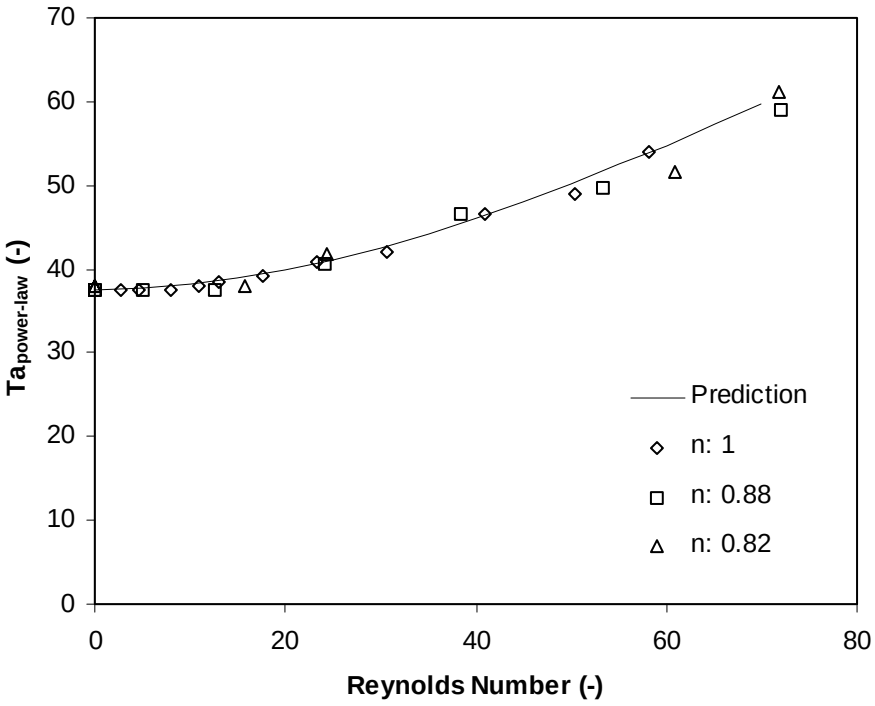

Figure 14.3-3 The onset of Taylor vortices in Newtonian and non-Newtonian fluids – experimental results (torque measurements) and predicted values

It may be seen from Figure 14.3-3 that for all fluids examined there is a good agreement between the predicted onset of turbulence and the actual measured value. The average error between the experimental results and the predicted value is 1.2% with a standard deviation 2.1%. These results demonstrate the validity of the stability criterion that has been developed for helical flow.

CHAPTER 15 INSTABILITIES IN HELICAL FLOW - CONCLUSIONS

Laminar Couette flow between rotating concentric cylinders may become unstable if certain criteria are met. Either both cylinders, or just the inner cylinder must be rotating for instabilities in the flow to develop as the rotation of just the outer cylinder has a stabilising effect on the flow. Couette flow is found in many practical applications, but one particular application is rheological measurements, where many of the geometries are based on the principles of Couette flow. If instabilities develop during a rheological measurement then the assumptions made in the analysis of the collected data will no longer be valid and the results will be subject to errors. It is therefore necessary to have available a method that can be used to determine whether the flow is stable or unstable. Analogous to the Reynolds number for pipe flow, the Taylor number may be used to determine the onset of instabilities in Couette flow.

The onset of instabilities in Newtonian Couette flow has been well defined in previous literature studies. Consequently this study has focused on developing an understanding of the onset of instabilities in non-Newtonian helical flow. To simplify the rheological behaviour of non-Newtonian fluids it was assumed that over the shear rate range near the critical rotational speed at which Taylor vortices form the rheological behaviour of the fluid could be describe by the power-law model. This model was used to develop a modified Taylor number to accommodate the dependence of the rheological properties of non-Newtonian fluids on the shear rate in the system. The modified Taylor number was experimentally examined and further modified based on experimental results.

Many practical rheological application of Couette flow involve acceleration rates of the rotating cylinder (usually the inner) greater than that which could be considered quasi-steady state or very slow. However, most research conducted into the onset of Taylor vortices in Couette flow has only considered the case where the acceleration rate of the rotating cylinder is very slow or quasi-steady state. Examination of a wide range of acceleration rates in this study identified that increases in the acceleration rate can have a destabilising effect on the critical speed at which Taylor vortices first appear in Couette flow. For acceleration rates well above that which is considered very slow, the critical speed for the onset of instabilities decreases in value by about 10% and it was also observed that the value of this decrease was dependent on the gap width between the cylinders. This lower value for the onset of turbulence was also observed to be independent of the rate of acceleration of the inner cylinder over a three-decade range of values of acceleration.

The introduction of axial flow to Couette flow can further complicate the analysis of the system, as both the axial and Couette flow may become unstable independently. However, the onset of instabilities in one component of the flow can also be influenced by the flow conditions of the other component. The operating conditions of the flow rheometer presented in Section B and in APPENDIX B are such that only the Couette portion of the flow is likely to become unstable. Thus the focus of this study was to investigate the effect of laminar axial flow on the onset of Taylor vortices in the Couette component of the flow.

It is well known that for Newtonian fluids the addition of an axial flow component can have a considerable stabilising effect on Couette flow. However, many practical applications involve non-Newtonian fluids and so the influence of axial flow on the onset of instabilities in non-Newtonian Couette flow was examined. The modified Taylor number previously mentioned for non-Newtonian fluids in Couette flow was used, as was a suitably modified Reynolds number. Experimental results showed that the effect of axial flow in non-Newtonian fluids was the same as that observed in Newtonian fluids providing that the appropriate Taylor and Reynolds numbers were used.

The ultimate objective of this study was to develop a stability criterion for helical flow so as to define a limit for stable operating conditions for the flow rheometer. A series of phenomena that influence the critical speed at which instabilities appear in the Couette component of helical flow are listed as follows:

- Acceleration rate of the inner cylinder
- Gap width
- Axial flow rate

A series of mathematical expression were developed to describe the effect that each of phenomena has on the onset of Taylor vortices. These expressions could then be combined to ultimately determine the critical speed and operating conditions for the onset of instabilities in the helical flow of a non-Newtonian fluid.

SECTION D APPLICATIONS OF THE FLOW RHEOMETER

CHAPTER 16 PREDICTING THE POWER REQUIREMENTS OF A MIXING IMPELLER

16.1 Introduction

The rheological properties of a slurry are an important criterion in the design and operation of process plant equipment and an accurate measurement of the properties of a slurry allows for improved process optimisation and control (Kemblowski et al. 1988). The flow rheometer, described in Section B was therefore designed to measure the rheological properties of settling slurries. The purpose of this investigation was to examine the effectiveness of using rheological measurements from the flow rheometer to predict the power requirements of an impeller in a mixing tank system (a simple process unit). It was not possible to take the flow rheometer onsite to test the power requirements in an industrial process, so a small laboratory scale-mixing tank was used instead.

.

16.2 Literature Review

Although mixing impellers have been used for many years, there have been very few theoretical developments in this field, particularly with regards to calculation relating to non-Newtonian fluids. Thus dimensional analysis and empirical correlations are widely used in the design of mixing tanks because of the complexities in modelling the fluid flow in the system (Skelland 1967).

In general it is expected that the power to rotate an impeller in a fluid will be a function of the following parameters.

Geometric Properties

C	height of impeller above tank bottom
D_I	impeller diameter
D_L	liquid depth
D_T	tank diameter
I_P	impeller pitch
J	width of baffles
L_B	length of impeller blade
M	mixing torque
N_B	number of baffles
N_I	number of impeller blades
W	width of impeller blade

Fluid Properties

ρ	density
μ	viscosity

Dynamic Quantities

Ω	rotational speed
g	gravitational acceleration

Thus a general expression for the power to rotate the impeller ($M\Omega$) may be written as follows.

$$M\Omega = f\,[C, D_I, D_L, D_T, I_P, J, L_B, N_B, N_I, W, \rho, \mu, \Omega, g] \qquad (16.2\text{-}1)$$

If dimensional analysis is performed then Equation (16.2-2) may be derived (Langhaar 106).

$$\frac{M\Omega}{D_I{}^5\Omega^3\rho} = f\left[\left(\frac{D_I{}^2\Omega\rho}{\mu}\right),\left(\frac{D_I\Omega^2}{g}\right),\left(\frac{D_T}{D_I}\right),\left(\frac{D_L}{D_I}\right),\left(\frac{C}{D_I}\right),\left(\frac{I_P}{D_I}\right),\left(\frac{L_B}{D_I}\right),\left(\frac{W}{D_I}\right),\left(\frac{J}{D_I}\right),N_I,N_B\right] \qquad (16.2\text{-}2)$$

The last nine terms on the right-hand side of Equation (16.2-2) define the geometry of a given system, thus if the system geometry remains constant these terms may be set to zero and thus Equation (16.2-3) may be written.

$$\frac{M\Omega}{D_I{}^5\Omega^3\rho} = f\left[\left(\frac{D_I{}^2\Omega\rho}{\mu}\right),\left(\frac{D_I\Omega^2}{g}\right)\right] \qquad (16.2\text{-}3)$$

The two remaining terms on the right-hand side of Equation (16.2-3) are forms of the Reynolds number and Froude number respectively. The term on the left-hand side of Equation (16.2-3) is defined as the power number Φ_P. If the baffles are adequate or the impeller is offset and the formation of surface waves and a vortex are minimised then the gravitational term in the Froude number is irrelevant and the term may be omitted (Rushton et al. 1950). This gives Equation (16.2-4).

$$\frac{M\Omega}{D_I{}^5\Omega^3\rho} = f\left(\frac{D_I{}^2\Omega\rho}{\mu}\right) \qquad (16.2\text{-}4)$$

Thus for a given system of fixed dimensions there must be a single defined relationship between the power number and a modified form of the Reynolds number.

For a non-Newtonian fluid the viscosity cannot be used to describe the rheological properties of the fluid and thus neither can the Reynolds number be used in the form presented in Equation (16.2-4). Metzner and Otto (1957) presented a generalised modified Reynolds number for a mixing tank system, Equation (16.2-5), which can be substituted for the Newtonian Reynolds number in Equation (16.2-4).

$$Re' = \frac{D_T{}^2 \Omega^{2-n} \rho}{A} 8 \left(\frac{n}{6n+2} \right)^n \qquad (16.2\text{-}5)$$

16.3 Experimental System - Mixing Tank

16.3.1 Experimental Apparatus

The experimental apparatus is shown schematically in Figure 16.3-1 and a picture is presented in Figure 16.3-2. The mixing tank was constructed from a clear perspex tube with an internal diameter of 142.6 mm and a wall thickness of 3 mm. Four 20 mm baffles were placed an equidistance around the inside of the tank. Liquid was placed in the tank to a depth equal to that of the tank's diameter. A four-blade bronze Rushton turbine of 61.6 mm diameter with a blade height of 17.6 mm was placed in both the vertical and radial centre of the fluid in the tank. The Rushton turbine was connected to an existing Haake VT 500 rheometer, which was used to control the speed of rotation (0-800rpm) and measure the torque acting on the Rushton turbine.

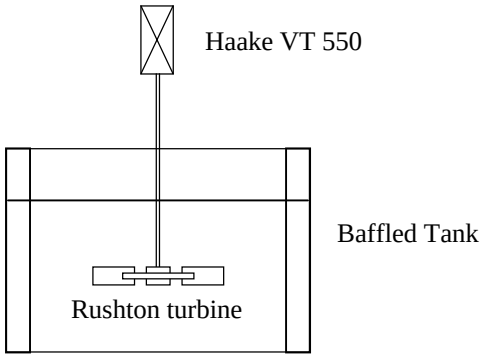

Figure 16.3-1 Schematic of the mixing tank system

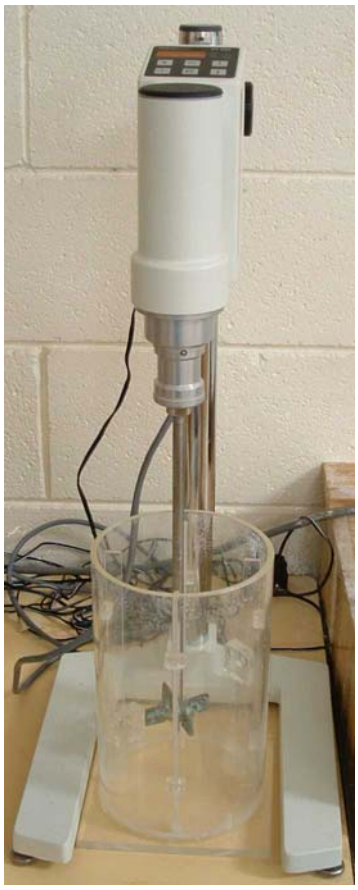

Figure 16.3-2 Photograph of the mixing tank and Haake rheometer

16.3.2 Experimental Technique

The test solution was placed in the tank and the impeller was lowered into position. A value of rotational speed was selected and the torque acting on the impeller was measured as a function of time. The test continued until a steady value of torque was observed, with a typical measurement period of between approximately two and three minutes. This procedure was then repeated for between sixteen and twenty different values of rotational speed. When particle settling was either very slow or not present the rotational speed was varied between approximately two and 500 rpm depending on the measured solutions viscosity and the maximum torque that could be measured on the Haake VT 550. When the settling rate of the particles was more rapid, then the minimum rotational speed was increased to a value that maintained the particle in a homogeneous suspension. Visual observations through the clear tank walls were used to ensure the rotational speed was high enough to prevent any particles settling.

16.4 Determination of the Experimental System Parameters

Numerous sets of data for the power requirements of various different mixing tank systems exist in the literature, of which a significant summary is presented in Skelland (1967). However, the data is extremely system specific and cannot be easily extrapolated to other systems, thus a power curve, which is a plot of the power number versus the Reynolds number, was prepared for the experimental system using a variety of different standard fluids, shown in Table 16.4-I. The rheological properties of these fluids were determined using the Haake VT 550 and the MV II concentric cylinder geometry using the procedure outlined in section 6.4.2.4. Several of the fluids used were characterised by yield stress behaviour, but the analysis technique presented in section 16.2, cannot accommodate the yield stress property of a fluid. However, at higher values of shear rate the rheological properties of a yield-pseudoplastic fluid can be described using a power-law model, so for the analysis of the experimental system it was assumed that the rheological properties of the yield stress fluids could be described by the power-law model over the range of shear rates

of interest. The power number for a baffled tank system with a Rushton turbine may be determined using Equation (16.4-1).

$$\Phi_P = \frac{M\Omega}{D_T{}^5\Omega^3\rho} \tag{16.4-1}$$

The Reynolds number of a fluid described by the power-law model may be determined using Equation (16.2-5) (Metzner and Otto 1957).

$$Re' = \frac{D_T{}^2\Omega^{2-n}\rho}{A} 8\left(\frac{n}{6n+2}\right)^n \tag{16.2-5}$$

Table 16.4-I: Experimental Fluids

Fluid	Temp (°C)	Density (kg/m^3)	A (Pa.s^n)	n
Glycerol solution	25	1244	0.416	1.0
CMC 0.5wt % (c600)	26.1	999.5	0.028	0.81
CMC 1.5wt % (c600)	24.5	1001	2.898	0.65
PEO 1.2wt%	26.2	999.5	0.041	0.91
Xanthan gum 0.25wt%	25.7	998.2	0.868	0.27

The power curves for the experimental fluids presented in Table 16.4-I are shown in Figure 16.4-1. Acceptably good agreement between the different types of fluids is observed in the laminar flow region, Re < 100, where the slope of line is approximately –1, which is consistent with other literature results (Skelland 1967). The transition region, 100 < Re < 2500, is very chaotic with very few common results between the data sets from the different fluids. In the fully turbulent region, Re > 2500, the Power number becomes independent of the Reynolds number as the slope approaches zero, which is consistent with other literature results (Skelland 1967).

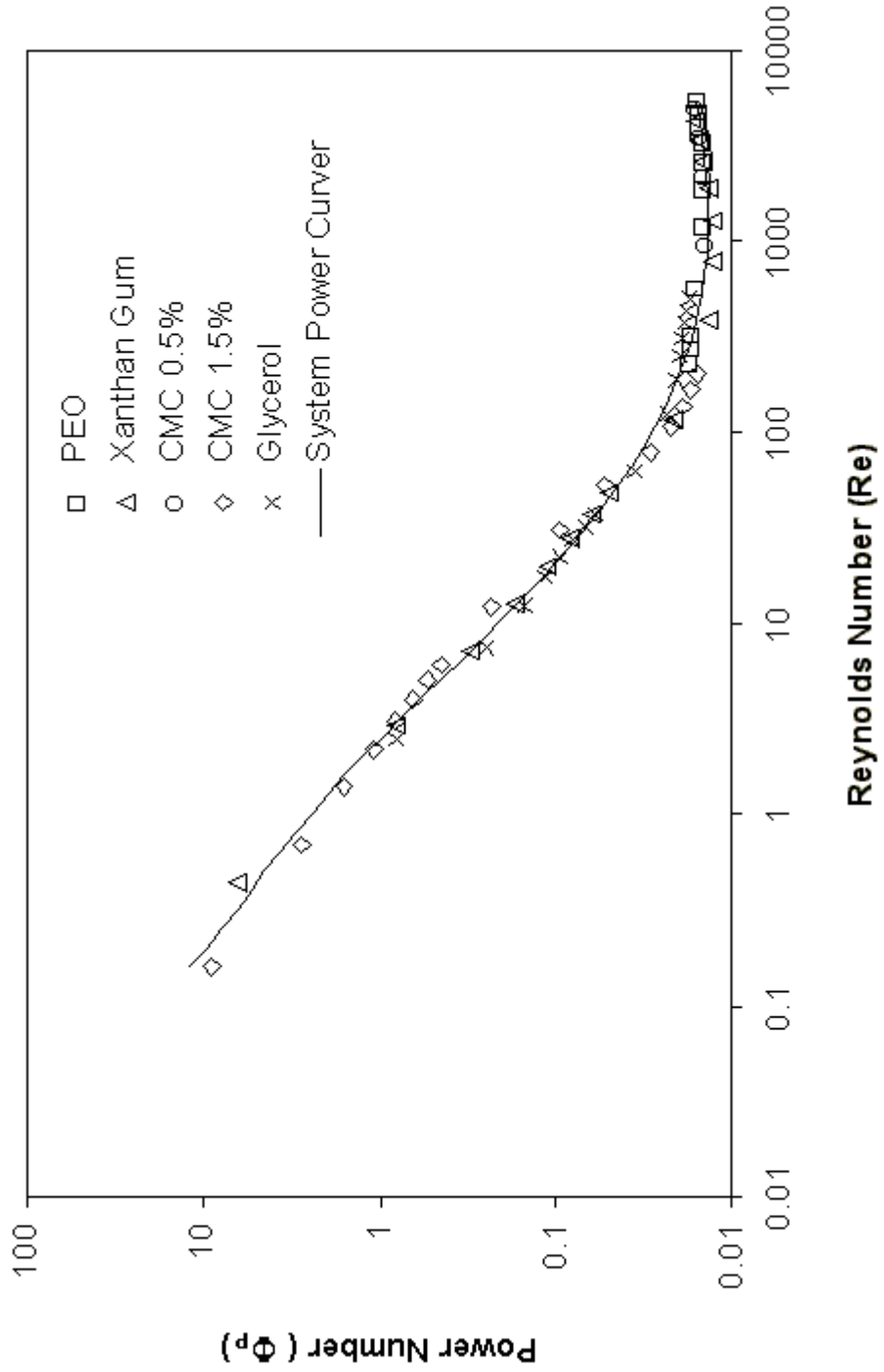

Figure 16.4-1 Power curves for ideal fluids in the experimental mixing tank system

16.5 Prediction of Power Requirements in a Slurries System

To test that the rheological measurements from the flow rheometer could be used to predict the power requirements of a mixing tank system, several different slurries were examined using the flow rheometer and the experimental mixing tank system. The physical and rheological properties of the slurries are presented in Table 16.5-I. Several of these slurries have rheological properties characterised by a yield stress. As with the pure liquids examined previously in section 16.4, the rheological properties of the slurries were modelled using the power-law model over the range of shear rates examined, thus in Table 16.5-I only the power-law model parameters are presented.

Table 16.5-I: Experimental Slurries

Slurry	Temp (°C)	Density (kg/m^3)	A ($Pa.s^n$)	n	Ω_{min} (rad/s)	Ω_{max} (rad/s)
Gold mine tailings 36wt%	17.8	1854	0.73	0.81	26.2	36.6
Clay slurry 71wt%	16.4	1788	8.47	0.32	0.2	31.4
Diamond mine tailings 49wt%	16.5	1442	2.5	0.30	10.5	36.6
PMMA 41vol%	23.4	1170	0.047	1.0	0.2	36.6

The slurries were examined in the mixing tank and the torque acting on the rotating impeller was measured for a variety of different values of rotational speed. The experimental procedure used was that described previously in section 16.3.2. Also as described in section 16.3.2 the minimal impeller speed used, was that which was required to maintain homogeneous conditions in the mixing tank.

The measured power values (measured torque × rotational speed) for the various slurries examined were compared with predicted power values. The predicted power values were determined using the Reynolds number, which was calculated from the operating rotational speed and the rheological properties measured using the flow

rheometer and the power curve for the experimental system, developed in section 16.4. The results of the comparison between measured and predicted power requirements for the different slurries are presented in Figure 16.5-1. As can be seen good agreement exists between the measured and predicted values of power with an average error of 4.6% and a standard deviation of 7.7%. This result demonstrates that rheological measurements from the flow rheometer can be used to successfully predict the power requirements of a mixing tank system.

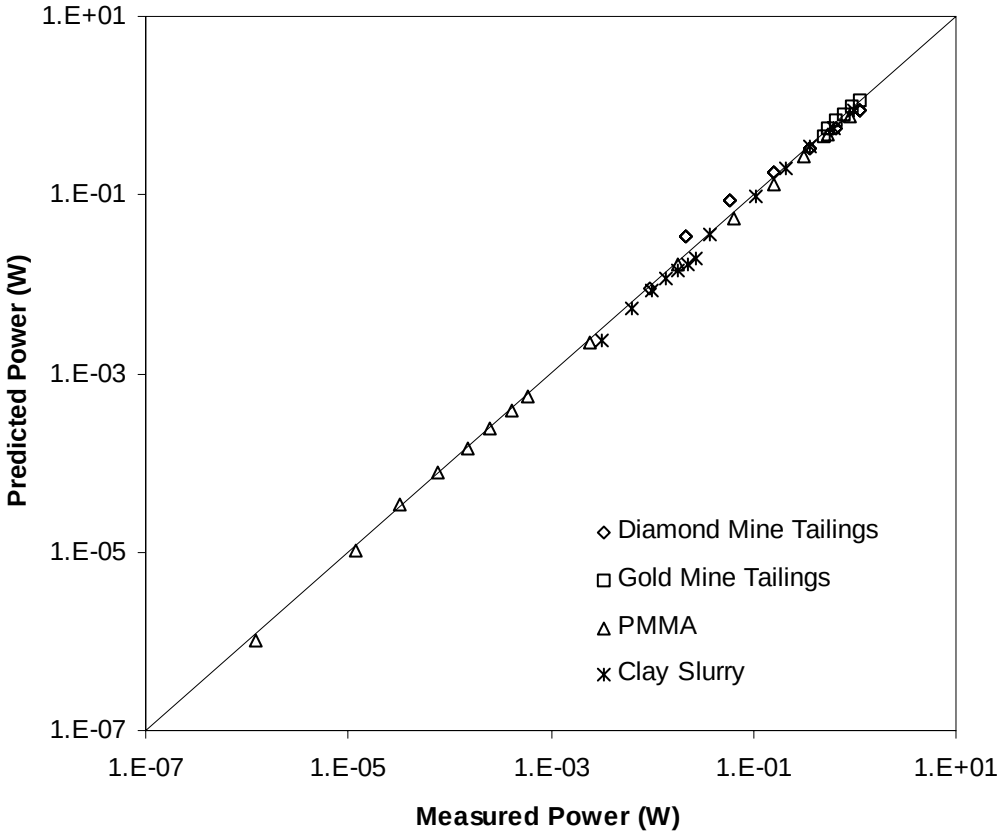

Figure 16.5-1 Comparison between predicted and measured power for a variety of different slurries

16.6 Conclusions

The rheological properties of a slurry and not the just the solid volume fraction are an important design and optimisation parameter in the construction and operation of equipment in a process plant. It was necessary to evaluate the effectiveness of using rheological measurements from the flow rheometer to predict the operating properties of a process unit. This evaluation was performed in a laboratory sized baffled mixing tank with a Rushton turbine impeller. Due to the complex nature of the mixing tank systems a power curve was developed for the experimental system using a variety of Newtonian and non-Newtonian liquids. This experimentally determined power curve and rheological measurements from the flow rheometer were used to predict the power requirements of the rotating impeller immersed in several different slurries. Predicted results were compared with measured results and good agreement was observed with an average error of only 4.6% between the two sets of data. This agreement demonstrates the applicability of the rheological measurements from the flow rheometer for use in simulations for the design and optimisation of process units.

CHAPTER 17 EFFECT OF CHANGES IN THE DENSITY OF THE SUSPENDING MEDIUM ON THE RHEOLOGY OF SETTLING SLURRIES

17.1 Introduction

The measurement of the rheological properties of settling slurries is extremely difficult as the solid particles settle creating a concentration gradient in the sample. The flow rheometer presented in Section B is one method by which homogeneous conditions may be maintained in a settling slurry during rheological measurements. Another option is to alter the density of the liquid to prevent or significantly slow the settling rate of the solid particles thereby maintaining homogeneous or quasi-homogeneous conditions during the period of measurement. However, it is likely that

the alteration to the suspending liquid density will change the rheological properties of the liquid and these changes in the rheology and density will affect the rheological properties of the slurry. A review of available literature shows that there has been minimal research in this field, so this investigation is aimed at defining the effect of altering the liquid density on the rheological properties of a slurry.

17.1.1 Altering the Density of the Solid Particles

Whilst there has been minimal research into the effect of altering the density of the suspending liquid on the rheological properties of a slurry, the effect of altering the density of the solid particles has been the subject of some research. Although the effect of altering the solid density may not be the same as altering the suspending liquid density, it may provide some insight into this phenomenon.

The effect of altering the density of the solid particles on the rheological properties of a slurry has been briefly reported by Clarke (1967) and by Saraf and Khullar (1975). In both investigations, an increase in the slurry viscosity was observed as the density of the solid phase was increased and this increase in the viscosity was attributed to an increase in the inertia of the more dense particles (Clarke 1967). The increased inertia of the more dense particles leads to a more chaotic motion of the particles because the fluid is less able to control the motion of these particles. The increase in the random motion of the particles leads to an increase in the overall viscosity of the slurry, through greater levels of energy dissipation.

The rheological measurements in the investigations by Clarke (1967) and by Saraf and Khullar (1975) were performed in Couette geometries with additional axial flow applied to prevent the particles from settling. However, in the analysis of the results the axial flow component was ignored, which compromises the results presented. Migration of particles is known to heavily influence the rheological measurements of slurries in Couette geometries (Abbott et al. 1991, Leighton and Acrivos 1987, Mondy et al. 1994, Phillips 1991, Tetlow 1998) but the influence of this effect on the results was not discussed. There is also the possibility that instabilities developed in the Couette flow during the measurements, because many of the results reported

showed slurries with shear thickening behaviour and in some instances the authors (Saraf and Khullar 1975) reported seeing Taylor vortices in the system. It is known that the presence of instabilities in Couette flow (Taylor vortices) will cause the measured torque to increase, see Section C and this increase in torque can be misinterpreted as shear thickening rheological behaviour. Despite these possible errors, a significant variation in the rheological properties of the slurries was observed with changes in the density of the solid particles and it therefore seems likely that a change in the density of the solid particles can influence the rheological properties of a slurry but the extent of this influence cannot be quantified.

As mentioned previously the effect of altering the density of the suspending liquid has not been extensively studied. However, the effect of altering the solid density has been the focus of some previous studies. These studies indicate that the change in the density of the solids affects the liquids ability to control the movement of the particles and that there is a greater energy dissipation when the density increases leading to a higher overall viscosity of the suspension. A similar effect may result when the density of the liquid is altered, however there is no previous evidence to support or disprove this assumption. Thus the objective of this study will be to identify any possible effects on the rheological properties of a suspension when the suspending liquid density is altered.

17.1.2 Altering the Suspending Liquid Viscosity

An increase in the viscosity of the suspending liquid in a suspension of smooth spheres has been shown by Ward and Whitmore (1950), to increase the viscosity of the suspension. However, the relative slurry viscosity was shown to be independent of changes in the suspending liquid viscosity (Ward and Whitmore 1950). The relative viscosity is the suspension or slurry viscosity divided by the viscosity of the pure suspending liquid.

17.1.3 Slurry Models – Suspensions of Spheres

The major physical factor that influences the rheological properties of a suspension or a slurry is the solids concentration. An equation to describe the viscosity of a dilute suspension of spheres was postulated by Einstein (1906) and is shown in Equation (17.1-1).

$$\eta_R = 1 + 2.5\Phi \qquad (17.1\text{-}1)$$

However, Einstein‘s equation is generally only valid for suspensions with a solids concentration of less than approximately 2 vol% (Batchelor and Green 1972). This is due to that fact that in the model it is assumed that individual particles in the suspension do not interact with any other particles in the suspension. Other values for the constant ‘2.5’ in Einstein’s equation have been quoted from different sources and range from between 4.5 (Hatschek 1913) and 5.5 (Happel 1957) to somewhere between 4.0 and 1.9 (Ward and Whitmore 1950). Particle shape can also have an effect on the value of the constant. For rods that are perfectly aligned the value of the constant has been shown to be close to 2.0, but in reality values greater than 2.5 are quoted for less perfectly aligned rods and this value increases as the axial length to radius ratio of the rods increase (Rutgers 1962). However, in general this model is rarely used due to limitations imposed by the range of solid concentrations covered.

As other factors that affect the viscosity of suspensions were identified, Einstein’s equation was further modified. These modifications are normally semi-theoretical or empirical where the equation is modified to match a series of experimental results.

Einstein’s equation was theoretically postulated for suspensions where the concentration is so low that the individual particles do not interact with each other. To take into account the interactions further terms may be added to Einstein’s equation, the simplest of these is a power series formula, shown in Equation (17.1-2) (Rutgers 1962).

$$\eta_R = 1 + 2.6\Phi + 12\Phi^2 \qquad (17.1\text{-}2)$$

This formula is valid for suspensions of spheres up to approximately 12 vol% concentration. Many other values for the two constants have been quoted for specific systems and specific sets of experimental results but typically they vary only by about ± 15%.

An Arrhenius type logarithmic relationship was proposed for a disperse system of spheres, Equation (17.1-3). The validity of this model however was quite poor. It was barely better than Einstein's equation with an applicable range up to 5 vol% concentration.

$$\ln(\eta_R) = 2.78\Phi \qquad (17.1\text{-}3)$$

Vand (1948a, 1948b) proposed a more complex version of the Arrhenius type logarithmic equation, shown in Equation (17.1-4). It incorporated the effect of collisions between two particles and hydrodynamic interactions between the particles and the suspending liquid. Experimental results for glass spheres (Vand 1948b) confirm the applicability of this model for up to 50 vol% concentration.

$$\ln \eta_R = \frac{2.5\Phi + 4(3.175 - 2.5)\Phi^2}{1 - 0.609\Phi} \qquad (17.1\text{-}4)$$

A combination of a power series and an Arrhenius type logarithmic relationship was proposed for polymer solutions, Equation (17.1-5) (Flory 1953), but it was also later found to be applicable for suspensions of spheres up to approximately 15 vol% concentration (Rutgers 1962).

$$\ln(\eta_R) = 2.74\Phi + 2.0\Phi^2 \qquad (17.1\text{-}5)$$

Instead of combining a power series with an Arrhenius type equation a power-law type equation may be used, Equation (17.1-6), (Papkow 1935). This model was originally proposed for concentrated polymer solutions, but it was later shown that the model could also be used to describe the behaviour of a suspension of spheres. With

the correct choice of parameters the model was shown to be valid for up to approximately 25 vol% concentration (Houwink and Klaassens 1942, Rutgers 1962).

$$\ln(\eta_R) = 2.3\Phi^{1.2} \qquad (17.1\text{-}6)$$

More complex versions of the power-law type equations have been proposed; Equation (17.1-7) (Mooney 1951) and Equation (17.1-8) (Krieger and Dougherty 1959).

$$\eta_R = \exp\left(\frac{2.5\Phi}{1-1.4\Phi}\right) \qquad (17.1\text{-}7)$$

$$\eta_R = \left(1-k_0\Phi\right)^{-2.5/k_0} \qquad (17.1\text{-}8)$$

Equation (17.1-7), with appropriate choices for the constants, as shown, may be used to model the apparent viscosity of a suspension of spheres up to a volume concentration of approximately 50% (Rutgers 1962). Equation (17.1-8) with the correct value for the constant k_0 is also applicable for a suspension of spheres up to approximately 50% volume concentration (Rutgers 1962).

17.2 Experimental slurries

Several different artificial slurries were used in a series of experiments aimed at determining the effect that altering density of the suspending liquid would have on the rheological properties of a slurry. Spheres of PMMA (poly-methyl-methacrylate) were used as the artificial solids in the slurries because the density of the PMMA is relatively low (1170 kg/m^3). Sodium Chloride salt was used to adjust the density of the liquid fraction, which was deionised water. The physical properties of the various different slurries are shown below in Table 17.2-I. Glycerol was used as a second substance to alter the suspending fluid density so as to provide a comparison with the sodium chloride results. The relevant physical properties of the glycerol slurries are presented in Table 17.2-II. The addition of salt or glycerol not only affects the density of the suspending liquid but also the viscosity. The viscosity data for the suspending

liquids at different glycerol and salt concentrations is also presented in the tables below. The preparation of these slurries is described in section 6.2.2.1 and the size distribution data of the PMMA spheres is presented in section 6.3.2.2.

Two instruments were used to determine the rheological properties of the PMMA slurries, the flow rheometer and a concentric cylinder geometry. The flow rheometer was used to measure the properties of all slurries in this investigation, but a problem was encountered during the operation of the flow rheometer and this is described in detail in section 17.3. The other instrument used was a standard concentric cylinder geometry, MV III connected to an existing Haake VT 550 rheometer. However, it was only possible to use this instrument when the density of the liquid was matched to that of the solids so that the particles would not settle and a concentration gradient develop during the measurement.

Table 17.2-I: Physical properties of PMMA - NaCl slurries at 25ºC

NaCl Conc. (Wt. %)	Liquid Density (kg/m^3)	Liquid Viscosity* (mPas)	Slurry Density (kg/m^3)				
			25 vol%	30 vol%	35 vol%	41 vol%	45 vol%
0.0	1000	1.01	1043	1051	1059	1070	1076
7.0	1050	1.12	1080	1086	1092	1099	1104
14.0	1100	1.31	1117	1121	1124	1129	1132
20.0	1150	1.56	-	1156	-	1158	-
22.5	1170	1.71	1170	-	1170	1170	1170
23.0	1175	1.74	-	1174	-	1173	-

* - Reference (Weast 1982)

Table 17.2-II: Physical properties of PMMA - glycerol slurries at 25ºC

Glycerol Conc. (Wt. %)	Liquid Density (kg/m^3)	Liquid Viscosity[+] (mPas)	Slurry Density (kg/m^3) 41 vol%
0.0	1000	1.01	1070
20.5	1050	1.67	1099
39.0	1100	3.68	1129
65.5	1170	12.2	1170

[+] - Reference (Dean 1985)

17.3 Modifications to the Experimental System

Initially the experimental system used in this investigation was that described previously in section 5.2. Soon after the helical rotor pump (manufactured by Mono Pumps Australia) was first used to circulate a PMMA slurry it unexpectedly seized and ceased to pump. Inspection of the pump revealed the presence of large agglomerates of fused PMMA in the pump and it was thought that the friction of the pumping action caused the PMMA spheres to semi-melt and fuse together. To eliminate this problem the helical rotor pump was replaced by a small centrifugal pump (manufactured by Charles Austin Pumps Ltd, UK). However, the flow rate delivery from a centrifugal pump cannot be as easily controlled as the flow from a positive displacement pump, which can be adjusted by changing the rotational speed of the motor. Centrifugal pumps transport fluids by applying energy to the fluid in the form of increased pressure (Davidson 1986) and the flow rate of the fluid is then dependent on the relationship between the system head and the head applied to the fluid by the pump. To reduce or adjust the flow rate the system head must be varied usually by the manipulation of a variable orifice device, typically a valve. A manually controlled ¼" ball valve was installed between the pump outlet and the inlet to the flow rheometer and a diagram of the modified system is shown in Figure 17.3-1.

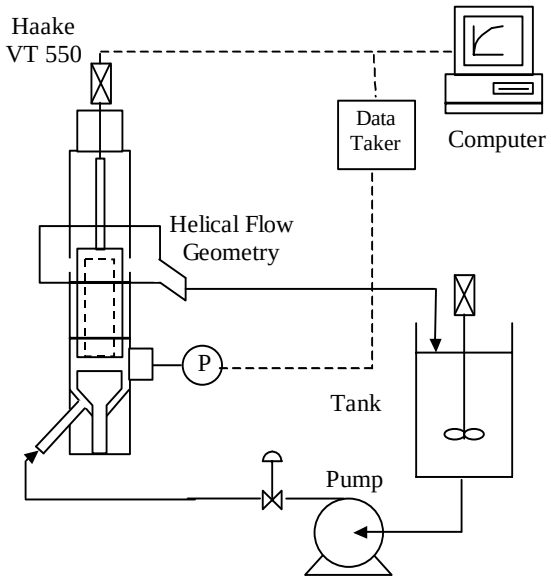

Figure 17.3-1 Schematic of the modified flow rheometer system

17.4 Experimental Procedure

A series of experiments were performed with the PMMA slurries using the flow rheometer. The particle size, Figure 6.3-3 of the PMMA restricted the size of the bob that could be used to the 32mm bob, which provided the larger gap width. For each slurry examined a series of measurements of torque versus time at rotational speeds from 10-80rpm were performed at constant values of differential pressure. Rotational speeds faster than 80rpm could not be tested, as the critical speed for the onset of instabilities would have been exceeded.

For the experiments performed with the Couette geometry a series of measurements of torque versus time at constant values of rotational speed were performed. Particle migration can affect the results from Couette geometries so to reduce this possible effect the slurry sample was removed from the geometry and stirred by hand with a spatula, before being replaced for testing at the next speed.

17.5 Particle Migration

The migration of small spheres in a suspension is a well-known phenomenon that can occur in rotating concentric cylinder systems (Abbott et al. 1991, Leighton and Acrivos 1987, Mondy et al. 1994, Phillips et al. 1991, Tetlow et al. 1998). In this series of experiments two rotational type geometries were used to examine the properties of the artificial PMMA slurries; the flow rheometer and a standard Couette geometry. The migration of particles in the flow rheometer has previously been discussed in CHAPTER 9 and it has been shown that particle migration is either not present or that it has no significant affect on the results. However, to test for the possibility of migration in the Couette geometry, the measured torque values were observed at constant values of rotational speed for a given period of time. A series of torque readings at different values of rotational speed for the 41vol% slurry are presented below in Figure 17.5-1. From the data presented there appears to be no particle migration, as the torque readings remain constant for the duration of the test period. The measurement time of the experiments was deliberately shortened to minimise any possible migratory effects.

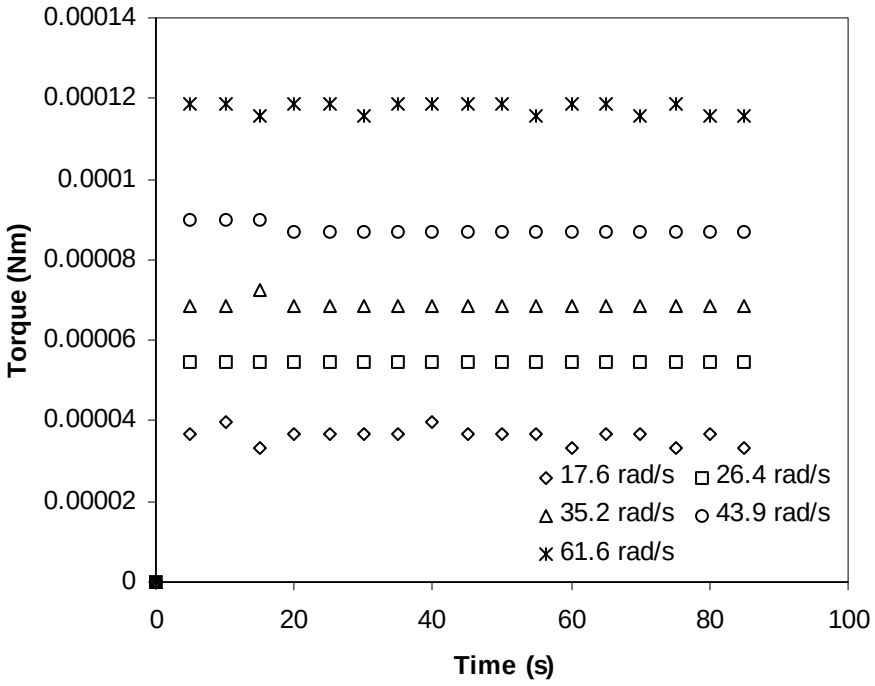

Figure 17.5-1 Torque readings from a Couette test with a PMMA –NaCl slurry, solid concentration 41vol%, liquid density 1170 kg/m^3

17.6 Experimental Results

17.6.1 Analysis of the Results for the 41 vol% PMMA - NaCl Slurry

The results from the investigation of the 41 vol% concentration (PMMA – NaCl) slurry are shown in Figure 17.6-1, as shear stress versus shear rate data. Newtonian rheological properties were observed in all slurries, at all the different liquid densities examined. Minimal variation was observed in the flow rheometer data at varying values of differential pressure, with an average error of approximately 1.3% and a standard deviation of approximately 2.7%. Good agreement was also observed between the flow rheometer data and the Couette geometry results, with an average error of 1.7%, verifying the accuracy of measurements from the flow rheometer.

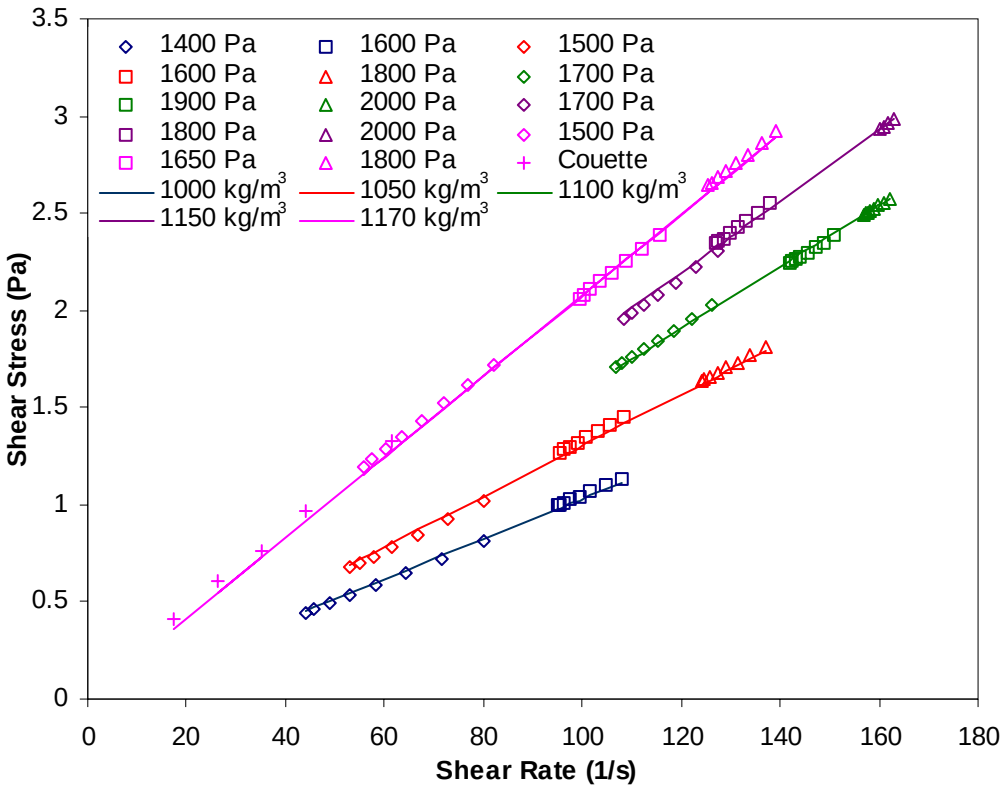

Figure 17.6-1 Rheological data for 41 vol% PMMA slurry at a variety of different liquid densities

17.6.2 Results for all Slurries

Because of the Newtonian nature of the slurries investigated the viscosity can be used to characterise the rheological properties of the slurries. The changes in the values of the viscosities of the different suspensions examined are presented in Figure 17.6-2. To distinguish between the NaCl slurries and the glycerol slurries, the glycerol slurries are marked with a ^{G}. Examination of the data shows that as the liquid density increases the viscosity of the slurries also increases. This phenomenon is consistent across all the different solid concentrations examined, though it is more pronounced in the higher solids concentration slurries.

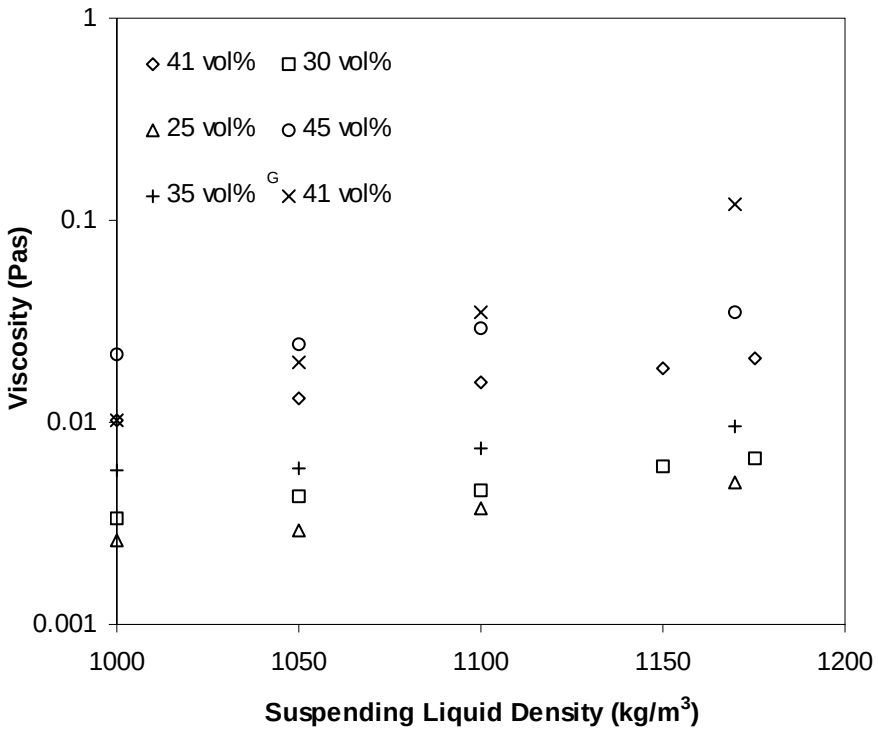

Figure 17.6-2 Viscosity data for PMMA slurries at a variety of different liquid densities

If the viscosity of the suspending liquids is examined in Table 17.2-I and Table 17.2-II it is clearly evident that as the concentration of either NaCl or glycerol increases the suspending liquid viscosity also increases. To examine the effect of the liquid density without the effect of the changing suspending liquid viscosity, Figure 17.6-3 is presented. The slurry viscosity has been normalised by dividing by the

suspending liquid viscosity. There is some random scattering of the data but this is to be expected, as the viscosity of the slurries measured was quite low and the Haake VT 550 was operating very low in its measurement range. However, in general there is no observed effect of changes in the suspending liquid density affecting the rheological properties of the slurry. The results are also confirmed by comparing the normalised data with a model for the viscosity of a suspension of spheres. The Mooney model for spheres (Mooney 1951) is also presented in Figure 17.6-3 for comparison and is used because of its applicability to volume concentrations of up to 50 vol% (Rutgers 1962). Good agreement between the model and the experimental data is noted at all of the different solid concentrations examined.

$$\eta_R = \exp\left(\frac{2.5\Phi}{1-1.4\Phi}\right) \qquad (17.1\text{-}7)$$

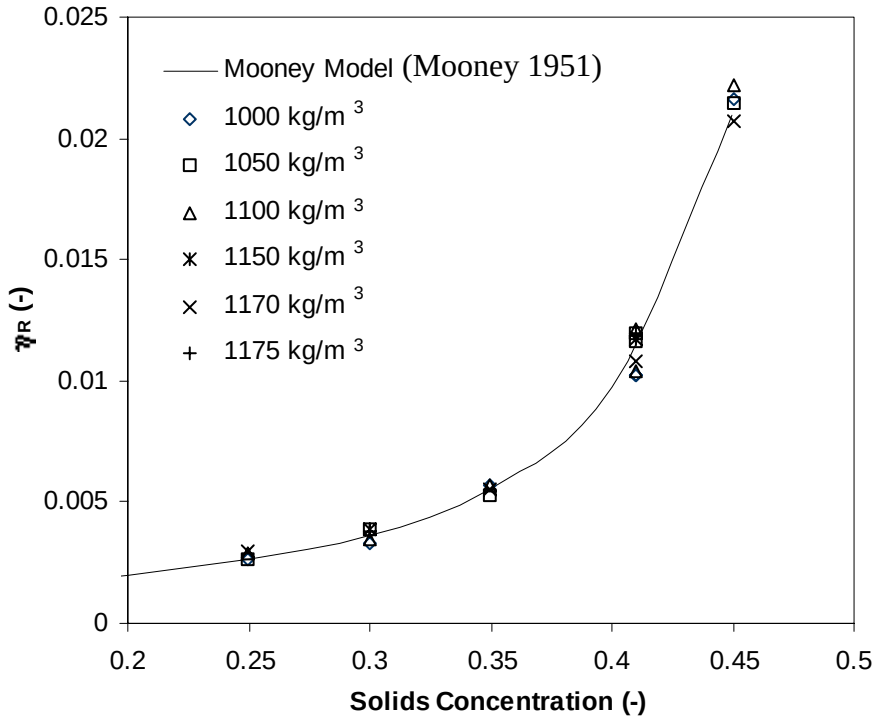

Figure 17.6-3 Effect of suspending liquid viscosity with normalised suspending liquid viscosity

The results from this investigation show that there is no relative effect of changing the density difference between the solid and liquid phases, which is in contrast to that

which has been previously reported (Clarke 1967, Saraf and Khullar 1975) for changes in the solid density. However, as previously discussed in section 17.1.1 the possibility of instabilities and particle migration in these systems, compromises these previous literature results. However, there may be another explanation for this apparent disparity between the results generated in this study and those previously reported in the literature. The changes observed in the slurry viscosity with changes in the suspending liquid density are primarily due to the changes in the liquid viscosity, which accompany the changes in density. This change in the liquid viscosity is readily measured and can then be accounted for, however, the effects due to changes in the solid density cannot be accounted for in this manner. In this way changes in the solid density will affect the slurry rheology but normalised changes in the liquid density will not. Therefore the effect of the density difference between the solid and the suspending liquid should not be treated as a single absolute density difference, but as two separate cases where changes in either the solid or suspending liquid density are examined separately.

It should also be noted that results from this study have only been generated with Newtonian slurries and that the findings presented here may not be valid for non-Newtonian slurries. Further research and experiments would be required to validate these results and conclusions for non-Newtonian slurries, as discussed in section 18.3.

17.7 Conclusions

A possible method for measuring the rheological properties of settling slurries is to alter the density of the suspending medium to match that of the solid particles, thus preventing or significantly reducing the particle-settling rate and thereby maintaining homogeneous conditions during any measurement. This change in the liquid density could however alter the rheological properties of the slurry.

The development of the flow rheometer and the ability to measure the rheological properties of settling slurries has enabled the effect of changing the suspending liquid density to be investigated. The effects of changing the liquid density were found to be negligible if the changes in the suspending liquid viscosity were properly accounted for. However, changes in the rheological properties of a slurry due to changes in the density of the solid particles cannot be so readily accounted for. Thus for this reason changes in the density difference between solid particles and the suspending liquid should not be considered as one absolute difference but rather changes in the liquid and solid densities should be considered independently.

The results presented in this chapter have particular practical significance as they provide a method for the measurement of the rheological properties of a settling slurry without the need for complex equipment with complex flow profiles to maintain homogeneous conditions. The liquid density could simply be adjusted so that the particles became neutrally buoyant and then the slurry could be examined in a more conventional geometry. The results could then be readily adjusted to account for the changes that occur in the suspending liquid viscosity due to the modification of its density. While this technique would render the flow rheometer redundant, the high density of the solid particles in most settling slurries means that matching the density could be difficult, thus the need for an instrument capable of measuring the rheological properties of settling slurries remains. It should also be noted that the rheological properties of many industrial slurries could be further affected by increasing the number of ions in solution, as this can lead to agglomeration and other surface chemistry effects. Therefore careful examination of each system on case-by-case basis would be necessary to determine the suitability of this method.

SECTION E CONCLUSIONS AND REFERENCES

CHAPTER 18 CONCLUSIONS AND RECOMMENDATIONS

18.1 Conclusions and Major Outcomes

To improve the optimisation of mineral-processing operations the rheological properties of settling slurries need to be accurately determined under conditions that realistically represent those found in actual site operations. However, this is not an easy task when dealing with high rate settling slurries, as most rheological instruments cannot maintain the particles in a homogeneous suspension. The major purpose of this study was to devise an instrument, including an appropriate analysis procedure for accurately determining the rheological properties of settling slurries.

18.1.1 Development of the Flow Rheometer

The major problem with most rheological instruments particularly the commonly used rotational type geometries is that when settling slurries are examined heterogeneous conditions rapidly develop. Many instruments have been developed to better maintain homogeneous conditions in the slurry during the measurement period and to do this the slurry is often circulated with an axial flow through a concentric cylinder geometry. However, the calculations associated with these instruments often ignore the contributions to the total shear rate made by the axial flow component, which can have serious implications when non-Newtonian fluids are examined and the correct shear rate is not determined. Experiments performed during this study showed that errors as high as 100% were observed in shear rate calculations when the axial flow component was ignored. However, the value of the error quoted (100%) is dependent on the physical size and operating conditions of the specific system but indicates the dangers posed by ignoring the axial flow component in the analysis of a helical flow system. The emphasis therefore in the development of the flow rheometer for settling slurries in this study was that the analysis procedure was based on the fundamental principles of helical flow; so as to eliminate the need for a calibration procedure and to enable the true rheological properties of a fluid to be directly measured.

Significant complications were introduced into the analysis procedure because the particle size distribution of many slurries meant that only a wide gap geometry could be used. The significant variation in shear rate across a wide gap in conjunction with the axial flow component prevented the use of simple Newtonian modelling techniques. To simplify the analysis of measurements from the flow rheometer it was assumed that over the range of shear rates examined, the rheological properties of a fluid could be predicted by the power-law model. An iterative numerical analysis procedure incorporating Levenberg-Marquardt non-linear regression was used to determine the best set of power-law model parameters, A and n to describe the rheological properties of the fluid over the measured shear rate range. Good agreement with both Newtonian and non-Newtonian fluids was observed between results from the flow rheometer and other laboratory rheological equipment.

The analysis procedure was complicated further when yield stress fluids were examined at low values of shear rate, where the power-law model cannot accurately predict the rheological properties of yield stress fluids. To reduce this error the experimental and analysis procedures were modified. Instead of using a single power-law model to describe the fluids behaviour over a wide range of shear rates, a multi-power-law model was used.

To compare and validate the results from the flow rheometer for settling slurries a second rheological instrument capable of measuring the properties of slow settling slurries was required and a specifically modified tube rheometer was developed for the purpose. This instrument incorporated a mixing impeller in the main reservoir, which was used to maintain homogenous conditions during the experiment. While this instrument was able to measure the properties of slow settling slurries, rapid settling slurries could not be reliably measured. However, good agreement was observed in results for slower settling slurries between the flow rheometer and the modified tube rheometer.

The design of the flow rheometer whilst proving very effective in its ability to measure the properties of settling mineral slurries could be further improved. Particular emphasis should be placed on the return of the slurry to the feed tank as particles can settle in the spill-over area around the flow rheometer before reaching the return pipe. Whilst this is not a problem if fresh feed is continuously used, in a laboratory there is usually only a small amount of sample available for analysis and recirculation of the sample is necessary. The effect of this problem could be reduced if the spill-over section were redesigned, such as to incorporate a downward slope towards the return pipe. This slope would maintain fluid and particle velocity in a downward direction and make it less likely for particles to settle before the return pipe was reached.

18.1.2 Instabilities in Helical Flow

Laminar Couette flow, which is found in concentric cylinder geometries, may become unstable as the speed of rotation of the inner cylinder increases. Helical flow is the

combination of Couette and axial flow and thus it is possible for Taylor vortices to develop in the Couette component of helical flow. Instabilities can also develop independently in the axial component of helical flow, but it was determined that for the operating conditions of the flow rheometer only the Couette component of the flow would become unstable. Therefore only the conditions surrounding the onset of instabilities (Taylor vortices) in the Couette component of helical flow were examined. The onset of Taylor vortices is particularly relevant in rheological measurements, as the onset of these instabilities will cause the measured torque values to significantly increase. Thus a good knowledge of the onset conditions of Taylor vortices is required so that any instrument based on Couette flow can be operated within the limits of laminar flow. Several key factors were identified as affecting the critical speed at which instabilities appear in helical flow; the rate of acceleration of the inner cylinder, the gap width between the cylinders, the axial flow Reynolds number and the non-Newtonian nature of the fluid. These factors, which are described individually below, were combined to develop a stability criterion for the helical flow of non-Newtonian fluids. This stability criterion was experimentally validated for a range of different fluids.

An increased rate of acceleration of the rotating inner cylinder was found to have a destabilising effect on Couette flow. For an increase in the rate of acceleration above quasi-steady state (or very slow) acceleration the critical speed for the onset of Taylor vortices decreased to a value approximately 10% lower than that presented in the literature for quasi–steady state acceleration. However, once this lower value was reached the critical rotational speed became independent of the rate of acceleration.

Unlike the value of the Reynolds number for the onset of instabilities in pipe flow, which is independent of the system geometry (the pipe diameter) the value of the Taylor number for the onset of instabilities in Couette flow is dependent on the gap width between the cylinders. Thus a factor for the effect of gap width was incorporated into the stability criterion developed for helical flow

It is known that the addition of an axial flow has a stabilising effect on the onset of Taylor vortices in a concentric cylinder system. Results in the literature show that for Newtonian fluids the critical rotational speed for the onset of Taylor vortices increases

with increases in the axial flow rate above an axial flow Reynolds number of 10. This study has shown that the effect of the axial flow in non-Newtonian fluids is identical to that observed in Newtonian fluids, provided that a suitable non-Newtonian Reynolds number is used.

The Taylor number like the Reynolds number is general presented with a viscosity term, which is used to describe rheological properties of the fluid. Many fluids and in particular mineral slurries are not Newtonian in nature and thus the concept of a single independent viscosity value to describe the rheological behaviour of the fluid cannot be used. In this study the Taylor number was suitably modified such that the stability of Couette flow in non-Newtonian fluids could be predicted. This modification to the Taylor number was experimentally validated with measurements from a specifically developed flow visualisation apparatus and torque measurements from several concentric cylinder geometries.

18.1.3 Predicting Mixing Impeller Power Requirements

A motivation for developing the flow rheometer was to enable improved design and optimisation of process units by providing a more accurate measurement of the rheological properties of mineral slurries. To test this ability to use flow rheometer data in design and optimisation, a small laboratory sized mixing tank was used. The specific laboratory mixing tank system was unique in design and was therefore first characterised using a variety of Newtonian and non-Newtonian liquids. The predicted power requirements (based on the system characteristics previously determined and the rheological measurements from the flow rheometer) for a variety of slurries were shown to correlate well with the actual measured power requirements.

18.1.4 Effect of Changes in the Density of the Suspending Medium on the Rheology of Settling Slurries

Instead of using a modified instrument that has a complex flow profile to maintain homogenous conditions in settling slurries during rheological measurements, another option is to alter the density of the suspending medium to match that of the solid

particles, thus preventing or significantly reducing the particle-settling rate. This change in density of the suspending liquid, will however affect the overall viscosity of the slurry. The development of the flow rheometer for settling slurries enabled slurries with different suspending liquid densities to be examined. The artificial slurries used in this investigation consisted of PMMA spheres and water with additions of either sodium chloride salt or glycerol to alter the density of the water. In increasing the water density through additions of either salt or glycerol the viscosity of the water was also increased. When the different slurry viscosities were normalised, no effects due to changes in the liquid density were observed. However, results were only generated for Newtonian fluids and further experiments would be required to validate this theory for non-Newtonian slurries.

18.2 Implications of the Present Work

The most significant implication of this work is the development of the flow rheometer and in particular the associated data analysis procedure. The addition of an axial flow component in a Couette system has been used by several previous researches to maintain homogeneous conditions during the measurement of settling slurries. However, in all cases where axial flow was used the contributions of the axial flow to the total shear rate were ignored. This has been shown to lead to significant errors in the determination of the rheological properties of non-Newtonian fluids, as the rheological properties are dependent on the total shear rate. Thus a particular focus of this study was the development of a correct method for the analysis of helical flow and thus the accurate determination of the rheological properties of non-Newtonian fluids.

The flow rheometer was specifically designed and optimised to operate in a settling slurry environment. A particular problem relating to the measurement of settling slurries is that the particles can settle and block pipes and conduits, which lead to unexpected equipment failure. The flow rheometer was specifically designed to minimise the chance of particles settling by incorporating a straight through design, which has minimal bends and regions of low flow rate. Most mineral slurries generally have relatively low values of viscosity, so the flow rheometer was also

optimised for the measurement of experimental variables including pressure and torque. End effects can generate errors in rheological measurements from a Couette geometry, so the flow rheometer was designed to minimise these effects with the use of hollow ended bobs.

Couette flow will become unstable and Taylor vortices will develop if the speed of rotation of either the inner cylinder or both cylinders exceeds a critical value, which is dependent on the system dimensions and the rheological properties of the fluid. The onset of vortices in Couette flow during rheological measurement will cause significant errors as the torque increases above that which would normally be expected. Much of the previous work into the onset of Taylor vortices in Couette flow assumed a quasi-steady state (or very slow) acceleration of the rotating cylinders. However, these conditions are rarely encountered in rheological measurements, as the acceleration rates are generally significantly faster. An important implication of this work was to define the effect of acceleration on the onset of Taylor vortices in Couette flow so that the onset of instabilities in Couette flow could be better predicted in more practical situations.

The Taylor number similar to the Reynolds number describes the rheological properties of a fluid using the single rheological model parameter, viscosity. However, this description is unsuitable for non-Newtonian fluids including most mineral slurries, which don’t have a constant viscosity. In this work the Taylor number was modified so as to include a more accurate description of the rheological properties of non-Newtonian fluids. This was particularly important for non-Newtonian rheological measurements as the onset of instabilities can now be predicted and avoided.

The effect of altering the liquid density on the rheological properties of a slurry were examined and compared to previous results where the solid density was altered. It was observed that the changes to the density of either phase should be considered individually and not combined. Whilst changes in the liquid density are readily accounted for by examining the associated changes in the liquid viscosity, changes in the solid phase cannot be predicted in this way. This result is extremely useful in the

measurement of settling slurries as it provides a method for measuring the rheological properties of these slurries without the need for a specialised instrument.

18.3 Recommendations for Future Work

The results and conclusions from this study generate the opportunity for future work, to further refine and build on the techniques and methods developed. The development of the flow rheometer and analysis procedure allows for the direct measurement of the actual rheological properties of settling mineral slurries. This ability to directly measure the actual properties of settling mineral slurries allows for new opportunities in the research, design and optimisation of mineral processing operations. The design of the instrument is such that it can be relatively easily transported to mineral processing site operations for actual onsite measurements.

The modified process by which the rheological properties of a yield stress fluid are measured in the flow rheometer is simple and effective but will still be subject to errors at very low values of shear rate. A development and improvement to the data analysis procedure would be to incorporate a yield stress rheological model such as the Herschel – Bulkley model instead of the power-law model. A three-parameter model such as the Herschel – Bulkley model can more accurately describe the behaviour of a yield stress fluid, though the implementation of such a change would be quite complex.

A further improvement of the analysis procedure for helical flow would be to incorporate the optimisation of both the rotational speed and axial flow in the determination of the rheological properties of an experimental fluid. This would also require the inclusion of a new and more accurate technique for the measurement of the axial flow rate.

Particle migration is known to affect the measurement of rotational and axial flow rheometers and whilst it was shown that the results from the flow rheometer were unaffected by particle migration, it would be an interesting exercise to examine the flow patterns within the instrument. An operating criterion to ensure minimal particle

migration could then be determined, similar to that determined in this study for the onset of Taylor vortices in non-Newtonian helical flow.

The effect of altering the liquid density was shown to have a minimal effect on the relative slurry viscosity for several different types of Newtonian slurries examined. However, many actual slurries are non-Newtonian in nature and so further experiments and investigations with different types of non-Newtonian slurries would be useful to confirm that the results observed in this study for Newtonian slurries can be extended to non-Newtonian slurries.

CHAPTER 19 REFERENCES

Abbott, J.R., Tetlow, N., Graham, A.L., Altobelli, S.A., Fukushima, E., Mondy, L.A. and Stephens, T.S., (1991), 'Experimental observations of particle migration in concentrated suspensions: Couette flow', *J. Rheol.*, **35**, pp. 773-795.

Albert, C., Dierckes, J.R. and Schowalter, W.R., (1966), *I & EC Fundamentals*, **5**, 2, pp. 263-271.

Allende, M. and Kalyon, D.M., (2000), 'Assessment of particle-migration effects in pressure-driven viscometric flows', *J. Rheol.*, **44**, pp. 79-90.

Andereck, D.C., Dickman, R. and Swinney, H.L., (1983), 'New flows in a circular Couette system with co-rotating cylinders', *Phys. Fluids*, **26**, pp. 1395-1401.

Andereck, D.C., Liu, S.S. and Swinney, H.L., (1986), 'Flow regimes in a circular Couette system with independently rotating cylinders', *J. Fluid Mech.*, **164**, pp.155-183.

Australian Bureau of Statistics, (2001), 'Water Account for Australia 1993-94 to 1996-97', <http://www.abs.gov.au/ausstats/abs@.nsf/Lookup/AusStats 4610_0 Water Account for Australia 1993-94to1996-97.htm>

Bagley, E.B., (1957), 'End corrections in the capillary flow of polyethylene', *J. Appl. Phys.*, **28**, pp. 624-627.

Barnes, H.A. and Nguyen, Q.D., (2001), 'Rotating vane rheometry – a review', *J. Non-Newtonian Fluid Mech.*, **98**, pp. 1-14.

Barnes, H.A. and Walters, K., (1985), 'The yield stress myth', *Rheol. Acta*, **24**, pp. 323-326.

Barnes, H.A., (1995), 'A review of the slip (wall depletion) of polymer solutions, emulsions and particle suspensions in viscometers: its cause, character and cure', *J. Non-Newtonian Fluid Mech.*, **56**, pp. 221-251.

Barnes, H.A., (1999), 'The yield stress – a review or 'παντα ρει' – everything flows?', *J. Non-Newtonian Fluid Mech.*, **81**, pp. 133-178.

Barnes, H.A., (2000), 'Measuring the viscosity of large-particle (and flocculated) suspensions – a note on the necessary gap size of rotational viscometers', *J. Non-Newtonian Fluid Mech.*, **94**, pp. 213-217.

Bartok, W. and Mason, S.G., (1959), 'Particle motions in sheared suspensions. VII. Singlets and doublets of fluid spheres', *J. Colloid Sci.*, **14**, pp. 13-26.

Batchelor, G.K. and Green, J.T., (1972), 'The determination of the bulk stress in a suspension of spherical particles to order C2', *J. Fluid Mech.*, **56**, pp .401-427.

Beavers, G.S. and Joseph, D.D., (1974), 'Tall Taylor cells in polyacrylamide solutions', *Phys. Fluids*, **17**, pp. 650-651.

Bender, J. and Wagner, N.J., (1996), 'Reversible shear thickening in monodisperse and bidisperse colloidal dispersions', *J. Rheol.*, **40**, pp. 899-916.

Bhattacharya, S.N., Chryss, A., Connell, H.J. and Shepard, J.J., (1990), 'Rotational rheometer for settling multiphase mixtures', *5th Nat. Conf. Rheol., Melbourne*, pp .15-18.

Bingham, E.C., (1922), 'Fluid and Plasticity', *McGraw-Hill Book Co., New York*, in, Skelland, A.H.P., (1967), 'Non-Newtonian Flow and Heat Transfer', *John Wiley and Sons, Inc. NewYork.*

Bird, R.B., Stewart, W.E. and Lightfoot, E.W., (1960), 'Transport Phenomena', John Wiley and Sons, New York.

Blaszczykl, J. and Petela, R., (1986), "Application of a modified rotary rheometer to the investigation of slurries", *Rheol. Acta*, **25**, 521-526.

Brenner, H., (1966) 'Hydrodynamic resistance of particles at small Reynolds numbers', *Adv. Chem. Eng.*, **6**, pp. 287-438.

Burkhalter, J.E. and Koschmieder, E.L., (1974), 'Steady supercritical Taylor vortices after sudden starts', *Phys. Fluids*, **17**, 1929-1935.

Butler, J.E. and Bonnecaze, R.T., (1999), 'Imaging of particle shear migration with electrical impedance tomography', *Phys. Fluids*, 11, pp. 1982-1994.

Calderbank, P.H. and Moo-Young, M.B., (1959), 'The prediction of power consumption in the agitation of non-Newtonian fluids', *Trans. Inst. Chem. Eng.*, **37**, pp. 26-33.

Calderbank, P.H. and Moo-Young, M.B., (1961), 'The power characteristics of agitators for the mixing of Newtonian and non-Newtonian fluids', *Trans. Inst. Chem. Eng.*, **39**, pp. 337-347.

Cameron, J.R., (1989), 'Viscometry of Nonhomogeneous Flows and the Behaviour of a Titanium-Crosslinked Hydroxypropyl Guar Gel in Couette flow', *J. Rheol.*, **33**, pp. 15-46.

Casson, N., (1959) 'A flow equation for pigment-oil dispersions of the printing-ink type', *Rheol. Disperse Systems, Proc. Conf. Univ.*, p. 84-104.

Castle, P. and Mobbs, F.R., (1967), 'Hydrodynamic Stability of the Flow Between Ecentric Rotating Cylinders: Visual Observations and Torque Measurements', *Proc. Inst. Mech. Eng.*, **182**, 3N, pp. 41-52.

Castle, P., Mobbs, F.R. and Markho, P.H., (1967), ' Visual Observations and Torque Measurements in the Taylor Vortex Regime Between Eccentric Rotating Cylinders', *J. Lubrication Tech.*, **93**, pp. 121-129.

Chandrasekhar, F.R.S., (1958), 'The stability of viscous flow between rotating cylinders', *Proc. R. Soc. London, A*, **246**, pp. 301-311.

Chandrasekhar, F.R.S., (1962), 'The stability of viscous flow between rotating cylinders II', *Proc. R. Soc. London, A*, **268**, pp. 145-152.

Chaplin, M., (2003), 'Xanthan gum', <http://www.sbu.ac.uk/water/xgum.html>

Chavan, V.V. and Ulbrecht, J. (1972), 'Power consumption for mixing of inelastic non-Newtonian fluids by helical screw agitators', **50**, *Trans. IChemE.*, pp. 147-155.

Cheng, D.C-H., (1986), 'Yield stress: a time dependent property and how to measure it', *Rheol. Acta*, **25**, pp. 542-554.

Chiera, C., Connell, H.J. and Shepard, J.J., (1992), 'Perturbation analysis of the helical flow of a bingham plastic model fluid in a narrow gap', *6th Nat. Conf. Rheol., Clayton*, pp. 11-14.

Chow, A.W., Sinton, S.W., Iwamiya, J.H. and Stephens, T.S., (1994), 'Shear-induced particle migration in Couette and parallel-plate viscoemters: NMR imaging and stress measurements', *Phys. Fluids*, **6**, pp. 2561-2576.

Chow, M.K. and Zukoski, C.F., (1995), 'Gap size and shear history dependencies in shear thickening of a suspension ordered at rest', *J. Rheol.*, **39**, pp. 15-32.

Chow, M.K. and Zukoski, C.F., (1995), 'Nonequilibrium behaviour of dense suspensions of uniform particles: Volume fraction and size dependence of rheology and microstructure', *J. Rheol.*, **39**, pp. 33-59.

Clarke, B., (1967), 'Rheology of coarse settling suspensions', *Trans. Inst. Chem. Eng.*, **45**, pp. T251-T256.

Clift, R., Grace, J.R. and Weber, M.E., (1978), 'Bubbles, drops and particles', *Academic Press*, New York, pp. 229-243.

Coleman, B.D. and Noll, W., (1959), 'Helical flow of general fluids', *J. Appl. Phys.*, **30**, 1508-1512.

Coles, D., (1965), 'Transitions in circular Couette flow', *J. Fluid Mech.*, **21**, pp. 385-425.

Coles, D., (1967), 'A note on Taylor Instability in circular Couette flow', J. App. Mech., Trans ASME, Series E, 34, pp. 529-534.

Cole, J.A., (1974), 'Taylor vortices with short rotating cylinders', *J. Fluids Eng.*, **96**, pp. 69-70.

Cole, J.A., (1976), 'Taylor-vortex instability and annulus-length effects', *J. Fluid Mech.*, **75**, pp.1-15.

Couette, M., (1890), Ann. Chim. Phys., 21, pp. 433-510, in, Taylor, G.I., (1923), 'VIII. Stability of a Viscous Liquid contained between Two Rotating Cylinders', *Phil. Trans. R. Soc.*, **223**, pp. 289-343.

Curran.S.J., Hayes, R.E., Afacan, A., Williams, M.C. and Tanguy, P.A., (2002), 'Properties of Carbopol Solutions as Models for Yield-Stress Fluids', *J. Food Sci.*, **67**, pp. 176-180..

da C.Andrade, E.N. and Fox, J.W., (1949), 'The mechanism of dilatancy', *Proc. Phys. Soc., B*, **62**, pp. 483-500.

Darabaner, C.L. and Mason S.G., (1967), 'Particle Motions in Sheared Suspensions XXII: Interactions of Rigid Spheres (Experimental)', *Rheol. Acta*, **6**, pp. 273-284.

Davidson, J., (1986), 'Process Pump Selection - A Systems Approach', *The Institution of Mechanical Engineers*, Suffolk, UK.

Davies, J.T., (1972), 'Turbulence Phenomena, An Introduction to the Eddy Transfer of Momentum, Mass and Heat, Particularly at Interfaces', *Academic Press, London*, pp. 5.

Dean, J.A., (1985), 'Lange's Handbook of Chemistry, 13th Edition', *McGraw-Hill Book Company*, New York.

Di Prima, R.C., (1960), 'The stability of flow between rotating cylinders with an axial flow', *J. Fluid Mech.*, **9**, pp.621-631.

Di Prima, R.C., (1963), 'A note on the Stability of Flow in Loaded Journal Bearings', *ASLE Trans.*, **6**, pp. 249-253.

Di Prima, R.C. and Eagles, P.M., (1977), 'Amplification rates and torque for Taylor-vortex flows between rotating cylinders', *Phys. Fluids*, **20**, pp.171-175.

Di Prima, R.C., Eagles, P.M. and Ng, B.S., (1984), 'The effect of radius ratio on the stability of Couette flow and Taylor vortex flow', *Phys. Fluids*, **27**, pp. 2403-2411.

Di Prima, R.C. and Pridor, A., (1979), 'The stability of viscous flow between rotating concentric cylinders with an axial flow', *Proc. R. Soc. London A.*, **366**, pp. 555-573.

Di Prima, R.C. and Stuart, J.T., (1972), 'Non-local Effects in the Stability of Flow Between Eccentric Rotating Cylinders', *J. Fluid. Mech.*, **54**, 393-415.

Di Prima, R.C. and Stuart, J.T., (1975), 'The Non-linear Calculations of Taylor Vortex Flow Between Eccentric Rotating Cylinders', *J. Fluid. Mech.*, **67**, 85-111.

Dierckes, A.C. and Schowalter, W.R., (1966), 'Helical flow of a non-Newtonian polyisobutylene solution', *I&EC Fundamentals*, **5**, pp. 263-271.

Donnelly, R.J., (1958), 'Experiments on the stability of viscous flow between rotating cylinders I. Torque Measurements', *Proc. R. Soc. A.*, **246**, pp. 312-325.

Donnelly, R.J., (1960), 'Experiments on the stability of viscous flow between rotating cylinders II. Visual Observations', *Proc. R. Soc. A.*, **258**, pp. 101-123.

Donnelly, R.J., (1965), 'Experiments on the stability of viscous flow between rotating cylinders IV. The ion technique', *Proc. R. Soc. A.*, **283**, pp. 509-519.

Donnelly, R.J. and Tanner, D.J., (1965), 'Experiments on the stability of viscous flow between rotating cylinders V. The theory of the ion technique', *Proc. R. Soc. A.*, **283**, pp. 520-530.

Donnelly, R.J., Schwarz, K.W. and Roberts, P.H., (1965), 'Experiments on the stability of viscous flow between rotating cylinders VI. Finite-amplitude experiments', *Proc. R. Soc. A.*, **283**, pp. 531-556.

Dostál, M., Źitný, R., Šesták, J. and Houška, M., (1993), 'Helical Flow of Power-Law Fluids', *AIChE J.*, **39**, pp. 189-192.

Einstein, A., (1906), 'Eine neue Bestimmung der Molekul dimension', *Ann. Phys.*, **19**, p. 289, in, Rajinder, P., (1999), 'Rheology of Blends of Suspensions and Emulsions', *Ind. Eng. Chem.*, **38**, pp. 5005-5010.

Ferrini, F., Ercolani, D., de Cindio, B., Nicodemo, L., Nicolais, L. and Ranaudo, S., (1979), 'Shear viscosity of settling slurries', *Rheol. Acta.*, **18**, pp. 289-296.

Flory, P.J., (1953), 'Principles of Polymer Chemistry', *Cornell Univ. Pr., New York*.

Frene, J. and Godet, M., (1974), 'Flow Transitions Criteria in a Journal Bearing', J. Lubrication Tech., **94**, pp. 135-140.

Gadala-Maria, F.A. and Acrivos, A., (1980), 'Shear-induced structure in a concentrated suspension of solid spheres', *J. Rheol.*, **24**, pp.799-814.

Garcia-Ramirez, R. and Isayev, A.I., (1992), 'Helical flow of a viscoelastic fluid – An approximation towards the analysis of rotational extrusion', J. Rheol., 36, pp. 1183-1211.

Gauthier, F., Goldsmith H.L. and Mason S.G., (1971), 'Particle motion in non-Newtonian media. I: Couette flow', *Rheol. Acta*, **10**, pp. 344-364.

Gauthier, F., Goldsmith H.L. and Mason S.G., (1971), 'Particle motion in non-Newtonian media. II: Poiseuille flow', *Trans. Soc. Rheol.*, **15**, pp. 297-330.

Gerhart, P.M., Gross, R.J. and Hochstein, J.I., (1992), 'Fundamentals of Fluid Mechanics', Addison-Wesley Publishing Company, New York.

Gorman, M. and Swinney, H.L., (1982), 'Spatial and temporal characteristics of modulated waves in the circular Couette system', *J. Fluid Mech.*, **117**, pp.123-142.

Graham, A.L., Altobelli, S.A., Fukushima, E., Mondy, L.A. and Stephens, T.S., (1991), 'Note: NMR imaging of shear-induced diffusion and structure in concentrated suspensions undergoing Couette flow', *J. Rheol.*, **35**, pp. 191-201.

Halow, J.S. and Wills, G.B., (1970), 'Experimental observations of sphere migration in Couette systems', *Ind. Eng. Chem. Fundam.*, **9**, pp.603-607.

Halow, J.S. and Wills, G.B., (1970), 'Radial migration of spherical particles in Couette systems', *AIChE J.*, **16**, pp. 281-286.

Hampton, R.E., Mammoli, A.A., Graham, A.L. and Tetlow, N., (1997), 'Migration of particles undergoing pressure driven flow in a circular conduit', *J. Rheol.*, **41**, pp. 621-640.

Han, M., Kim, C., Kim, M. and Lee, S., (1999), 'Particle migration in tube flow of suspensions', *J. Rheol.*, **43**, pp. 1157-1174.

Happel, J., (1957), 'Viscosity of Suspensions of Uniform Spheres', *J. Appl. Phys.*, **28**, pp.1288-1292.

Hasoon, M.A. and Martin B.W., (1977), 'The stability of viscous axial flow in an annulus with a rotating inner cylinder', *Proc. R. soc. London, A.*, **352**, pp 351- 380.

Hatschek, E., (1913), 'The General Theory of the Viscosity of Two-phase Systems', *Trans. Far. Soc.*, **9**, pp. 80-93, in, Rutgers, R., (1962), 'Relative Viscosity and Concentration', *Rheol. Acta*, **2**, pp 305-348

Herschel, W.H. and Bulkley, R., (1926), *Kolloid-Z.*, **XXXIX**, pp. 291, in, Skelland, A.H.P., (1967), 'Non-Newtonian Flow and Heat Transfer', *John Wiley and Sons, Inc. New York.*

Herschel, W.H. and Bulkley, R., (1926), 'Measurement of consistency as applied to rubber-benzene solutions', *Proc. Am. Soc. Test. Mat*, **XXVI**, pp. 621, in, Skelland, A.H.P., (1967), 'Non-Newtonian Flow and Heat Transfer', *John Wiley and Sons, Inc. New York.*

Ho, B.P. and Leal, L.G., (1974), 'Inertial migration of rigid spheres in two-dimensional unidirectional flows', *J. Fluid Mech.*, **65**, pp. 365-400.

Houwink, R. and Klaassens, K. H., (1942), 'The viscosity-concetration relation in concentrated solutions', *Kolloid-Z*, 79, pp. 160-171, in, Rutgers, R., (1962), 'Relative Viscosity and Concentration', *Rheol. Acta*, **2**, pp 305-348.

Hubbe, M., (2003), 'Mini-Encyclopedia of Papermaking Wet-End Chemistry – Polyethylene oxide (PEO)', <http://www4.ncsu.edu:8030/~hubbe/MiniEncy/PEO.html>

Hughes, T.H. and Reid, W.H., (1968), ' The stability of spiral flow between rotating cylinders', *Phil. Trans. R. Soc. Series A*, **263**, pp. 57-91.

Huilgol, R.R., (1990), 'Helical flow of non-Newtonian fluids', *Proc. 5th Nat. Conf. Reol., Melbourne*, pp. 43-46.

Kamal, M. M., (1966), 'Separation in the Flow Between Eccentric Rotating Cylinders', *J. Basic Eng., Trans. ASME, Series D.*, **88**, 717-724.

Karnis, A. and Mason S.G., (1966), 'Particle motions in sheared suspensions XIX. Viscoelatic media', *Trans. Soc. Rheol.*, **10**, pp. 571-592.

Kassim, H.O. and Killick, E.G., (1996), 'Application of the impeller viscometry technique to the rheology of liquids containing particulate solids', *IChemE Symposium Series*, **140**, pp. 259-270.

.

Kataoka, K., Doi, H., Hongo, T. and Futagawa, M., (1975), 'Ideal plug-flow properties of Taylor vortex flow', *J. Chem. Eng. Japan*, 8, pp.472-476.

Kawatra, S.K. and Bakshi, A.K., (1995), 'On-line Viscometry in Particulate Processing', *Miner. Proc. Extract. Met. Review*, **14**, pp. 249-273.

Kawatra, S.K. and Bakshi, A.K., (1996), 'On-line measurement of viscosity and determination of flow types for mineral suspensions', *Int. J. Miner. Process.*, **47**, pp. 275-283.

Kawatra, S.K., Bakshi, A.K. and Eisele, T.C., (1999), 'An on-line pressure vessel rheometer for slurries', *Powder Tech.*, **105**, pp. 418-423.

Kearsey, H.A. and Cheney, A.G., (1961), 'A note on the effect of temperature on the rheology of thoria slurries' *Trans. Inst. Chem. Eng.*, **39**, pp. 91-92.

Kemblowski, Z., Sek, J. and Budzynski, P., (1988), 'The concept of a rotational rheometer with a helical screw impeller', *Rheol. Acta*, **27**, pp. 82-91.

Klein, B., Laskowski, J.S. and Partridge, S.J., (1995), 'A new viscometer for rheological measurements on settling suspensions', *J. Rheol.*, **39**, pp. 827-840.

Koh, C.J., Hookham, P. and Leal, L.G., (1994), 'An experimental investigation of concentrated suspension flows in a rectangular channel', *J. Fluid Mech.*, **266**, pp. 1-32.

Koschmieder, E.L., (1979), 'Turbulent Taylor vortex flow', *J. Fluid Mech.*, **93**, 515-527.

Krueger, E.R. and Di Prima, R.C., (1964), 'The stability of a viscous fluid between rotating cylinders with an axial flow', *J. Fluid Mech.*, **19**, pp. 528-538.

Kreyszig, E., (1993), 'Advanced Engineering Mathematics', 7th Ed', John Wiley and Sons, Inc., New York, pp. 1040.

Krieger, I.M., (1968), 'Shear rate in the Couette Viscometer', *Trans. Soc. Rheol.*, **12**, pp.5-11.

Krieger, I.M., (1990), 'Bingham Award Lecture – 1989, The role of instrument inertia in controlled-stress rheometer', *J. Rheol.*, 34, pp. 471-483.

Krieger, I.M. and Dougherty, T.J., (1959), 'A mechanism for non-newtonian flow in suspensionsof rigid spheres', *Trans. Soc. Rheol.*, **3**, pp. 137-152.

Krieger, I.M. and Maron, S.W., (1953), 'Direct Determination of Flow Curves of Non-Newtonian Fluids. II. Shearing Rate in the Concentric Cylinder Viscometer', *J. Appl. Phys.*, **24**, pp. 134-136.

Krieger, I.M., and Maron, S.W., (1954), 'Direct Determination of Flow Curves of Non-Newtonain Fluids. III. Standardised Treatment of Viscometric Data', *J. Appl. Phys.*, **25**, pp. 72-75.

Langhaar, H.L., (1951), 'Dimensional Analysis and Theory of Models', *John Wiley and Sons Inc., New York*, p. 20.

Leal, L.G., (1979), 'The motion of small particles in non-Newtonian fluids', *J. Non-Newtonian Fluid Mech.*, **5**, pp. 33-78.

Leighton, D. and Acrivos, A., (1987), 'The shear-induced migration of particles in concentrated suspensions', *J. Fluid Mech.*, **181**, pp. 415-439.

Lewis, J.W., (1928), 'An experimental Study of the Motion of a Viscous Liquid contained between Two Coaxial Cylinders', *Proc. R. Soc. A*, **117**, pp. 388-407.

Lueptow, R.M., Docter, A. and Kyungyoon, M., (1992), 'Stability of axial flow in an annulus with a rotating inner cylinder', *Phys. Fluids A*, **4**, pp. 2446-2455.

Mallock, A., (1896), 'Experiments on fluid viscosity', *Phil. Trans. R. Soc. A*, **187**, pp.41-56.

Marquardt, D.W., (1963), 'An algorithm for least-squares estimation of non-linear parameters', *J. Soc. Indust. Appl. Math.*, **11**, pp. 411-431.

Martin, B.W. and Payne, A., (1972), 'Tangential flow development for laminar flow in an annulus with a rotating inner cylinder', *Proc. R. Soc. London, A*, 328, pp. 131-141.

McGuire, J.T., (1993), *Encyclopedia of Chemical Processing and Design*, **45**, Marcel Dekker Inc., New York, USA, pp. 362-390.

McKelvey, J.M., Gavis, J. and Smith, T.G., (1957), *SPE J.*, **13**, p. 29., in, Van Wazer, J.R., Lyons, J.W., Kim, K.Y. and Colwell, R.E., (1963), 'Viscosity and Flow Measurement, A laboratory handbook of Rheology', *Interscience Publishers, New York*.

McMurry, J., (1992), 'Organic Chemistry', *Brooks/Cole Publishing Company*, California.

Metzner, A.B., (1956), 'Non-Newtonian Technology', *Adv. Chem. Eng.*, **1**, *Academic Press, New York*, pp. 77-153.

Metzner, A.B. and Otto, R.E., (1957), 'Agitation of non-Newtonian fluids', *AIChE J.*, **3**, pp. 3-10.

Metzner, A.B. and Taylor, J.S., (1960), 'Flow patterns in agitated vessels', *AIChE J.*, **6**, pp. 109-114.

Metzner, A.B. and Whitlock, M., (1958), 'Flow Behaviour of Concentrated Dilatant Suspensions', *Trans. Soc. Rheol.*, **2**, pp. 239-254.

Mobbs, F.R. and Ozogan, M.S., (1984), 'Study of sub-critical Taylor vortex flow between eccentric rotating cylinders by torque measurements and visual observations', *Int. J. Heat and Fluid Flow*, **5**, pp. 251-253.

Mondy, L.A., Brenner, H., Altobelli, S.A., Abbott, J.R. and Graham, A.L., (1994), 'Shear-induced particle migration in suspensions of rods', *J. Rheol.*, **38**, pp. 444-452.

Mooney, M., (1951), 'The viscosity of a concentrated suspension of spherical particles', *J. Colloid Sci.*, **6**, pp. 162-170.

Moreland, C., (1963), 'Viscosity of suspensions of coal in mineral oil', *Can. J. Chem. Eng.*, **41**, pp. 24-28.

Murdoch, R. and Kearsey, H.A., (1960), 'Pumping studies on aqueous thoria slurries', *Trans. Inst. Chem. Eng., London*, **38**, pp. 165-175.

Ostwald, W., (1926), *Kolloid-Z*, **38**, pp. 261., in, Skelland, A.H.P., (1967), 'Non-Newtonian Flow and Heat Transfer', *John Wiley and Sons, Inc.*

Nakagawa, M., Altobelli, S.A., Caprihan, A. and Fukushima, E., (1997), 'NMRI study: axial migration of radially segregated core of granular mixtures in a horizontal rotating cylinder', *Chem. Eng. Sci.*, **52**, pp. 4423-4428.

Nguyen, Q.D. and Boger, D.V., (1985), 'Direct yield stress measurement with the vane method', *J. Rheol.*, **29**, pp. 335-347.

Nguyen, Q.D., Devasagayam, C. and Bown, D.J., (2000), 'Development of an on-line flow rheometer', *Mineral Processing and Extractive Metallurgy Review*, **20**, pp. 75-91.

Nott, P.R. and Brady, J.F., (1994), 'Pressure-driven flow of suspensions: simulations and theory', *J. Fluid Mech.*, **275**, pp. 157-199.

Papkow, S., (1935), *Kunststoffe*, **25**, p.253., in, Rutgers, R., (1962), 'Relative Viscosity and Concentration', *Rheol. Acta*, **2**, pp 305-348.

Park, K., Crawford, G.L. and Donnelly, R.J., (1981), 'Determination of Transitions in Couette Flow in Finite Geometries', *Phys. Rev. Let.*, 47, pp. 1448-1450.

Phan-Thien, N., Graham, A.L., Altobelli, S.A., Abbottt, J.R. and Mondy, L.A., (1995), 'Hydrodynamic particle migration in a concentrated suspension undergoing flow between rotating eccentric cylinders', *Ind. Eng. Chem. Res.*, **34**, pp.3187-3194.

Phillips, R.J., Armstrong, R.C. and Brown, R.A., (1991), 'A constitutive equation for concentrated suspensions that account for shear-induced particle migration', *Phys. Fluids A.*, **4**, pp. 30-41.

Press, W.H., Flannery, B.P., Teukolsky, S.A. and Vetterling, W.T., (1990), 'Numerical recipes in Pascal – The art of scientific computing', Cambridge Uni Press, pp. 572-580.

Purdom, G.J. and Richardson, S.M., (1991), 'Lateral migration, A simple continuous separation mechanism for dilute suspensions', *Trans I ChemE*, **69 A**, pp. 193-194.

Purghit, N.K., Roy, A.N., (1965), 'Studies on the rheological properties of rapidly settling suspensions including minerals', *Proc. 8th Commonwealth Mining and Metallurgical Congr. Aust. and New Zealand*, pp. 455-466.

Rabinowitsch, B., (1929), 'The viscosity and elasticity of sols', *Z. physik. Chem., Leipzig*, **145A**, p. 1-26., in, Van Wazer, J.R., Lyons, J.W., Kim, K.Y. and Colwell, R.E., (1963), 'Viscosity and Flow Measurement, A laboratory handbook of Rheology', *Interscience Publishers, New York.*

Rayleigh, Lord, (1916), 'On the dynamics of revolving fluids', *Proc. R. Soc., A.*, **93**, pp. 148-154.

Rea, D.R., and Schowalter, W.R., (1967), 'Velocity Profiles of a non-Newtonian Fluid in Helical Flow', *Trans. Soc. Rheol.*, **11**, pp. 125-143.

Reeves, T.J., (1985), 'On-line viscometer for mineral slurries', *Trans. I.M.M.*, **94**, C201-C208.

Renehan, M.J., Snow, R.J., Leong, Y.K. and Boger, D.V., (1987), 'Rheological characterisation using a mixing bowl – coaxial cylinder viscometer', *Proc. CHEMECA 87, Melbourne*, **V.2**, 69.1-69.9.

Reynolds, O., (1883), 'An Experimental Investigation of the Circumstances which determine whether the Motion of Water shall be Direct or Sinuous, and of the Law of Resistance in Parallel Channels', *Phil. Trans. R. Soc. London*, **174**, pp. 935-982.

Ritchie, G. S., (1968), 'On the Stability of of Viscous Flow Between Eccentric Rotating Cylinders', *J. Fluid Mech.*, **32**, 131-144.

Rivlin, R.S., (1956), 'Solution of Some Problems in the Exact theory of Visco-Elasticity', *J. Rational Mech. Anal.*, **5**, pp. 179-188.

Rushton, J.H., Costich, E.W. and Everett, H.J., (1950), 'Power characteristics of mixing impellers. I', Chem. Eng. Prog., **46**, pp 395-404.

Rutgers, R., (1962), 'Relative Viscosity and Concentration', *Rheol. Acta*, **2**, pp 305-348.

Saraf, D.N. and Khullar, S.D., (1975), 'Some Studies on the Viscosity of Settling Suspensions', *Canadian J. Chem. Eng.*, **53**, pp. 449-452.

Sarmiento, G., Crabbe, P.G., Boger, D.V. and Uhlherr, P.T., (1979), 'Measurements of the Rheological Characteristics of Slowly Settling Flocculated Suspensions', *Ind. Eng. Chem. Process Des. Dev.*, **18**, pp. 746-751.

Savaş, Ö., (1985), 'On flow visualisation using reflective flakes', *J. Fluid Mech.*, **152**, pp. 235-248.

Schlichting, H., (1968), 'Boundary-Layer Theory 6th ed.', *McGraw-Hill Book Company*.

Schulz-Grunow, F., (1959), Zur Stabilität der Couetteströmung', *ZAMM*, **39**, p. 101.

Schwarz, K.W., Springett, B.E. and Donnelly, R.J., (1964), 'Modes of instability in the spiral flow between rotating cylinders', *J. Fluid Mech.*, **20**, pp. 281-289.

Shauly, A., Wachs, A. and Nir, A., (1998), 'Shear-induced particle migration in a polydisperse concentrated suspension', *J. Rheol.*, **42**, pp. 1329-1348.

Segre, G. and Silberberg, A., (1962), 'Behaviour of macroscopic rigid spheres in Poiseuille flow, Part 1', *J. Fluid Mech.*, **14**, pp.115-135.

Segre, G. and Silberberg, A., (1962), 'Behaviour of macroscopic rigid spheres in Poiseuille flow, Part 2', *J. Fluid Mech.*, **14**, pp.136-157.

Shi, F.N. and Napier-Munn, T.J., (1996), 'Measuring the rheology of slurries using an on-line viscometer', *Int. J. Miner. Process.*, **47**, pp. 153-176.

Simmers, D.A. and Coney, J.E.R., (1979), 'The effect of Taylor vortex flow on the development length in concentric annuli', *J. Mech. Eng. Sci.*, **21**, pp. 59-64.

Sinevic, V., Kuboi, R. and Nienow, A.W., (1986), 'Power numbers, Taylor numbers and Taylor vortices in viscous Newtonian and non-Newtonian fluids', *Chem. Eng. Sci.*, **41**, pp. 2915-2923.

Sinton, S.W. and Chow, A.W., (1991), 'NMR flow imaging of fluids and solid suspensions in Poiseuille flow', *J. Rheol.*, **35**, pp. 735-772.

Skelland, A.H.P., (1967), 'Non-Newtonian Flow and Heat Transfer', *John Wiley and Sons, Inc. New York.*

Snyder, H.A., (1962), 'Experiments on the stability of spiral flow with low axial Reynolds numbers', *Proc. R. Soc. Series A.*, **265**, pp. 198-214.

Snyder, H.A., (1969), 'Change in wave-form and mean flow associated with wavelength variations in rotating Couette flow', *J. Fluid Mech.*, **35**, pp. 337-352.

Snyder, H.A., (1969), 'Wave-number selection at finite amplitude in rotating Couette flow', *J. Fluid Mech.*, **35**, pp. 273-298.

Sparrow, E.M. and Lin, S.H., (1964), 'The Developing Laminar Flow and Pressure Drop in the Entrance Region of Annular Ducts', *Trans. ASME, J. Basic Eng., Series D*, **86**, pp. 827-834.

Sparrow, E.M., Munro, W.D. and Jonsson, V.K., (1964), 'Instability of the flow between rotating cylinders: the wide gap problem', *J. Fluid Mech.*, **20**, pp.35-46.

Spells, K.E., (1955), 'Correlations for use in transport of Aqueous suspensions of fine solids through pipes', *Trans. Instn. Chem. Engrs*, **33**, pp. 79-84.

Steffe, J.F., (1992), 'Rheological Methods in Food Process Engineering', *Freeman Press*, East Lansing, Michigan.

Tachibana, M., (1973), 'On the behaviour of a sphere in the laminar tube flow', *Rheol. Acta.*, **12**, pp. 58-69.

Takeuchi, D.I. and Jankowski, D.F., (1981), 'A numerical and experimental investigation of the stability of spiral Poiseuille flow', *J. Fluid Mech.*, **102**, pp 101-126.

Tan, W.H., von Ellenrieder, K.D., Lim, T.T. and Soria, J., (2001), 'Stability of Taylor-Couette Flow with Axial Flow', *14th Australasian Fluid Mechanics Conference, Adelaide.*

Tanner, R.I., (1963), 'Helical Flow of Elastico-Viscous Liquids – Part I Theoretical', *Rheol. Acta*, **3**, pp. 21-26.

Tanner, R.I., (1963), 'Helical Flow of Elastico-Viscous Liquids – Part II Experimental', *Rheol. Acta*, **3**, pp. 26-34.

Taylor, G.I., (1923), 'VIII. Stability of a Viscous Liquid contained between Two Rotating Cylinders', *Phil. Trans. R. Soc., A*, **223**, pp. 289-343.

Taylor, G.I., (1936), 'Fluid Friction Between Rotating Cylinders I – Torque Measurements', *Proc. R. Soc., A.*, **157**, pp. 546-564.

Tehrani, M.A., (1996), 'An experimental study of particle migration in pipe flow of viscoelastic fluids', *J. Rheol.*, **40**, pp. 1057-1077.

Tetlow, N., Graham, A.L., Ingber, M.S., Subia, S.R., Mondy, L.A. and Altobelli, S.A., (1998), 'Particle migration in a Couette apparatus: Experiment and modeling', *J. Rheol.*, **42**, pp. 307-327.

Thomas, A.D., Cowper, N.T. and Venton, P.B. (1998), 'On-line viscosity measurement for the mineral processing industry', *Proc. 10th Int. Congr. Rheol. Sydney*, **V.2**, pp. 326-328.

Tuoc, T.K. and McGiven, J.M., (1994), 'Laminar flow of non-Newtonian fluids in annuli', *Trans IChemE, Series A*, **72**, pp. 669-676.

Valverde, J.L., Zumalacarregui, L., De Leucas, A. and Suris, G., (1997), 'An Improved Method for Determining Rheological Parameters of Suspensions: Statistical Approach', *Trans. IChemE*, **75 A**, pp. 784-791.

Vand, V., (1948), 'Viscosity of Solutions and Suspensions I, Theory', *J. Phys. Colloid Chem*., **52**, pp. 277-299.

Vand, V., (1948), 'Viscosity of Solutions and Suspensions II, Experimental Determination of the Viscosity-Concentration Function of Spherical Suspensions', *J. Phys. Colloid Chem*., **52**, pp. 300-321.

Van Dyke, M., (1982), 'An Album of Fluid Motion', *The Parabolic Press, California*.

Van Wazer, J.R., Lyons, J.W., Kim, K.Y. and Colwell, R.E., (1963), 'Viscosity and Flow Measurement, A laboratory handbook of Rheology', *Interscience Publishers*, New York.

Vlachou, V. and Piau, J., (2000), 'A new tool for the rheometric study of oil well cement slurries and other settling suspensions', *Cement and Concrete Res.*, **20**, pp. 1551-1557.

Vlaev, S.D., Valeva, M.D. and Mann, R., (2002), 'Some effects of rheology on the spatial distribution of gas hold-up in a mechanically agitated vessel', *Chem. Eng. J.*, **87**, pp. 21-30.

Vohr, J.H., (1968), 'An experimental study of Taylor vorticies and turbulence in the flow between eccentric rotating cylinders', *J. Lub. Tech., Trans. ASME, Series F*, **90**, pp. 275-296.

Von Kármán, T., (1934), 'Some aspects of the turbulence problem', *Proc. 4th Int. Congr. Appl. Mech., Cambridge*, pp. 54-59., in White, F.M., (1974), 'Viscous Fluid Flow', *McGraw-Hill Book Company*, New York.

Ward, H.T., and Kammermeyer, K., (1940), 'Sedimentation in the Laboratory, Design Data from Laboratory Experimentation', *Industr. Eng. Chem.*, **32**, pp. 622-626.

.

Ward, S.G. and Whitmore, R.L., (1950), 'Studies of the viscosity and sedimentation of suspensions, Part 1 – The viscosity of suspensions of spherical particles', *British, J. Appl. Phys.*, **1**, pp. 286-290.

Warren, L.J., (1975), 'Shear-Flocculation of Ultrafine Scheelite in Sodium Oleate Solutions', *J. Coll. Int. Sci.*, **50**, pp. 307-318.

Weast, R.C., (1982), 'CRC – Handbook of Chemistry and Physics, 63rd Edition', *CRC Press Inc.*, Boca Raton, Florida.

Wei, T. and Willmarth, W.W., (1992), 'Modifying turbulent structure with drag-reducing polymer additives in turbulent channel flows', *J. Fluid Mech.*, **245**, pp. 619-641.

Wendt, F., (1933), 'Turbulente Strömung zwischen zwei rotierenden koaxialen Zylindern', *Ing. Arch.*, **4**, pp. 577-595., in, Schlichting, H., (1968), 'Boundary-Layer Theory 6th ed.', *McGraw-Hill Book Company*.

Wills, B.A., (1976), 'Mineral Processing Technology', *Pergamon Press*, New York.

Wright, A.R., (1999), Private Communication.

Yu, Y. and Sun, D., (1964), 'Stability of a Viscous Flow Between Two Rotating Coaxial Cylinders', *J. Franklin Inst.*, **277**, pp. 140-149.

Zarti, A.S., Robati, B. and Mobbs, F.R., (1979), 'Misalignment Effects on the Stability of the Flow Between Eccentric Rotating Cylinders', *ASLE Transactions*, **22**, 361-364.

APPENDICES

APPENDIX A PROOF THAT PARAMETER B IS CONSTANT

Simplifying a momentum balance over a defined length of a concentric cylinder system gives:

$$\frac{d}{dr}\left(r\tau_{rz}\right)=\left(\frac{\Delta\wp}{L}\right)r$$

Integrating with respect to r yields:

$$\tau_{rz}=\left(\frac{\Delta\wp}{2L}\right)+\frac{c_1}{r}$$

The constant c_1 cannot be directly determined because the boundary conditions at either wall are unknown. However, the velocity curve will reach a maximum at an undetermined point ($r = \lambda R$) and at this point the momentum flux will be zero and thus c_1 can be determined as follows (Bird et al. 1960).

$$c_1 = -\frac{\Delta \wp}{2L}(\lambda R)^2$$

The shear stress across the radial section of the annulus may be therefore defined as.

$$\tau_{rz} = \frac{(\Delta \wp)R}{2L}\left(\frac{r}{R} - \lambda^2 \frac{R}{r}\right)$$

For a power-law model fluid the shear stress may be determined as a function of the change in the axial velocity with r.

$$\tau_{rz} = -A\left(\frac{dv_z}{dr}\right)^n$$

By combining the above two equations the shear rate or velocity gradient of the fluid may be determined.

$$-A\left(\frac{dv_z}{dr}\right)^n = \frac{(\Delta \wp)R}{2L}\left(\frac{r}{R} - \lambda^2 \frac{R}{r}\right)$$

$$\therefore \frac{dv_z}{dr} = \left(\frac{-(\Delta \wp)R}{2AL}\left(\frac{r}{R} - \lambda^2 \frac{R}{r}\right)\right)^{1/n}$$

$$\therefore \frac{dv_z}{dr} = \left(\frac{-(\Delta \wp)R}{2AL}\right)^{1/n}\left(\frac{r}{R} - \lambda^2 \frac{R}{r}\right)^{1/n}$$

The following boundary conditions may be assumed.

$v_z = 0 \quad @ \quad r = R$

$v_z = 0 \quad @ \quad r = \kappa R$

While it is not possible to solve for λ, it is possible to determine the parameters on which λ is dependent.

$\lambda\ (\kappa, R, L, A, n, \Delta\wp)$

The parameter b also represents the peak in the velocity profile and thus b is directly proportion to λ.

Therefore b is a function of the following variables.

$b\ (\kappa, R, A, n, \Delta\wp)$

Therefore b is only a function of the system dimensions, fluid properties and the dependent variable $\Delta\wp$. Thus for a given set of experiments preformed at constant $\Delta\wp$ and providing the rheological properties of the fluid do not dramatically change the value of b will be constant.

APPENDIX B SAMPLE CALCULATION – SIMULATION OF INSTABILITIES IN THE FLOW RHEOMETER

This set of sample calculations simulates the onset of turbulence in the flow rheometer. The rheological properties of the fluids are assumed to be Newtonian to simplify the calculations. The appropriate physical properties are outlined below.

R:	0.019	m	μ:	0.01	Pas
κ:	0.842		ρ:	1000	kg/m^3
L:	0.116	m			

The onset of instabilities in pipe flow can be predicted by the Reynolds number. For applications of helical flow the Reynolds number for annular flow between two concentric cylinders is required and is shown below.

$$\mathrm{Re} = \frac{2R(1-\kappa)\langle v_z \rangle \rho}{\mu} \qquad (11.2\text{-}1)$$

Thus this equation may be re-arranged to determine the average axial velocity $\langle v_z \rangle$ at which instabilities will develop (Re ≈ 2100).

$$\langle v_z \rangle = \frac{\mu \,\mathrm{Re}}{2R(1-\kappa)\rho}$$

$$\langle v_z \rangle = \frac{(0.01)(2100)}{2(0.019)(1-0.842)(1000)}$$

$$\langle v_z \rangle = 3.49 \ \text{m/s}$$

Thus the axial volumetric flow rate may be determined.

$$Q = \pi R^2 \left(1-\kappa^2\right)\langle v_z \rangle$$

$$Q = \pi(0.019)^2 \left(1-0.842^2\right)(3.49)$$

$$Q = 1.15\times10^{-3}\,\text{m}^3/\text{s}$$

$$Q = 69.1 \text{ L/min}$$

The maximum flow rate attainable with the current helical rotor pump is approximately 4 L/min, which is well below the onset value of 69.1 L/min. Thus there should be no situation in which instabilities would develop in the axial component of the flow.

A similar set of calculations can be performed to determine the critical speed at which Taylor vortices will develop in the Couette component of the flow. The Taylor number may be determined using the following equation.

$$Ta = \frac{v_\theta R(1-\kappa)}{\nu}\sqrt{\frac{(1-\kappa)}{\kappa}} = 41.3 \qquad (11.3\text{-}4)$$

This equation may be re-arranged to determine the velocity of the rotating inner cylinder at which Taylor vortices will appear.

$$v_\theta = \frac{\frac{\mu Ta}{\rho R(1-\kappa)}}{\sqrt{\frac{(1-\kappa)}{\kappa}}}$$

$$v_\theta = \frac{\frac{(0.01)(41.3)}{(1000)(0.019)(1-0.842)}}{\sqrt{\frac{(1-0.842)}{0.842}}}$$

$$v_\theta = 0.318 \text{ m/s}$$

Thus the angular velocity of the inner cylinder may be determined.

$$\Omega = \frac{v_\theta}{\kappa R}$$

$$\Omega = \frac{0.318}{(0.842)(0.019)}$$

$$\Omega = 19.8 \text{ rad/s}$$

$$\Omega = 190 \text{ rpm}$$

This rotational speed of 190 rpm for the critical onset of Taylor vortices is well inside the operating range of the Haake VT550 (0.5 – 800rpm) and thus it is possible that Taylor vortices may develop during rheological measurements.

APPENDIX C SAMPLE CALCULATIONS FOR THE DETERMINATION OF RHEOLOGICAL PROPERTIES FROM MEASUREMENTS WITH THE FLOW RHEOMETER

This set of sample calculations refers to the experimental measurements of the CMC 1.5wt % solution, measured at an operating differential pressure of 1500Pa using the wide gap geometry (32mm bob).

The density of the CMC, measured using a 50mL density bottle, was 1003kg/m^3 at 24ºC.

The analysis procedure to determine the fluids rheological properties is presented in CHAPTER 4. A flow chart of the calculation procedure is presented in Figure C-1.

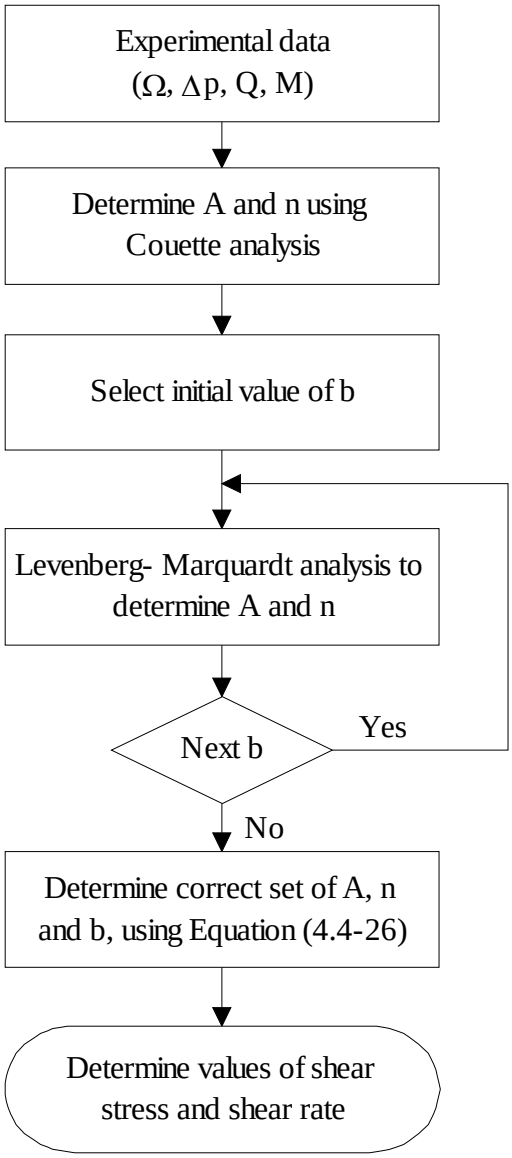

Figure C–1 Calculation procedure to determine the rheological properties of a non-Newtonian fluid from measurements performed with the flow rheometer

The first step in the calculation procedure is to consolidate the experimental readings from the flow rheometer. This is achieved by determining an average torque value for each value of rotational speed examined. The torque measurements from the Haake VT 550 are present below in Figure C-2 as a function of time and rotational speed.

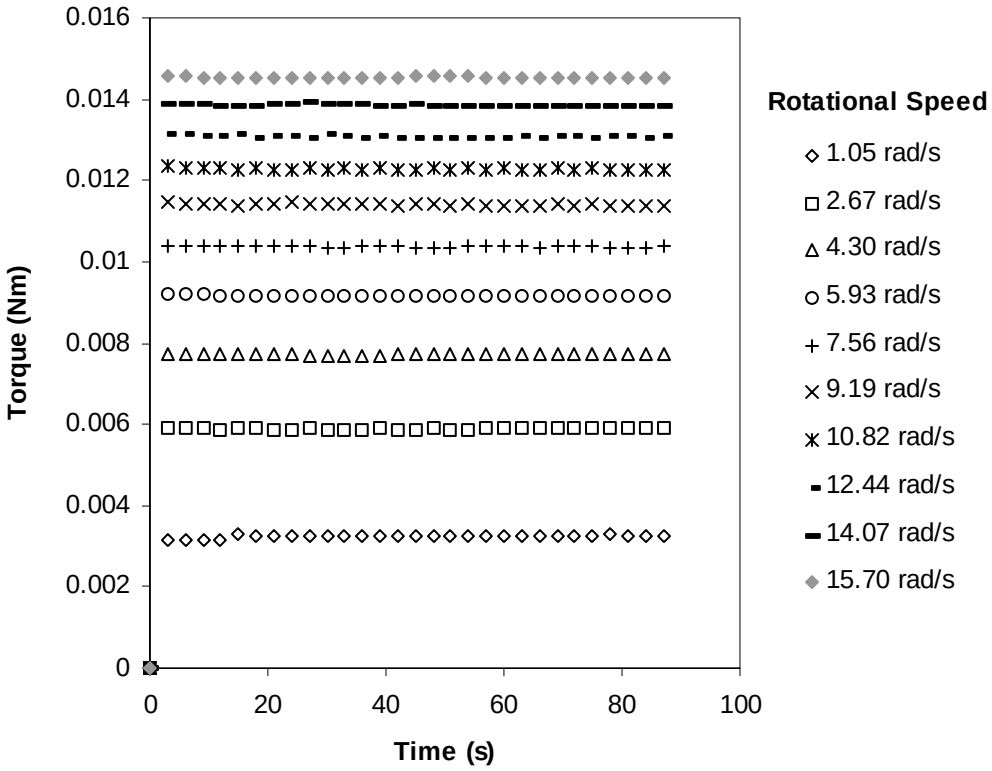

Figure C–2 Torque measurements from 1.5wt% CMC experiments, with an operating pressure of 1500Pa

The pressure drop as previously mentioned was held constant at 1500Pa. The flow rate measurements are redundant because the system is fully specified without them, as described in section 8.4.

Before the Levenberg – Marquardt method can be used an appropriate guess is required for the parameters to be optimised (A and n). These guessed values can be determined by ignoring the axial flow component and performing calculations based on Couette flow theory. The averaged values of torque and rotational speed are used to determine values of shear stress and shear rate respectively. An example is presented below.

The system dimensions and experimental readings:

L:	0.116 m	M:	0.00916 Nm
R:	0.019 m	Ω:	5.93 rad/s
κ:	0.842		

The shear stress at the bob may be calculated using the following equation.

$$\tau = \frac{M}{2\pi(\kappa R)^2 L} \qquad (3.2\text{-}5)$$

$$\tau = \frac{0.00916}{2\pi(0.019 \times 0.842)^2 (0.116)}$$

$$\tau = 49.1 \text{ Pa}$$

To simplify the calculations the shear rate is determined using a formula that would normally only be applicable for a Newtonian fluid. This is not the correct method as many fluids examined are likely to be non-Newtonian, however this procedure is only to generate approximate starting values for the Levenberg-Marquardt procedure.

$$\dot{\gamma} = \frac{2\Omega}{(1-\kappa^2)} \qquad (3.2\text{-}6)$$

$$\dot{\gamma} = \frac{2 \times 5.93}{(1-(0.842)^2)}$$

$$\dot{\gamma} = 40.8 \text{ rad/s}$$

For each measurement at a different rotational speed a value of shear stress and shear rate is calculated. A complete list of the Couette shear stress and shear rate values are presented in Table C–I and from these shear stress and shear rate values the guesstimate values of A and n are determined using a least square fit of log values of

shear stress and shear rate. The various variable necessary for this calculation are also presented in Table C–I.

Table C–I Values necessary for a least square regression to determine the parameters A and n

Shear Rate (1/s)	Shear Stress (Pa)	ln ($\dot{\gamma}$), X	ln (τ), Y	X^2	XY
7.2	17.4	1.97	2.86	3.90	5.64
18.4	31.6	2.91	3.45	8.48	10.05
29.6	41.4	3.39	3.72	11.47	12.61
40.8	49.1	3.71	3.89	13.75	14.44
52.0	55.6	3.95	4.02	15.61	15.87
63.2	61.1	4.15	4.11	17.19	17.05
74.4	65.8	4.31	4.19	18.57	18.04
85.6	70.1	4.45	4.25	19.80	18.91
96.8	74.2	4.57	4.31	20.91	19.69
108.0	77.9	4.68	4.36	21.92	20.39

$\Sigma X = 38.09$

$\Sigma Y = 39.16$

$\Sigma(X^2) = 151.59$

$\Sigma XY = 152.70$

The slope of the line of best fit on a plot of ln(shear stress) versus ln (shear rate) gives the value of n.

Thus

$$n = \frac{\Sigma XY - \left(\frac{\Sigma X \, \Sigma Y}{\text{no of data points}} \right)}{\Sigma\left(X^2\right) - \left(\frac{(\Sigma X)^2}{\text{no of data points}} \right)}$$

$$n = \frac{152.70 - \left(\frac{38.09 \times 39.16}{10}\right)}{151.59 - \left(\frac{(38.09)^2}{10}\right)}$$

$$n = 0.55$$

The y-intercept of the line of best gives ln(A).

Thus

$$A = e^{\left(\frac{\Sigma Y - n\Sigma X}{\text{no of data points}}\right)}$$

$$A = e^{\left(\frac{39.16 - 0.55 \times 38.09}{10}\right)}$$

$$A = 6.24$$

The correct value of the parameter b cannot be determined before the Levenberg-Marquardt regression is performed and so a range of possible b values are selected. The maximum and minimum values of b are based on the following equation.

$$\left(-\frac{\partial p}{\partial z} + \rho g\right)\frac{R^2}{2} < b < \left(-\frac{\partial p}{\partial z} + \rho g\right)\frac{(\kappa R)^2}{2} \qquad (4.4\text{-}11)$$

Therefore

$$b_{max} = \left(-\frac{\partial p}{\partial z} + \rho g\right)\frac{(\kappa R)^2}{2}$$

$$b_{max} = \left(\frac{-1500}{0.116} + 1003 \times 9.81\right)\frac{(0.016)^2}{2}$$

b_{max} = -0.396

and

$$b_{min} = \left(-\frac{\partial p}{\partial z} + \rho g \right) \frac{R^2}{2}$$

$$b_{min} = \left(\frac{-1500}{0.116} + 1003 \times 9.81 \right) \frac{(0.019)^2}{2}$$

b_{min} = -0.558

Twenty values of b are selected ranging between the maximum and minimum values and these values are presented in Table C-II. For each value of b a value of A and n is determined from the Levenberg-Marquardt method. Two other variables are also determined as part of the Levenberg-Marquardt method; X^2 and the evaluation of the integral, Equation (4.4-26). The evaluation of the integral is used to determine the correct value of b from the selection chosen. The variable X^2 is used to determine the accuracy of the fit and is calculated as follows.

$$X^2 = \sum_{i=1}^{n} \left(Y_i - \hat{Y}_i \right)^2$$

Where $\hat{Y}_i$ is the predicted value of Y at the i^{th} data point.

A plot of X^2 versus b and the evaluation of the integral versus b is presented in Figure C-3 to show the trend of these two variables over the range of b values from minimum to maximum.

Table C–II Summary of results from Levenberg-Marquardt non-linear regression

b	A	n	X^2	Evaluation of Equation (4.4-26)
-0.558	7.647	0.480	0.296	-1.670E-03
-0.550	7.627	0.481	0.301	-1.443E-03
-0.542	7.608	0.481	0.306	-1.236E-03
-0.534	7.591	0.482	0.311	-1.046E-03
-0.526	7.577	0.482	0.315	-8.727E-04
-0.518	7.564	0.482	0.319	-7.138E-04
-0.509	7.553	0.483	0.322	-5.678E-04
-0.501	7.544	0.483	0.325	-4.328E-04
-0.493	7.537	0.483	0.327	-3.070E-04
-0.485	7.531	0.483	0.328	-1.883E-04
-0.477	7.528	0.483	0.329	-7.471E-05
-0.469	7.527	0.483	0.330	3.606E-05
-0.461	7.527	0.483	0.329	1.460E-04
-0.453	7.530	0.483	0.329	2.576E-04
-0.445	7.534	0.483	0.327	3.730E-04
-0.437	7.540	0.483	0.326	4.947E-04
-0.429	7.548	0.483	0.323	6.251E-04
-0.420	7.558	0.482	0.320	7.667E-04
-0.412	7.570	0.482	0.317	9.217E-04
-0.404	7.584	0.482	0.313	1.093E-03

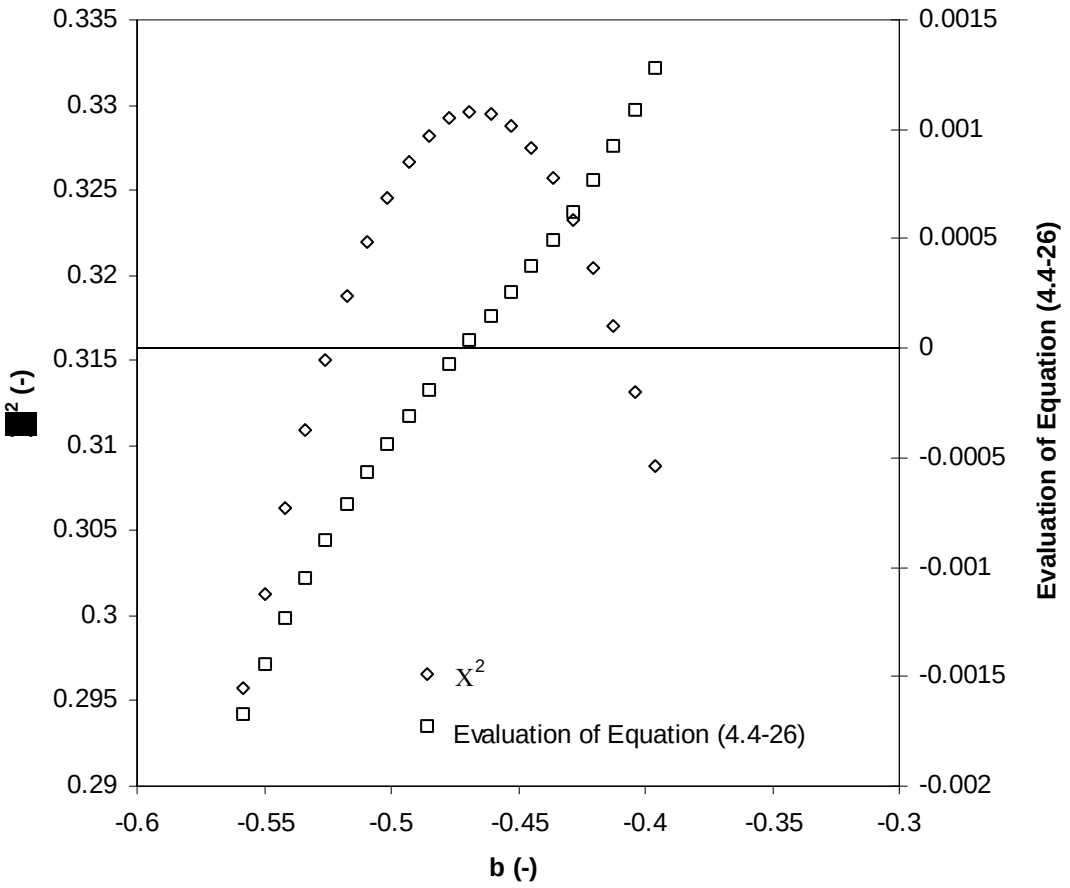

Figure C–3 Graphical presentation of results from the Levenberg-Marquardt non-linear regression

The correct value of b is determined by examining Equation (4.4-26). From the graph and the table it is clear that the value of b that gives a value of the integral closest to zero is –0.469. Thus the correct values of A and n are 7.527 and 0.483 respectively.

The correct values of shear stress may then be calculated as shown. The example continues to uses the same set data presented at the start of the calculation.

$$\tau = \sqrt{\left[\frac{M}{2\pi(\kappa R)^2 L}\right]^2 + \left[\frac{b}{\kappa R} - \frac{c(\kappa R)}{2}\right]^2} \qquad (4.4\text{-}21)$$

The value of the variable c is required and can be determined thus.

$$c = -\frac{\partial p}{\partial z} + \rho g \qquad (4.4\text{-}9)$$

$$c = \left(\frac{-1500}{0.116} + 1003 * 9.81\right)$$

$$c = -3091.6$$

Therefore

$$\tau = \sqrt{\left[\frac{0.00916}{2\pi(0.016)^2(0.116)}\right]^2 + \left[\frac{-0.469}{0.016} - \frac{-3091.6(0.016)}{2}\right]^2}$$

$$\tau = 49.3$$

The shear rate cannot be directly determined from the experimental measured variables and so the optimised values of A and n are used to determine the shear rate at each value of shear stress.

$$\dot{\gamma} = \left(\frac{\tau}{A}\right)^{\frac{1}{n}} \qquad (4.4\text{-}22)$$

$$\dot{\gamma} = \left(\frac{49.4}{7.527}\right)^{\frac{1}{0.483}}$$

$$\dot{\gamma} = 49.0$$

A complete list of the calculated values of shear stress and shear rate are presented in Table C-III. All the results for the 1.5wt% CMC solution are presented in Figure 7.3-2.

Table C-III Calculated values of shear stress and shear rate for the 1.5wt% CMC solution measured at 1500Pa with the wide gap geometry in the flow rheometer.

Shear Stress (Pa)	Shear Rate (1/s)
18.0	6.1
31.9	19.9
41.6	34.5
49.4	49.0
55.8	63.1
61.3	76.7
66.0	89.4
70.3	101.8
74.4	114.4
78.0	126.4

APPENDIX D MANIPULATION OF THE TAYLOR NUMBER

Taylor (1923) initial derived the expression presented below as a criterion for the onset of instabilities in Couette flow with either the inner, outer or both cylinders rotating.

$$P = \frac{\pi^4 \nu^2 (R + \kappa R)}{2\Omega_2^2 (R - \kappa R)^3 (\kappa R)^2 \left[1 - \left(k R^2 / (\kappa R)^2\right)\right](1 - k)} = 0.0571 \qquad (11.3\text{-}2)$$

When the outer cylinder is stationary, k, the ratio of the speed of rotation of the two cylinders will be zero and Taylor's expression can be simplified thus.

$$P = \frac{\pi^4 \nu^2 (R + \kappa R)}{2\Omega^2 (R - \kappa R)^3 (\kappa R)^2} = 0.0571$$

The parameter P is redefined as the Taylor number, Ta', as shown.

$$Ta' = \frac{\pi^4}{P} = \frac{2(\kappa R)^2 \Omega^2 (R - \kappa R)^3}{\nu^2 (R + \kappa R)} = \frac{1}{0.0571} \times \pi^4$$

The following simplification to the Taylor number can be made.

$$Ta' = \frac{2 v_\theta^2 (R - \kappa R)^3}{\nu^2 (R + \kappa R)} = 1706 \qquad (11.3\text{-}3)$$

$$Ta' = \frac{v_\theta^2 (R - \kappa R)^3}{\nu^2 (R + \kappa R)} = \frac{1706}{2}$$

$$Ta' = \frac{v_\theta^2 (R - \kappa R)^3}{\nu^2 (R + \kappa R)} = 853$$

$$Ta = \sqrt{\frac{v_\theta^2 (R - \kappa R)^3}{\nu^2 (R + \kappa R)}} = \sqrt{853}$$

$$Ta = \frac{v_\theta (R - \kappa R)}{\nu} \sqrt{\frac{(R - \kappa R)}{(R + \kappa R)}} = 29.2$$

If a narrow gap is assumed $\kappa R \approx R$ then the above expression may be simplified as follows, to yield the Taylor number definition used in this study, Equation (11.3-4).

$$Ta = \frac{v_\theta (R - \kappa R)}{\nu} \sqrt{\frac{(R - \kappa R)}{2(\kappa R)}} = 29.2$$

$$Ta = \frac{v_\theta (R - \kappa R)}{\nu} \sqrt{\frac{(R - \kappa R)}{(\kappa R)}} = 29.2 \times \sqrt{2}$$

$$Ta = \frac{v_\theta R(1 - \kappa)}{\nu} \sqrt{\frac{(1 - \kappa)}{\kappa}} = 41.3 \qquad (11.3\text{-}4)$$

APPENDIX E SAMPLE CALCULATIONS – PREDICTION OF THE INSTABILITIES IN HELICAL FLOW

This set of sample calculations refers to the prediction of the onset of instabilities in the polyox solution, section 14.3.3. The following list summarises the values of the variables that will be used in these calculations.

R:	0.019 m	Ω:	11.4 rad/s
κ:	0.842	A:	0.0095 Pas
L:	0.116 m	n:	0.82
Q:	420 mL/min	ρ:	998 kg/m^3

The effect due to each of the following parameters must be determined.

- Acceleration rate of the inner cylinder, E_A
- Gap width, E_G
- Axial flow rate, E_{Re}

The rate of acceleration was ~15.3 rad/s/s, which is in the fast region and thus the value of E_A is 0.87.

Given that the acceleration is in the fast region the value of the gap width parameter may be calculated as follows.

$$E_G = 0.87(1-\kappa)^2 + 0.21(1-\kappa)+1 \qquad (14.3\text{-}8)$$

$$E_G = 0.87(1-0.842)^2 + 0.21(1-0.842)+1$$

$$E_G = 1.05$$

The axial flow Reynold's number may be determined as follows.

$$Re = \frac{[2R(1-\kappa)]^n \langle v_z \rangle^{2-n} \rho}{(8\varphi)^{n-1} A'} \qquad (11.2\text{-}2)$$

where

$$\varphi(\kappa) = \frac{(1-\kappa)^2}{\frac{\left(1-\kappa^2\right)}{\ln(\kappa)} + \left(1+\kappa^2\right)} \qquad (11.2\text{-}3)$$

$$\varphi(\kappa) = \frac{(1-.0842)^2}{\frac{\left(1-0842^2\right)}{\ln(0842)} + \left(1+0842^2\right)}$$

$$\varphi = 1.499$$

and

$$A' = A\left[\frac{3n+\varphi}{(3+\varphi)n}\right]^n \qquad (11.2\text{-}4)$$

$$A' = 0.0095\left[\frac{3(0.82)+1.499}{(3+1.499)(0.82)}\right]^{0.82}$$

$$A' = 0.0101$$

and

$$\langle v_z \rangle = \frac{Q}{\pi R^2\left(1-\kappa^2\right)}$$

$$\langle v_z \rangle = \frac{420/60\times 1000\times 1000}{\pi(0.019)^2\left(1-(0.842)^2\right)}$$

$$\langle v_z \rangle = 0.021 \text{ m/s}$$

Therefore

$$Re = \frac{[2(0.019)(1-0.842)]^{0.82}(0.021)^{2-0.82}(998)}{(8\times 1.499)^{0.82-1}(0.0101)}$$

$$Re = 24.4$$

The axial flow axial flow parameter can be determined using the following equation.

$$E_{Re} = \sqrt{1+3.12\times 10^{-4}\,Re^2} \qquad (14.3\text{-}10)$$

$$E_{Re} = \sqrt{1+3.13\times 10^{-4}(24.4)^2}$$

$E_{Re} = 1.09$

The predicted onset of instabilities in the helical flow under these conditions can now be determined as follow.

$$\text{Prediction} = E_A E_G E_{Re}\, 41.3 \qquad (14.3\text{-}11)$$

$$\text{Prediction} = (0.89)(1.05)(1.09)(41.3)$$

$$\text{Prediction} = 42.1$$

The measured value for the onset of Taylor vortices can be determined by examining a plot of rotational speed versus torque measurement, see Figure E-1 below.

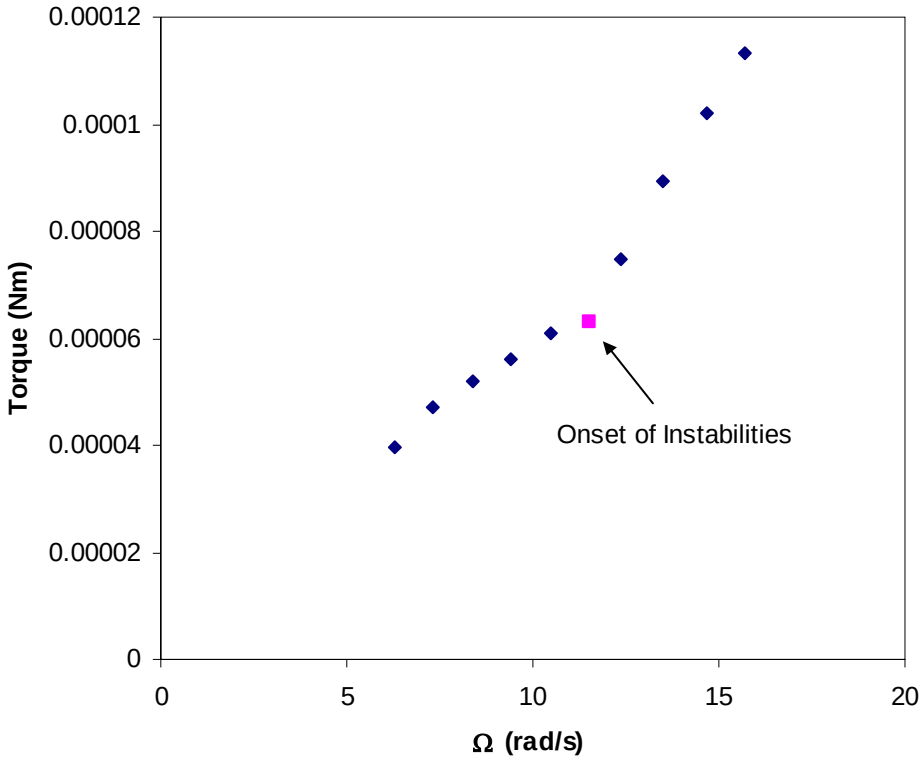

Figure E–1 Torque measurements as a function of rotational speed for the polyox solution with an axial flow rate of 420 mL/min

From this figure it can be seen that Taylor vortices first appear at a value of rotational speed of 11.4 rad/s. Thus the non-Newtonian Taylor number can be determined as follows.

$$Ta_{power\text{-}law} = n\frac{\Omega\rho(\kappa R)(R-\kappa R)}{A\left(\left(\frac{2\Omega}{n}\right)\left(\frac{1}{1-\kappa^{2/n}}\right)\right)^{n-1}}\sqrt{\frac{(R-\kappa R)}{(\kappa R)}} \qquad (13.4\text{-}4)$$

$$Ta_{power\text{-}law} = 0.82\frac{(11.4)(998)(0.016)(0.019-0.016)}{A\left(\left(\frac{(2)(12.2)}{0.82}\right)\left(\frac{1}{1-(0.842)^{2/0.82}}\right)\right)^{0.82-1}}\sqrt{\frac{(0.019-0.016)}{(0.016)}}$$

$$Ta_{power\text{-}law} = 41.9$$

The experimentally determined Taylor number for the onset of Taylor vortices in helical flow compares extremely well to the predicted value (41.9 compared to 42.1), which demonstrates the accuracy of the stability criterion developed.